ΠΑΝΕΠΙΣΤΗΜΙΟ ΚΡΗΤΗΣ

ΙΑΤΡΙΚΗ ΣΧΟΛΗ

ΤΟΜΕΑΣ ΒΑΣΙΚΩΝ ΕΠΙΣΤΗΜΩΝ

ΕΡΓΑΣΤΗΡΙΟ ΒΙΟΧΗΜΕΙΑΣ

Διδακτορική διατριβή

Μελέτη των μηχανισμών μοριακής σηματοδότησης και των αθηροπροστατευτικών δράσεων της HDL στα ενδοθηλιακά κύτταρα

Θεοφιλάτος Δημήτρης

Επιβλέπων Καθηγητής: Δ. Καρδάσης

Ηράκλειο, 2019

UNIVERSITY OF CRETE

SCHOOL OF MEDICINE

DEPARTMENT OF BASIC SCIENCES-BIOCHEMISTRY

Ph.D. thesis

Study the signaling cascades and the atheroprotective properties of HDL in endothelial cells

Theofilatos Dimtris

Supervisor: Prof. D. Kardassis

Heraklion, 2019

Ευχαριστίες

Σε αυτό το σημείο θα ήθελα να ευχαριστήσω κάποιους ανθρώπους που συνέβαλαν αποφασιστικά στην επιτυχή ολοκλήρωση αυτής της Διδακτορική Διατριβής (ΔΔ) και συνεπώς στην διαμόρφωση της επιστημονικής μου σκέψης.

Αρχικά, θα ήθελα να ευχαριστήσω θερμά, τον επιβλέποντα Καθηγητή μου Δρ. Καρδάση Δημήτρη που από την πρώτη στιγμή που ήρθα στο εργαστήριο του (ως μεταπτυχιακός φοιτητής) μου έδειξε εμπιστοσύνη, μου έδωσε την δυνατότητα να εκτεθώ σε πολλές διαφορετικές τεχνικές και σε διαφορετικά βιολογικά ερωτήματα και ήταν πάντα εκεί για να με καθοδηγεί. Επίσης, εκτός από εξαιρετικός Καθηγητής είναι και ένας εξαιρετικός άνθρωπος που με το ήθος και την ευγένεια του αποτελεί παράδειγμα για τον τρόπο που πρέπει να διαμορφώνονται οι σχέσεις εντός και εκτός ενός εργαστηρίου.

Εν συνεχεία, θα ήθελα να ευχαριστήσω τα μέλη της Τριμελούς μου Επιτροπής, τον Καθηγητή Δρ. Τσατσάνη Χρήστο και την Αναπλ. Καθηγήτρια Δρ. Σανούδου Δέσποινα, οι οποίοι ήταν πάντα διαθέσιμοι και βοηθητικοί για οποιοδήποτε ζήτημα πρόεκυπτε. Επίσης, θα ήθελα να ευχαριστήσω και τα υπόλοιπα μέλη της Επταμελούς μου Επιτροπής, τον Επικ. Καθηγητή Δρ. Μπερτσιά Γιώργο, τον Αναπλ. Καθηγητή Δρ. Χαραλαμπόπουλο Ιωάννη, την Επικ. Καθηγήτρια Δρ. Παπακωνσταντή Ευαγγελία και τον Διευθυντή Ερευνών Δρ. Ταλιανίδη Ιωάννη για τις πολύτιμες συμβουλές τους.

Ιδιαίτερες ευχαριστίες στον Ομότιμο Καθηγητή Δρ. Ζαννή Βασίλη, ο οποίος μου παρείχε πολύτιμες συμβουλές καθ' όλη την διάρκεια του διδακτορικού μου.

Επίσης, θα ήθελα να ευχαριστήσω τον Καθηγητή Δρ. Ηλιόπουλο Δημήτρη, ο οποίος μου έδωσε την δυνατότητα να πραγματοποιήσω κάποια πειράματα για το project του let-7b στο εργαστήριο του στο UCLA στο Los Angeles. Ιδιαίτερες ευχαριστίες στον Δρ. Κούκο Γιώργο, ο οποίος εκτός του ότι οργάνωσε κάθε πτυχή της συγκεκριμένης επίσκεψης, ήταν και ο άμεσος συνεργάτης μέσα στο εργαστήριο παρέχοντας μου πολύτιμες συμβουλές.

Ένα ξεχωριστό ευχαριστώ σε όλα τα μέλη του εργαστηρίου του κυρίου Καρδάση για το εξαιρετικό κλίμα συνεργασίας και συναδελφικότητας που υπήρχε εντός του εργαστηρίου. Στην Βέτα, στην Έφη, στην Ιωάννα, στη Νικολέτα, στην Μαρία, στην Βίκυ, στην Κατερίνα, και στον Δημήτρη με τους οποίους περάσαμε πολλές ώρες μαζί, συζητάγαμε γύρω από τα project μας (και όχι μόνο), κάναμε πειράματα και εν τέλει χαιρόμασταν και απογοητευόμασταν μαζί. Ειδικά με την Κατερίνα και τον Δημήτρη που συνέπεσαν οι φάσεις των διδακτορικών μας, ήταν πολύ μεγάλη μου χαρά που βίωσα μαζί τους αυτές τις στιγμές. Επίσης και στα υπόλοιπα παιδιά που βρέθηκαν είτε για λιγότερο είτε για περισσότερο στο εργαστήριο.

Επιπρόσθετα, θα ήθελα να ευχαριστήσω το πρόγραμμα Μεταπτυχιακών Σπουδών 'Μοριακή Βάση των Νοσημάτων του Ανθρώπου' που μου έδωσε την δυνατότητα να

ξεκινήσω την ερευνητική μου διαδρομή. Ιδιαίτερες ευχαριστίες στην γραμματέα του προγράμματος, Κα Αδαμάκη Μαίρη που είναι πάντα εκεί για όλους μας. Σε αυτό το σημείο θα ήθελα να ευχαριστήσω και τις γραμματείες των μεταπτυχιακών και διδακτορικών σπουδών της Ιατρικής Σχολής, Κα. Εφεντάκη Νίκη, Κα Φλουρή Σοφία και την Κα Σκουλά Μαρία για την άριστη συνεργασία που είχαμε σε όλη τη διάρκεια του διδακτορικού.

Ξεχωριστές ευχαριστίες σε κάποιους ανθρώπους οι οποίοι εκτός του ότι είναι συνάδελφοι και οποτεδήποτε τους χρειάστηκα ήταν εκεί αλλά είναι και αγαπημένοι φίλοι που ανεχόντουσαν τις ερωτήσεις μου οποιαδήποτε ώρα μέσα στην ημέρα. Πιο συγκεκριμένα την Δρ. Κανελίνα Καραλή, τη Νάντια Γεωργιλά και τον Πέτρο Τζέρπο οι οποίοι με την στάση τους αποτελούν πηγή έμπνευσης για τους συναδέλφους τους. Ξεχωριστές ευχαριστίες στην Δήμητρα Μαυροειδή, η οποία πορεύτηκε μαζί μου σε όλη αυτή τη διαδρομή, ανέχτηκε τα ωράρια μου, αγκάλιασε την αγωνία μου και έπαιξε καταλυτικό ρόλο ώστε να αρχίσω (επιτέλους) να γράφω την διατριβή μου.

Αυτή η διαδρομή δεν θα ήταν ίδια χωρίς τους αγαπημένους μας φίλους. Άνθρωποι που συναντήθηκαν τα άγχη μας στους διαδρόμους του Πανεπιστημίου Κρήτης και στην πόλη του Ηρακλείου, επιλέξαμε να τα αντιμετωπίσουμε από κοινού και καταφέραμε να δημιουργήσουμε όμορφες καταστάσεις που ήταν η καλύτερη συντροφιά μέσα στην καθημερινότητα. Επίσης, αγαπημένοι φίλοι και στις δυο άλλες πόλεις που έχω ζήσει, Πάτρα και Αθήνα, που κάθε φορά που συναντιόμασταν φροντίζαμε να «γεμίζουμε τις μπαταρίες μας» με όμορφες στιγμές.

Ξεχωριστές ευχαριστίες στους γονείς μου Θύμιο και Κέλλυ που – παρά την γεωγραφική απόσταση- καταφέρνουν να είναι πάντα δίπλα μου και να στηρίζουν κάθε βήμα μου! Χωρίς την στήριξή τους, τα πράγματα θα ήταν σίγουρα πολύ διαφορετικά. Επίσης, στον αδερφό μου Γεράσιμο και στην όμορφη οικογένειά του που είναι πάντα δίπλα μου!

Κλείνοντας, είναι σημαντικό να ειπωθεί πώς αυτό το διδακτορικό πραγματοποιήθηκε σε δύσκολες εποχές για την ελληνική κοινωνία. Μέσα σε αυτές τις συνθήκες, ο ρόλος της επιστήμης για την πρόοδο των ανθρώπινων κοινωνιών φαντάζει ακόμα πιο σημαντικός. Μια επιστήμη που θα πραγματοποιείται με γνώμονα της ανάγκες των ανθρώπων και τα αποτελέσματά της θα είναι άμεσα διαθέσιμα σε αυτούς φαίνεται πώς αποτελεί αναγκαία συνθήκη για να επιτευχθεί ουσιαστική κοινωνική πρόοδος, όπου οι άνθρωποι και το περιβάλλον θα ζουν αρμονικά.

Η παρούσα έρευνα έχει χρηματοδοτηθεί από την Γενική Γραμματεία Έρευνας και Τεχνολογίας μέσω του μέσω του Προγράμματος «ΘΑΛΗΣ», με κωδικό MIS 377286 στο Επιχειρησιακό Πρόγραμμα "Εκπαίδευση και Δια Βίου Μάθηση. Επίσης και από προσωπική υποτροφία από το κληροδότημα ‘Αντώνιου Παπαδάκη’ που διαχειρίζεται το Εθνικό και Καποδιστριακό Πανεπιστήμιο Αθηνών.

Table of Contents

Περίληψη

Πολυάριθμες επιδημιολογικές μελέτες έχουν δείξει ότι τα χαμηλά επίπεδα της λιποπρωτεΐνης υψηλής πυκνότητας (High Density Lipoprotein – HDL) στον ορό αποτελούν ισχυρό δείκτη κινδύνου για την ανάπτυξη Καρδιαγγειακών Νοσημάτων (ΚΝ). Παράλληλα, έχουν ανακαλυφθεί αρκετές προστατευτικές ιδιότητες της HDL απέναντι στην ανάπτυξη της αθηροσκλήρωσης, η οποία είναι η παθολογική αιτία των ΚΝ. Ωστόσο, σε ασθενείς με ΚΝ, η χρήση φαρμάκων που στόχευαν στην αύξηση της συγκέντρωσης της HDL στον ορό δεν οδήγησε σε μείωση του κινδύνου εμφάνισης καρδιαγγειακών γεγονότων. Επιπρόσθετα, πρόσφατες έρευνες ανέδειξαν ότι οι ασθενείς με ΚΝ φέρουν 'μη λειτουργική/δυσλειτουργική' HDL, η οποία αδυνατεί να πραγματοποιήσει τις φυσιολογικές προστατευτικές της δράσεις. Από αυτά τα δεδομένα προκύπτει πώς από μόνη της η αύξηση των επιπέδων της HDL δεν αρκεί για να παρέχει αθηροπροστασία αλλά πρέπει να συνοδεύεται και από την ύπαρξη λειτουργικής HDL. Παράλληλα, κάποια φάρμακα που στοχεύουν στην αύξηση των επιπέδων της HDL προκάλεσαν σημαντικές παρενέργειες στους ασθενείς αναδεικνύοντας την πολυπλοκότητα των μεταβολικών μονοπατιών αλλά και την ελλιπή, μέχρι σήμερα, κατανόησή τους.

Οι ερευνητικοί στόχοι της παρούσας διδακτορικής διατριβής ήταν οι εξής:

- **Κεφάλαιο 1**: Να διευκρινιστούν οι μοριακοί μηχανισμοί μέσω τον οποίων η HDL επιφέρει την αθηρο-προστατευτική της δράση στα ενδοθηλιακά κύτταρα. Για αυτό τον στόχο, στις *Ενότητες Ι και ΙΙ* επικεντρωθήκαμε στην ανίχνευση γονιδίων-στόχων της HDL στα ενδοθηλιακά κύτταρα αλλά και στη μελέτη των μηχανισμών μέσω των οποίων πραγματοποιούνται οι συγκεκριμένες ρυθμίσεις, ενώ στην *Ενότητα ΙΙΙ,* μελετήσαμε την λειτουργικότητα της HDL που έχει απομονωθεί από ασθενείς με μια χρόνια φλεγμονώδη νόσο (την αγκυλοποιητική σπονδυλίτιδα).

- **<u>Κεφάλαιο 2:</u>** Να διερευνηθούν σε μοριακό επίπεδο νέα γονίδια και miRNAs που ρυθμίζουν την βιογένεση της HDL στα ηπατικά κύτταρα. Για τον σκοπό αυτόν, στην *<u>Ενότητα IV</u>* μελετήσαμε την ρύθμιση του γονιδίου του μεταγραφικού παράγοντα LXRα από τον ηπατικό μεταγραφικό παράγοντα HNF-4α, ενώ στην *<u>Ενότητα V</u>* μελετήσαμε τον ρόλο του miRNA let-7b στην ρύθμιση της απολιποπρωτεΐνης E (apoE) στα ηπατικά κύτταρα HepG2.

Ο τραυματισμός ή 'δυσλειτουργική' δράση του ενδοθηλίου έχει συσχετιστεί με την έναρξη και ανάπτυξη της αθηρωματικής πλάκας. Η HDL αποτελεί ρυθμιστή της φυσιολογικής λειτουργίας του ενδοθηλίου και ενεργοποιεί μηχανισμούς προστασίας του μετά από τραύμα, ενώ η 'δυσλειτουργική' HDL δεν έχει αυτές τις δράσεις. Για αυτό τον λόγο, στον **Κεφάλαιο 1** θέλαμε να ανιχνεύσουμε τους μοριακούς μηχανισμούς δράσης της φυσιολογικής HDL στο ενδοθήλιο. Τα γονίδια στα οποία επικεντρωθήκαμε στις δύο πρώτες ενότητες, αντλήθηκαν από microarray δεδομένα, τα οποία είχαν παραχθεί σε προηγούμενες μελέτες της ερευνητική μας ομάδας ύστερα από επίδραση ενδοθηλιακών κυττάρων με ανασυσταθείσα HDL που φέρει την ανθρώπινη απολιποπρωτεΐνη A-I (rHDL-AI). Εμείς μελετήσαμε την ανταπόκριση αυτών των γονιδίων ύστερα από επίδραση με φυσική HDL που απομονώθηκε από διαγονιδιακούς ποντικούς που εξέφραζαν την ανθρώπινη απολιποπρωτεΐνη-A-I (tgHDL).

Πιο συγκεκριμένα, στην <u>ενότητα I</u> επικεντρωθήκαμε στη ρύθμιση του γονιδίου της Angiopoietin-like 4 (ANGPTL4), το οποίο έχει σημαντικό ρόλο στον μεταβολισμό των λιπιδίων και στην αθηρωμάτωση. Παρατηρήσαμε ότι τόσο η φυσική HDL (tgHDL) όσο και η ανασυσταθείσα HDL (rHDL-AI) ενεργοποιούν την έκφραση της *ANGPTL4*. Για την ανίχνευση των μηχανισμών μέσω του οποίου η tgHDL ενεργοποιεί το συγκεκριμένο γονίδιο χρησιμοποιήσαμε γνωστούς αναστολείς κινασών και παρατηρήσαμε ότι η δράση της tgHDL γίνεται μέσω των μονοπατιών της AKT και της p38-MAPK. Επιπρόσθετα, με πειράματα διαχωρισμού πυρηνικών από κυτταροπλασματικές πρωτεΐνες και ανοσοϊστοχημείας,

παρατηρήσαμε ότι η tgHDL έχει την ικανότητα, μέσω του μονοπατιού της ΑΚΤ, να επάγει την φωσφορυλίωση του πυρηνικού μεταγραφικού παράγοντα Forkhead Box O1 (FOXO1) με αποτέλεσμα την μετατόπισή του στο κυτταρόπλασμα και την απενεργοποίηση της μεταγραφικής του δράσης. Συνδυάζοντας διαφορετικές πειραματικές προσεγγίσεις για την απενεργοποίηση του FOXO1 στα ενδοθηλιακά κύτταρα με παράλληλη επίδραση ή όχι της tgHDL, είδαμε ότι ο FOXO1 έχει ανασταλτικό ρόλο στην ενεργοποίηση του γονιδίου της *ANGPTL4*, όπου η απενεργοποίηση του από την HDL οδηγεί σε καταστολή της έκφρασης της *ANGPTL4*.

Στην ενότητα ΙΙ επικεντρωθήκαμε στην ρύθμιση του γονιδίου της ενδοθηλιακής λιπάσης (LIPG), η οποία εμπλέκεται στον καταβολισμό της HDL. Αρχικά παρατηρήσαμε ότι η φυσική HDL (tgHDL) μείωνε την έκφραση της LIPG σε αντίθεση με την rHDL-AI που την αύξανε. Επικεντρωθήκαμε στην δράση της tgHDL και διαπιστώσαμε ότι όχι απλά μείωνε την έκφραση της LIPG αλλά εμπόδιζε την ενεργοποίηση του γονιδίου σε συνθήκες έλλειψης θρεπτικού ορού (starvation). Πειράματα αποσιώπησης της έκφρασης του FOXO1 με siRNAs οδήγησαν σε μείωση των επιπέδων της LIPG, αναδεικνύοντας ότι ο FOXO1 είναι σημαντικός για την ενεργοποίηση του συγκεκριμένου γονιδίου από το starvation αλλά και ότι η HDL μειώνει την έκφραση της LIPG μέσω της απενεργοποίησης του FOXO1. Επιπρόσθετα της δράσης του FOXO1, παρατηρήσαμε ότι η HDL εμποδίζει την έκφραση ενός επιπλέον γονιδίου ώστε να αναστείλει την ενεργοποίηση της LIPG από το starvation.

Στην ενότητα ΙΙΙ διερευνήσαμε την λειτουργικότητα της HDL που έχει απομονωθεί από ασθενείς με αγκυλοποιητική σπονδυλίτιδα (ΑΣ), μια χρόνια φλεγμονώδη νόσο. Παρατηρήσαμε ότι η HDL που είχε απομονωθεί από υγιή άτομα είχε την ικανότητα να φωσφορυλιώνει την κινάση ΑΚΤ ενώ αντίθετα, η HDL που απομονώθηκε από ασθενείς με ΑΣ οδήγησε σε μειωμένη φωσφορυλίωση της ΑΚΤ στα ενδοθηλιακά κύτταρα υποδεικνύοντας την παρουσία μη-λειτουργικής HDL στους ασθενείς αυτούς.

Παρότι η HDL συγκροτείται εξωκυττάρια, το ήπαρ αποτελεί την κύρια πηγή παραγωγής των πρωτεϊνών που εμπλέκονται στη βιογένεση της HDL. Για αυτό τον λόγο, στο **Κεφάλαιο 2** χρησιμοποιήσαμε κύτταρα ανθρώπινου ηπατοβλαστώματος HepG2 ώστε να μελετήσουμε τους μηχανισμούς ρύθμισης της έκφρασης γονιδίων που συμμετέχουν στον μεταβολισμό της HDL.

Στην ενότητα IV μελετήσαμε τον μηχανισμό με τον οποίο ρυθμίζεται στο ήπαρ το γονίδιο του μεταγραφικού παράγοντα LXRα. Ο LXRα (Liver X Receptor α) διαδραματίζει σημαντικό ρόλο στο μεταβολισμό των λιπιδίων και της χοληστερόλης, διότι ελέγχει άμεσα την έκφραση των γονιδίων που εμπλέκονται σε αυτά τα μονοπάτια (για παράδειγμα των ABCA1, ABCG1, SREBP κλπ). Παρατηρήσαμε ότι ο υποκινητής του γονιδίου του LXRα του ανθρώπου (hLXRα) ενεργοποιείται από την δράση του HNF-4α, ο οποίος είναι ένας μεταγραφικός παράγοντας που εκφράζεται κυρίως στο ήπαρ και αποτελεί γενικό ρυθμιστή των γονίδιων που ενεργοποιούνται στο ήπαρ. Με πειράματα ChiP και DNAP εντοπίσαμε το σημείο πρόσδεσης του HNF-4α στον υποκινητή του LXRα στην περιοχή -50 με -40. Μετάλλαξη στο συγκεκριμένο μοτίβο πρόσδεσης οδήγησε σε απώλεια της ικανότητας του HNF-4α να ρυθμίζει θετικά την ενεργότητα του υποκινητή του LXRα. Αποσιώπηση του γονιδίου του HNF-4α οδήγησε σε μείωση των επιπέδων της πρωτεΐνης LXRα.

Στην ενότητα V μελετήσαμε την ικανότητα του micro-RNA let-7b να ρυθμίζει την έκφραση του γονιδίου της απολιποπρωτεΐνης Ε (apoE) σε HepG2 κύτταρα. Η αποΕ παίζει σημαντικό ρόλο στην απομάκρυνση των υπολειμμάτων των λιποπρωτεϊνών από την κυκλοφορία αλλά και στην βιογένεση της HDL. Υπερέκφραση του let-7b προκάλεσε μείωση των επιπέδων τόσο του mRNA όσο και της πρωτεΐνης της apoE. Ωστόσο, η υπερέκφραση του let-7b δεν επηρέασε την ενεργότητα ενός πλασμιδίου που είχε κλωνοποιημένη την 3'-UTR περιοχή του mRNA της αποΕ υποδηλώνοντας ότι το let-7b δεν ρυθμίζει άμεσα, μέσω της 3'-UTR περιοχής, την έκφραση της apoE. Επιπρόσθετα, σε πειράματα όπου συνεκφράσαμε τον υποκινητή της apoE (-500/+73) με το let-7b είδαμε την ενεργότητα του υποκινητή να μειώνεται επιβεβαιώνοντας τον έμμεσο τρόπο ρύθμισης αυτού του γονιδίου

από το let-7b. Παράλληλα, διαπιστώσαμε την ικανότητα του let-7b να ρυθμίζει την έκφραση και της αποA-I, η οποία είναι η κύρια πρωτεΐνη της HDL. Παρατηρήσαμε ότι υπερέκφραση του let-7b μείωσε τόσο το mRNA της αποA-I όσο και την ενεργότητα του υποκινητή (-1020/-24) της. Βιοπληροφορική ανάλυση στο mRNA της αποA-I δεν ανέδειξε κάποιο σημείο πρόσδεσης του let-7b προτείνοντας ότι η αποA-I, όπως και η αποE, ρυθμίζονται με διαφορετικό από τον κλασσικό τρόπο από το let-7b.

Συμπερασματικά, τα ευρήματα της παρούσας διατριβής προσφέρουν νέα γνώση πάνω στους μηχανισμούς που ελέγχουν τα επίπεδα και την λειτουργικότητα της HDL. Τα γονίδια που βρέθηκαν στην παρούσα μελέτη να μεσολαβούν στις δράσεις της HDL στα ενδοθηλιακά και στα ηπατικά κύτταρα θα μπορούσαν να έχουν διαγνωστική και θεραπευτική αξία σε ασθενείς με χαμηλά επίπεδα HDL ή με μη-λειτουργική HDL όπως ασθενείς με Καρδιαγγειακά Νοσήματα ή χρόνια φλεγμονώδη νοσήματα.

Abstract

Numerous epidemiological studies have shown that low levels of High Density Lipoprotein Cholesterol (HDL-C) in the serum are a strong and independent risk factor for the development of Cardiovascular Diseases (CVDs). Furthermore, a great number of reports have revealed that HDL exerts pleiotropic functions protecting against the development of atherosclerosis, which is the leading cause of CVDs. However, drugs that were designed to increase HDL-C failed to counteract CVD risk in human clinical studies. In addition, recent studies showed that HDL isolated from patients with CVDs is “dysfunctional” and it is unable to exert its known anti-atherosclerotic functions. These findings indicate that only by raising HDL-C levels is not sufficient for atheroprotection, but it must be accompanied by the presence of functional HDL. Also, it should be mentioned that some drugs aiming to raise HDL-C levels caused significant side-effects, highlighting the complexity of the metabolic pathways as well as their poor understanding.

The main goals of this PhD thesis were:

- **Chapter 1:** To investigate the molecular mechanisms underlying the atheroprotective roles of HDL in the endothelium. For this purpose, in *parts I and II*, we focused on identifying genes targeted by HDL in endothelial cells as well as the mechanisms through which HDL regulates their expression, while in *part III* we studied the functionality of HDL isolated from patients with a chronic inflammatory disease (Ankylosing Spondylitis, AS).
- **Chapter 2:** To identify novel transcription factors and miRNAs in the liver that control the expression of genes involved in the biogenesis of HDL. In *part IV* we studied the regulation of the transcription factor LXRα by the master hepatic transcription factor HNF-4α, while in *part V* we studied the role of the miRNA let-7b in the regulation of the expression of *apolipoprotein E* (*apoE*) gene.

Endothelium injury or 'dysfunctional' endothelium has been associated with the initiation and the progression of the atherosclerotic plaque. HDL not only is a positive regulator of the physiological function of endothelium, but also protects endothelium against injury, while dysfunctional HDL is unable to promote these actions. For this purpose, in **Chapter 1**, we wanted to elucidate the molecular mechanisms underlying HDL functionality in endothelium. The genes that we focused on in the first two parts were derived from microarray data, which had been generated previously by our research group following the treatment of endothelial cells with reconstituted HDL containing the human apolipoprotein A-I (rHDL-AI). We studied the expression of these genes after treatment with natural HDL, which was isolated from transgenic mice expressing the human apoA-I gene (tgHDL).

Specifically, in part I we studied the regulation of the Angiopoietin-like 4 (ANGPTL4) gene, which plays an important role in lipid metabolism and atherosclerosis. We observed that both natural HDL (tgHDL) and reconstituted HDL (rHDL-AI) were able to induce the expression of *ANGPTL4*. To investigate the molecular mechanisms through which tgHDL activates the expression of this gene, we utilized known inhibitors for signaling cascades and we observed that both the AKT and the p38-MAPK pathways are involved in this regulatory effect of tgHDL. Furthermore, by utilizing the separation of nuclear from cytoplasmic protein extracts technique as well as immunofluorescence, we revealed that tgHDL, through the AKT pathway, promotes the phosphorylation of the nuclear transcription factor Forkhead Box O1 (FOXO1) resulting in its translocation to the cytoplasm and, subsequently, its inactivation. By combining different experimental approaches to inactivate FOXO1 in endothelial cells followed by treatment with tgHDL, we identified that FOXO1 suppresses the expression of *ANGPTL4*, while the FOXO1-mediated inactivation by HDL results in the induction of *ANGPTL4*.

In part II, we focused on the expression of the endothelial lipase (LIPG) gene, which mediates HDL catabolism. Initially, we observed that natural HDL (tgHDL) inhibited the expression of *LIPG* in contrast to reconstituted HDL (rHDL-AI) which induced its expression. We focused on the effect of tgHDL and we found that not only tgHDL inhibited the expression of LIPG but also prevented the induction of *LIPG* by growth deprivation (starvation). Silencing the expression of FOXO1 by utilizing a specific siRNA led to reduction of the LIPG mRNA levels indicating that FOXO1 is an important transcriptional activator of this gene in starvation conditions. TgHDL, by promoting FOXO1 transcriptional inactivation, inhibits *LIPG* expression. In addition to FOXO1 inactivation, tgHDL may inhibit the expression of an additional gene – still uncharacterized- in order to prevent LIPG-mediated induction by starvation.

In part III we studied the functionality of HDL isolated from patients with Ankylosing Spondylitis (AS), a chronic inflammatory disease. We reported that HDL isolated from healthy people was able to phosphorylate AKT kinase, while HDL isolated from patients with AS showed reduced AKT phosphorylation indicating the existence of dysfunctional HDL in AS patients.

Although HDL is synthesized extracellularly, liver is the main source of proteins participating in HDL biogenesis. Therefore, in **Chapter 2** we used the human liver cell line, HepG2, in order to identify the mechanisms underlying the expression of genes involved in HDL metabolism.

In part IV we studied the regulation of the transcription factor LXRα in the liver. LXRα (Liver X Receptor α) is a key regulator of lipid and cholesterol metabolism by controlling directly the expression of genes participating in these pathways (for instance ABCA1, ABCG1, SREBP etc.). We observed that the promoter of human LXRα gene (hLXRa) is activated by HNF-4α, a transcription factor expressed in the liver which regulates the expression of several liver-specific genes. By performing ChiP and DNAP analysis, we

identified the binding site of HNF4a in the proximal region of the hLXRa promoter and specifically in the region from -50 to -40. Disruption of this site in the hLXRα promoter with site-specific mutagenesis abolished the transactivation by HNF-4α. Moreover, silencing of HNF-4α in HepG2 resulted in reduction of LXRα protein levels.

In part V, we studied the ability of the micro-RNA let-7b to regulate the expression of apolipoprotein E (apoE) gene in HepG2 cells. ApoE is a crucial apolipoprotein since it not only mediates the clearance of triglyceride-rich lipoproteins from the circulation, but also participates in the biogenesis of HDL. Overexpression of let-7b in HepG2 caused a reduction in both mRNA and protein levels of apoE. However, let-7b overexpression did not affect the luciferase activity of a plasmid containing the 3'-UTR region of the mRNA of apoE. This observation indicates that let-7b does not regulate directly, though the 3'-UTR region, the expression of *apoE*. Furthermore, co-expression of a plasmid containing the (-500/+73) promoter of apoE with let-7b led to reduced luciferase activation confirming the indirect effect of let-7b in the regulation of *apoE* expression. Interestingly, we identified that let-7b also regulates the expression of apoA-I, the main protein of HDL. We found that let-7b overexpression resulted in a reduction of the mRNA levels of apoA-I as well as in the luciferase activity of a plasmid containing the (-1020/-24)-apoA-I promoter. Bioinformatic analysis in the mRNA region of the human apoA-I gene did not reveal any putative let-7b binding sites suggesting that apoA-I, similar to apoE, is regulated by let-7b independently of the 3'-UTR region.

In conclusion, the findings from this PhD thesis provide new insights into the mechanisms that control HDL serum levels as well as its functionality. Genes found in the present study to mediate HDL functions in endothelial and liver cells may be of great diagnostic and/or therapeutic value in patients with low HDL or dysfunctional HDL such as patients with CVDs or chronic inflammatory diseases.

1. INTRODUCTION

1.1 Atherosclerosis

1.1.1 Cardiovascular Diseases

Cardiovascular diseases (CVDs) refer to a group of disorders affecting the heart and blood vessels such as the coronary artery disease, the cerebrovascular disease, heart failure and cardiomyopathies and are the major cause of mortality globally. According to the Global Burden of Disease (GBD), in 2017 CVDs had an estimated global prevalence of 73 million people, causing nearly 18 million deaths representing the 31% of all global deaths (1). In Europe, an epidemiological study in 2016 showed that CVD deaths account for 45% of all deaths (2). The pathophysiological cause of CVDs is atherosclerosis which is characterized by the gradual thickening of the arterial wall as a result of lipid accumulation and chronic inflammation. Both environmental and genetic factors, as well as the interplay between them, are implicated in the pathogenesis of atherosclerosis and subsequently to CVDs (3). Many clinical studies have shown that age, cigarette smoking, physical inactivity, hypertension and obesity lead to an increased risk of presenting CVDs. Similarly, dyslipidemias and especially high levels of LDL-cholesterol and low levels of HDL-cholesterol in the plasma are considered as high risk factors for CVDs, since they play a crucial role for both the initiation and the development of atherosclerosis (4).

1.1.2 The pathogenesis of Atherosclerosis

Atherosclerosis is a pathological disorder of the large and medium-sized arteries (5) driven by two underlying processes: a build-up of lipid deposit in the wall of arteries followed by a strong inflammatory response against it. The interplay between these two processes leads to the formation of the atherosclerotic plaque which gradually becomes thicker resulting in the narrowing of the artery lumen. Consequently, the amount of blood supplied to the organs is reduced, most commonly affecting the heart and the brain. Plaques can

abruptly rupture, causing blood clots and often a heart attack or stroke (6). It has been shown that atherosclerosis starts at a young age, indicating that it progresses slowly and silently over decades before it results in cardiovascular events (7).

A plethora of factors including lipids (mainly cholesterol), lipid transporters (primarily LDL which transfers cholesterol from liver to peripheral tissues) and cells (endothelial cells, leukocytes and smooth muscle cells) are involved in the development of the atherosclerotic plaque (5) which can be divided into three stages: initial lesion, fatty streak and complex lesion (8) (Fig. 1.1).

Initial lesion: Circulating LDL enters the sub-endothelium layer (intima) either through passive diffusion or through transcytosis via SR-BI-DOCK4 mechanism (9). There, LDL is trapped by proteoglycans which are expressed in the surface of endothelial cells (10). The trapped LDL undergoes a plethora of modifications, mainly oxidation, resulting in the formation of oxidized LDL particles (oxLDL) (11). Then, these oxLDL particles stimulate endothelial cells to express adhesion molecules including vascular cell adhesion molecule-1 (VCAM-1) and intercellular adhesion molecule-1 (ICAM-1) and various chemokines such as the monocyte chemoattractant protein-1 (MCP-1) and Interleukin 8 (IL-8). This leads to monocyte recruitment, adhesion, and transmigration into the intima followed by their differentiation to macrophages (12).

Fatty streak: In the arterial wall, macrophages engulf the oxLDL particles through the scavenger receptors CD-36, SR-A and LOX-1. However, macrophages cannot further catabolize oxLDL resulting in the accumulation of these particles and the formation of cholesterol-laden macrophages called foam cells. In turn, foam cells secrete proinflammatory cytokines to recruit additional monocytes, as well as T cells to the vascular endothelium (12). Interestingly, it has been shown that ox-LDL, by interacting with the monocytes, provokes epigenetic histone modifications leading to increased production of proinflammatory cytokines and foam cell formation (13). The accumulated foam cells begin

to undergo apoptosis and necrosis, resulting in the release of cellular debris and cholesterol crystals into the intima of the arteries (14).

Complex lesion: The apoptotic cells and the fatty contents accumulate to form a lipid-rich necrotic core (14). While the inflammatory response is maintained with the accumulation of both T and B cells (12), foam cells regulate the migration and the proliferation of vascular smooth muscle cells (VSMC) in the intima. VSMCs secrete large amounts of extracellular-matrix components (ECM), such as collagen, resulting in the formation of a fibrous cap over the lipid core stabilizing the plaque (15). Complex mechanisms triggered by the inflammatory response, including the inhibition of collagen production by VSMCs, could result in an unstable lesion that can rupture and lead to thrombosis (16).

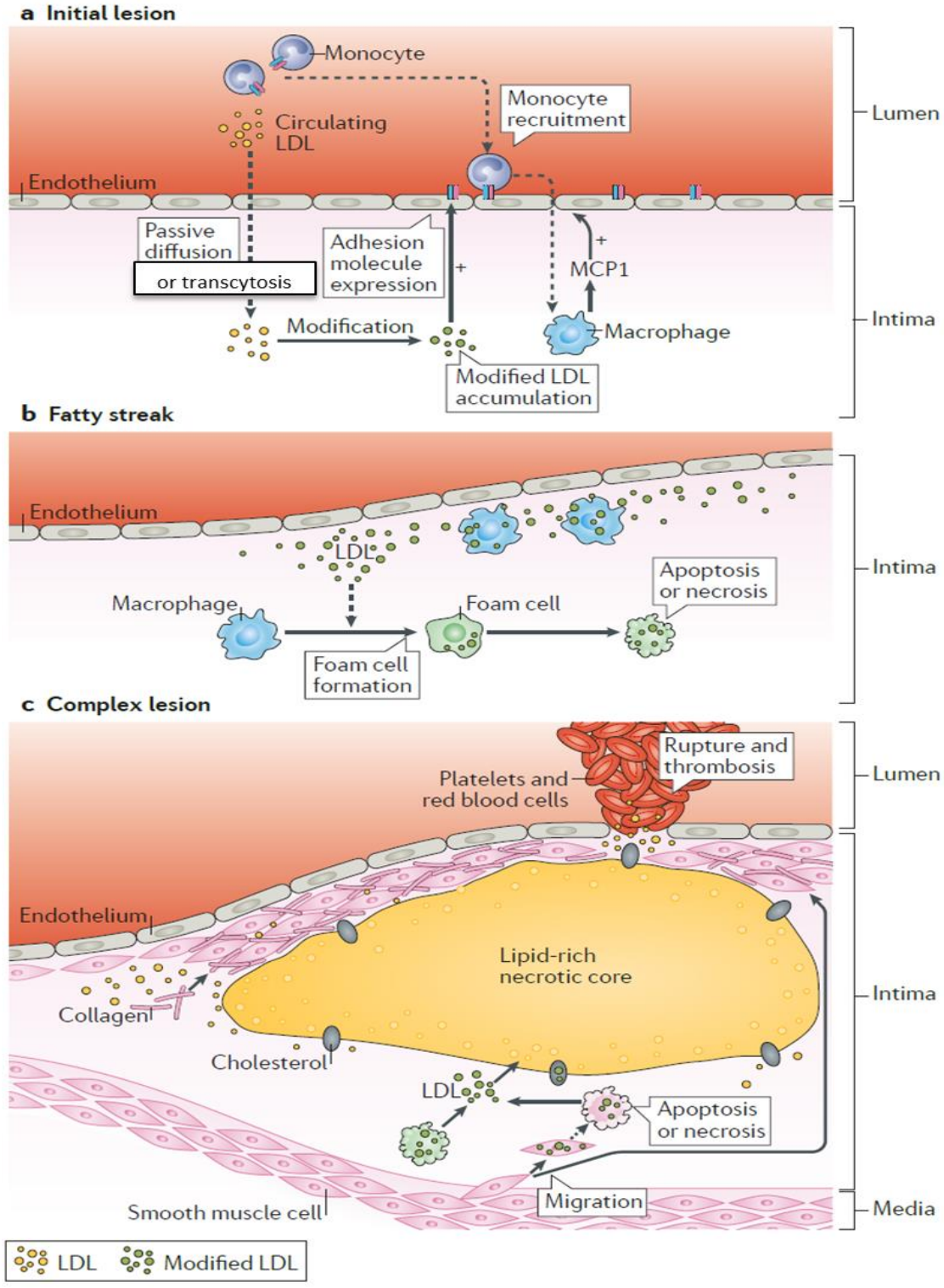

Figure 1.1 The stages of atherosclerotic plaque formation (8)

1.1.3 The role of endothelial dysfunction in atherosclerosis

Endothelium is a single layer of endothelial cells that covers the inner surface of blood arteries forming a selectively permeable barrier between circulating blood and the arterial wall. Besides its function as a barrier, endothelium synthesizes and secretes a wide range of biologically active mediators (vasodilators, extracellular matrix proteins, growth factors, cytokines) affecting different aspects of vascular biology (17). The secretory ability of endothelial cells is under the regulation of a plethora of stimuli such as physical forces (sheer stress), lipoproteins, hormones, platelet products, and cytokines (18). Alterations in the endothelial function because of pathophysiological stimuli precede the formation of plaque lesion contributing to the initiation and the maintenance of atherosclerosis (17).

In healthy conditions, endothelium controls vascular tone, blocks leukocyte adhesion and migration, inhibits platelet activation and thrombosis and suppresses SMCs proliferation (19). It is noteworthy that these effects are mediated mainly by the vasodilator molecule nitric oxide (NO). NO is produced by the endothelial isoform of NO synthase (eNOS) during the conversion of L-arginine to L-citrulline and is then diffused through the endothelial plasma membrane to the neighboring cells (Fig. 1.2) (17). NO functions mainly through two different mechanisms: a) by the activation of the soluble guanylate cyclase in the adjacent VSMCs leading to a profound increase in intracellular cGMP and thus resulting in their relaxation and vasodilation; and b) by promoting the s-nitrosylation of cysteine residues in a wide range of proteins (the transcription factor NF-κB, cell cycle controlling proteins, proteins involved in generation of tissue factor), resulting in their inactivation (20).

Besides NO production, endothelial cells exhibit also anticoagulant and fibrinolytic properties by releasing additional mediators including prostacyclin (PGI_2), heparin-like molecules, thrombomodulin and the tissue plasminogen activator, as well as by providing a luminal surface (21). It should be mentioned that the structural and functional integrity of endothelium is regulated by complex cell-cell junctions such as adherens junctions, gap junctions and desmosomes (22).

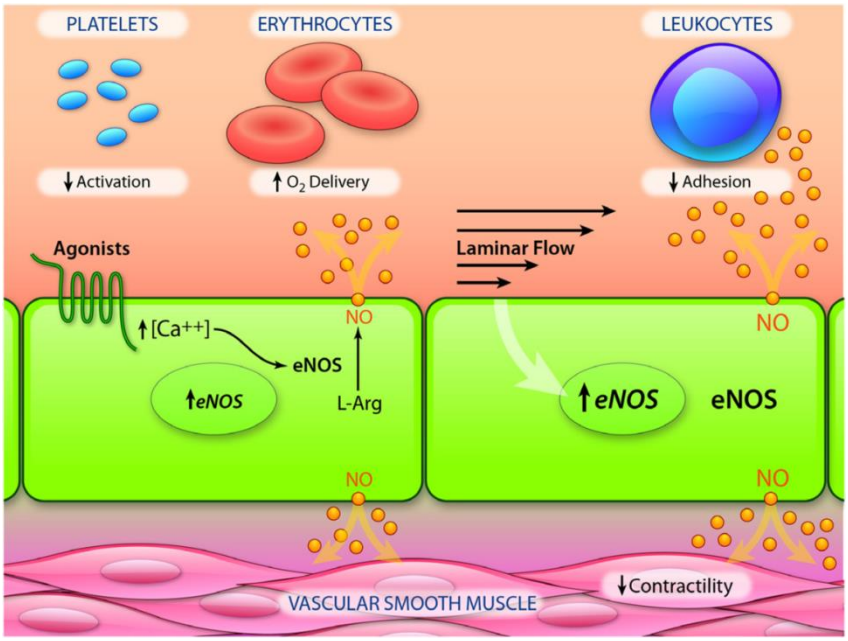

Figure 1.2 The production and the biological actions of endothelial NO (17).

In the pathogenic state of atherosclerosis, the endothelial phenotype changes to a proinflammatory and prothrombotic state, a process referred to as *endothelial dysfunction* or *endothelial activation* (23). Critical step for the development of endothelial dysfunction is the loss of endothelial integrity (endothelial injury) which leads to the entry and the accumulation of LDL particles in the arterial wall (19). Numerous proatherogenic factors such as disturbed blood flow (17), hypercholesterolemia, obesity and hypertriglyceridemia have been determined to promote endothelial cell injury (24).

As was described above, the trapped LDL particles in the intima are oxidized and play a crucial role for the development of endothelial dysfunction. On the one hand, oxLDL, either by inhibiting eNOS activation or by enhancing NO degradation, prevents the production of NO and subsequently its protective effects (Fig. 1.3) (25). On the other hand, oxLDL orchestrates the endothelial inflammatory response by inducing the activation of NF-κB resulting in the overexpression of NADPH oxidase 1 (NOX-1), vascular cell adhesion molecule 1 (VCAM-1), intercellular adhesion molecule 1 (ICAM-1), monocyte chemoattractant protein 1 (MCP-1), and other chemokines (Fig. 1.3) (17). As a result of

these responses, the endothelium permeability is impaired, reactive oxygen species (ROS) are generated and the adherence and migration of monocytes is augmented. ROS and cytokines produced by the monocytes also contribute to both the reduction of NO and the inflammatory response (26).

Injury of the endothelium also triggers thrombotic response by both releasing thromboxane A2 (TxA2) which promotes platelet aggregation, and expressing adhesive co-factors for platelets such as von Willebrand factor and fibronectin (27). In parallel, the expression of antithrombotic substances is decreased. Moreover, activated endothelial cells can express both the tissue factor, which activates the fibrin-generating coagulation cascade (21) and the plasminogen activator inibitor-1 (PAI-1) which inhibits the fibrinolytic pathway (28). These effects facilitate the process of thrombosis, causing devastating consequences.

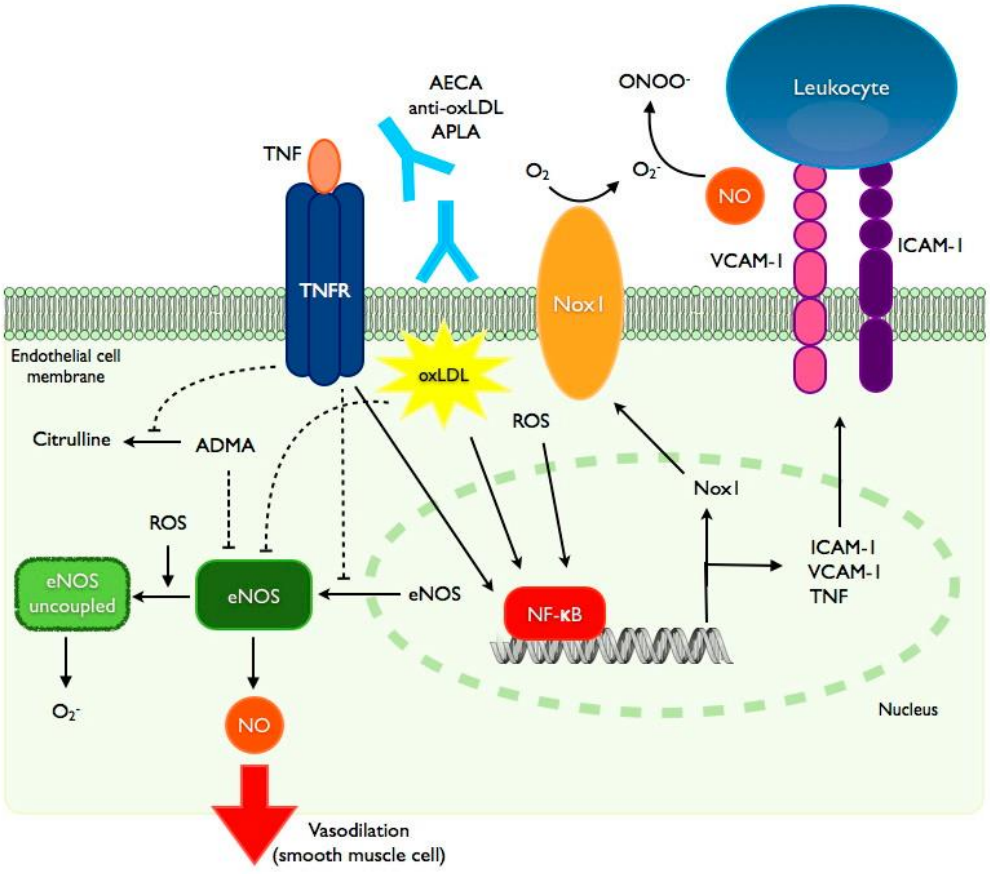

Figure 1.3 Mediators inducing inflammatory response in the endothelial cells (26)

1.2 Lipoproteins

1.2.1 The biological role of lipoproteins

Lipoproteins are complex particles of lipids and proteins that serve as vehicles for lipid transport throughout the body to tissues where they are required. Lipoproteins consist of non-polar lipids (including cholesterol esters (CE) and triglycerides (TG)), amphipathic lipids (including free cholesterol (FC) and phospholipids (PL)) and proteins (apolipoproteins) such as apoA-I, apoA-II, apoB, apoC-II, apoC-III, apoE and apoM (29, 30). The basic structure of lipoproteins is the spherical one in which the non-polar lipids are in the core of the molecule surrounded by a single membrane layer of amphipathic lipids. Apolipoproteins are also enclosed in the membrane, both stabilizing the complex and providing its functional specificity (31, 32).

The composition and the ratio of lipids to proteins within each lipoprotein molecule determine its size and density. In general, the size of each particle is inversely related to its density. Based on their density, lipoproteins are classified into five groups (lower to higher density): chylomicrons, very low density lipoproteins (VLDL), intermediate-density lipoproteins (IDL), low-density lipoproteins (LDL), and high-density lipoproteins (HDL) (33). Lipoproteins of each group consist of characteristic apolipoproteins and have distinctive lipid compositions (Table 1.1).

	Chylomicrons	VLDL	IDL	LDL	HDL
Density (g/ml)	<0.94	0.94-1.006	1.006-1.019	1.019-1.063	1.063-1.21
Diameter. (nm)	75-1200	30-80	25-50	18-30	5-12
		Components			
Protein (%)	1-2	6-10	18	18-20	45-55
FC (%)	1-3	4-8	29	6-8	3-5
CE (%)	2-4	16-22	32-35	45-50	15-20
PL (%)	3-6	15-20	22	18-24	26-32
TG (%)	80-95	45-65	31	4-8	2-7

Table 1.1 Lipoprotein classification, lipid and protein content (modified from(32))

1.2.2 Pathways of lipoprotein metabolism

The successful transfer of lipids and their subsequent distribution into the body is achieved by sequential rounds of biosynthesis and catabolism of lipoproteins. Several proteins including apolipoproteins, plasma enzymes, lipoprotein receptors and lipid transporters are involved in these processes. The metabolism of lipoproteins is performed through three distinct but interrelated pathways: the chylomicron pathway, the VLDL/IDL/LDL pathway and the HDL pathway.

Chylomicrons pathway: through this pathway the dietary lipids are absorbed by the small intestine and are available for the rest of the tissues. Briefly, dietary free fatty acids and cholesterol are transferred through different pathways to the endoplasmic reticulum of enterocytes and undergo modifications resulting in the formation of triglycerides and cholesterol esters respectively. Then, these lipids interact with apolipoprotein B-48 (apoB-48) producing chylomicrons, which in turn are secreted into the circulation. In the circulation, the enzyme lipoprotein lipase (LPL) catalyzes the triglyceride component of chylomicrons

releasing free fatty acids which now can be absorbed by peripheral tissues. The chylomicron remnants are subsequently taken up by the liver (34).

VLDL/IDL/LDL pathway: through this pathway the lipids synthesized by the liver are transferred to peripheral tissues. The newly synthesized triglycerides and cholesterol, as well as the triglycerides from chylomicrons, interact with apolipoprotein-B100 (apoB-100) resulting in the formation of VLDL particles which in turn are secreted into the circulation. VLDL particles are also triglyceride-rich but they have a higher ratio of cholesterol to triglycerides compared to chylomicrons. As with chylomicrons, the triglycerides of VLDL are hydrolyzed by LPL in the circulation releasing free fatty acids and converting VLDL to IDL particles. The triglycerides of IDL are further hydrolyzed by hepatic lipase (HL) resulting in the formation of the cholesterol-rich LDL particles. LDL is responsible for the transfer of cholesterol to peripheral cells. Both IDL and LDL particles are taken up by the liver via the LDL receptor ffor further catabolism (35).

HDL pathway: through this pathway excess lipids from peripheral tissues are transferred back to the liver. HDL is synthesized extracellularly through a complex pathway in which many proteins such plasma enzymes and lipoprotein receptors are participating. HDL is enriched with cholesterol and phospholipids, while the main apolipoprotein of HDL is apolipoprotein-AI (apoA-I) which is produced and secreted by the liver and the intestine. HDL particles promote the efflux of cholesterol from peripheral cells and its transfer back to the liver, a process referred to as the Reverse Cholesterol Transport (RCT). Additionally, HDL is implicated in the transport of triglycerides and phospholipids, while additional functions of HDL, such as the anti-inflammatory and anti-oxidative properties, have been described (36). In the following chapters, we will discuss in detail HDL metabolism and its functions.

1.3 The Metabolic Pathway of HDL

1.3.1 HDL structure

HDL comprises a heterogeneous group of macromolecules which differ in composition, structure and functionality. The main apolipoprotein component of HDL is apoA-I, representing ~ 70% of the total protein in HDL and plays a key role in the biogenesis, structure stability and function of HDL (37). However, additional apolipoproteins have been identified to bind to HDL particles including apoA-II, apoA-IV, apoC-III, apoE, apoM and apoJ.

In the plasma, HDL particles are found either in discoidal or in spherical structures (Fig. 1.4). Discoid HDL particles are small and lipid-poor representing the pre-mature forms of HDL and consisting of phospholipids, free cholsterol and apoA-I in a bilayer conformation (38). On the other hand, the spherical HDL particles are larger consisting of a hydrophobic core of cholesterol esters and triglycerides surrounded by the polar lipids and apoA-I (38). In healthy conditions, the spherical type is the most abundant type of HDL in the circulation.

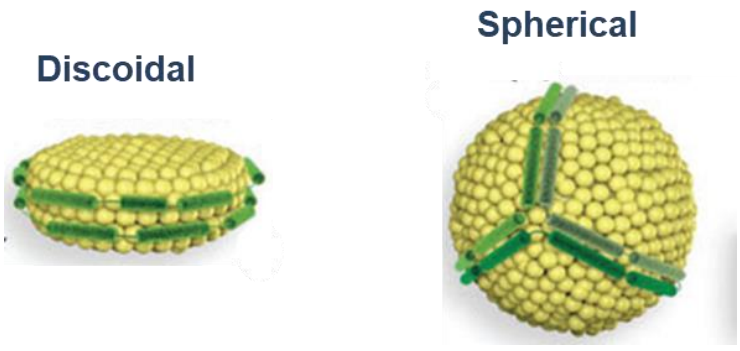

Figure 1.4 The discoidal and the spherical type of HDL particles.

1.3.2 HDL biogenesis/remodeling/catabolism

The pathways of biogenesis, remodeling and catabolism of HDL are complex in which a variety of membrane-bound and plasma proteins are involved (39). These pathways are depicted in Fig. 1.5 and briefly described below:

Biogenesis: The initial step for HDL biogenesis is the synthesis and the secretion of apoA-I by the liver and the intestine (40). Lipid-free apoA-I interacts with the transmembrane lipid transporter ATP Binding Cassette Transporter A1 (ABCA1) promoting the transfer of cellular phospholipids and cholesterol generating the lipid-poor apoA-I particles (41). These particles are further lipidated via interaction with ABCA1 from peripheral cells resulting in the formation of the discoidal β-HDL particles. These particles are enriched with unesterified cholesterol representing the pre-mature type of HDL. In the presence of the enzyme lecithin:cholesterol acyl transferase (LCAT), these discoidal particles are converted to spherical ones (maturation) (39). Specifically, LCAT catalyzes the esterification of free cholesterol with a fatty acid derived from lecithin thus forming the hydrophobic cholesterol esters, which in turn are inserted into the non-polar core of the particle creating the spherical type of HDL (42). The spherical type is the most abundant type in the blood circulation of healthy people. It should be mentioned that apoE and apoA-IV can also interact with the above mediators and participate in the biogenesis of HDL (43, 44).

Remodeling: In the circulation, the newly synthesized spherical HDL particles are in a continuous process of remodeling. Specifically, spherical HDL also promotes the efflux of cellular cholesterol by interacting with the lipid transporter ABCG1 (45). Additionally, phospholipids are transferred from VLDL/LDL particles to HDL by the action of the phospholipid transfer protein (PLTP) (46). Both of these processes lead to the generation of larger HDL particles. On the other hand, a variety of mechanisms are implicated in the formation of smaller HDL or even lipid-poor apoA-I particles, which in turn can initiate a new cycle of maturation and remodeling. Specifically, HDL by interacting with the scavenger receptor class B type I (SR-BI) mediates the selective uptake of cholesterol esters by the

cells (47). It should mentioned that in some cases SR-BI can promote the efflux to HDL (47). Moreover, cholesterol esters are transferred from HDL to VLDL/LDL particles by cholesterol ester transfer protein (CETP) (48). Finally, the hydrolysis of phospholipids and residual triglycerides of HDL is mediated by endothelial lipase and hepatic lipase respectively (49).

Catabolism: HDL transfers cholesterol esters back to the liver either through the VLDL/LDL pathway or through the selective CE uptake via the hepatic SR-BI. Then, cholesterol is secreted into the bile via the ABCG5/G8 transporters and then to feces for final removal from the body (39). Besides the removal of CE, the whole particle of HDL can be removed from the plasma for further degradation through two different mechanisms. The first one is the endocytosis of HDL holoparticle by the liver via the synergistic action of the ecto-F1-ATPase and P2Y13 receptors (50). The second one refers to the lipid-poor apoAI particles which are removed from the kidney by binding to cubilin/megalin receptors (39).

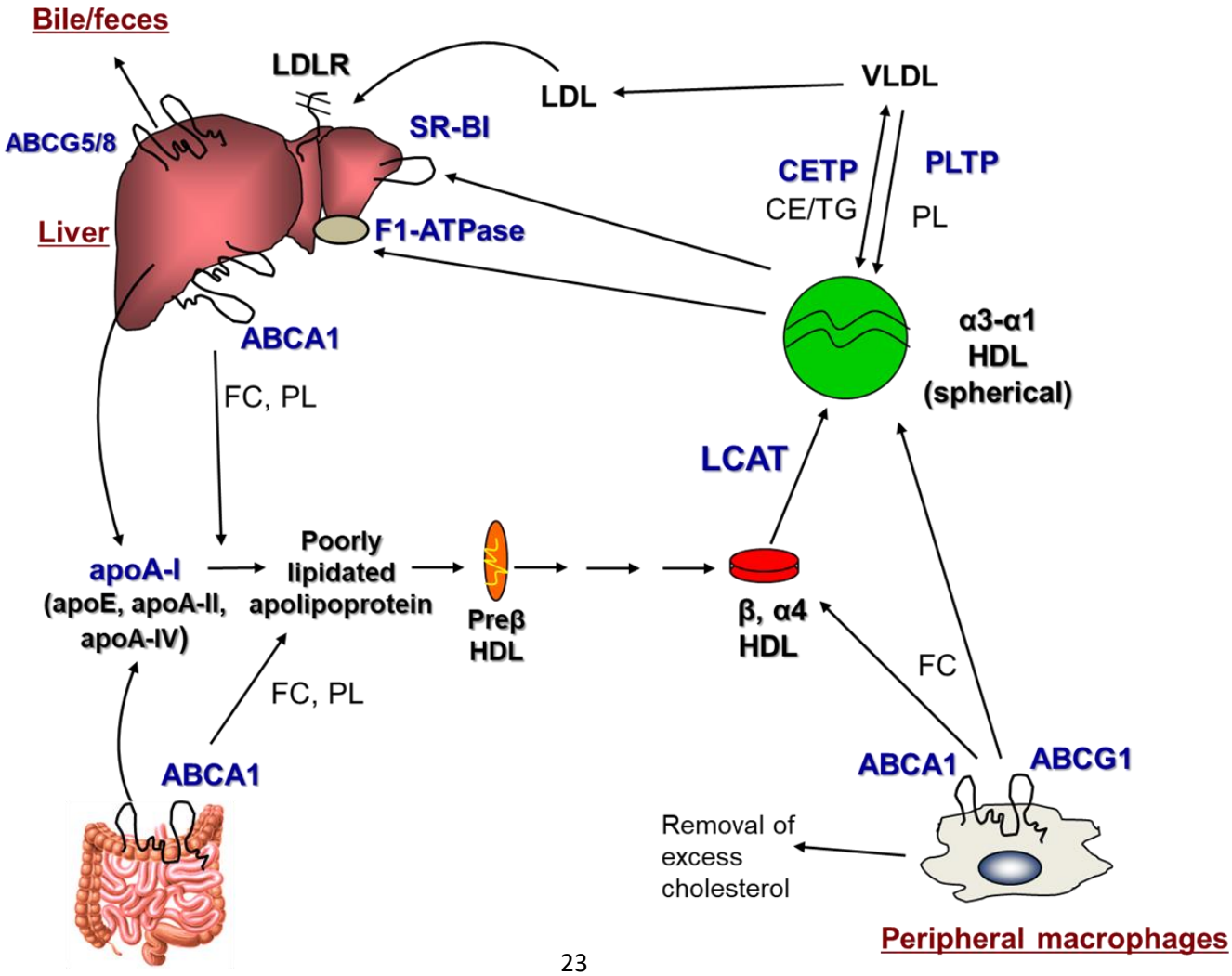

Figure 1.5 Schematic representation of the metabolic pathway of HDL (modified (51)).

1.3.3 HDL subpopulations

A consequence of the continuous remodeling of HDL particles is the generation of a variety of HDL subpopulations which differ in density, size, lipid and protein composition, and surface charge. Several methods have been developed in order to subfractionate HDL particles (52).

Using ultracentrifugation, HDL particles are separated on the basis of their density into two major subfractions: HDL2 (1.063-1.125 g/ml) and HDL3 (1.125-1.21 g/ml) (Fig. 1.6A) (53). To separate HDL particles depending on their size two distinct methods have been developed. The classical one is by utilizing non-denaturing polyacrylamide gradient gel electrophoresis (GGE) in which HDL particles are separated into five distinct subpopulations: HDL2b (~10.6 nm), HDL2a (~9.2 nm), HDL3a (~8.4 nm), HDL3b (~8.0 nm), HDL3c (~7.6 nm) (Fig. 1.6 A, B) (54). The most recent one is by utilizing the nuclear magnetic resonance (NMR) in which three HDL subclasses can be identified: large HDL (8.8–13.0 nm diameter), medium HDL (8.2–8.8 nm) and small HDL (7.3–8.2 nm) (55).

Utilizing immunoaffinity-based methods, HDL particles are classified depending on their apolipoprotein composition into two major subpopulations: HDL containing apoA-I (LpAI) or HDL containing both apoA-I and apoA-II (LpA-I:A-II) (56).

Based on surface charge, HDL can be separated by agarose gel electrophoresis into three subpopulations (α-, preβ- and γ- migrating particles). α-migrating particles (α-HDL) include the spherical particles of HDL. Pre-β particles (pre-β HDL) are either discoidal or lipid-poor apoA-I particles, while γ-particles (γ-HDL) contain the spherical apoE-HDL particles (57, 58). Additionally, HDL particles can be distinguished based both on their size and on surface charge. This is performed with non-denaturing two-dimensional gel electrophoresis (2D-PAGE) and shows the existence of twelve subpopulations: preβ-1a,

preβ-1b, preβ-2a, preβ-2b, preβ-2c, α1, α2, α3, α4, preα-1, preα-2 and preα-3 (Fig. 1.6C) (59).

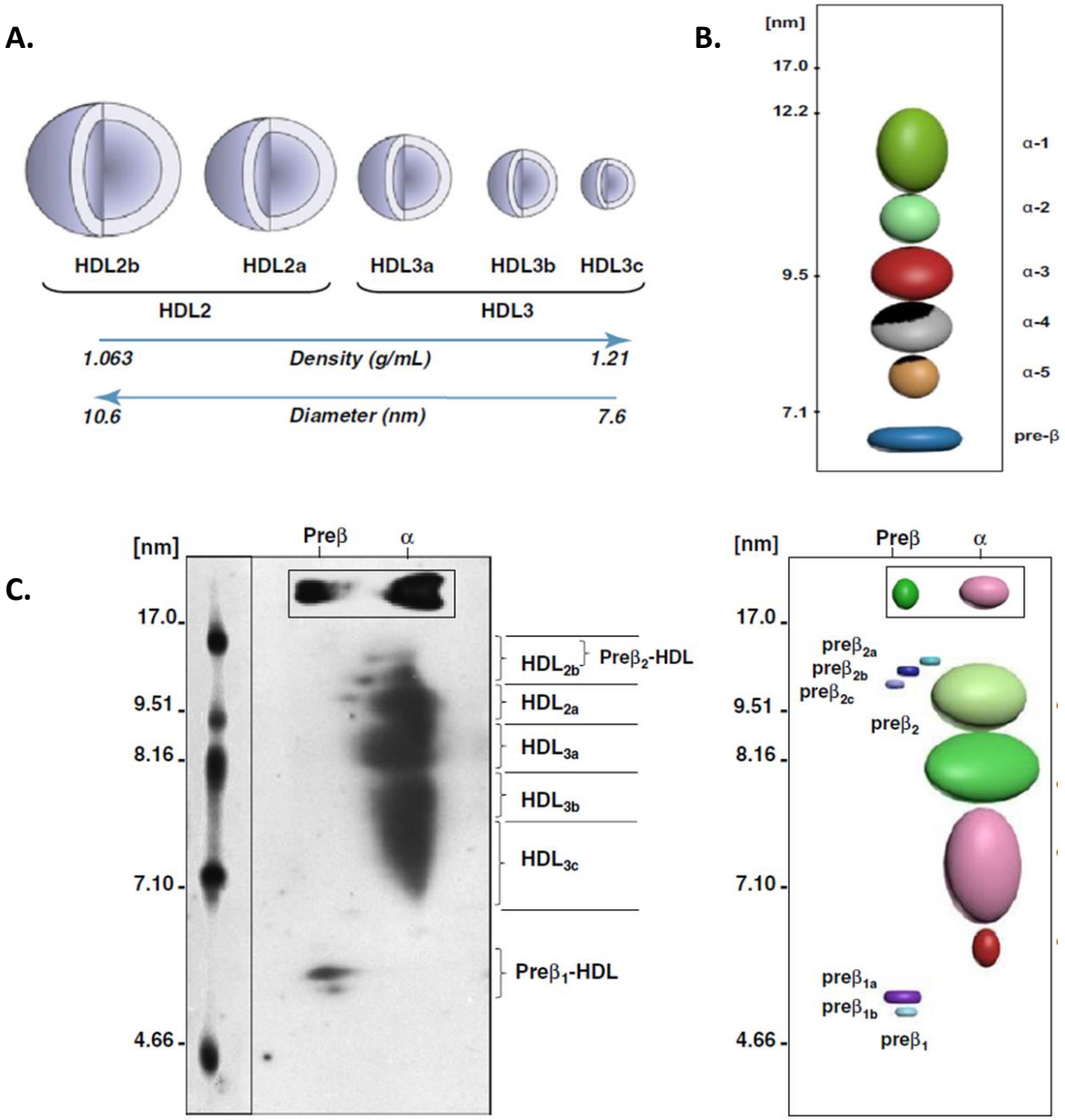

Figure 1.6 HDL heterogeneity. A) Distribution of HDL based on their density or their size (60). B) Schematic representation of the distribution of HDL particles after GGE (52). C) (left panel) 2D-PAGE in order to separate HDL particles based on both their surface charge and their size. (right panel) Schematic diagram of all the apoA-I containing HDL particles after 2D PAGE (52).

1.3.4 The role of apoA-I and apoE in HDL Biogenesis

1.3.4.1 apoA-I-HDL particles

Apolipoprotein A-I (apoA-I) is the major protein of HDL and plays central roles in all aspects of HDL biology, from HDL biogenesis to proper HDL functionality. It is synthesized mainly by the liver and the intestine and secreted in a precursor form (pro-apoA-I) which undergoes proteolytic processing resulting in the mature apoA-I (61, 62). The structure of mature apoA-I consists of eight alpha-helical amphipathic domains of 22 amino acids and two repeats of 11 amino acids (63). These amphipathic domains allow apoA-I to interact with lipids. Additionally, its structure is characterized by a high degree of flexibility allowing apoA-I to readily adopt different conformations. This low stability structure facilitates the functional remodeling of HDL particles as well as the interactions between apoA-I and membrane receptors or transporters (63)

ApoA-I plays a key role in the formation of HDL particles. Specifically, it interacts with ABCA1 promoting cholesterol efflux and it also functions as the scaffold protein that accepts these lipids (39). Indeed, structural-functional studies utilizing apoA-I isoforms with mutations in the C-terminal segment (amino acids 220-231), which is responsible for the interaction with ABCA1, resulted in decreased HDL levels due to impaired cholesterol efflux (64-67). Additionally, apoA-I acts as coactivator of LCAT enzyme (39). Mice expressing the natural mutations of apoA-I, L141R$_{Pisa}$ and L159R$_{FIN}$, had decreased HDL-C levels consisting of small size HDL particles (preb2 and a3, a4) due to impaired capacity of apoA-I to activate LCAT (Fig. 1.7) (68). Beyond biogenesis, apoA-I interacts directly with ABCG1 and SR-BI transporters regulating also the steps of remodeling and catabolism of HDL (39). Furthermore, apoA-I by directly binding to SR-BI and ecto-F1-ATPase receptors activates intracellular signaling cascades resulting in a variety of atheroprotective effects (discussed in detail below).

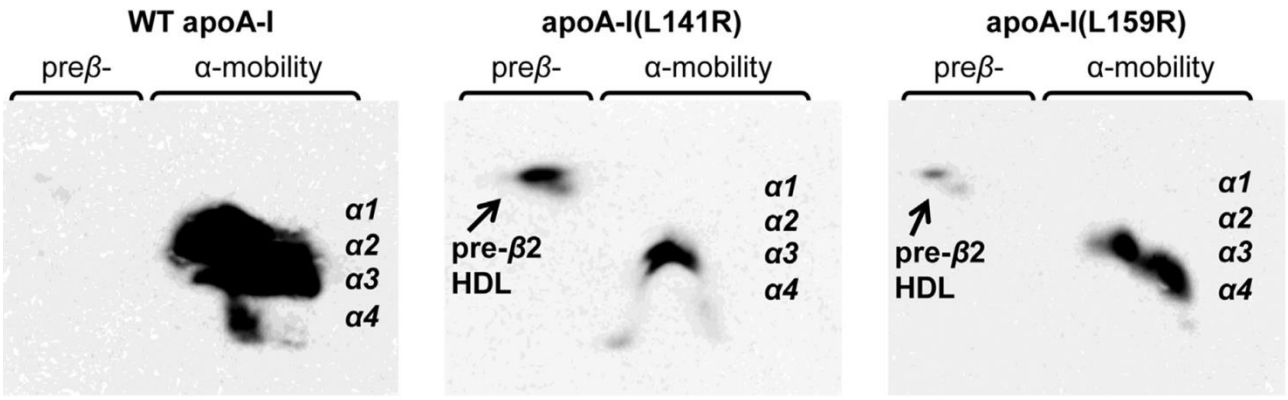

Figure 1.7 Characterization of apoA-I-containing HDL subpopulations in the serum of transgenic mice expressing human apoA-I (wild type or the mutations L41R and L159R) on chow diet. The serum was analyzed by two-dimensional gel electrophoresis and western blotting using anti-human apoA-I antibody (68).

1.3.4.2 apoE-HDL particles

Apolipoprotein E (apoE) is an essential apolipoprotein of lipid metabolism in all tissues and organs. It is synthesized mainly by the liver but also by macrophages, endocrine tissues and central nervous system (40, 69, 70). Human apoE is a polymorphic protein. There are 3 isoforms of apoE: isoforms E2, E3 and E4, differing by a single unit of net charge (71). The three isoforms are expressed from multiple alleles at a single apoE genetic locus. E3 allele is considered the wild type because it is expressed in highest frequency in all populations studied (~78%) (72, 73). E2 allele is found in 7.5% of the general population and is associated with type III hyperlipoproteinemia (type III HLP) (72), while E4 is found in 13.4% of the general population and is considered a risk factor for the development of Alzheimer's disease (72, 74).

Similar to apoA-I, apoE contains eight amphipathic alpha-helical repeats allowing its association with lipids and the formation of lipoproteins (75). The major fraction of circulating apoE is carried by triglyceride-containing lipoproteins where it serves as a ligand for LDL receptor (LDLr) as well as for other receptors, promoting the clearance of the lipoprotein remnants (76-78). Furthermore, apoE is a critical component of the RCT pathway (39). Although apoE is a minor component of HDL, it has the ability to promote cholesterol efflux

and to form functional HDL particles in a process similar to that of apoA-I (43, 79). Infection of apoA-I$^{-/-}$ mice with apoE4-expressing adenoviruses increased HDL-C levels and generated discoidal HDL particles that were converted to spherical upon co- infection with an adenovirus expressing human LCAT. ABCA1$^{-/-}$ mice treated similarly failed to form HDL particles, suggesting that the biogenesis of apoE-containing HDL particles requires the functions of both ABCA1 and LCAT (43). Importantly, apoE is the only apolipoprotein present in the brain and by generating apoE-HDL particles controls the lipid homeostasis in this tissue (76, 80). The importance of apoE in lipid homeostasis is evident in mice with apoE deficiency which develop atherosclerotic lesions spontaneously (i.e. without a high fat diet), similar to those observed in humans, and these lesions exacerbate when mice are fed a high fat diet (81). Therefore, apoE$^{-/-}$ mice became the best animal model to study atherosclerosis in cardiovascular research (82, 83).

1.3.5 HDL heterogeneity

Proteomic and lipidomic analysis have shown that many proteins and lipids are associated with the molecule of HDL affecting its structure and its function. Several proteomic studies utilizing different methods of HDL isolation have identified up to 80 distinct proteins associated with HDL (84). Besides apolipoproteins, there are proteins belonging into several subgroups including enzymes, lipid transfer proteins, acute-phase response proteins, complement components, proteinase inhibitors and other protein components (Table 1.2).

The HDL lipidome is dominated by phospholipids that contribute to 27-32% of total HDL mass. Technological advances in mass spectrometry (MS) reveal more than 200 individual molecular lipids species in the five major HDL subpopulations (85). Table 2 presents the major lipid subclasses. It should be mentioned that among sphingolipids, HDL binds the important bioactive sphingosine-1-phosphate (S1P).

Importantly, many studies in the last decade have shown that HDL binds miRNAs and delivers them to cells and tissues (Table 2). The circulating levels of these miRNAs are altered in pathophysiological conditions, while some of them have been correlated with CVDs (86).

> 80 proteins	>200 lipid species	miRNAs
Apolipoproteins: ApoA-I, ApoA-II , ApoA-IV, ApoC-I, ApoC-II, ApoC-III, ApoC-IV, ApoD, ApoE, ApoF, ApoH, ApoJ, ApoL-I, ApoM	**Phospholipids:** Phosphatidylcholine, PC-plasmalogen, LysoPC, Phosphatidylethanolamine, PE-plasmalogen, Phosphatidylinositol, Cardiolipin, Phosphatidylserine, Phosphatidylglycerol, Phosphatidic acid	miR-223 miR-33 miR-24 miR-30c Mir-146a miR-155
Enzymes: LCAT, PON1, PAF-AH, GSPx-3	**Sphingolipids:** Sphingomyelin, Ceramide, Hexosyl Cer , Lactosyl Cer, S1P, SPC	
lipid transfer proteins: PLTP, CETP	**Neutral lipids:** Cholesteryl esters, Free cholesterol, Triacylglycerides, Diacylglycerides	
acute-phase response proteins: SAA1, SAA4, Fibrinogen alpha chain	**Minor lipids:** Free fatty acids, Isoprostane-containing PC	
Complement components: C3		
proteinase inhibitors: Alpha-1-antitrypsin, Hrp		
other protein components: Transthyretin, Serotransferrin, Vitamin, D-binding protein, Alpha-1Bglycoprotein, Hemopexin		

Table 1.2 Proteins, lipids and miRNAs that are associated with HDL particles ((38, 86))

1.4 Molecular Mechanisms Regulating HDL Metabolism

The proper quantity and functionality of HDL in the circulation requires a rigorous cooperation among the different steps (biogenesis, remodeling and catabolism) of HDL metabolism. Therefore, the expression of proteins participating in these steps is under a tight regulation at multiple levels. Indeed, it has been reported that these proteins are under the regulation of: a) transcription factors including nuclear receptors and SREBPs, at the transcription level (87), b) several miRNAs at the post-transcriptional level (88), c) long-non coding RNAs at both transcriptional and post-transcriptional levels (89) and d) enzymes and ubiquitinases at the post-translational level (87). In the context of this thesis, we will focus on the role of nuclear receptors and miRNAs in liver HDL metabolism.

1.4.1 The impact of Nuclear Receptors on HDL metabolism

Nuclear receptors (NRs) comprise a superfamily of transcription factors that transduce different metabolic signals to modulate gene transcription. Forty eight NRs have been identified in humans and 49 in mice (90). The majority of NRs are activated in a ligand-dependent manner by steroid hormones, retinoids, thyroids and products of intermediate metabolism such as bile acids, fatty acids and cholesterol derivatives (91). Still, some members of this family do not need ligand binding to regulate transcription and are classified as “orphans” (92).

All proteins of the NR superfamily share a common structure (Fig. 1.8A) that includes the following domains: a) a N-terminal transactivation domain called Activation Function 1 (AF-1) for interaction with cofactors; b) a conserved DNA binding domain (DBD) that contains two zinc fingers; c) a variable hinge region that connects the DBD with the ligand-binding domain (LBD); and d) the LBD which is unique for each NR and also contains a

second transactivation domain called AF-2 (93). Nuclear receptors bind to specific DNA sequences called Hormone Response Elements (HREs) on the promoters of target genes either as homodimers or as heterodimers with the Retinoid X Receptor (RXR) (87). HREs variously contain direct repeats (DRs), inverted repeats (IRs) or palindromic repeats (PRs) of the sequence 5'-AG(G/T)TCA-3'. These repeats are separated by one, two, three, four, or five nucleotides and are designated DR1, DR2, etc. (for direct repeats), IR1, IR2, etc. (for e inverted repeats), and PR1, PR2, etc. (for palindromic repeats) (94). The exact sequence of the repeats and spacing as well as the 5' extension of the HREs define the specificity of different nuclear receptor heterodimers. In the absence of ligand, NRs bind to DNA and associate with corepressors resulting in the repression of transcription. Upon ligand binding, NRs undergo conformational changes leading to the recruitment of transcriptional co-regulators, chromatin remodelers and the general transcription machinery to activate the target gene (Fig. 1.8B) (95).

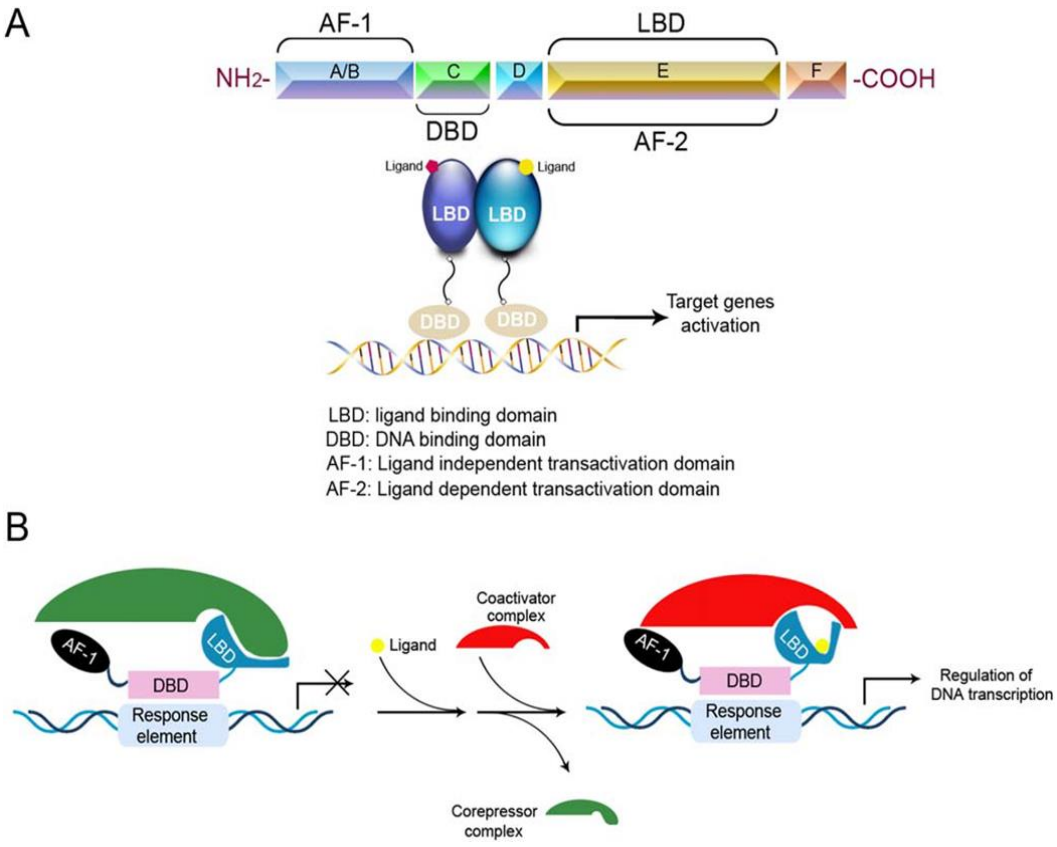

Figure 1.8 A) Schematic representation of structure, dimerization process and DNA binding of Nuclear receptors, B) Schematic diagram of ligand-dependent activation of nuclear receptors (92).

Accumulating evidence reveals that the promoters of genes associated with HDL metabolism, such as *apoA-I, apoA-II, apoE, apoM, LCAT, ABCA1* and *SR-BI*, are rich in HREs (51, 87, 92). *In vitro* and *in vivo* studies have confirmed the binding of several NRs in these sites in response to various intracellular and extracellular ligands. The main NRs binding to HDL-related genes are LXRs, HNF-4α, PPARs, RXR, RAR, T3β and FOXA2, which control important steps of HDL biology, by regulating the expression of the corresponding genes (51, 87, 92). An example of the regulation of a promoter by NRs is depicted in Figure 1.9.

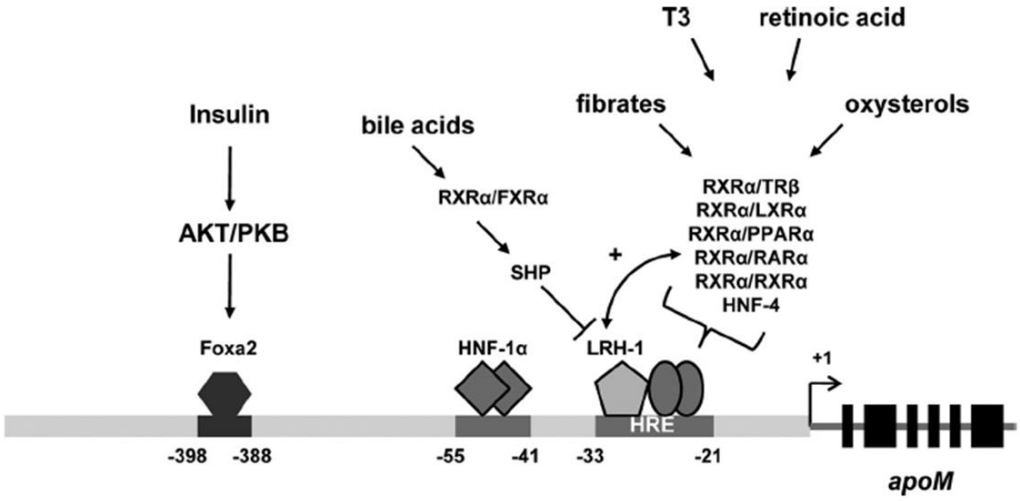

Figure 1.9. Regulatory elements and Nuclear Receptors that participate in the control of human apoM promoter (96).

1.4.1.1 LXRs

Liver X receptors (LXRs) are sterol-activated members of the NR superfamily and play crucial roles in the transcriptional control of lipid metabolism. There are two members of LXR family, LXRα (*NR1H3)* and LXRβ *(NR1H2)*, whose genes are located in chromosomes 11 and 19 respectively (97, 98). LXRα and LXRβ proteins have considerable sequence homology, sharing about 77% identity in their DBD and LBD domains both in humans and rodents, but they present distinct tissue distributions (99). LXRα is highly expressed in metabolic tissues such as liver, adipose tissue, intestine, kidney and macrophages, while LXRβ is expressed ubiquitously (100). Activation of LXRs is performed by endogenous ligands, including cholesterol derivatives such as oxysterols and 24(S), 25-epoxycholesterol, and by intermediate precursors in the cholesterol biosynthetic pathway, such as desmosterol (101, 102). Additionally, the synthetic agonists GW3965 and T0901317 have high affinity and activate LXRs (103). To induce the expression of target genes, LXRs form obligate heterodimers with RXR and bind to a specific DNA site known as an LXR response element (LXRE) of DR-4 type (98).

The importance of LXRs in maintaining cholesterol homeostasis was observed when LXRα-knockout mice were fed a high cholesterol diet and developed cholesterol-rich livers which resulted in impaired hepatic function (104). Nowadays, it is clear that LXRs control the expression of a plethora of genes participating in different steps of cholesterol homeostasis (Fig. 1.10). Specifically, LXRs by inducing the expression of transporters ABCA1 and ABCG1 (105-107), the lipoprotein remodeling enzymes CETP, PLTP and LPL (108-110), and apolipoproteins ApoE, ApoC-I, ApoC-II and ApoC-IV (111, 112) control the transport of cholesterol from peripheral tissues to the liver (RCT). Moreover, LXRs induce the expression of ABCG5 and ABCG8 that together form a functional heterodimeric protein which promotes the excretion of cholesterol from the liver to the bile and decreases the absorption of dietary cholesterol by the intestine (113-115). The absorption of dietary cholesterol is also decreased by LXRs through inhibition of the expression of the Niemann-pick C1-like 1

(Npc1l1) transporter (116). Interestingly, it has been reported that LXRs also inhibit hepatic cholesterol biosynthesis through the induction of the non-coding RNA LXR-induced sequence (LeXis) (117). In this context, LeXis interferes with a co-activator and RNA-binding protein, RALY, for the transcription of genes in the cholesterol biosynthetic pathway (117). Furthermore, LXRs inhibit cholesterol uptake by macrophages by inducing the expression of IDOL, a degrader of LDL receptor (LDLr) (118).

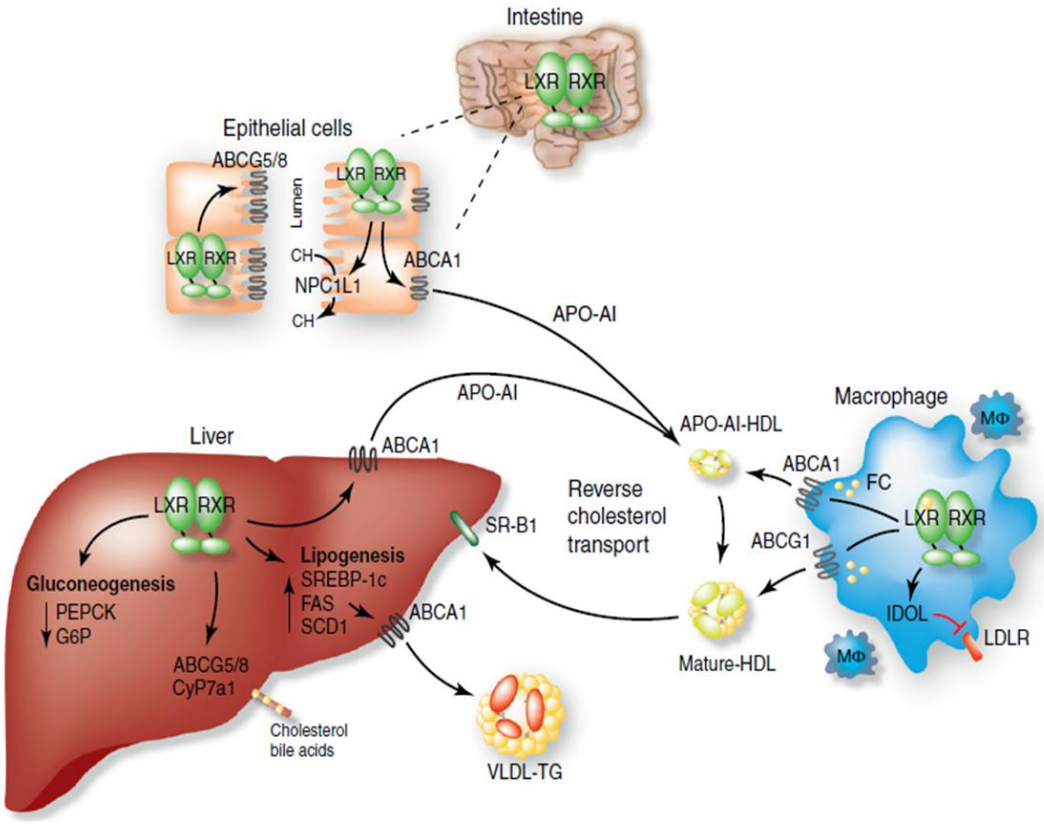

Figure 1.10 The impact of LXRs on lipid metabolism via regulation of the expression of a variety genes in different cells (119).

The impact of LXRs in RCT and subsequently in atherosclerosis has been extensively studied in mice (120). Mice lacking total (121), hepatic (122), intestinal (123) and myeloid (124) LXRs in an atherosclerotic background (ApoE-/- or LDLr-/-) develop severe atherosclerosis with increased plaque lesions. In contrast, administration of LXR ligands(125) or tissue specific overexpression of LXRα in the intestine (123) and in macrophages (126) resulted in attenuation of atherosclerosis. Interestingly, the atheroprotective role of LXRs in macrophages is not only by promoting cholesterol efflux or decreasing the uptake of cholesterol, but also by exerting anti-inflammatory functions (120). Indeed, it has been demonstrated that LXRs activation in macrophages reciprocally represses a set of inflammatory genes such as COX-2, IL-6, IL-1β, and MCP-1(127), through inhibition of the NF-kB pathway (128, 129).

In addition to their importance in modulating cholesterol homeostasis, LXRs also control additional liver-specific metabolic processes (Fig. 1.10). LXRs are key regulators of de novo lipogenesis in the liver by inducing the expression the central activator of fatty acid biosynthesis sterol regulatory element binding protein 1c (SREBP-1c) (130), as well as of several lipogenic genes such as the fatty acid synthase (Fasn) and the stearoyl-coenzyme A desaturase 1 (Scd1) (131, 132). Moreover, LXRs exhibit antidiabetic action by suppressing the expression of glucose 6-phosphatase (G6Pase) and phosphoenolpyruvate carboxykinase (PEPCK) and subsequently inhibit hepatic gluconeogenesis (133). Indeed, LXRs activation has been reported to improve glucose tolerance in diabetic mouse (133) and rat models (134).

Studies in mice lacking either LXRα or LXRβ revealed a preferential role of LXRα in preserving liver cholesterol homeostasis (104, 135-137). The expression of LXRα is driven by two promoters giving rise to five transcript variants (LXRα1-5), which differ in transactivation activity and tissue distribution (138, 139). LXRα1 is the main variant, however, the contribution of the other variants in the different aspects of LXRα biology is poorly understood. Interestingly, the expression of LXRα is autoregulated through direct

binding to three LXREs which are located at 2.9kb, 2.1kb and 1.7kb upstream of the transcriptional start site of LXRα1 (140, 141). Furthermore, transcription of LXRα is induced by PPARγ (through a PPARE at the distal region of the promoter) (141) and Thyroid Hormone Receptor β1 (TRβ1) (the site of TRβ1 in the human LXRα promoter has not been identified) (142). Moreover, the expression of liver LXRα is under the regulation of inflammatory and metabolic stimuli. Specifically, it has been reported that TNFα and IL-1β (143) downregulate the expression of LXRα, while insulin upregulates its expression (144) suggesting that the stimulatory effect of insulin on hepatic lipogenesis may be partially mediated via LXRα (145, 146).

1.4.1.2 HNF-4α

Hepatocyte nuclear factor 4 alpha (HNF-4α or NR2A1) is an orphan member of the NRs superfamily and is highly conserved among species (147). It has been reported that linoleic acid (LA, C18:2) binds to the LBD of HNF-4α, however the activation of this NR is independent of ligand-binding (148). HNF-4α forms homodimers and binds to HREs of DR-1 type. Also, it binds to a novel HNF4-specific binding motif (H4-SBM) with the consensus sequence 5' xxxxCAAAGTCCA 3' (149).

HNF-4α is essential for embryonic development, since mice deficient for HNF-4α are embryonically lethal due to impairment in gastrulation (150). The expression of HNF-4α is in abundance in the liver and to a lesser degree in kidney, intestine and pancreas (151). Hepatic HNF-4α is a master regulator of liver development, differentiation and functionality by controlling the expression of a great number of genes. Conditional liver-specific inactivation of the HNF-4α gene in mice caused weight loss, increased mortality, liver steatosis, lipid abnormalities, defective ureagenesis and gluconeogenesis due to impaired expression of genes involved in these processes (152-155). Importantly, HNF-4α not only regulates genes by directly binding to their promoters and/or enhancers but also appears to

be fundamental for establishing a network of transcription factors that governs the expression of additional hepatic mRNAs (156). Furthermore, studies in livers from adult humans revealed that more than 40% of the promoters of active genes were bound by HNF-4α (157), whereas reduced expression and/or activity of HNF-4α is associated with all major liver diseases, such as alcoholic and non-alcoholic steatohepatitis, viral hepatitis, liver cirrhosis, and liver cancer (158). Additionally, heterozygous mutations in the HNF-4α gene are associated with an early onset form of type II diabetes called maturity onset diabetes of the young 1 (MODY1) characterized by impaired lipid metabolism and insulin secretion (159, 160). Of note, until today no homozygous mutations in human *HNF4a* gene have been reported (161).

In vitro and *in vivo* studies have revealed that HNF-4α is a positive regulator of many proteins implicated in HDL metabolism, including apoA-I, apoA-II, apo-A-IV, apoE and ABCA1 (87), whereas mice deficient in hepatic HNF-4α are characterized by low levels of plasma HDL (152, 162). In agreement with this finding, GWAS studies identified a common variant in the coding region of the HNF-4α gene (rs1899861) associated with low HDL concentrations in humans (163). Besides the role of HNF-4α in HDL metabolism, it has been reported that HNF-4α affects also HDL functionality, since HNF-4α induces hepatic apoM expression through an HRE element in the proximal region of the apoM promoter (Fig. 1.9) (96). ApoM functions as a carrier for the atheroprotective molecule S1P in the HDL molecule (164). As we will discuss below, many atheroprotective functions of HDL are mediated through the apoM-S1P constituent.

The expression and transcriptional activity of HNF-4α are regulated at multiple levels. At the transcription level, the expression of HNF-4α is driven by two promoters (P1 and P2) giving rise to 9 isoforms that exhibit varying levels of transactivation activity and are expressed in a temporal and spatial-specific fashion (165). P2 promoter-driven HNF-4α isoforms (HNF-4α1-6) are expressed in fetal liver and adult pancreas, whereas P1 promoter–driven isoforms (HNF-4α7-12) are expressed in adult liver. HNF-4α2 is the most

predominant isoform in adult liver. A complex network of transcription factors are implicated in the activation of these promoters, while FOXA1 inhibits P1 promoter in embryonic states and HNF-4α1 inhibits P2 promoter after birth (161). Moreover, *HNF-4α* expression is regulated by a variety of physiological and pathological conditions, including fasting (upregulates *HNF-4α*), refeeding (downregulates *HNF-4α*), hyperinsulinemia (downregulates *HNF-4α*) (166) and inflammation (downregulates *HNF-4α*) (167). HNF-4α transcriptional activity is regulated by post-translational modifications including methylation, phosphorylation and acetylation (167). Furthermore, HNF-4α recruits coactivators (such as PGC1α), co-repressors (Hes6) and interacts with a plethora of transcription factors (such as SP1, COUP-TF, SMAD, KLF9) orchestrating cell transcription (167).

1.4.2 miRNAs: novel regulators of HDL metabolism

MicroRNAs (miRNAs) are short (18–25 nucleotides), single-stranded, non-coding RNAs involved in post-transcriptional regulation of gene expression. miRNAs function, mainly, as repressors by direct binding to their target mRNA promoting its degradation or inhibiting its translation (168). This binding is mediated through sequence-specific complementarity between the 5' 'seed' region of miRNA (2-8 nucleotides) and the 3' untranslated region of the target mRNA (3' UTR) (168). Importantly, most mammalian miRNAs bind with either mismatches or bulges (non-canonical interactions), while the mode of binding determines the type of post-transcriptional repression (169). Additionally, it has been reported that some miRNAs can interact with other mRNA target regions including the 5′ UTR (170) or the coding sequence (171), while other miRNAs increase rather than decrease translation of their target mRNA (172). Interestingly, recent data showed that certain miRNAs are localized in the nucleus and bind directly to promoter (173) or enhancer (174) regions regulating the transcription of the corresponding genes.

Human genome encodes about 2.000 miRNAs and prediction algorithms suggest that 60 % of human protein-coding genes have conserved targets for pairing with miRNAs

within their 3' UTR (175). Furthermore, computational methods and validation studies have revealed that a single miRNA can target multiple genes, while a single mRNA may have different miRNA binding sites (168, 169). Thus, miRNAs are implicated in all cellular biological processes such as differentiation, proliferation, apoptosis and aging, while abnormal expression of miRNAs has been associated with the development of several diseases including cancer, neureodegenerative and cardiovascular diseases (176). Interestingly, the finding that some miRNAs are circulating in the plasma, indicates that these miRNAs may also participate in the communication between different organs (177), and to be potential biomarkers during the progression of pathophysiological processes (178). Of note, HDL functions as a carrier for circulating miRNAs (177).

Accumulating data revealed that miRNAs are important regulators of HDL metabolism by targeting several proteins participating in it (179-181). Characteristically, a number of reports have shown that ABCA1 is targeted by several miRNAs including miR-33a/b, miR-10b, miR-20a/b, miR-144 and miR-148 resulting in impaired cholesterol efflux *in vitro* and RCT *in vivo* (179-181) (Fig. 1.11). Interestingly, silencing of miR-33 (182-184) or miR-20a/b (185) attenuated atherosclerosis progression in mouse models of atherosclerosis. Specifically, miR-33 isoforms (miR-33a and miR-33b) play a crucial role in cholesterol homeostasis overall. On one hand, miR-33a/b inhibit both ABCA1 and ABCG1 expression regulating cholesterol efflux, and on the other they regulate the last phase of RCT by inhibiting factors involved in the synthesis (CYP7A1) and secretion (ATP8B1 and ATCB11) of bile acids (179) (Fig. 1.11). Besides the regulation of proteins participating in cholesterol efflux, it has been demonstrated that several miRNAs (miR-185, miR-96, miR-233) also target SR-BI inhibiting its expression and leading to impaired HDL-C uptake in hepatic cells *in vitro* (179, 180) (Fig. 1.11). Recently, it was shown that overexpression of a novel miRNA, miR-24, decreased hepatic SR-BI expression and promoted plaque formation in apoE$^{-/-}$ mice (186). Besides the proteins participating directly to RCT, miRNAs regulate the expression of

the master regulator of cholesterol metabolism LXRα (miR-1, miR-206, miR-613, and miR-155), as well as its partner RXRα (miR-128-2) (179).

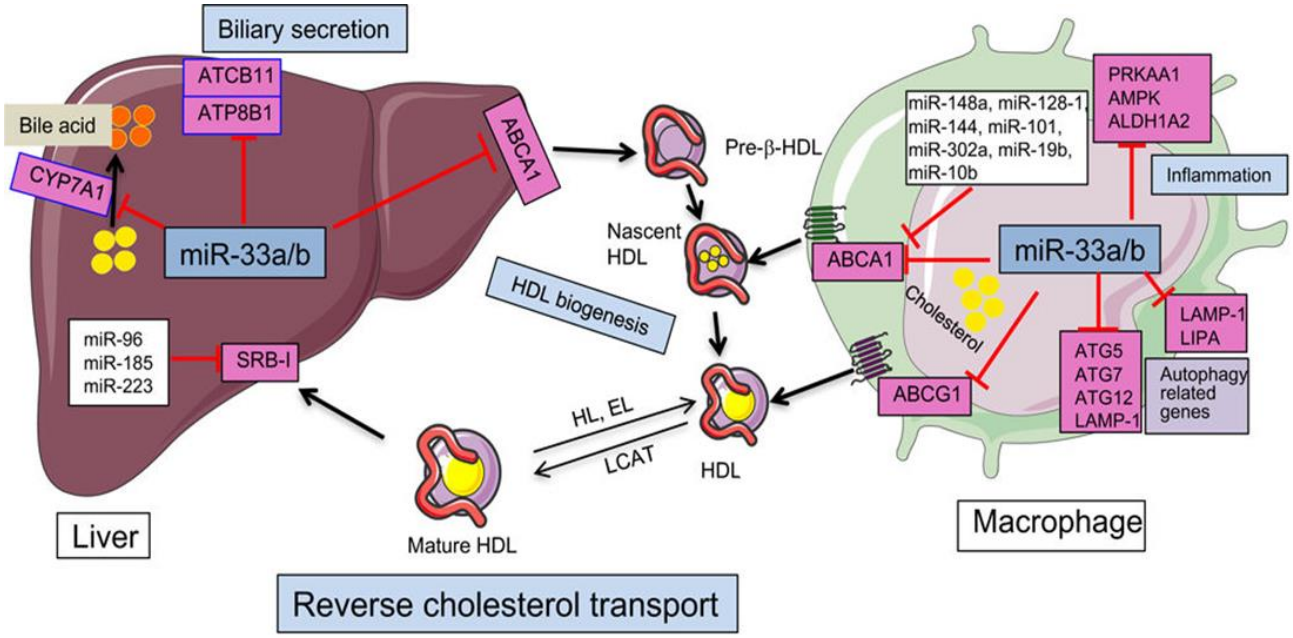

Figure 1.11 Schematic representation of regulation of ABCA1, ABCG1 and SR-BI by miRs in liver and macrophages. MiR-33a/b play key regulatory roles in several metabolic processes. In the liver, besides the regulation of ABCA1, miR-33a/b regulate also the expression of genes involved in bile acid metabolism (CYP7A1, ATP8B1, ATCB11). Additionally, in macrophages they regulate the expression of the key autophagy effectors ATG5, ATG7, ATG12, LAMP-1 and LIPA and control macrophage polarization by regulating the expression of PRKAA1, AMPK and ALDH1A2 (181).

1.4.2.1 Let-7

Let-7 (lethal-7) was one of the first miRNAs to be discovered. It was originally identified in the nematode *C. elegans* to control the transition from late-larval to adult cell fates (187). The let-7 miRNA is evolutionarily conserved across various animal species, including flies and mammals, but it is not found in plants (188, 189). In humans let-7 family consists of nine members (let-7a, let-7b, let-7c, let-7d, let-7e, let-7f, let-7g, let-7i and mir-98) encoded by twelve different genomic loci, some of which are clustered together (190). These

members share an almost identical seed sequence (spans nucleotides 2 through 8) indicating that at least some targets and functions are common (191).

The most characteristic function of let-7 is as tumor-suppressor. Multiple let-7 members were found to be down-regulated in human cancers and cancer stem cells (190, 192). Additionally, it has been reported that let 7 directly targets oncogenes. Specifically, let-7g inhibits the Rat sarcoma (RAS) resulting in suppressing tumorigenesis in non-small cell lung cancer (NSCLC) (193), while all members of let-7 family inhibit the oncofetal High-mobility group AT-hook 2 *(*HM*GA2)* which is involved in self-renewal of stem cells (194, 195) and let-7a suppresses *MYC*-induced cell growth in Burkitt lymphoma cells (196). Moreover, let-7 was found to suppress cell-cycle progression in cancer cells by repressing cell cycle regulators such as cyclins A, D1, D3, and CDK4 (190, 192).

Several studies have revealed an important role of let-7s in cardiovascular biological processes and cardiovascular diseases (197). Specifically, let-7g levels were found reduced both in high-fat diet-fedmice and hypercholesterolemic humans (198). Let-7d and let-7i levels are down-regulated in CAD patients (199, 200), while all members of let-7 family are up-regulated in patients suffering from atherosclerotic abdominal aortic aneurysm (201). Interestingly, it was reported that overexpression of let-7g in macrophages inhibited the NF-κB pathway leading to reduction of foam cell formation, decreased accumulation of macrophages in atheromatic plaques as well as reduction of the size of these plaques (202). In contrast, it has been reported that both global and pancreas-specific overexpression of Let-7 in mice resulted in impaired glucose tolerance and reduced glucose-induced pancreatic insulin secretion by directly targeting components of the insulin-signaling pathway, such as Igf1r, Insr, Irs2, Pik3ip1, Akt2, Tsc1, and Rictor, while specfic knockdown of Let-7 in Let-7 transgenic mice rescued the phenotype by improving insulin sensitivity in muscle and adipose tissues (203, 204).

1.5 The Atheroprotective Properties of HDL

From the early studies about the characterization of CVDs, it appeared that patients with coronary artery disease had less HDL cholesterol (HDL-C) levels in their plasma (205). Since then, multiple epidemiological studies have confirmed that low levels of HDL-C are a strong, consistent and independent risk factor for the development of CVDs (206-208). Importantly, it has been shown that low levels of HDL-C remains predictive of future CVD risk even when the concentration LDL-C has been reduced to low levels by treatment with statins (209). Consequently, HDL is thought to be an atheroprotective molecule and thus research has focused on elucidating its protective properties. It has been established that HDL exerts pleiotropic functions in order to protect against the development of atherosclerosis. These functions include: reverse cholesterol transport, positive regulator of endothelial biology, anti-oxidant and anti-inflammatory effects (36).

1.5.1 Reverse Cholesterol Transport (RCT)

The most characterized atheroprotective role of HDL is its ability to remove excess cholesterol from macrophages and to transport it to the liver for excretion in the bile, a mechanism also referred to as reverse cholesterol transport (RCT) (36). As we discussed in the chapter 1.1.2, the formation and subsequently the accumulation of cholesterol-laden macrophages (foam cells) in the intima of the arteries constitutes a crucial step in the development of atherosclerosis. Thus, HDL through RCT protects both macrophages and the arterial wall from cholesterol accumulation. In fact, macrophage cholesterol efflux capacity of HDL has been postulated as a more appropriate predictor for cardiovascular disease than HDL-cholesterol levels (202).

A crucial step for RCT is the efflux of free cholesterol from macrophages to HDL particles (either the mature or the lipid-poor particles). This is performed through four pathways, two active and two passive, which are depicted in Figure 1.12. The active pathways are mediated by either ABCA1 or ABCG1 transporters. Specifically, ABCA1 promotes the transport of cholesterol to lipid-free apoA-I or lipid-poor HDL particles (210), while ABCG1 delivers cholesterol to the mature HDL particles (45). The impact of these transporters in RCT and subsequently to atherosclerosis has been described by Yvan-Chavret and colleagues by utilizing transplantation experiments. They transplanted bone marrow from ABCA1$^{-/-}$, ABCG1$^{-/-}$ and ABCA1$^{-/-}$/ABCG1$^{-/-}$ mice into LDLr$^{-/-}$ mice and observed that individual deficiency of each receptor led to atherosclerosis, while the lack of both receptors resulted in an accelerated atherosclerosis development and extensive infiltration of the myocardium and spleen with macrophage foam cells (211).

In addition to the active cholesterol efflux pathways, aqueous diffusion and diffusion facilitated by SR-BI are two passive pathways primarily driven by cholesterol concentration gradient, in which spherical HDL particles are the major acceptors (212). The main function of SR-BI is to facilitate the selective uptake of cholesterol esters from HDL particles into the cells (213). However, it has been shown that in macrophages SR-BI is involved in the opposite pathway promoting the efflux of free cholesterol to HDL (47). The exact role of SR-BI in macrophage RCT is controversial. A study from Wang and colleagues showed that macrophage ABCA1 and ABCG1, but not SR-BI, promote macrophage RCT *in vivo* (214). Interestingly, in another study from Van Eck's lab in Leiden, they showed, using transplantation experiments, that in the absence of ABCA1 the relative importance of SR-BI-mediated cholesterol efflux from macrophages becomes really apparent under conditions where the efflux to lipid-poor apoA-I1 via the ABCA1 was also disrupted (215).

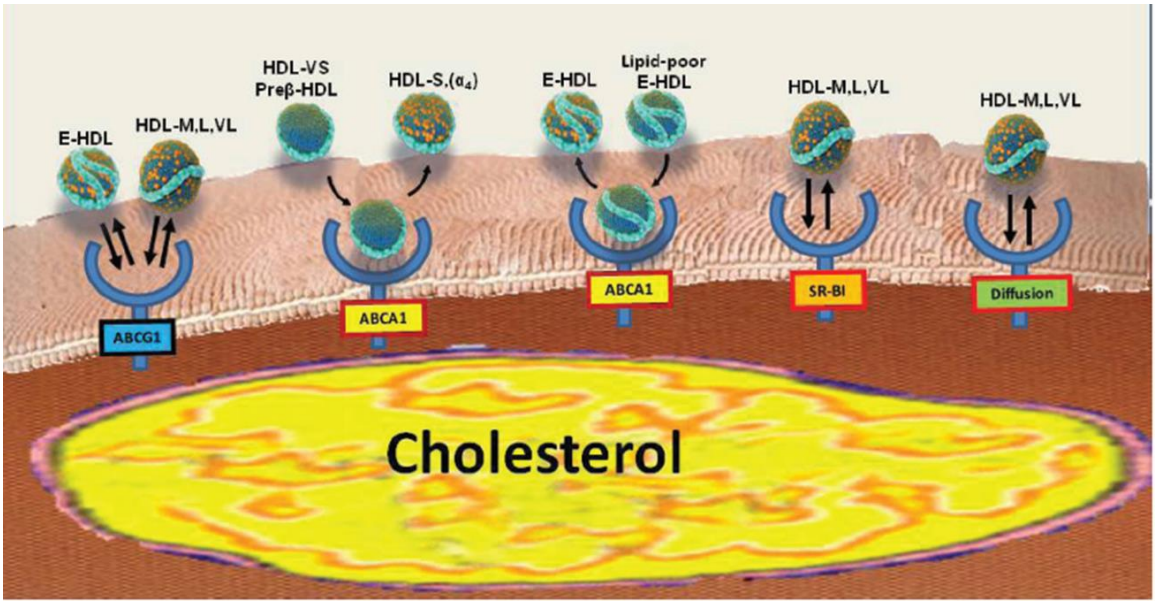

Figure 1.12 Schematic representation of the cholesterol efflux mechanisms (216).

1.5.2 HDL as a positive regulator of endothelial biology

Endothelial cells are highly exposed to HDL, both at the luminal and at the sub-endothelial side (217). In order to reach the sub-endothelial compartment, HDL particles are transferred through the endothelium via a mechanism called “transcytosis” which includes the endocytosis of the particles from one side of a polarized endothelial cells and its exocytosis from the other side (218). ABCA1 was identified as a limiting factor for binding, uptake, and transport of lipid-free apoA-I through by endothelial cells while ABCG1, SR-BI, and endothelial lipase were found to limit binding, uptake, and transport of mature HDL (219).

The effect of HDL on NO production

The endothelial NO production is an essential feature for the maintenance of the vascular homeostasis. Therefore, it was of great importance when it was demonstrated that HDL can directly stimulate the endothelial NO production via interaction with SR-BI (220). It has been shown that HDL modulates eNOS activity through three mechanisms: a) by

preventing oxLDL-mediated eNOS displacements from caveolae and restoring enzyme stimulation (221); b) by direct phosphorylation at Ser1117, which is known to activate the enzyme (220); and c) by increasing the abundance of eNOS protein by increasing its half-time but not the mRNA levels (222). Also, the capacity of HDL to activate NO production and subsequently vasodilation has been confirmed *in vivo* (223), as well as in humans after applying intravenous rHDL infusion (224).

The interaction between HDL components and endothelial receptors is critical for the HDL-mediated eNOS activation. Specifically, HDL-bound apoA-I, but not the lipid-free apoA-I form, interacts with SR-BI and induces the activation of the tyrosine kinase Src, which in turn activates the phosphoinositide (PI) 3-kinase (PI3K). Then, the PI3K activates both the Akt and Erk pathways, which independently provoke the phosphorylation of eNOS at ser1177 and subsequently the activation of eNOS (225). In addition to this pathway, the interaction of HDL with SR-BI activates the AMP-activated protein kinase (AMPK) via the activation of the calcium/calmodulin-dependent protein kinase (CaMK) and the serine-threonine kinase B1 (LKB1). Then, AMPK activates the AKT pathway, but not ERKs, leading to the activation of eNOS (226). The exact functionality of SR-BI in the HDL-mediated eNOS activation has been studied further. The ability of SR-BI to promote cholesterol efflux plays important role for the SR-BI-mediated signaling activation (227). Interestingly, it has been found that SR-BI through its transmembrane (TM) domain binds plasma membrane cholesterol and acts as cholesterol sensor allowing the signaling activation (227). A single mutation (Q445A) on this TM domain reduced its binding to cholesterol by 71% and this resulted in an impaired HDL-induced signaling without altering cholesterol efflux to HDL (228). Additionally, the binding of SR-BI through a cytoplasmic domain to the adaptor protein PDZK-I is indispensable for the downstream signaling activation (227). The absence of either of these domains or both of them resulted in impaired HDL-mediated signaling activation and subsequently eNOS stimulation (227).

Another important mechanism of eNOS activation involves the HDL-associated sphingosine 1 phosphate (S1P). HDL is the main carrier of plasma S1P and apolipoprotein M (ApoM) is considered as the sole S1P binding protein on HDL (164) . S1P interacts with the G-protein-coupled receptors S1P1 and S1P3 activating a plethora of downstream signaling cascades leading to the production of NO (229, 230). One pathway includes the activation of the GPCR/Src/RAK1/PI3K/AKT axis resulting in the phosphorylation of eNOS at Ser1117 (231). Another pathway implicates the activation of AMPK by CaMK leading to the PI3K/AKT/eNOS activation (226). Additionally, it has been observed that S1P promotes the mobilization of intracellular Ca^{2+} which in turn disrupts the inhibitory interaction of eNOS with caveolin promoting NO production (232).

The interaction of HDL with ABCG1 has also been identified to provoke NO production in the presence of hypercholesterolemia (233). As observed in mice fed a high-cholesterol diet, HDL, oxysterols and specifically 7-ketosterol, are accumulated in endothelial cells and induce the production of reactive oxygen species and the disruption of the active eNOS dimer (233). The HDL-mediated cholesterol and oxysterol efflux via ABCG1 reduced the inhibitory interaction of eNOS with caveolin-1 and thereby restored eNOS activity (234). An overall picture of the mechanisms through which HDL activates NO production is depicted in Figure 1.13.

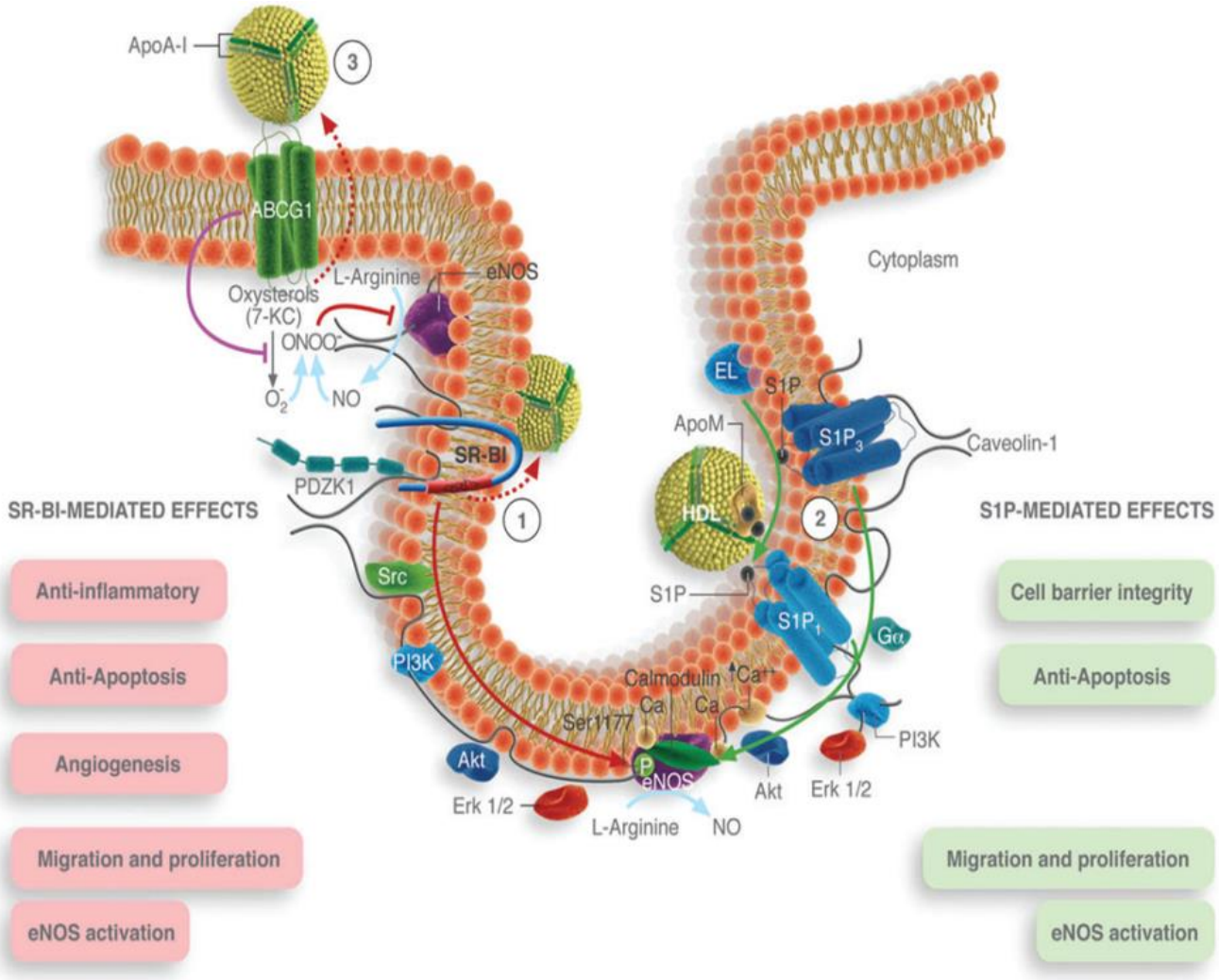

Figure 1.13 HDL activates NO production through (1) SR-BI signaling, (2) S1P signaling and ABCG1-mediated efflux (235).

The anti-inflammatory effects of HDL on endothelium

At the sites of initial lesions, endothelium obtains a pro-inflammatory state expressing leukocyte adhesion molecules and pro-inflammatory cytokines. Thus, endothelium contributes to the migration, infiltration and accumulation of monocytes/macrophages and T lymphocytes into the arterial intima. HDL prevents endothelial inflammation through different pathways. *In vitro* studies have shown that HDL or reconstituted HDL containing apoA-I (rHDL-AI) inhibits the expression of the key endothelial adhesion molecules VCAM-1, ICAM-1 and E-selectin that are activated by TNF-α (236, 237) or IL-1 (236). Additionally, the oxLDL-mediated production of the chemoattractant MCP-1 is prevented in the presence of

HDL (238), as well as the adhesion of monocytes (U937 cells) to the endothelial monolayers mediated by oxLDL (239).

Furthermore, the potent anti-inflammatory effects of HDL have been demonstrated by several *in vivo* studies. In mouse (240) and rabbit (241) models of acute vascular inflammation, utilizing carotid artery cuff injury or the implant of non occlusive carotid periarterial collars respectively, rHDL-AI reduced neutrophil infiltration and endothelial cell inflammatory activation. ApoA-I infusion after the induction of acute vascular inflammation in rabbits also inhibited the endothelial VCAM-1 and ICAM-1 expression and the neutrophil infiltration (242). Additionally, in a rabbit model of vascular inflammation mediated by high-fat diet, apoA-I infusion suppressed the expression of leukocyte adhesion proteins (243). In human studies, it has been shown that administration of reconstituted HDL increased the anti-inflammatory capacity of HDL from patients with type-2 diabetes (244).

Several mechanisms have been proposed to explain the inhibitory effects of HDL on endothelial inflammatory activation. Most of them focused on the suppression of the pro-inflammatory transcription factor NF-κB. HDL prevents NF-κB activation by TNFα, through the activation of the signaling axis SRBI/PI3K/AKT/eNOS and subsequently the induction of NO (245). A NO-independent mechanism of NF-kB inhibiton by HDL has also been reported. Specifically, it was shown that rHDL-AI interacts with SR-BI and up-regulates the 24-dehydrocholesterol reductase (DHCR24) and the well-known anti-inflammatory protein heme oxygenase I (HO-1), both of them preventing the activation of NF-κB by TNFα (246). In addition to the apoA-I component of HDL, HDL-S1P promotes the formation of a cell surface $S1P_1$–β-arrestin 2 complex and attenuates the ability of TNFα to activate NF-κB and increase ICAM-1 abundance (247). Besides the inhibitory effect of HDL to NF-κB, the ABCG1-mediated cholesterol efflux has been reported to contribute to the anti-inflammatory effects (248). Interestingly, apoA-I has also been shown to attenuate palmitate-induced NF-κB activation by reducing toll-like receptor-4 recruitment into lipid rafts (249).

The phopsholipid constituents of HDL have been also proposed to exert the anti-inflammatory effects of HDL. The VCAM-1-mediated inhibition by rHDL-AI varied substantially when different phosphatidylcholine species were compared (250), while the activation of E-selectin by TNFα was prevented by two lysosphingolipids associated with HDL (251).

The effect of HDL on endothelial cell apoptotic pathways

Apoptotic cell death following injury of vascular endothelium is assumed to play an important role in the pathogenesis of atherosclerosis. Notably, it has been reported that HDL inhibits apoptosis triggered by various proatherogenic factors, such as TNFα (252, 253), and growth factor deprivation (254). Additionally, in a mouse model of atherosclerosis the administration of HDL resulted in the reduction of endothelial apoptosis (255).

Several mechanisms have been proposed for the endothelial anti-apoptotic effects of HDL. Suc and colleagues reported that HDL inhibits ox-LDL cell death by preventing the oxLDL-mediated increase in intracellular calcium (253). Additionally, HDL has been identified to suppress the Caspase 3 (Cas-3) activation and as a result, to inhibit the ox-LDL- (256) and the TNFα- (252) mediated apoptosis. Interestingly, these effects were mimicked by lipid-free apoA-I which was shownto inhibit apoptosis through binding to the F1-ATPase receptor (257). However, the exact mechanism of this effect is not clearly understood. It has also been shown that HDL through the PI3K/AKT pathway upregulates the anti-apoptotic molecule Bcl-xL preventing from apoptosis which is induced by growth deprivation (255). Interestingly, this effect of HDL was mediated by the apolipoprotein J (apoJ) in a NO-independent pathway (255).

Besides the protein component, the lipid component has also been reported to mediate the anti-apoptotic effects of HDL. Nofer and colleagues observed that the two lysosphingolipids associated with HDL, sphingosylphosphorylcholine and lysosulfatide,

mimicked HDL functionality in the inhibition of apoptosis caused by growth deprivation (254). Specifically, they observed that the inhibitory effect was mediated through the activation of PI3K/AKT pathway which in turn prevented both Cas-3 and Cas-9 activation (254). In addition to this effect, PI3K/AKT activation inhibited, via phosphorylation, the Bcl-2-associated death promoter Bad, preventing it from binding to Bcl-xL and thus allowing Bcl-xL to inhibit mitochondria-mediated apoptosis (254). Moreover, S1P bound to HDL by interacting with the S1P1 receptor inhibited Cas-3 activation and consequently apoptosis caused by growth deprivation. This effect was mediated independently by the activation of PI3K/AKT and ERKs (258). Recently, it was reported that plasmalogens, which are a low abundance lipid subgroup of phospholipids, inhibits the apoptotic effect of growth deprivation (259).

Effects of HDL on endothelial repair processes

Injury of the endothelium and consequently disruption of endothelial permeability is a hallmark for the progression of atherosclerosis. It has been demonstrated that HDL induces endothelial repair mechanisms by affecting the proliferation and migration of adjacent endothelial cells (260), by recruiting endothelial progenitor cells (EPC) (261) and by promoting angiogenesis (262).

HDL stimulates endothelial proliferation through both apoA-I (263) and S1P (260) constituents. Interestingly, HDL and mainly apoA-I induces proliferation through binding to the ecto-F1-ATPase receptor and activating the PI3Kβ isoform, which in turn activates the AKT pathway (263).

In vitro studies utilizing wound healing assays or trans-wells have indicated the ability of HDL to induce endothelial cell migration via the activation of the small GTPase Rac (264, 265). In a work by Seetharam et al., Rac was activated by native HDL or rHDL-AI through the binding to SR-BI receptor and the following activation of Src, AKT and ERKs. This

regulation was independent of the NO production (264). Interestingly, in the same study they observed that Rac activation promoted the formation of lamelipodia, a characteristic feature of migration (264). Importantly, the SR-BI adaptor protein, PDKZ-I, was required for the SR-BI-mediated migration (266). Further studies showed that carotid artery re-endothelialization after perivascular electric injury was ameliorated in apo-AI$^{-/-}$ mice, and adenoviral overexpression of apoA-I rescued normal re-endothelialization (264). Moreover, S1P has, also, been reported to stimulate migration through the activation of Rac (265). This regulation was mediated through S1P1 or S1P3 receptors and involved the activation of AKT and p38-MAPK (265). Recently, an additional mechanism of S1P-mediated migration was reported. Specifically, HDL-S1P induced both the expression and the activation of VEGFR2 resulting in cell migration (260).

Several studies have demonstrated that, upon injury of the endothelium, the circulating endothelial progenitor cells (EPCs), which are bone-marrow derived mononuclear cells, are recruited to the injury areas participating in re-endothelialization and neovascularization processes (267). Interestingly, in mouse models of atherosclerosis, either adenoviral overexpression of apoA-I (268) or intravenous infusion of rHDL-AI (261) led to an increase of the circulating EPCs and the induction of their incorporation into the regenerating endothelium, while the neointima formation was attenuated. SR-BI deficiency in bone marrow abrogates EPC incorporation induced by HDL (269). *In vitro* and *ex vivo* studies have confirmed that HDL stimulated EPCs differentiation through the activation of PI3K/AKT pathway (270) and affects their functionality and viability through NO-dependent pathways (269, 271). Recently, it has been reported that ABCG1 (272) and ecto-F1-ATPase receptor (263) also play an important role in EPCs functionality mediated by HDL.

Another beneficial effect of HDL is its capacity to promote capillary tube formation *in vitro* (273) and hypoxia-driven angiogenesis *in vivo* (262). Hypoxia-driven physiological angiogenesis is critical for tissue neovascularization after ischemic injury such as myocardial infraction (MI) (274). Of note, both *in vivo* and *in vitro*, rHDL augmented hypoxia-induced

angiogenesis but inhibited the inflammation-induced angiogenesis (275). The molecular basis of this difference is the conditional regulation of hypoxia-inducible factor-1a (HIF-1α), VEGF and VEGFR2, which were attenuated in response to TNFα, but augmented by rHDL in response to hypoxia (275). Furthermore, it has been indicated that HDL augments hypoxia-mediated angiogenesis through the post-translational regulation of HIF-1α (262). Specifically, HDL through SR-BI/PI3K/AKT axis upregulates the expression of the ubiquitin ligases Siah1 and Siah2, which target and promote the degradation of the prolyl hydroxylases, PHD2 and PHD3, leading to HIF-1α stabilization, which in turn induces VEGF expression promoting angiogenesis (Fig. 1.14) (262). Additionally, in mouse models of impaired ischemic-mediated angiogenesis the intravenous infusion of rHDL-AI restored blood flow recovery and capillary density, while the topical application of rHDL-AI rescued impaired wound closure (276, 277). These effects of rHDL-AI implicated VEGF (276) and HIF-1 (277) regulation and were attenuated in SR-BI$^{-/-}$ mice (277).

.

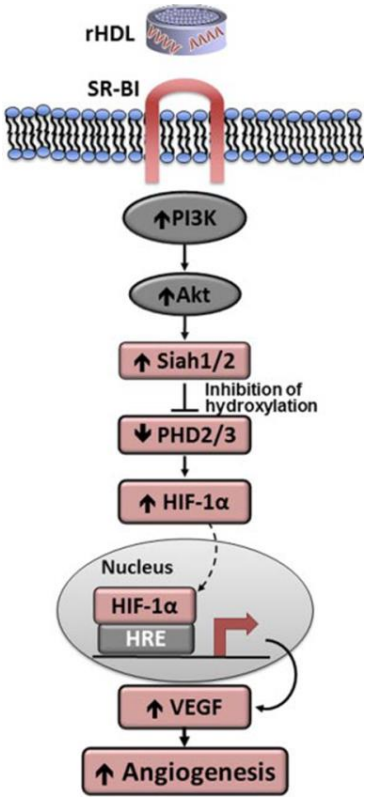

Figure 1.14 The mechanism of action of rHDL in hypoxia-driven angiogenesis (262)

Effects of HDL on endothelial thrombotic activation

As lesion development progresses, rupture or erosion of the plaque leads to platelets aggregation and thrombus formation resulting in rapid occlusion of the vessel and subsequent deleterious effects. Under physiological conditions, endothelium exhibits anticoagulant and fibrinolytic properties, while injury of endothelium triggers thrombotic response. An anti-thrombotic effect of HDL in humans was suggested by a study in healthy subjects where infusion of reconstituted HDL limited their procoagulant state after endotoxin exposure (278).

The main mechanism contributing to anti-thrombotic effects of HDL is its ability to induce endothelial prostacyclin (PGI_2) synthesis (279). The vasodilator PGI_2 acts synergistically with NO to induce vascular smooth muscle relaxation, inhibits platelet activation, and diminishes the release of growth factors that stimulate the local proliferation of smooth muscle cells (280). HDL-mediated release of PGI_2 occurs by both the provision of arachidonate (281) and upregulation of Cox-2 expression (279). Interestingly, it has been reported that HDL through ABCA1 activates a signaling cascade including p38-MAPK, ERKs and JAK2 activation resulting in Cox-2 upregulation (282). Additionally, it has been demonstrated that the effect of HDL on Cox-2 expression and PGI_2 production is mediated by SR-BI and the activation of PI3K/AKT/eNOS signaling axis (283).

Besides the HDL-mediated release of PGI_2, HDL affects the expression of additional proteins participating in the thrombotic response. Specifically, HDL inhibits the thrombin-mediated (284, 285) and TNFα-mediated (286) expression of endothelial tissue factor (TF), which is the primary initiator of coagulation. Moreover, HDL increased endothelial tissue factor pathway inhibitor (TFPI) expression and tissue plasminogen activator (tPA) release, and inhibited thrombin-induced plasminogen activator inhibitor type 1 (PAI-1) expression (284). These effects of HDL were dependent of NO production (284). Recently, it was shown that HDL prevents self-association of VWF reducing the extent of VWF fiber formation and resulting in the inhibition of platelet adhesion to stimulated endothelial cells (287). These

observations were consistent with *in vivo* experiments in a mouse model of thrombotic microangiopathy where HDL was able to reduce thrombocytopenia when co-injected with vWF (287).

1.5.3 The antioxidant properties of HDL

As we described above, oxidation of the trapped LDL particles in the sub-endothelial space is a hallmark for atherogenesis. Of note, many studies have shown that HDL prevents LDL oxidation through different mechanisms (288). HDL directly inhibits oxidation of LDL via transfer of oxidation products (such as lipid hydroperoxides (LOOH)) from LDL to HDL (289). This transfer can occur directly between lipoprotein phospholipid monolayers, either spontaneously or mediated by lipid transfer proteins, including CETP (290). ApoA-I plays a crucial role in the anti-oxidant effects of HDL since it binds and removes LOOH from LDL (291). Also, apoA-I inactivates by reduction the HDL-associated LOOH (292, 293). Besides apoA-I, other apolipoproteins, including apoE, apoA-II, apoJ and apoM, have been identified to have anti-oxidant effects (288). Notably, HDL carries also anti-oxidant enzymes that may be involved in prevention of lipid oxidation or degradation of LOOH, such as paraoxonase-1 (PON1), LCAT and platelet-activating factor acetylhydrolase (PAF-AH) (294, 295). In particular, PON1 has been suggested to be crucial mediator of HDL anti-oxidant properties (296, 297).

1.5.4 The immunomodulatory effects of HDL

In addition to the anti-inflammatory effect of HDL on endothelial cells, accumulating evidence suggest a critical role of HDL in regulating immunologic functions of both innate and adaptive immune responses (298). It has been reported that HDL, by suppressing the expression of the monocyte adhesion molecule CD11b, prevents the adhesion of monocytes (299) and neutrophils (300) to endothelial cells. These effects were dependent of ABCA1-

mediated cholesterol efflux leading to disruption of the specific membrane microdomains enriched in cholesterol and sphingolipids called lipid rafts.

Once monocytes leave the circulation and migrate into the atherosclerotic lesion area, they differentiate into two main macrophage populations, based on the different cytokines produced in the microenvironment: M1—classically activated, which promote inflammation or M2—alternatively activated known to decrease immune reactions (301). Notably, in a mouse transplantation model of atherosclerosis regression, HDL enhanced macrophage polarization to the M2 population contributing to atherosclerotic plaque regression (302). Moreover, many studies have shown that HDL prevents macrophages from TLR-mediated inflammatory response (298, 303). Toll-like receptors (TLRs) are receptors that recognize several conserved pathogen-associated molecular patterns (PAMPs) and induce a signal transduction cascade resulting in the expression of pro-inflammatory cytokines (304). TLRs are localized in lipid rafts and thereby one potent mechanism of the inhibitory effect of HDL is through the disruption of lipid rafts (298). On the meanwhile, De Nardo and colleagues suggested an additional mechanism, which is independent of disruption of TLR signaling but depends on the induction of transcription regulator ATF3 (305). Specifically, they observed that pre-incubation of bone marrow derived macrophages (BMDMs) with HDL induced both the mRNA levels of ATF3 and its binding to the genome. Therefore, ATF3, which acts as a negative transcription factor, inhibits the induction of cytokines in the presence of TLR stimuli (305). In contrast to the anti-inflammatory effects of HDL, a recent study indicated a pro-inflammatory effect of HDL on macrophages via passive cholesterol depletion highlightening the complexity of HDL functionality (306).

Accumulating evidence also indicate the involvement of inflammasome activation in the process of atherosclerosis (307, 308). Importantly *in vitro* studies utilizing THP-1 macrophages indicated that both native HDL and rHDL-AI, by decreasing the expression of several key inflammasome components, such as IL-1β and NLRP3, inhibit the

inflammasome activation mediated by cholesterol crystals (309). Additionally, in a mouse model of obesity, adenoviral apoA-I gene transfer led to a decrease in aortic NLRP3 mRNA levels (310). Again, cholesterol efflux mechanisms in myeloid cells mediated by ABCA1 and ABCG1 seem to be crucial for the modulation of inflammasome activity (311).

Finally, HDL has been associated with inhibition of T cell and B cell activation (312). Besides the fact that T-cell receptor (TCR) and B-cell receptor (BCR) are localized in lipid rafts suggesting that their activity is strictly modulated by alterations in the lipid raft composition (313), HDL also prevents T cell activation by the antigen presentation cells (APCs) such as B cells, macrophages and dendritic cells (DCs) (314). This effect is also mediated through the disruption of lipid rafts and subsequently the reduction in the density of major histocompatibility complex II (MHCII) (314). Interestingly, it has been reported that rHDL-AI suppresses dendritic cell functionality through the inhibition of NF-κB/MyD88 axis resulting in a reduction of T-cell proliferation and subsequently attenuating Th1 and th17 autoimmune responses (315). Recent studies in mice identified a key role of apoE expressed by myeloid cells in dendritic cell functionality and the subsequent T cell activation regardless of the onset of hypercholesterolemia (316).

The protective properties of HDL against the development of atherosclerosis are summarized in Figure 1.15.

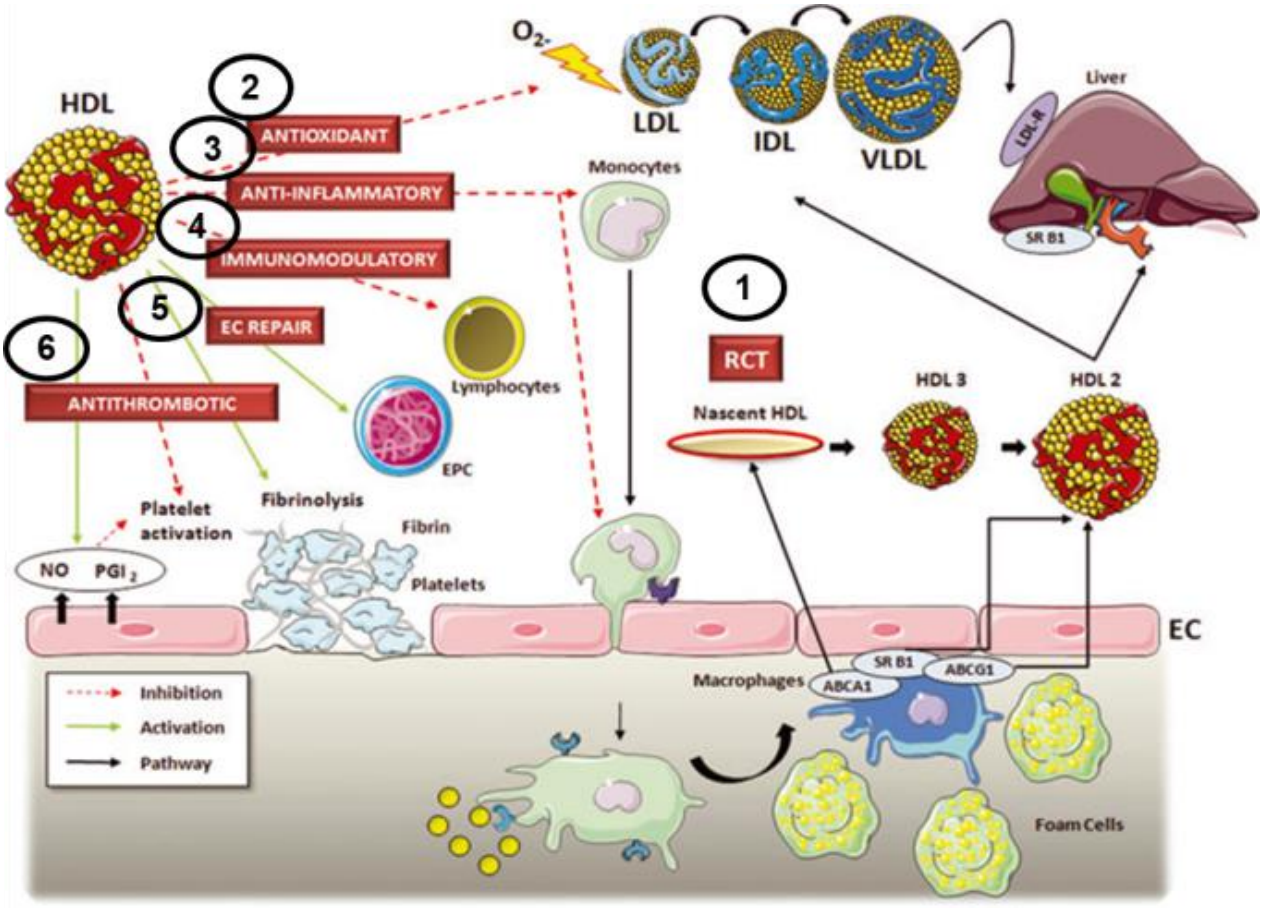

Figure 1.15 A schematic representation of the atheroprotective properties of HDL (4).

1.6 The Impact of Atherosclerosis on HDL Functionality

1.6.1 Dysfunctional HDL in Patients with CVDs

A study from Landmesser group in 2011 demonstrated that HDL isolated from patients with Coronary Artery Disease (CAD) had lost its protective properties in endothelium (317). Specifically, they treated primary human endothelial cells (HUVECs) with HDL isolated from healthy subjects, patients with stable CAD and patients with acute coronary syndrome (ACS) and they observed that HDL from all patients was unable to promote NO production (317). As a consequence, HDL from patients (either with CAD or ACS) did not inhibit TNFα-mediated endothelial adhesion molecule expression (impaired anti-inflammatory properties), while it also failed to promote re-endothelialization in a mouse model with carotid artery injury (impaired endothelial repair capacity) (317). Since then, a broad spectrum of dysfunctions of HDL in patients with CAD has been described (294), including a reduced cholesterol efflux capacity from macrophages and other cells (318), lack of the anti-apoptotic (255) and anti-thrombotic (284) effects in endothelium, as well as impaired anti-oxidative properties (319). In several cases, HDL was not only characterized by loss or reduced functionality but also by the gain of atypical functions. For example, HDL from patients with CAD or ACS not only failed to inhibit apoptosis in endothelial cells but also stimulated pro-apoptotic pathways (255). Besides CAD and ACS, dysfunctional HDL has been detected in almost all CVDs including heart failure (320), ischemic cardiomyopathy (321), stroke (322) as well as in many conditions that are known to increase cardiovascular risk such as type 2 diabetes (323), chronic kidney disease (324, 325), chronic inflammatory diseases (326), and familial hypercholesterolemia (327, 328).

1.6.2 Compositional Changes and Modifications in Dysfunctional HDL

The molecular changes that underlie HDL dysfunction may relate to compositional changes of the lipoprotein's proteome, alterations of the lipid moiety and other cargo molecules, or post-translational modifications of the HDL-associated proteins. Many studies have shown that in the state of chronic inflammation, such as atherosclerosis, the composition of HDL is altered leading to impaired functionality (329, 330). In fact, proteomic studies from patients with CAD revealed that HDL particles are enriched in the acute phase inflammatory proteins Serum Amyloid A (SAA) and Complement C3, while the levels of the atheroprotective apoA-I and the anti-oxidant PON1 and PAF-FH are decreased (331-333). Interestingly, Riwanto and colleagues identified an increase of the pro-inflammatory protein apoC-III in HDL particles with a parallel decrease of the anti-apoptotic clusterin (apoJ) converting HDL from an anti-apoptotic molecule to a pro-apoptotic one (255). Furthermore, lipidomic studies also revealed changes in the lipid content of HDL isolated from patients including higher triglyceride levels and lower total phospholipid levels, while the levels of oxidized phospholipids were increased (330, 334). Importantly, the levels of HDL-bound S1P are also decreased in dysfunctional HDL (330, 335).

Under inflammatory and oxidative conditions proteins of HDL undergo certain post-translational modifications which also compromise the beneficial properties of HDL. Such a case is the modifications in the apoA-I molecule mediated by MPO resulting in impaired ability of HDL to promote ABCA1-mediated cholesterol efflux (330). Myeloperoxidase (MPO) is a heme protein released by macrophages, monocytes and neutrophils, that causes oxidative modifications to a plethora of proteins (336). MPO targets apoA-I directly, mainly in the subendothelial compartment (337), causing oxidative chlorination and nitration to multiple residues of apoA-I (338). ApoA-I with nitrated or chlorinated residues Tyr-192, Tyr-18, and Tyr-166 or oxidized Trp-72 has been isolated from human atheroma tissues (338-341). *In vitro* and *ex vivo* studies showed that MPO-mediated modifications of apoA-I generate HDL particles with impaired atheroprotective properties (330, 338). Interestingly, it

was demonstrated that in mouse models of atherosclerosis, the infusion of MPO-modified apoA-I did not promote beneficial alternations to plaque composition compared to infusion with non-oxidized apoA-I (342).

1.7 HDL as a Therapeutic Target for CVDs

1.7.1 HDL-based therapies

Pharmacologic intervention for the treatment of atherosclerosis originally focused on lowering serum LDL-C concentrations as a therapeutic target. Indeed, the use of HMG-CoA reductase inhibitors (statins) has resulted in reduction of cardiovascular events and overall mortality (343). However, residual risk among high-risk patients remains (344), while other individuals have been intolerant to statins either incompletely or completely (345) suggesting that complementary therapy is needed. Of note, patients with low LDL-C levels, after receiving treatment with statins, show low HDL-C levels that remain predictive of future CVD event (209). Based on epidemiological evidence and on the biological properties of HDL, it was hypothesized that raising HDL-C levels will lead to a decrease in cardiovascular events (named “HDL hypotheses”). Therefore, research was focused in developing drugs that raise HDL-C levels.

The first class of drugs utilized for targeting HDL-C levels was the established hypolipidemic drugs: statins, fibrates and niacin which promote an increase in HDL-C levels by 2-10%, 5-15% and 15-30% respectively (346). However, this increase was not associated with a reduction of the risk for cardiovascular events in clinical trials. For instance, the cardioprotective effects of statins are due to the decrease in the LDL-C levels and not to the increase in HDL-C (347). Moreover, neither fibrates (348) nor niacin (349) administration resulted in cardiovascular benefits beyond statin therapy in recent outcome studies.

A different approach to raise the endogenous levels of HDL is the intervention in the metabolic pathway of HDL and thus a variety of drugs targeting different steps of this pathway have been developed (Fig.1.16). Among the most promising drugs are: inhibitors for CETP (HDL remodeling), agonists for LXRs (HDL biogenesis), agonists for PPARs (HDL

hydrolysis), recombinant LCAT (HDL maturation) and RVX-208 which inhibits the BET transcription regulatory proteins (apoA-I inducers) (350, 351). There is a considerable piece of evidence from animal studies that most of the above drugs promote an important increase in the concentration of HDL which is associated with inhibition or even reversion of atherosclerosis (352). Nevertheless, these treatments have not been successful in clinical trials (352-354). Furthermore, some of the interventions caused important side effects such as torcetrapib (first generation CETP inhibitor) which increased HDL-C levels by 80%, but it also increased morbidity and mortality (355). In line with the results from clinical trials, Mendelian randomization studies did not report any relationship between polymorphisms in genes that influence HDL cholesterol levels (such as ABCA1, SR-BI, LIPG and LCAT) and cardiovascular event rates (356-358). Interestingly, Zanoni and colleagues observed recently that a rare variant in SR-BI that abrogates selective HDL-cholesterol uptake, raised HDL-cholesterol but it increased the risk of coronary heart disease (359). From this result, combined with the deleterious effects of torcetrapib, we could conclude the following: 1) intervening with the complexity of the metabolic pathways could produce deleterious side effects; 2) HDL-C concentration in plasma should no longer be considered to reflect the atheroprotective capacity of HDL. At this point we should mention the unexpected results from a recent epidemiological study, in which individuals with extremely high HDL-C levels were paradoxically associated with elevated mortality as compared to normal HDL-C individuals (360).

Since the therapeutic approaches targeting only the raising of HDL-C levels were insufficient to produce the anticipated clinical benefits, the focus has been shifted toward strategies to improve HDL functionality. ApoA-I is the major functional component of HDL and so therapies designed to mimic apoA-I function are being developed, and include: full length apoA-I, mutated variants of apoA-I with improved functionality (apoA-I Milano), reconstituted HDL particles (rHDL) and apoA-I mimetic peptides (Fig. 1.16) (354).

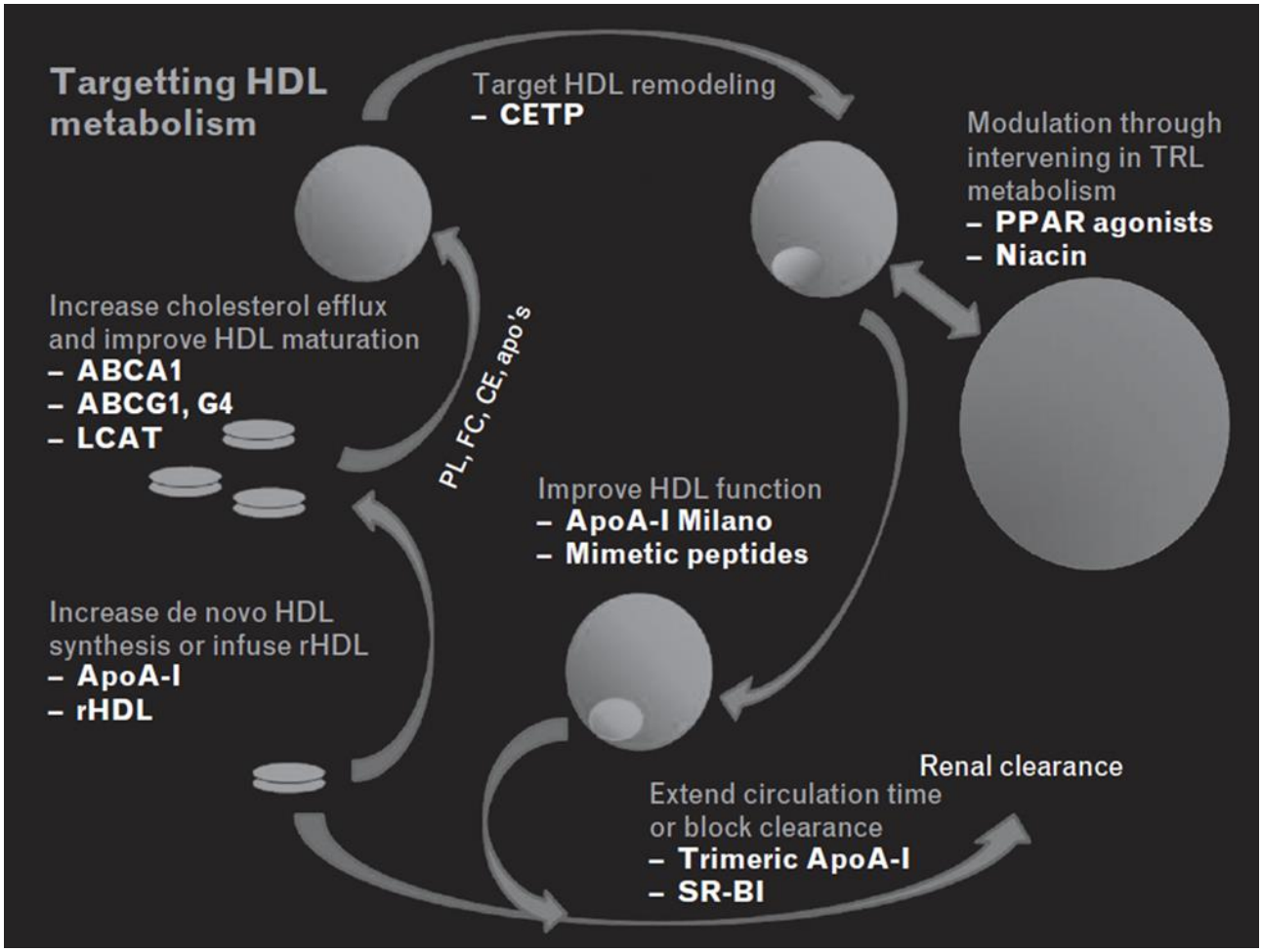

Figure 1.16. Therapeutic interventions targeting HDL metabolism (350).

As we discussed in previous chapters, numerous *in vitro*, animal and small clinical studies have reported the atheroprotective effects of rHDL and consequently make it a promising target for the reduction of CVD risk. Therefore, a variety of rHDL compounds have been checked in clinical trials with patients with an acute coronary syndrome (ACS) event. The first rHDL compound that was used in that type of studies was ETC-126 which consists of the apoA-I_{Milano} variant and phospholpids and it showed promising results (361). Specifically, administration of ETC-126 over a 5-week period produced a reduction of atheroma volume by 4.2% compared with baseline (361). However, in a recent larger study (MILANO-PILOT study), MDCO-216 compound (ETC-216; renamed by the new license owner) failed to reproduce the previous results since its administration did not result in

plaque regression (362). The main difference between these two studies is that all the patients from the latter study have received background statin therapy, while this was not the case for all patients in the former study. According to the authors of MILANO-PILOT study this fact may reflect a false-positive finding in the former study (362). Furthermore, rHDL compound containing the wild type apoA-I has also been used in clinical trials in patients with an ACS event. Among them, the most prominent are CER-001 and CSL-112. CER-001 consists of wild type apoA-I, diphosphatidylglycerol and sphingomyelin and mimics nascent pre-β HDL (363). The promising role of CER-001 has been reported in studies with patients with familial hypoalphalipoproteinemia (FHA) (364) and homozygous familial hypercholesterolemia (365). In these two small studies, infusions of CER-001 (over a period of 6 months) resulted in regression of atherosclerosis, as it was assessed with MRI scans of the carotid arteries. However, in the recent CARAT study with patients following an ACS event within 14 days, CER-001 did not promote regression of coronary atherosclerosis (365). Moreover, the prominent compound CSL-112, which consists of wild type apoA-I and phospholipids, it is now tested in the ongoing phase III AEGIS-II study which is expected to be concluded in 2022 (366).

Till today there is not a large clinical study to confirm that targeting HDL will lead to a reduction either of CVD risk or an ACS event. However we should take into account that the majority of these studies were performed in patients with stable cardiovascular disease after having an ACS event. In this case, there is a great atheromatic environment that affects the functionality of HDL and probably the functionality of the newly synthesized or infused HDL particles. As a result, the potential anti-atherogenic effects of the treatment are compromised. Therefore, different approaches should be followed. Such an approach could be to target to the mediators or effectors of HDL action.

1.8 Transcriptomics as a Tool to Understand HDL Functionality

The transcriptomics applications combined with bioinformatics has contributed substantially to the understanding of the physiology and pathophysiology of all biological processes. Specifically for complex disorders, such as CVDs, the use of DNA Microarrays or RNA-seq technologies helped to: 1) elucidate the molecular mechanisms underlying the impaired functionality of endothelial cells, vascular smooth muscle cells and macrophages during the development of atherosclerosis (367); 2) understand the impact of environmental factors for the initiation and progress of the disease (368); 3) validate the causality of genes identified from GWAS studies (367); and 4) identify biomarkers in order to improve the treatment of the disease (368).

In the field of HDL, transcriptomic studies performed by De Nardo and colleagues revealed that HDL regulates the macrophage inflammatory response at the transcriptional level (305). Specifically, they observed that HDL induces the expression of the transcriptional repressor *ATF3,* which in turn inhibits the pro-inflammatory cytokine-mediated induction by TLRs (305). In the same context, transcriptomic studies were performed by the collaboration between Dr. V.I. Zannis and Dr. D. Kardassis in order to characterize the impact of HDL on the global gene expression profile of the endothelium. Specifically, endothelial cells were treated with rHDL-AI and then microarray analysis was performed (369). Among the genes that their expression was changed by HDL were the genes for ANGPTL4 and LIPG. In the context of this thesis, we focused on these genes in order to validate that they are true HDL-target genes and also to elucidate the mechanisms through which HDL regulates their expression.

1.8.1 ANGPTL4

Structure and Expression Patterns

Angiopoietin-like protein 4 (ANGPTL4) is a secreted protein that belongs to the family of angiopoietin-like proteins (ANGPTL1–8). Like other proteins of this family, ANGPTL4 contains a C-terminal fibrinogen-like domain (CCD) and an N-terminal coiled-coil folding domain (FLD) which are connected via a cleavage linker (370). ANGPTL4 is expressed in many cells and tissues, including adipose tissue, liver, endothelium, intestine, and muscle, whereas the expression patterns of the other members of the ANGPTL family are more cell-specific (371). The human *ANGPTL4* gene is located on chromosome 19p13.3 and is well preserved amongst various species (372). The encoded full length ANGPTL4 protein (flANGPTL4), with a molecular mass of 50 kDa, undergoes several post-translational modifications including glycosylation, oligomerization, and cleavage (373). ANGPTL4 can form higher order structures such dimers and tetramers through the formation of intermolecular disulfide bonds (374). After secretion, the flANGPTL4 protein is cleaved into a 37-kD C-terminal (cANGPTL4) and a 15-kD N-terminal (nANGPTL4) fragments by proprotein convertases (375, 376) (Fig. 1.17). The cleavage of ANGPTL4 is tissue-dependent and as a result ANGPTL4 can be detected in the bloodstream in different isoforms such as glycosylated, oligomerized, native, and cleaved. Adipose tissue secretes full-length ANGPTL4, while the liver secretes nANGPTL4 isoforms (377).

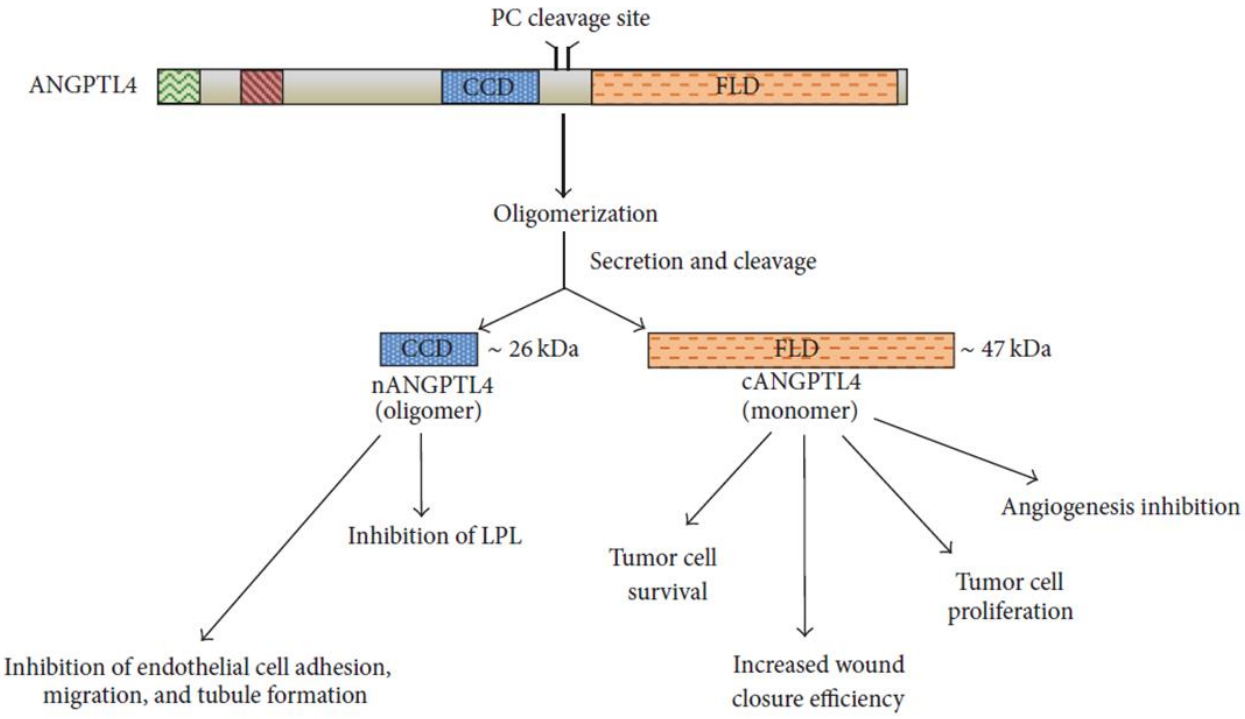

Figure 1.17 Structure and function of ANGPTL4 domains (378).

ANGPTL4 Function

ANGPTL4 is a protein known primarily for its role as an inhibitor of lipoprotein lipase (LPL) (371). LPL is an enzyme that hydrolyzes the triglycerides from circulating lipoproteins (chylomicrons and VLDL) generating free fatty acids which in turn are distributed to the neighboring tissues for storage or utilization (379). Consequently, ANGPTL4 is an important regulator of lipid metabolism. Indeed early studies showed that overexpression of ANGPTL4 in mice leads to hypertriglyceridemia, whereas its deficiency leads to reduced circulating lipids (380). ANGPTL4 inhibits LPL activity through its nANGPTL4 domain (Fig. 1.17), while it has been reported that ANGPTL4 also promotes the intracellular cleavage and degradation of LPL in the adipose tissue (381). Besides participating in lipid metabolism, ANGPTL4 has been also reported to be involved in several biological processes including angiogenesis, vascular permeability, cell differentiation, tumorigenesis, glucose

homoeostasis, energy homeostasis, wound healing, inflammation, and redox regulation (382) (Fig. 1.17).

Accumulating evidence from genetic studies revealed a strong correlation between a loss-of-function variant of ANGPTL4 (E40K) and CAD risk (383). The E40K mutation substantially reduces the ability of ANGPTL4 to inhibit LPL, likely by destabilizing ANGPTL4 via cooperative unfolding of the first a-helix of the coiled-coil domain (384). Most large-scale genetic studies have shown that the E40K mutation in humans results in reduced circulating TG levels, increased HDL-C levels, and protection against CAD (385-390). There was, however, one exception in a study, which showed that individuals with E40K mutation have an increased risk for CAD, despite having an athero-protective lipid profile (391). These discrepancies could have resulted from variations in the sample size and the ethnic diversity of the subjects used in the different studies. Moreover, plasma levels of ANGPTL4 have been shown to be a risk factor CAD independently of other traditional risk factors (392). Despite the promising results from genetic studies, inactivation of ANGPTL4 in mice causes a lethal phenotype upon feeding a standard high-fat diet characterized by chylous ascites, a massive acute phase response, and enlarged mesenteric lymph nodes filled with Touton giant cells (387, 393, 394). Disposal accumulation of lipids in mesenteric lymph nodes was also observed in several female monkeys treated with an anti- ANGPTL4 antibody (387).

In contrast to genetic studies, mouse models of atherosclerosis reported an atheroprotective role of ANGPTL4 through is function on macrophages. Specifically, Georgiadi and colleagues observed that overexpression of ANGPTL4 in apoE3.Leiden mice (in a high fat diet background) reduced atherosclerosis by 34% (Fig. 1.18A) by decreasing foam cell formation, the macrophage content of the plaques and the number of monocytes adhering to the endothelium (395). Thus, overexpression of ANGPTL4 leads to a less inflammatory lesion phenotype. An additional study from Fernandez-Hernando lab confirmed the atheroprotective role of ANGPTL4 expressed by macrophages. In this study, they initially observed that total deficiency of ANGTPL4 in a mouse model of atherosclerosis attenuated

atherosclerosis. However, these mice were characterized by severe gut inflammation and decreased survival. Importantly, they observed that ANGPTL4 deficiency in haematopoietic cells promoted monocyte expansion and atherosclerosis progression (396). Specifically, it was shown that ANGPTL4 deletion in haematopoietic cells resulted in larger plaque area (Fig. 1.18B) with bigger necrotic core and increased macrophage apoptosis. Furthermore, ANGPTL4 deficiency in macrophages promoted foam cell formation by enhancing CD36 expression and reducing ABCA1 localization in the cell surface (396). In contrast, in a subsequent study from the same lab, it was shown that ANGPTL4 deficiency in adipose tissue attenuated the progression of atherosclerosis. This effect was mainly by improving the circulating lipid profile, while no differences in the circulating inflammatory leukocytes were observed. From both of these studies we conclude that the exact ANGPTL4 functionality is dependent on the tissue in which it is expressed (397).

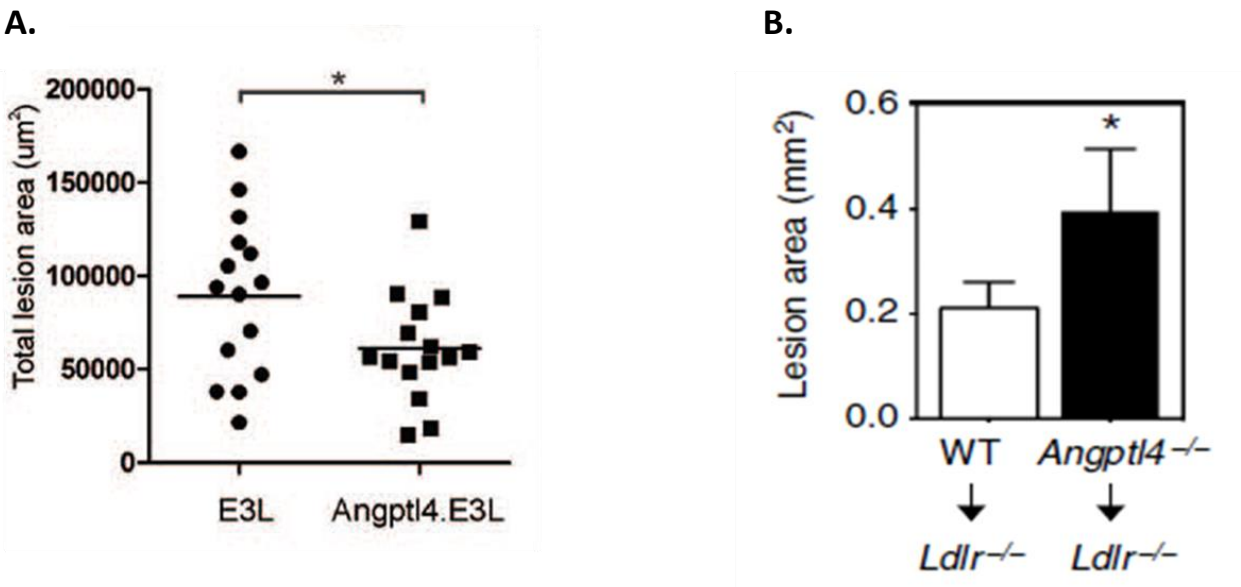

Figure 1.18 The atheroprotective role of ANGPTL4. A) Transgenic ApoE3*Leiden mice (E3L) overexpressing ANGPTL4 (Angptl4.E3L) had reduced size of lesions compared to E3L mice after 24 weeks of Western-type diet (WD) (395). E3L mice represent a human-like model of atherosclerosis. B) Ldlr-/- mice, another model of atherosclerosis, were transplanted with ANGPTL4-deficient bone marrow (BM) and resulted in significantly larger

atherosclerotic lesions size compared with the ones transplanted with WT BM after 12 weeks WD (396)

Regulatory mechanisms of ANGPTL4 expression

The expression of ANGPTL4 is under the regulation of a plethora of physiological stimuli including: fasting, hypoxia, chronic caloric restriction, short-term cooling, high-fat diet, and free fatty acids (382). Depending on the stimuli, several transcription factors have been identified to be involved in the regulation of this gene with PPARs and HIF1 act as the main upregulators. Indeed, a functional PPAR element has been identified at the third intron of ANGPTL4 gene (2kb downstream of the TSS), through which PPARs activate this gene (398). A potent mechanism through which PPARs regulate ANGPTL4 has been proposed by Jin and colleagues after studies in MEFs (399). Briefly, in the absence of ligand, PPARδ is bound on the PPRE motif of the ANGPTL4 gene recruiting transcription corepressors to repress ANGPTL4 expression. Ligand binding leads to a conformational change of PPARδ, which dissociates from co-repressors and associates with the CBP/p300 coactivator. The recruited CBP/p300 specifically acetylates the histones H3K18 and H3K27 on the ANGPTL4 promoter resulting in the recruitment of Pol II to initiate transcription. (399) Furthermore, HIF1 upregulates the expression of the *ANGPTL4 gene* through the binding to a hypoxia responsible element (HRE), which is located on the distal region of the promoter (2kb upstream of the TSS) (400). Of note, Inoue and colleagues reported a synergistic action between PPARβ/δ and HIF1 in order to induce ANGPTL4 expression (401). By utilizing Chromatin Conformation Capture (3C) and ChIP-seq analysis, they observed that this induction was dependent on the conformational proximity of the two elements (401). This is not the first report that shows a synergistic action between two transcription factors in order to regulate ANGPTL4 expression. Previous work in human myofibroblasts revealed that a novel TGFβ-responsive upstream enhancer (TGF-E) which is located at the -8kb region upstream of the TSS of the human ANGPTL4 gene cooperates with the PPAR-E in the third

intron of the gene to mediate synergistic ANGPTL4 upregulation by TGFβ signalling and PPARγ ligands the synergistic action between (402).

1.8.2 LIPG

Structure and expression patterns

Endothelial lipase (LIPG) belongs to the triglyceride lipase family which catalyzes TG from lipoproteins. The other members of this family are the lipoprotein lipase (LPL), which is the most studied, hepatic lipase (HL) and pancreatic lipase (PL) and they present differential expression patterns. LPL is mainly synthesized by adipocytes, skeletal muscle cells, and cardiac muscle cells, HL is found in the liver, PL is produced by the pancreas and LIPG is primarily synthesized by vascular endothelial cells (403). *LIPG* gene is located on chromosome 18 and encodes a 55 kDa protein which undergoes post-translational glycosylation and then is secreted from the cell as a 68 kDa protein. After secretion, LIPG binds to proteoglycans on the cell surface where it exerts its function (404). Mature LIPG shares amino acid sequence similarity of 44% with LPL, 41% HL and 27% with PL. All four enzymes share a similar catalytic region indicating functional conservation (403, 405). The main difference between LIPG and the other lipases lies within “lid” region which determines the substrate specificity. LIPG predominantly catalyzes phospholipids, while LPL, HL and PL function mainly with triglyceride substrates (403, 405, 406) . Therefore, HDL is the preferred substrate of LIPG.

LIPG Function

The primary role of LIPG is to mediate HDL catabolism through the hydrolysis of HDL-phospholipids (HDL-PL). LIPG overexpression in transgenic mice reduced the serum concentration of HDL-C levels (403, 407), while either LIPG deficiency in mice (408), or inhibition of mouse LIPG activity(409) resulted in a significant increase in plasma HDL-C and phospholipid levels, which was attributed to increased HDL particle size and reduced HDL phospholipid clearance. Besides its phospholipase functionality, LIPG maintains a minor

triglyceride lipase activity and thus is capable of hydrolyzing apo-B containing lipoproteins (410). By mediating HDL-PL hydrolysis, LIPG supplies cells with free fatty acids (both saturated and unsaturated) and lysophospholipids supporting cellular metabolism (411). Interestingly, LIPG-mediated hydrolysis of HDL has been reported to mediate HDL functionality on endothelium. For instance, Ahmed and colleagues demonstrated that the LIPG-mediated hydrolysis of HDL activates PPARα, which in turn inhibits VCAM-1 expression in endothelial cells and subsequently suppresses leukocyte adhesion (412). Researchers from the same lab also reported that endothelial LIPG expression is determinant for the HDL-S1P mediated angiogenesis (413). Specifically, LIPG-mediated hydrolysis of HDL releases and activates S1P, which binds to $S1P_1$ receptor and promotes AKT and eNOS phopshorylation resulting in endothelial cell migration and angiogenesis (413). Additionally, it has been reported that LIPG mediates the IL-6-induced HDL translocation through the endothelium (414).

Moreover, LIPG has been shown to exert non-catalytic functions that are independent of its enzymatic activity. Strauss et al. demonstrated the ability of LIPG to facilitate the binding and uptake of HDL holoparticles, and the selective uptake of HDL-cholesterol esters (CE) in HepG2 cells (415). LIPG can also mediate the binding and uptake of apoB-lipoproteins. This process is dependent on heparin sulfate proteoglycans (HSPGs) on the cell membrane, which bind to LIPG. In this way, LIPG serves as a bridging molecule between plasma lipoproteins and cells (415, 416).

LIPG, through both its catalytic and non-catalytic functions, promotes HDL clearance from the circulation and, as a consequence, is a crucial determinant for HDL-C levels. This finding has been also supported by genetic studies in humans, in which SNPs in LIPG locus or loss-of-function LIPG variants are correlated with elevated plasma HDL-C levels (417). Since low HDL-C levels are correlated with high CVD risk, it was assumed that these polymorphisms in LIPG locus would be also correlated with CVD risk. However, none of these polymorphisms have been associated with CVD risk in large GWAS till today (417).

Additionally, the effect of LIPG in atherosclerosis is still unclear. In one study, LIPG deficiency in apoE$^{-/-}$ mice decreased the atherosclerotic plaque (418), while in another study LIPG deficiency in either apoE$^{-/-}$ or LDLR$^{-/-}$ mice fed a high fat diet was unable to inhibit atherosclerosis development (419). Interestingly, Hara and colleagues observed that HDL particles isolated from LIPG deficient mice have enhanced anti-inflammatory properties (420). Recently, it was reported that transgenic rabbits expressing the human LIPG gene in the liver exhibited significantly lower hypercholesterolemia and less atherosclerosis after feed with HFD compared to wild type rabbits (421).

Regulatory mechanisms of LIPG expression

Both *in vitro* and *in vivo* studies have shown that LIPG expression is under the regulation of inflammatory stimuli. It has been reported that TNFα, IL-1β (422) and IL-6 (414) upregulate LIPG in endothelial cells, while angiotensin 2 and hypertension (423) induce the expression of this gene in vascular smooth muscle cells. The activation of NF-κB plays crucial role in LIPG-mediated induction by cytokines. Studies by Kempe and colleagues demonstrated that there are two NF-κB sites in the promoter of the LIPG gene located at 467 and 1250kb upstream of the TSS (424). Endothelial NF-κB, after activation by TNFα, binds to these sites promoting the induction of LIPG expression (424). However, the exact role of LIPG in inflammatory conditions should be investigated further.

Moreover, it has been reported that systemic cholesterol and lipid levels could regulate the expression of LIPG. Specifically, in macrophages LIPG is upregulated by the saturated fatty acid palmitic acid, while the anti-inflammatory polyunsaturated fatty acid, eicosapentaenoic acid, decreased its expression (425). Furthermore, Kivella and colleagues showed that endothelial LIPG is upregulated in starvation conditions. This effect was mediated by the sterol regulatory element binding protein 2 (SREBP-2), which binds to three binding sites located at 292, 1901 and 2190 bp upstream from the transcription start site (426). This effect of starvation was inhibited in the presence of VEGFA making VEGFA a potent endogenous LIPG inhibitor (426).

2. MATERIALS AND METHODS

2.1 Materials

2.1.1 Reagents

Dulbecco's modified Eagle's medium, penicillin/streptomycin for cell culture, Dynabeads M-280 streptavidin, M-MLV Reverse Transcriptase and dNTPs were purchased from Invitrogen/Life Technologies (Carlsbad, CA, USA). Fetal bovine serum was purchased from BioChrom Labs (Terre Haute, IN, USA). Restriction enzymes were purchased from New England Biolabs (Beverly, MA, USA). Modifying enzymes (T4 DNA ligase, shrimp alkaline phosphatase) and human recombinant TNFα were purchased from Minotech (Heraklion, Greece). The luciferase assay system was purchased from Promega (Madison, WI, USA). PCR cleanup system was purchased from Macherey-Nagel (Duren, Germany). Protein G sepharose were purchased from GE healthcare (Waukesha, WI). The Super Signal West Pico chemiluminescent substrate was purchased from Pierce (Rockford, IL, USA). ONPG (onitrophenyl β-D-galactopyranoside), PMSF, aprotinin, benzamidine and the eNOS inhibitor L-NMMA (M7033) were purchased from Sigma (St. Louis, MO, USA). The PI3K/AKT inhibitor LY294002 and cycloheximide were purchased from Cayman Chemicals (Ann Arbor, USA). Lipopolysaccharides (LPS), the JNK inhibitor SP600125 and the p38 inhibitor SB203580 were purchased from Calbiochem/Merck (Billerica, USA). The ERK inhibitor UO126 and the FOXO1 inhibitor AS1842856 were purchased from Millipore/Merck (Billerica, USA). Lipofectamine RNAiMAX transfection reagent, Opti-MEM™ I Reduced Serum Medium and Hoechst 33342 were purchased from Thermo Scientific (Waltham, USA). Polyethylenimine (PEI) reagent was purchased from Polysciences (Warrington, USA). Universal cDNA Synthesis Kit II and LNA-optimized miRNA PCR primer sets were purchased by Exiqon (Vedbaek, Denmark). Biotinylated oligonucleotides were synthesized at VBC Biotech (Vienna, Austria). The HiPerFect transfection reagent, FOXO1 siRNA (Hs_FOXO1A_7 FlexiTube siRNA) and the negative control siRNA (AllStars Negative Contrl siRNA) were purchased by Qiagen (Hilden, Germany). All other oligonucleotides were

synthesized at the microchemical facility of the Institute of Molecular Biology and Biotechnology (IMBB) (Heraklion, Greece) or purchased from Eurofins MGW Operon (Ebersberg, Germany). HNF-4a siRNA and scrambled si-RNA were also synthesized at MWG. The 4–20% Mini Protean TGX precast gels (4561095) were purchased by Bio-Rad Laboratories (Hercμles, USA).

2.1.2 Antibodies

The primary antibodies utilized in this study are depicted in Table 2.1. The anti-mouse peroxidase-conjugated secondary antibody was purchased from Jackson Immunoresearch (West Grove, PA, USA), the anti-rabbit peroxidase-conjugated secondary antibody was purchased from Millipore/Merck (Billerica, USA) and the anti-goat peroxidase-conjugated secondary antibody was purchased from Sigma (St. Louis, MO, USA). Alexa fluor488 secondary was purchased from Thermo Scientific (Waltham, USA).

2.2 Animal Models

For the purpose of this study, we utilized transgenic mice carrying the human apoA-I/apoC-III gene cluster along with the human apoA-I gene as they have been described previously (427). These mice were lacking the expression of the endogenous mouse apoA-I gene. Mice were maintained at the animal facility of the Institute of Molecular Biology and Biotechnology of Crete on a 12 h light/dark cycle and fed standard rodent chow. For the isolation of HDL, blood was collected by cardiac puncture following a 4 h fasting period.

Table 2.1 Antibodies used for analysis of protein expression.

Antibody	**Application**	**Dilution***	**Incubation**
anti-phospho-AKT *Cell Signaling; Cat. No. 4060*	Western Blot	1:2000 in 5% BSA	Overnight at 4^{o}C
anti-total AKT *Cell Signaling; Cat. 4691*	Western Blot	1:2000 in 5% BSA	Overnight at 4^{o}C
anti-phospho-ERK *Cell Signaling; Cat. 4376*	Western Blot	1:1500 in 5% BSA	Overnight at 4^{o}C
anti-total ERK *Cell Signaling; Cat. 4695*	Western Blot	1:1500 in 5% BSA	Overnight at 4^{o}C
anti-phospho-p38MAPK *Cell Signaling; Cat. 4511*	Western Blot	1:2000 in 5% BSA	Overnight at 4^{o}C
anti-total p38MAPK *Cell Signaling; Cat. 8690*	Western Blot	1:2000 in 5% BSA	Overnight at 4^{o}C
anti-phospho-eNOS *Cell Signaling; Cat. No. 9570*	Western Blot	1:10.000 in 5% BSA	Overnight at 4^{o}C
anti-total FOXO1 *Cell Signaling; Cat. 2880*	• Western Blot • Immunofluorescence	• 1:1500 in 5% BSA • 1:35**	• Overnight at 4oC • Overnight at 4oC
anti-Histone 3 *Cell Signaling; Cat. 4620*	Western Blot	1:3000 in 5% BSA	Overnight at 4^{o}C
anti-phospho-JNK *Cell Signaling*	Western Blot	1:400 in 5% BSA	Overnight at 4^{o}C
anti-total JNK *Cell Signaling*	Western Blot	1:1000 in 5% BSA	Overnight at 4^{o}C
anti-phospho FOXO1 *Abcam; Cat. No. ab131339*	Western Blot	1:1500 in 5% BSA	Overnight at 4^{o}C
anti-LXRa *Abcam; Cat. No. ab41902*	Western Blot	1:500 in 2.5% BSA	Overnight at 4^{o}C
anti-HNF-4a *Santa Cruz Biotechnology; Cat. No.M19*	• Western Blot • ChIP	• 1:1000 in 5% not-fat milk • 5μg**	• Overnight at 4oC • Overnight at 4oC
anti-ANGPTL4 *Novus Biologicus; Cat. No. NBP2-19016*	Western Blot	1:500 in 5% BSA	Overnight at 4^{o}C
anti-actin *Chemicon Int.; Cat. No.MAB1501*	Western Blot	1:5000 in TBS-T	Overnight at 4^{o}C
anti-human apoA-I *Millipore; Cat No AB740*	Western Blot	1:4000 in 5% non-fat milk	Overnight at 37^{o}C
Rhodamine pholadin *Molecμlar Probes Cat. No.R415*	Immunofluorescence	1:100**	40min RT
Antibodies used for Western Blot were diluted in TBS supplemented with 1% Tween buffer (TBS-T) * Antibodies were diluted as described in the corresponding protocol			

2.3 Lipoproteins Manipulation Techniques

2.3.1 Serum isolation

Blood from either mice or human was collected in covered test tube containing no anticoagulant. Then, the blood was allowed undisturbed to clot at room temperature for about 30 minutes. The clot was removed by centrifuging at 2500 rpm for 15 minutes. After centrifugation, the supernatant (serum) was transferred immediately into a clean polypropylene tube. Serum is stored at -80 ^{0}C.

2.3.2 Preparation of HDL

HDL was purified from either the pooled serum of transgenic mice expressing human apoA-I (tgHDL) or from human healthy volunteers (hHDL). We utilized two different protocols for purifying HDL depending on the downstream application.

- Protocol 1: Separation of HDL from serum proteins

To study the effects of natural HDL on endothelial cells, HDL was separated from the other serum proteins (albumin, apoB-lipoproteins, lipid free proteins) using the density gradient ultracentrifugation method as described previously (428). Briefly, 0.3ml of pooled serum were diluted with 1XPBS (table 2.2) to a total volume of 0.5ml and then was adjusted to a density of 1.23 g/ml with KBr. This mixture was added in the bottom of centrifugal tubes (Beckman Coutler, Brea, USA) and then was overlaid sequentially with 1ml of KBr solution of a density (*d*) of 1.21g/ml, then with 2.5ml of KBr solution of *d*= 1.063 g/ml, then with 0.5ml of KBr solution of *d*= 1.019 g/ml and final with 0.5 ml 1XPBS. The mixture was centrifuged for 22h in a SW55 rotor at 30.000 rpm. Following ultracentrifugation, 0.5 ml fractions from the top of the centrifugal tube were collected separately into 10 plastic tubes. Next the fractions were dialyzed against 3L of 1XPBS (pH.7) for 22h at 4^{o}C using membranes with a molecular weight cut-off of 12,000-14,000 Daltons. The apolipoprotein composition of each fraction

was determined by SDS–PAGE and Coomassie Brilliant Blue staining (described below). Fractions containing the lipid bound apoA-I (fractions from 5 to 8) correspond to the different types of serum HDL (HDL_3, HDL_2) and therefore they were pooled forming a complete HDL solution. Then, HDL was sterilized through a 0.22-μm filter and stored at 4°C. Since apoA-I is the main protein that is present in the HDL preparation, HDL concentration was determined by the Lowry method.

- Protocol 2: Separation of HDL from apo-B Lipoproteins

In order to determine the levels of cholesterol bound on HDL, HDL was separated from the apo-B lipoproteins (LDL, VLDL) using the dextran-$Mg2^+$ method. Briefly, equal volumes of dextran sulfate (MP biomedicals) and $MgCl_2$ stock solutions were mixed to produce the precipitation solution consisting of 10 g/L dextran sulfate (pH=7.0) and 0.5 M $MgCl_2$ (pH=7.0). Serum samples were mixed thoroughly with precipitation solution at a volume ratio of 10:1 and incubated for 10 min at RT. After centrifigation at 1.400xg for 40 min at 4^oC, the HDL-containing supernatant was collected.

Table 2.2 Composition of 10XPBS

10XPBS (500ml)
5.75g Na_2HPO_4
1g KH_2PO_4
40g NaCl
1g KCl
Final volume with dH_20

2.3.3 Plasma lipids and FPLC analysis

Both HDL and total serum cholesterol levels were measured using the Infinity cholesterol reagent (Thermo Scientific, Waltham, MA), according to the manufacturer's instructions. Free cholesterol, phospholipids and triglycerides in the serum were determined

using the Free Cholesterol E, Labassay Phospholipid and Labassay Triglyceride reagents (Wako Chemicals Inc., Neuss, Germany), respectively. The concentration of cholesteryl esters in the serum was determined by subtracting the concentration of free cholesterol from the concentration of total cholesterol. For FPLC analysis, 40µl of plasma were loaded onto a Sepharose 6 PC column (GE Healthcare, Freiburg, Germany) and eluted with 1XPBS. A total of 70 fractions of 50 µl volume each were collected and then total cholesterol levels were measured.

2.4 Molecular Cloning Protocols

2.4.1 Plasmid constructs

The luciferase reporter constructs containing the human *ANGPTL4* promoter, (-2362/+77)-ANGPTL4 or the human *LIPG* promoter, (-2097/+171)-h*LIPG*-luc, were generated by PCR amplification of the corresponding fragments (table 2.2) using human genomic DNA as template and subsequent cloning into the KpnI-HindII sites of the pGL3basic vector (Promega Corp.).

The promoter constructs for both the human *LXRα* promoter, (2625/+385)-h*LXRa*-luc, and the mouse *LXRα* promoter, (-3000/+30)-mLXRa have been previously described (142) and were provided provided by Dr. Hashimoto. The promoter constructs containing consecutive 5' deletions of the h*LXRa* promoter, (-844/+384)-h*LXRa*-luc, (-457/+384)-h*LXRa*-luc, (-300/+384)-h*LXRa*-luc, (-111/+384)-h*LXRa*-luc, were generated as described previously (429). The reporter plasmids (-111/+384)-h*LXRa*-luc, (-42/+384)-h*LXRa*-luc and (-25/+384)-h*LXRa*-luc were generated by cloning the corresponding fragments into the KpnI-HindII sites of the pGL4 basic vector. These fragments were purified after PCR amplification

using the (-844/+384)-h*LXRa*-luc plasmid as template and the appropriate primers (table 2.3).

The (-844/+384)-mut-hLXRa plasmid bearing three point mutations in the HNF-4α binding site was generated by site-directed mutagenesis using the QuickChange Site-Directed Mutagenesis Kit (Stratagene) and the primers shown in Table 2.4 according to the manufacturer's instructions.

The plasmid constructs containing the wild type of 3-UTR of *apoE*, h*apoE*-3'UTR-luc, or a mutated isoform of it, h*apoE*-3'UTRmut-luc and the expression vectors sh-HNF-4α and sh-scramble were generated as previously described (430). The expression vectors pMT2-*HNF4a* and CMV-*bgal* and the human *apoAI*, *apoE*, *apoC3* and *ABCAI* promoter constructs, (-1020/+24)-h*apoAI*-luc, (-500/+73)-h*apoE*-luc, (-890/+24)-h*apoC3*-luc and (-204/+205)-h*ABCAI*-luc respectively, were available at the lab.

Table 2.3 Primers used in cloning

Name	**Sequence**
-2362-hANGPTL4-FW	5'- GGGGTACCCCCTGGGTCTGTGATGTGTTTTGT -3'
+77ANGPTL4-REV	5'- CCCAAGCTTGGTAAGACCCGCTTGGTTGCA -3'
-2097-hLIPG-FW	5'- CGGGGTACCTGCAGGACTACCTTCCAACAAT -3'
+171-hLIPG-Rev	5'- CCCAAGCTTCGGTAAGACCCTTCTCTCGG -3'
-111-hLXRa - FW	5'- GGGTACCAAGGGAGGAGGAGGGAGG -3'
-42-hLXRa - FW	5'- GGGTACCTTTGCTCCACGAGGTGCCTA -3'
-25-hLXRa - FW	5'- GGGGTACCCTATGGAGGGGAGGGAA -3'
+384-hLXRa - Rev	5'- CCAAGCTTTGTCCAGAAGTCTCGGT -3'
KpnI (GGTACC) and HINDIII (AAGCTT) restriction sites are underlined	

Table 2.4 Primers used in mutagenesis

Name	**Sequence**
(-59/-26)-hLXRa-FW	5' - CGGGCCGTGCTGGGA**TA**T**C**TGCTCCACGAGGTGC - 3'
(-59/-26) hLXRa-Rev	5' – GCACCTCGTGGAGCA**G**A**TA**TCCCAGCACGGCCCG - 3'
Nucleotide substitutions in the primers are in bold and underlined	

2.4.2 DNA isolation from agarose gel electrophoresis

PCR products and digestion reactions, run on agarose gels, are purified with the use of Wizard SV Gel and PCR Clean-Up System according to the manufacturer's instructions. In cases a single enzyme is used for vector digestion, 1μl shrimp alkaline phosphatase (SAP) is added to the digestion reaction followed by incubation at 37^{o}C for 30min to 1h to catalyze the dephosphorylation of 5' phosphates from DNA and prevent recircularization.

2.4.3 Ligation reaction

Ligation was performed by combining digested DNA fragment (insert) with digested plasmid DNA (vector) and the molar ratio of insert to vector was 3:1 molecules by using 50-100ng of the vector. Then, 1xT4 DNA ligation buffer (New England BioLabs) supplemented with ATP and 1μl T4 DNA ligase were added to the mixture and the final volume of the reaction was adjusted to 12μl by adding (dd)H_20. Then, the mixture was incubated overnight at 4^{o}C.

2.4.4 Transformation

We performed transformation of plasmid DNA into E.*Coli* DH10β competent cells using the heat shock method. Briefly, 100μl of frozen competent cells were thawed on ice and the appropriate amount of DNA (6μl of the ligation reaction or 5-50 ng of plasmid) was added to the cells. The cells were incubated for 30 min on ice, heat-shocked at 42°C for 45 sec and immediately placed on ice for 2-3 min. Subsequently, 0.9ml of growth medium (LB)

was added and the cells were incubated at 37°C for 1h. If the DNA that was used for transformation derived from a ligation reaction, the cells were centrifuged at 3000rpm for 5 min at RT, resuspended in 150μl LB and the entire amount of resuspended bacteria was spread on LB plate with the appropriate antibiotic. If plasmid DNA was used for transformation, 100μl of cells were spread on the appropriate selective plate. The plates were then incubated at 37°C for 16-18 h.

2.4.5 Purification of plasmid DNA

- Mini-preparation

For the preparation of up to 10-20 μg of plasmid DNA, single bacterial colonies were picked from selective plates and used to inoculate 2ml of the appropriate selective LB medium. Following 16-18 h incubation at 37^{o}C in a shaking incubator, the mini cultures were transferred in eppendorf tubes and centrifuged at 15,000 x g for 1min. Plasmid extraction and purification was performed using the QIAGEN Plasmid Mini Kit according to the manufacturer's instructions. Briefly, the supernatant was removed and the cell pellet was resuspended in the appropriate suspension buffer, lysed and centrifuged to pellet cell debris. The plasmid-containing supernatant was collected and plasmid DNA was precipitated, air-dried and resuspended in 40 μl ddH_2O.

- Midi-preparation

For the preparation of up to 500 μg of plasmid DNA, a single colony from a freshly streaked selective plate was used to inoculate a starter culture of 3 ml LB medium containing the appropriate selective antibiotic. Following 6h incubation at 37^{o}C with vigorous shaking, the starter culture was diluted and was used to inoculate 200ml selective LB medium. Following 16h incubation at 37^{o}C, plasmid extraction and purification was performed according to the QIAGEN Plasmid Midi Kit.

2.5 Cell Cultures Protocols

2.5.1 Cell cultures

For the purpose of this study, we used the EA.hy926 (human umbilical vein endothelial hybrid cell line), the HepG2 (human hepatocellular liver carcinoma cells and the HEK293T (human embryonic kidney 293T cells) cell lines. The stocks of the cultures are kept at -80^{o}C. All cell lines were cultured in T75 flasks in complete growth medium containing Dulbecco's modified Eagle's medium (DMEM) supplemented with 10% fetal bovine serum (FBS) and 2% penicillin/streptomycin solution (P/S) and maintained at 37°C in a 5% CO_2 incubator. EA.hy926 cells were grown in low glucose DMEM with GlutaMAX supplement (Invitrogen, Cat. No. 21885), while HepG2 and HEK293T cells were grown in high glucose DMEM (Invitrogen, Cat. No. 41966). The growth medium was replenished every 48h. When the cells in the flask were between 80 to 90% confluent, they were subcultured to an appropriate concentration by using trypsin/EDTA.

2.5.2 Transient Transfection Assays

- Plasmid DNA transfection of HepG2 and HEK293T cells

Transient transfections of these cells were performed using the calcium phosphate [$Ca_3(PO_4)_2$] co-precipitation method. The experimental procedure is prepared as follows and the amounts given are for one well of a 6-well plate:

- ✓ One day before the transfection, the appropriate number of cells ($25*10^4$ HEK293T and $50*10^4$ HepG2) was seeded in plates and incubated in 1ml final volume of complete medium (containing FBS and antibiotics).
- ✓ At the day of transfection the desired confluency of the cells should be 60-80%. Then, 1-6μg of DNA and 15.5μl of $CaCl_2$ (2M) were diluted in ddH20 in a final volume of 125μl (pre-mix transfection solution).

- ✓ The pre-mix transfection solution was added dropwise while vortexing to a tube containing an equal amount of 2x HBS (274mM NaCl, 10 mM KCl, 1.5 mM $Na_2HPO_4 \cdot H_2O$, 12mM Dextrose, 42mM Hepes, pH 7±0.1). This mixture is the transfection solution.
- ✓ The transfection solution was incubated for 15min at RT. In parallel, the medium from the cells was replenished with 0.75 ml fresh complete medium.
- ✓ Then, the transfection solution (250µl final volume) was added to the cells dropwise. Next, the cells were incubated at 37 ^{o}C in a CO_2 incubator.
- ✓ After 12-18 h post-transfection, the medium was renewed. The cells were further incubated for 24h then harvested.

➢ <u>Plasmid DNA transfection of EA.hy926 cell line</u>

Transient transfections of endothelial cells with plasmid constructs were performed using the Polyethylenimine (PEI) reagent as described previously (431) with some modifications. The experimental procedure is prepared as follows and the amounts given are for one well of a 12-well plate:

- ✓ Two days before the transfection, $20*10^4$ endothelial cells were seeded in 12-well plates and incubated in 0.5 ml final volume of complete medium (containing FBS and antibiotics). The desired confluency of the cells at the date of transfection is about 70-80%.
- ✓ At the day of transfection, 1.5µg of DNA was diluted in serum free DMEM (tube 1 – final volume 25µl). Also, 1.5µl of PEI reagent was diluted in serum free DMEM (tube 2 – final volume 25µl).Vortex and flash spin was performed to each tube.
- ✓ After 5min of incubation at RT, the tube 2 was added to tube 1 (transfection solution). Vortex and flash spin were performed, followed by 20min incubation at RT.
- ✓ The transfection solution was added to the cells dropwise and the cells were incubated at 37^{o}C in a CO_2 incubator.

- ✓ After 4h of incubation, the media was replenished with fresh complete media and the cells were further incubated for 24-48h.

- ➢ <u>siRNA transfection of HepG2 cells</u>

HepG2 cells were transfected with siRNA against HNF-4a (5'-AAAGCGGCCACGCGAGUCAUACUGG -3') or scrambled siRNA (5'-UGCGCUAGGCCUCGGUUGC -3') using the Hiperfect transfection reagent (Qiagen). We performed 2 rounds of transfection utilizing the Fast-Forward protocol as follows:

- ✓ The first round of transfection was performed at the same day of cell plating. HepG2 cells ($6*10^4$) were seeded in 24-well plates in 0.4ml of complete medium (with FBS and P/S).
- ✓ Then, we prepared the transfection mixes. 6μl of Hiperfect reagent were diluted in 44μl of serum and antibiotic free DMEM (tube1). Also, 100nM of siRNA were diluted in serum and antibiotic free DMEM to a final volume of 50μl (tube2).
- ✓ The tube 2 was added to the tube 1 (transfection solution). Vortex and flash spin were performed, followed by incubation for 10min at RT.
- ✓ Then, the transfection solution was added dropwise in the plates and the cells were incubated at 37 ^{o}C in a CO_2 incubator.
- ✓ After 24h of the first round of transfection, we performed the second round of transfection. The mixes were prepared as described above. Before adding the transfection solution, the medium of the cells was replenished with 0.4 ml fresh complete medium.
- ✓ Cells were harvested 48h after the first round of transfection. The silencing efficiency of HNF4a was confirmed by western blotting.

- ➢ <u>siRNA transfection of EA.hy926 cells</u>

EA.hy926 cells were transfected with siRNA targeting FOXO1 (Hs_FOXO1A_7 FlexiTube siRNA, Qiagen) or with a control (scrambled) siRNA (All Stars Negative Control

siRNA, Qiagen) utilizing the Lipofectamine RNAiMAX reagent according to the manufacturer's instructions with some modifications. FOXO1 silencing was achieved following two rounds of 100 nM siRNA transfection. Specifically:

- ✓ One day before the first round of transfection, endothelial cells were seeded in 24well plates ($7*10^4$/well) in 0.5ml final volume of complete medium.
- ✓ At the day of transfection, the transfection mixes were prepared as follows:
    - 1.5μl of RNAiMAX reagent was diluted in 25μl of OptiMEM (tube A). Also, 100nM of siRNA was diluted in 25μl of OptiMEM (tube B).
    - Then, tube B was added to tube A (transfection solution). Vortex and flash spin were performed and followed by 10min incubation at RT.
    - In the meantime, medium of the cells was removed followed by two washes with OptiMEM.
    - The transfection solution was added in the cells dropwise. Then, 200μl of OptiMEM were added in the cells and afterwards the cells were incubated at 37^oC in a CO_2 incubator
    - After 6h of incubation, 250μl of complete medium was added in the cells and the cells were incubated further.
- ✓ Next day, the medium was replenished with fresh complete medium (0.5ml)
- ✓ Two days after the first round of transfection, cells were split and subcultured at 1:2 ratio to new 24-well plates by using the trypsin/EDTA method.
- ✓ Next day, we performed the second round of transfection, which was prepared as described in the first round.
- ✓ 24h after the second round of transfection, the medium was renewed and the cells were further incubated. Cells were harvested at the time indicating at each experiment. The silencing efficiency of FOXO1 was confirmed by western blot analysis and qPCR (described below).

- Co-transfections with plasmid constructs and siRNAs or miRNAs mimicks

HepG2 cells were co-transfected with plasmid constructs and siRNAs or mimics of miRNAs. For this purpose, the Attractene transfection reagent (Qiagen) was used according to the manufacturer's instruction. Specifically:

- ✓ One day before the transfection, HepG2 cells were plated in 24-well plates ($8*10^4$ cells/ well) in 0.5ml complete medium.
- ✓ At the day of transfection, 0.3μg of plasmid DNA was diluted to serum free DMEM to a final volume of 60μl (pri-transfection solution).
- ✓ Then, 10nM of miRNA mimics or 100nM of siRNA were added to the pri-transfection solution (pre-transfection solution).
- ✓ Next, 1.5 μl of attractene reagent was added to the pre-transfection solution (transfection solution) followed by incubation 15min at RT. Then, the transfection solution was added to the cells dropwise and afterwards the cells were incubated at 37^oC in a CO_2 incubator.
- ✓ After 24h, the medium was replenished. The cells were harvested in the appropriate time.

2.5.3 Luciferase assays

For the experiments studying the activity of promoters, we performed luciferase assays using the luciferase assay kit from Promega Corp. according to the manufacturer's instructions. Normalization for transfection efficiency was performed by β-galactosidase. Briefly, 40h post-transfection cells were lysed in 1X lysis reagent (Promega) and incubated for 5min at RT in a shaking platform. Cells were scraped, collected and after a cycle of freeze-thaw the lysates were purified by centrifugation at 13.000rpm for 1min at RT. The supernatant was collected as total cell lysate and used for measurement of luciferase and β-galactosidase activity.

- Measurement of luciferase activity

60µl of cell extract were mixed with 60µl luciferase substrate (Promega) and the relative light units (RLU) were measured in the luminometer.

- Measurement of β-galactosidase activity

5µl of cell extracts were mixed with 149µl sodium phosphate buffer (P buffer), 44µl ONPG (8mg/ml) and 2µl Mg^{+2} buffer (table 2.5) and incubated at 37^{o}C using the TECAN Infinite 200 PRO instrument. B-galactosidase activity was measured from the absorbance at 410nm by TECAN Infinite 200 PRO at different time points until the samples are colored yellow.

Table 2.5 Buffers used for β – galactosidase activity

Sodium phosphate buffer (P buffer):	0.1M Na_2HPO_4 pH7.3 (pH is adjusted with 0.1M NaH_2PO_4)
ONPG:	The appropriate amount of O-nitrophenyl-galactopyranoside (ONPG) is resuspended in P buffer to a final concentration of 8 mg/ml
Mg2+ buffer:	1M KCl, 0.1M $MgCl_2$, 352mM β-mercaptoethanol

2.5.4 Cell Treatments with HDL and Inhibitors

Two days before the treatment, the EA.hy926 cells were seeded in 12-well plates ($20*10^4$ cells/ well) and incubated in complete medium. 3h before the treatment, the medium was replenished with medium containing 0.5% FBS (starvation medium). Treatments were performed with either human HDL or a humanized type of HDL (TgHDLapoA-I) and for various time points. For the experiments with the inhibitors, cells were pre-incubated with inhibitors in the starvation medium for 1h before the addition of HDL and remained in the culture medium for the entire duration of the experiment. The following inhibitors were used:

phosphatidylinositol 3-kinase (PI3K)/Akt inhibitor LY294004, p38 mitogen-activated protein kinase inhibitor SB203580, extracellular signal-regulated kinase (ERK) inhibitor UO126, c-Jun N-terminal kinase (JNK) inhibitor SP600125, endothelial nitric oxide synthase inhibitor (L-NMMA), the protein synthesis inhibitor cycloheximide (CHX) and the forkhead box O1 (FOXO1) inhibitor AS1842856. For the experiments with siRNAs, HDL treatment was performed 48h after the second round of transfection.

2.5.5 Immunofluorescence

Two days before the experiment, the cells were seeded onto glass coverslips (coated with 1% gelatin) in 24-well plates (105cells/ well) and incubated in 0.4ml of complete medium. When the cell-confluency reached approximately 90%, the cells were starved for 3h and then HDL was added to the cell cultures. At the end of HDL treatment we performed the immunofluorescence protocol as follows:

- ✓ The cells were washed with 1XPBS and fixed in 4% paraformaldehyde for 10 min at RT.
- ✓ After three washes with 1XPBS, cells were permeabilized in 0.1% 1XPBS-T (1XPBS containing 0.1% Triton X-100) for 5min and then blocked with 0.3% 1XPBS-T containing 5% normal serum and 0.5% BSA for 1hr at RT while shaking.
- ✓ After blocking, cells were incubated overnight with the primary antibody (table 2.1), which was diluted in 1% normal serum in 0.1% 1XPBS-T, at 4°C.
- ✓ Next day, three washes were performed with 0.1% 1XPBS-T followed by incubation for 1hr at RT with the appropriate fluorescent-conjugated secondary antibody diluted to 1:1000 in 0.1%PBS-T.
- ✓ Then, the cells were washed three times with 0.1% 1XPBS-T, incubated for 15 min with Hoechst dye (dilution 1:10.000 in 1XPBS), washed two times with 1XPBS and mounted on glass slides using mounting solution (1:1 glycerol/1XPBS).
- ✓ All washes were performed for 5minutes at a rotor at RT.

Fluorescently-labelled cells were imaged at a Leica TCS SP8 inverted confocal microscope using a 40x oil-immersion objective lens. Z-projections of images were acquired using Fiji ImageJ software.

2.6 Purification and Analysis of Protein Extracts

2.6.1 Purification of protein extracts

Depending on the localization of the protein of interest, we used different lysis protocols to obtain protein extracts from the cells. Protein extracts were then stored at -80^{o}C. The composition of buffers used for protein extraction is depicted in the table 2.6.

- Purification of whole extracts

To isolate whole extracts, we used the Co-IP lysis buffer. Briefly, cells were washed with ice-cold 1XPBS and lysed in a Co-IP buffer supplemented with protease and phosphatase inhibitors. The cell lysates were collected in eppendorf tubes by scraping and rotated at 4^{o}C for 30 min. After the rotation, cell lysates were centrifuged at 13,000 rpm for 10min at 4^{o}C and subsequently the supernatant containing the protein extracts was collected in new eppendorf tubes.

- Purification of nuclear extracts

Nuclear proteins were separated from cytoplasmic proteins utilizing a two buffers protocol (Buffer A and Buffer B). Briefly, cells were washed with ice-cold 1XPBS, lysed in buffer A supplemented with protease and phosphatase inhibitors and incubated in RT for 10min. After incubation, cells were scraped and centrifuged at 13000 rpm at 4°C for 5 min. The supernatant containing the cytoplasmic proteins was collected and stored at -80^{0}C, while the pellet was re-suspended in buffer A and centrifuged. The supernatant was

discarded and the nuclear pellet was re-suspended in buffer B supplemented with the protease and phosphatase inhibitors. Extracts were incubated on ice for 30min and then were centrifuged at 13000 rpm at 4°C for 6min. The supernatants containing the nuclear proteins was collected.

- Secreted proteins

To detect secreted proteins, the incubation media was collected and the proteins were precipitated with TCA as described previously (432) with some modifications. Briefly, TCA (to a final concentration of 10%) was added in 400μl of medium and the mixture was incubated overnight on ice and centrifuged at 13000rpm for 30 min at 4 °C. The supernatant was removed, the pellet was washed with ice-cold acetone and centrifuged at 13000rpm at 4 °C for 10 min. The acetone-containing supernatant was removed and the protein pellet was air dried and diluted in a 4x Laemmli buffer.

Table 2.6 Buffers used for protein extraction

CoIP lysis bufer	Buffer A	Buffer B
20mM Tris-Cl pH7.5	10mM Hepes 7.9	20mM Hepes pH7.9
150mM NaCl	10mM KCl	0.4M NaCl
10% Glycerol	0.1mM EDTA	0.1 mM EDTA
1% TritonX-100	0.4% NP40	10% Glycerol

2.6.2 Protein samples preparation

After protein purification, protein concentration was determined by measuring the absorbance at 750nm in the TECAN Infinite 200 PRO instrument using the DC Protein Assay kit (BioRad Hercules, CA) according to the manufacturer's instructions. Before electrophoresis, protein samples were diluted in a 4x-Laemmli buffer (table 2.7) and boiled

for 10min. In experiments detecting the ANGPTL4 tetramers, samples were diluted in a non-reduced 4x Laemmli buffer (table 2.7) without boiling. The samples analyzed by Native Electrophoresis were diluted in a non-reduced, non-denaturated 4xLaemmli buffer (table 2.7) without boiling.

Table 2.4 Sample buffers for protein preparation

4xLaemmli	Non-reduced 4xLaemmli	Non-reduced, non-denaturated 4x Laemmli
0.25M Tris	0.25M Tris	0.25M Tris
8% β-mercaptoethanol	8% SDS	20% Glycerol
8% SDS	20% Glycerol	0.004% Bromophenol Blue
20% Glycerol	0.004% Bromophenol Blue	
0.004% Bromophenol Blue		

2.6.3 Analysis of protein extracts

- SDS-PAGE:

Based on the size, the appropriate amount of protein samples were loaded on 8.5%, 10.5% or 12.5% SDS polyacrylamide gels consisting of the separating and stacking gel (table 2.8). Then we performed electrophoresis in 1XTGS buffer (table 2.9), at 140 V using Mini-PROTEAN Tetra Cell System (Bio-Rad). The BenchMark Prestained Protein Ladder (Invitrogen) was used as a size marker. For visualization of the protein bands, gels were either stained with Coomassie Brilliant Blue R-250 or used for Western blot analysis as described below.

- Non-denaturating (Native) PAGE

During Native PAGE all procedures were performed under native conditions, particularly in the absence of SDS. Briefly, the medium of EA.hy926 cells was collected and the proteins were precipitated using Amicon Mltra-0.5 Centrifugal Filter Devices (Millipore).

The concentrated protein samples were diluted with 4x native sample buffer (table 2.7) and gel electrophoresis was performed in 1XTG buffer (table 2.9), at 110 V utilizing the 4–20% Mini Protean TGX precast gels. The electrophoretic pattern of apoAI-particles of HDL (isolated from healthy human donors) was used as a size marker. The protein bands were visualized utilizing Western blot analysis.

Table 2.8 Buffers used for the preparation of polyacrylamide gels

	Separating Buffer	**Stacking Buffer**
Tris	18.165 g (1.5 M)	6.05 g (0.5 M)
SDS	0.4 g (0.4% w/v)	0.4 g (0.4% w/v)
pH (with HCl)	8.8	6.8
Final Volume (with dH_20)	*100 ml*	*100 ml*

Stacking Gel		**Separating Gel**			
			8.5%	**10.5%**	**12.5%**
dH20	3.6ml	dH20	4.6ml	3.9ml	3.2ml
30% acrylamide	900µl	30% acrylamide	2.8ml	3.5ml	4.2ml
Stacking buffer	1.5ml	Separating buffer	2.5ml	2.5ml	2.5ml
10% APS	60µl	10% APS	160µl	160µl	160µl
TEMED	6µl	TEMED	8µll	8µll	8µll

Table 2.9 Buffers used for SDS and Native Page

	10X TGS	**12.5X TG**
Tris	30.3g	30g
Glycine	144.2g	144g
SDS	10g	(-)
Final Volume (with dH_20)	*1L*	*800ml*

- Coomassie Brilliant Blue Staining:

For visualization of the protein bands the Coomasie Brilliant Blue staining was used. Briefly, polyacrylamide gels were stained with Coomassie Brilliant Blue (2.5 g Coomassie Brilliant Blue R in 45 % methanol and 10% acetic acid) for 20min and then destained in destaining solution (50% methanol, 8.5% acetic acid) overnight while shaking. The gels were rehydrated in dH_2O for 4-5h and dried in a Hoefer SE 1160 gel dryer under vacuum at 80 ^oC for 1 h.

- Western Blot:

Following SDS and Native PAGE, proteins were transferred onto nitrocellulose membranes (GE Healthcare Life Sciences) by electroblotting at 400 mA for ~1.5 h using transfer buffer with or without SDS respectively (table2.10). The transfer was performed using Mini-PROTEAN Tetra Cell System (Bio-Rad). Membranes were then blocked in 5% non-fat milk in TBS-Tween 20 (TBS-T) for 1 h. Incubation with primary antibodies was performed as shown in Table 2.1. After the incubation, the membranes were washed three times with TBS-T for 10 min per wash. Then, incubation with HRP-conjugated secondary antibodies diluted 1:10,000 in 5% non-fat milk in TBS-T was performed at RT for 1 h. After the final incubation, the membranes were washed again with TBS-T for three times followed by a wash with TBS for 5 minutes. Signals were detected by enhanced chemiluminescence (Thermo Scientific) and proteins were visualized on a ChemiDoc XRS+ imaging system (Bio-

Rad) and band intensities were quantified using the Image Lab Software (Bio-Rad). Actin levels were used for normalization.

Table 2.10 Buffers used for Western Blot

Transfer Buffer (SDS)		**Transfer Buffer (Native)**		**10XTBS**	
10XTGS	100ml	12.5XTG	80ml	NaCl	180g
Methanol	200ml	Methanol	200ml	Tris	121.14
dH20	700ml	dH20	720ml	pH (with HCl)	7.3
Final Volume	1L	Final Volume	1L	Final volume (with dH20)	1L

2.7 RNA Purification and Expression

Total RNA was isolated from cells using RNAiso reagent according to the manufacturer's protocol (Takara, Japan). RNA concentration was determined by measuring the absorbance at 260nm. To assess the purity of RNA, we measured the absorbance at 280nm and at 230nm and then we calculated the 260/280 ratio and the 230/280 ratio. 260/280 ratio determines the purity of RNA from protein contaminants and the acceptable range of values is 1.8-2.0. 260/230 ratio determines the purity of RNA from unwanted organic contaminants such as Trizol and phenol and the acceptable range of values is 2.0-2.2. All measurements were performed in TECAN's NanoQuant plate.

Pure isolated RNA (1μg) was reverse-transcribed using the M-MLV reverse transcriptase and random primers. The cDNAs produced were used for quantitative PCR analysis with the appropriate pair of primers which were designed using the Lasergene PrimerSelect software (DNASTAR) (Table 2.11). qPCR was performed on a StepOnePlus Real-Time PCR system (Applied Biosystems, Foster City, CA) using KAPA SYBR FAST qPCR Master Mix (Kapa Biosystems, Wilmington, MA). Melting curve analysis was performed to ensure primer specificity. The expression of the target genes was normalized

to the expression of the housekeeping gene and the relative gene expression levels were determined by the comparative Ct method (ΔΔCt method), as described in Applied Biosystems Guide.

- MicroRNA qPCR analysis:

To study the expression levels of let-7 family genes in HepG2, pure isolated RNA (200ng) was reverse transcribed with Universal cDNA Synthesis Kit II according to the manufacturer's protocol. Then, qPCR analysis was performed as described above utilizing the specific Exiqon PCR Primer Sets. U6 expression was used as an internal control.

Table 2.11 Primers used in Quantitative PCR

Name	Sequence
ANGPTL4-FW	5'- AAGCCTGCCCGAAGAAAGAG - 3'
ANGPTL4-REV	5'- ACTGTCCAGCCTCCATCTGA - 3'
HMOX1-FW	5'– CAGTCAGGCAGAGGGTGATAGA – 3'
HMOX1-Rev	5'– GGGCAGAATCTTGCACTTTGTTG – 3
LIPG-FW	5'- GGAAACCCAGCGGAAACTGACA -3'
LIPG-REV	5'- CCATCCCGACACTTGCGAAACC -3'
APOA-I-FW	5'- TGGATGTGCTCAAAGACAGC - 3'
APOA-I-REV	5'- TCCAGGTTATCCCAGAACTCC - 3'
APOE-FW	5'- GAACTGAGGGCGCTGATGGAC -3'
APOE-REV	5'- CGGGGTCAGTTGTTCCTCCAGT -3'
GAPDH-FW	5' CTCCTGTTCGACAGTCAGCC -3'
GAPDH-REV	5'- TTTACCAGAGTTAAAAGCAGCCCT -3'
GusB-FW	5'- CACAAGAGTGGTGCTGAGGA -3'
GusB-REV	5' ACCAGGTTGCTGATGTCGG -3'
RPLPO-FW	5'- GGCACCTGGAAAACAACCC -3'
RPLPO-REV	5'- AGCAACATGTCCCTGATCTCA -3'
FOXO1-FW	5'- ACTTCAAGGATAAGGGTGACAGCA -3'
FOXO1-REV	5'- CCACCCTCTGGATTGAGCATC -3'

2.8 DNA Affinity Precipitation

For the in vitro identificaton of DNA-protein interactions, we performed DNA affinity precipitation (DNAP) utilizing nuclear extracts from HepG2 cells and biotinylated PCR products or biotinylated oligonucleotides. DNAP protocol is performed in three steps.

- Step1. Extracts purification and double stranded biotinylated oligonucleotides preparation

Nuclear extracts were collected as described above. Biotinylated PCR products were amplified with the use of a biotinylated primer and a non-biotinylated primer (table 2.12) and isolated by gel extraction. The amount used in the reaction was calculated based on the fact that for a 600bp fragment, 2 μg of the PCR product is required.

Biotinylated oligonucleotides were prepared by utilizing the annealing protocol. Briefly, 5 μg biotinylated oligonucleotide, 5 μg unbiotinylated complementary oligonucleotide and 10xNEB2 buffer were diluted in ddH_20 up to a final volume of 20 μl (synthesis mix). The synthesis mix was incubated at 92^oC for 2 min and then was allowed to cool gradually. The final concentration was induced to 5 μM by adding the appropriate volume of H_20. Bio-products and bio-oligos were stored at -20^oC.

Table 2.12 Oligonucleotides used in DNAP assays

Name	Sequence
-111-hLXRa - FW	5'- GGGTACCAAGGGAGGAGGAGGGAGG -3'
-25-hLXRa - FW	5'- GGGGTACCCTATGGAGGGGAGGGAA-3'
+384-hLXRa-Rev-bio	5'- bio TGTCCAGAAGTCTCGGTGGC -3'
-52/-23-hLXRa-bio FW	5'- bio TGCTGGGACCTTTGCTCCACGAGGTGCCTA -3'
-52/-23-hLXRa REV	5'- TAGGCACCTCGTGGAGCAAAGGTCCCAGCA -3'
-52/-23-hLXRa-bio mut FW	5'- bio TGCTGGGATATCTGCTCCACGAGGTGCCTA -3'
-52/-23-hLXRa mut Rev	5'- TAGGCACCTCGTGGAGCAGATATCCCAGCA -3'

- Second Step: Beads-DNA interactions

For this purpose we used the M-280 Streptavidin Dynabeads. The DNA-beads mixture was prepared as follows:

- ✓ 50μg beads were washed with 1xB&W buffer (table 2.13).
- ✓ Beads were mixed with 7μl 2xB&W buffer and 7μl biotinylated oligo (0.58μM). (for control samples beads were mixed with 14μl of 1xB&W buffer)
- ✓ The DNA-beads mixture was then incubated for 15 minutes at RT, with occasional shaking.
- ✓ Washes with 1xB&W buffer were performed twice.
- ✓ One final wash with BBRC buffer (table 2.13) was performed.

- Third Step: DNA-Protein binding interactions

The DNA-protein mixture was performed as follows:

- ✓ 500μl of BBRC buffer supplemented with 1mM PMSF and 0.5mM benzamidine, 60μg NE and 3μg of competitor poly dI-dC were added in the mixture of DNA-coupled beads.
- ✓ Then, the DNA-protein mixture was incubated for 1h on a rotator at 4^{o}C.
- ✓ Three washes with BBRC buffer supplemented with 1mM PMSF and 0.5mM benzamidine were performed
- ✓ After the final wash, the protein-DNA mixture was resuspended in 15μl 4xLaemmli buffer and then boiled for 10min.

Table 2.13 Buffers used in DNAP assays

2xB&W	BBRC
10mM Tris-HCL pH7.5	10mM Tris-HCL pH 7.5
1mM EDTA	50mM KCl
2mM NaCl	4mM $MgCl_2$
	0.2mM EDTA
	10% glycerol

2.9. Chromatin immunoprecipitation (ChIP)

For the in vivo identification of DNA-protein interactions, we performed Chromatin immunoprecipitation (ChIP). ChIP protocol was performed in six steps as described below:

- Step 1. Chromatin Preparation from HepG2 cells
  - ✓ HepG2 cells were seeded in p100 plates ($4*10^6$ cells/ plate) and incubated in complete medium.
  - ✓ Upon reaching the desired confluency (about 90%), the cells were crosslinked with formaldehyde as follows:
  - The medium from the plates was replenished with 9ml DMEM (without FBS).
    - 1 ml formaldehyde (from 10% stock) was added to the plates followed by shaking
    - Cells were incubated for 10 min at 37^{o}C.
  - ✓ The cross-linking reaction was stopped by adding 1ml glycine (from 1.375M stock).
  - ✓ The cells were washed three times with ice cold 1XPBS supplemented with 0.5mM PMSF and finally were collected in 7 ml ice-cold 1XPBS supplemented with 0.5% NP-40 and 0.5 mM PMSF by scraping.

- ✓ After centrifugation at 1000rpm for 5min at 4^{o}C, the pellets were lysed in swelling buffer (table 2.14) supplemented with complete Protease Inhibitor Cocktail and incubated on ice for 10min. Subsequently, the cells were homogenized utilizing a Dounce homogenizer (30 times up-down). To confirm this process, the nuclei were checked in microscope by mixing 5μl with equal volume of 0.4%Trypan Blue.
- ✓ The nuclei were precipitated by centrifugation at 2000rpm for 5min at 4^{o}C and re-suspended in 2ml sonication buffer (table 2.14) supplemented with complete Protease Inhibitor Cocktail and sonicated for 12 times for 30sec at 50% amplitude on ice.
- ✓ The sonicated chromatin was cleared by two sequential centrifugations at 2000rpm for 15 min at 4^{o}C. After the final centrifugation, 50μl of the sample were kept for sonication check and the rest was stored at -80^{o}C.

➢ Step 2. Sonication check

- ✓ The sample with 50μl of chromatin was mixed with 150μl H_2O and 10.5μl NaCl (from 4M stock) and incubated overnight at 65^{o}C.
- ✓ Next day, 2μl RNAse A (10mg/ml stock) were added in the mixture, followed by incubation for 1h at 37^{o}C.
- ✓ Then, 2 μl EDTA and equal volume of phenol/chloroform/isoamylalcohol were added in the mixture and followed by centrifugation at 13000 rpm for 5min.
- ✓ The upper phase of centrifugation was collected in a new eppendorf and mixed with equal volume of chloroform and 4 μl glycogen (from 5 μg/μl stock) and followed by centrifugation at 13000 rpm for 5min.
- ✓ The upper phase was collected again in a new eppendorf and mixed with 1/10 volume Na-acetate (from 3M stock) and 2.5 volume 100% Ethanol, incubated for 30min at -80^{o}C.

- ✓ After centrifugation at 13000 rpm for 10min, the pellet, containing the chromatin, was washed with 75% Ethanol, air-dried and resuspended in 20 μl sterile dH_2O
- ✓ The quality of the fragmented chromatin was checked on a 1.5% agarose gel.

➢ Step 3. Equilibration and blocking of beads

- ✓ For each sample a total amount of 160μl protein G sepharose beads were used (40μl for the immunoprecipitation (IP) reaction, 40μl for the control reaction and 80μl for preclearing chromatin).
- ✓ The beads were washed three times with 1.5 ml sonication buffer as follows:
    - Rotation 10min at 4^oC
    - Centrifugation at 2000rpm for 3min at 4^oC
    - Supernatant was removed
- ✓ Then, the beads were blocked with 494μl sonication buffer, 5μl BSA (100mg/ml stock) and 1μl sonicated λ DNA (0.5ug/μl stock) and rotated for 2h at 4^oC.
- ✓ After rotation, 200μl from the beads were stored at 4^oC, while the rest were used for preclearing chromatin.

➢ Step 4. Preclearing and Immunoprecipitation (IP)

- ✓ Chromatin stored at -80^oC, was thawed on ice and quantified by measuring the OD at 260nm and 280nm.
- ✓ In the meantime, the beads that had been kept for the preclearing process were centrifuged at 6000rpm for 3min at 4^oC and the supernatant was removed.
- ✓ After preparing chromatin and beads, 1500μl chromatin, 15μl BSA (100mg/ml stock) and 3μl sonicated λ DNA were added in the beads and subsequently the mixture was rotated for 2h at 4^oC.
- ✓ Then, the beads were removed from the mixture by centrifugation at 3000rpm for 10min at 4^oC. The supernatant was collected to a new eppendorf tube. One-tenth

of the volume of the supernatant (input) was transferred to a new eppendorf tube and stored at 4^{o}C.

- ✓ The remaining volume of the supernatant was used for the IP method. Specifically, the appropriate amount of the supernatant was mixed with 5μg of a-HNF4a (IP sample) or with no Ab (control sample) and followed by rotation for 2h at 4^{o}C. Meanwhile, the equilibrated beads stored at 4^{o}C, were isolated by centrifugation at 6000 rpm for 3 minutes.
- ✓ After the rotation, the immunoprecipitated chromatin (and the control chromatin) were mixed with the equilibrated beads and followed by overnight rotation at 4^{o}C.

➢ <u>Step 5. Washes of beads and De-crosslinking</u>

- ✓ Next day, the samples were centrifuged at 6000 rpm for 3 min at 4^{o}C and the supernatant was removed.
- ✓ Then, the samples were washed twice with buffer A, buffer B, buffer C and TE buffer as follows:
    - 1ml buffer was added
    - 10min rotation at 4^{o}C was performed
    - The supernatant was removed by centrifugation at 6000rpm for 3 min at 4^{o}C followed by the addition of the next buffer in the sample
- ✓ After the washes, DNA was eluted in 300μl of elution buffer. Then DNA was mixed with 100μl H_20 and 21μl NaCl (4M stock) followed by overnight incubation at 65^{o}C so as to promote de-crosslinking.
- ✓ Chromatin kept as input was also mixed with elution buffer up to 300μl, 100μl H_20 and 21μl NaCl and incubated overnight at 65^{o}C.

- Step 6. DNA purification and PCR amplification

  - ✓ Next day, the samples were subjected to RNAse A treatment for 1h and then mixed with 2μl EDTA (0.5M) and 2μl Proteinase K (10mg/ml) and incubated for 2h at 42^{o}C.
  - ✓ DNA was purified by phenol-chloroform extraction and ethanol precipitation as follows:
    - 200μl H_2O, 1/10 volume Na-acetate and equal volume of phenol/chloroform/isoamylalcohol 25:24:1 were added in the samples followed by vortexing.
    - After centrifugation of the samples at 13000 rpm for 5 minutes, the upper phase was collected in new eppendorf tube and mixed with equal volume of chloroform.
    - The samples were again centrifuged at 13000 rpm for 5min and the upper phage was collected in a new eppendorf tube and mixed with 4μl glycogen (5ug/μl stock) and 2.5 volumes 100% Ethanol and incubated overnight at -20^{o}C.
  - ✓ Next day, the samples were centrifuged at 13000rpm for 30min at 4^{o}C and the pellet containing the precipitated chromatin was washed with 75% Ethanol, centrifuged at 13000 rpm for 10min, air dried and re-suspended in 10mM Tri-Cl pH 7.5 (input samples were re-suspended in 100μl 10mM Tri-Cl pH 7.5, while the IP samples in 50μl 10mM Tri-Cl pH 7.5).

The IP samples and 1% chromatin input were analyzed by the SYBR-Green quantitative PCR (KAPA SYBR® FAST qPCR kit) utilizing the StepOnePlus™Real-Time PCR System (Applied Biosystems) according of the manufacturer's instructions. The CT values of the ChIP signals detected by q PCR were converted to the percentage of the input DNA using the “percent input method” as recommended by the manufacturer. Primers used for ChIP analysis are depicted in table 2.15

Table 2.6 Buffers used for ChIP assays

Swelling buffer	**Sonication buffer**	**Wash Buffer A**	**Wash Buffer B**	**Wash Buffer C**
25mM Hepes pH7.9	50mM Hepes pH7.9	50mM Hepes pH7.9	50mM Hepes pH7.9	20mM Tris-Cl pH8.0
1.5mM MgCl2	140mM NaCl	140mM NaCl	500mM NaCl	1mM EDTA pH8.0
10mM KCl	1mM EDTA pH8.0	1mM EDTA pH8.0	1mM EDTA pH8.0	250mM LiCl
0.5% NP-40	1% Triton X-100	1% Triton X-100	1% Triton X-100	0.5% NP-40
1mM DTT	0.1% Na-deoxycholic acid	0.1% Na-deoxycholic acid	0.1% Na-deoxycholic acid	0.5% Na-deoxycholic acid
2µg/ml Aprotinin	0.1% SDS	0.1% SDS	0.1% SDS	2µg/ml Aprotinin
0.5mM PMSF	2µg/ml Aprotinin	2µg/ml Aprotinin	2µg/ml Aprotinin	0.5mM PMSF
	0.5mM PMSF	0.5mM PMSF	0.5mM PMSF	

TE buffer	**Elution Buffer**
10mM Tris-Cl pH8.0	50mM Tris-Cl pH8.0
1mM EDTA pH8.0	1mM EDTA pH8.0
2µg/ml Aprotinin	1% SDS
0.5mM PMSF	50mM $NaHCO_3$

Table 2.15 Primers used in ChIP assays

Name	**Sequence**
-147-hLXRa-ChIP-FW	5'- CTAGTGGGGAGAGCTTCTTGG -3'
+78-hLXRa-ChIP-Rev	5'- CTCCTTACCCAGCGCTCTTAG -3'
+3461-hLXRa-ChIP-FW	5'- ATTTGGCCCTGTCCTTAGGTGT -3'
+3694-hLXRa-ChIP-Rev	5'- CAAGTACCGTGACTCGAAGCC -3'

2.10 Statistical Analysis

Data are expressed as mean ± SD. Statistical significance was determined using two-tailed Student's t-test or one-way analysis of variance and Tukey's post-hoc test to evaluate differences between three or more groups. For all results, $p < 0.05$ was considered statistically significant. Analysis was performed using GraphPad Prism (GraphPad Software, Inc., La Jolla, USA).

3. RESULTS AND DISCUSSION

Chapter I: Endothelial signaling pathways and genes that contribute to HDL-mediated atheroprotection.

As it was discussed in the introduction, HDL affects the endothelium functionality in order to promote atheroprotection by interacting with endothelial receptors. However, little is known about the ability of HDL to induce changes in the expression of endothelial genes and whether these genes could mediate the atheroprotective functions of HDL. In the first two parts of this chapter, we examined the ability of HDL to affect the expression of endothelial genes. We focused on genes with atheroprotective properties (such as ANGPTL4 and LIPG) and we investigated the cellular mechanisms that are employed by HDL in order to regulate these genes. In the third part, we utilized the ability of the functional HDL to activate signaling pathways and specifically the AKT pathway, in order to examine the functionality of HDL isolated from patients with inflammatory diseases.

<u>Part I:</u> ANGPTL4 is a target gene of HDL in the endothelium

Effects of rHDL-AI on global endothelial gene expression

To unravel new target genes of HDL in the endothelium, we utilized the microarray data that had been produced by the collaboration of Dr. V.I. Zannis and Dr. D. Kardassis as described previously (369). Briefly, primary Human Aortic Endothelial Cells (HAECs) were treated for 12h in starvation medium with 250μg/ml of reconstituted HDL containing the human apolipoprotein A-I (rHDL-AI) and then RNA was extracted. In control experiments, HAECs were treated with PBS for the same time period. The mRNAs from the rHDL-treated and PBS-treated cells were purified, labeled and hybridized with GeneChip Human Gene 1.0 ST Arrays (Affymetrix) followed by bioinformatics analysis which was performed in collaboration with Dr. D. Sanoudou (Bioacademy of Athens).

As depicted in Figure 3.1A, the expression of 410 transcripts was significantly changed in the presence of rHDL-AI, and more than half of the differentially expressed transcripts were downregulated by rHDL-AI (263 transcripts or 64% of the total). Gene ontology classification of the differentially expressed transcripts based on the cellular localization of the encoded proteins revealed that the majority of the transcripts encoded for nuclear (186), followed by cytoplasmic (103), plasma membrane (43), secreted (31), as well as other proteins with unknown localization (47) (Fig. 3.1B).

We focused on the transcripts coding for secreted proteins, since they could mediate the atheroprotective signal of HDL. Interestingly, we observed that ANGPTL4 was the most upregulated transcript among them. As presented in the Introduction, ANGPTL4 is a key player of lipid metabolism that, by inhibiting the lipoprotein lipase (LPL), controls the triglyceride levels in the circulation (433). Moreover, accumulating evidence indicates that ANGPTL4 protects against the development of atherosclerosis (395, 396), confirming the

physiological significance of our observation. Therefore, we focused on the mechanisms by which HDL regulates the expression of this specific gene in endothelial cells.

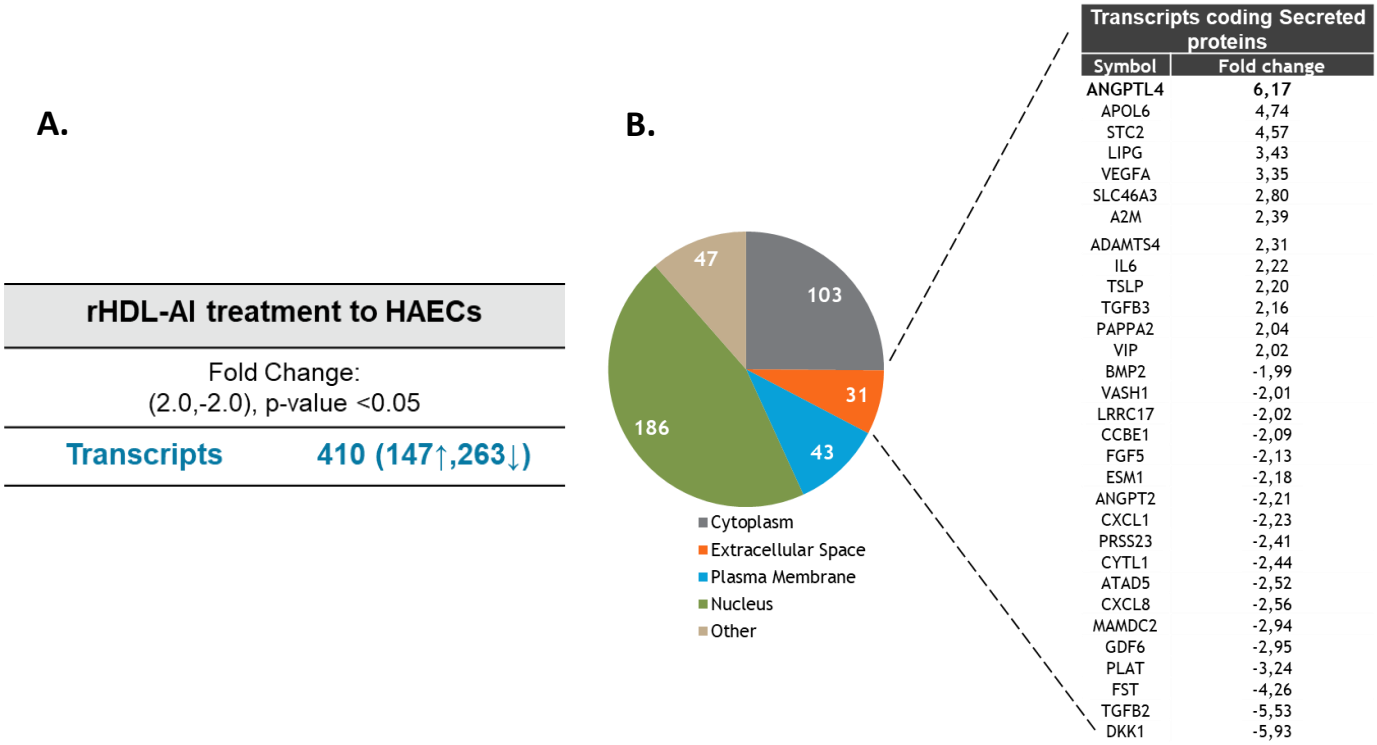

Figure 3.1 Microarray analysis of the response of endothelial cells to rHDL-apoAI.
A) Primary human aortic endothelial cells were treated with 250μg/ml of rHDLA-I for 12 h. Total RNA was extracted and microarray analysis was performed as described in Materials and Methods section. Transcripts with a fold change of ≥|2.00| were selected and a false discovery rate (FDR) threshold of > 0.05 was applied. B) The pie chart shows the classification of the differentially expressed transcripts based on the cellular localization of the encoded proteins. The Table shows genes encoding for extracellular proteins that were differentially expressed in response to rHDL-AI. ANGPTL4 was the gene with the strongest upregulation.

ANGPTL4 is a target gene of all types of HDL

In the circulation HDL is represented in two different types, the spherical type which is the most abundant type in healthy people and the discoidal one. As rHDL-AI resembles to the discoidal type of HDL, we wondered whether and the spherical type of HDL affects ANGPTL4 gene expression. Therefore, we isolated native HDL from the serum of two different sources: a healthy human donor (hHDL) and transgenic mice expressing the human apolipoprotein A-I gene (tgHDL). Native HDL contains mainly the spherical type of HDL.

Initially we examined the concentration, the structure and the functionality of HDL that is produced from the transgenic mice to make sure that it has no major structural differences from the HDL that is normally found in mice or humans. It was found that tgHDL had structural and functional properties similar to human HDL, such as the distribution of apoA-I in the HDL_2/HDL_3 region and the inhibition of TNFα-induced expression of the pro-Inflammatory Cytokine Intercellular Adhesion Molecule 1 (ICAM-1) in endothelial cells (Fig. 3.2A-C). These mice had high levels of plasma total and HDL cholesterol, a normal ratio of CE/TC and normal phospholipids and triglycerides (Fig. 3.2D).

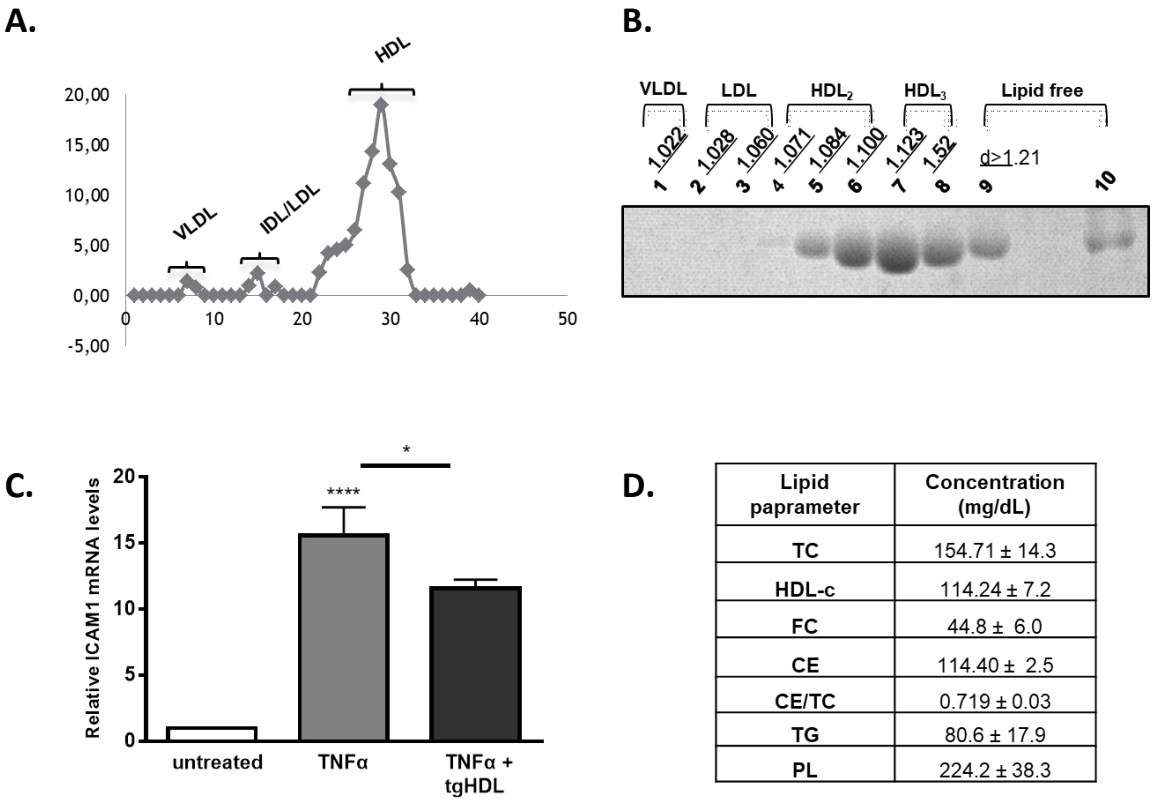

Lipid paprameter	Concentration (mg/dL)
TC	154.71 ± 14.3
HDL-c	114.24 ± 7.2
FC	44.8 ± 6.0
CE	114.40 ± 2.5
CE/TC	0.719 ± 0.03
TG	80.6 ± 17.9
PL	224.2 ± 38.3

Figure 3.2 Structural and functional properties of the HDL isolated from the human apoA-I transgenic mice. (A) Cholesterol distribution to different lipoprotein fractions in serum isolated from transgenic mice expressing human apoA-I as determined by FPLC. Data are representative of two independent experiments with identical profiles. (B) Distribution of apoA-I-containing HDL subpopulations in the serum of human apoA-I transgenic mice. Fractionation of the plasma was performed with density gradient ultracentrifugation. The apoA-I composition of each fraction was determined by SDS–PAGE and Coomassie Brilliant Blue staining. (C) EA.hy926 cells were treated with 250μg/ml of tgHDL or with PBS for 16h and then stimulated with TNFα (1ng/ml) or PBS (control) for additional 5 hr. Total RNA was extracted and quantitative RT-PCR was performed to determine ICAM1 mRNA levels, which were normalized relative to the RPLPO mRNA levels. The relative ICAM1 mRNA levels are expressed as mean (±SD) from at least three independent experiments. (D) Total cholesterol (TC), HDL-cholesterol (HDL-C), free cholesterol (FC), cholesteryl esters (CE), triglycerides (TG) and phospholipid (PL) levels in the serum of human apoA-I transgenic mice (n=5). Data represent mean ± SD.

Next, we determined the mRNA levels of ANGPTL4 following treatment of endothelial cells for 12h with rHDL-AI, tgHDL, hHDL or PBS (control experiment). For this purpose, we utilized the endothelial cell line EA.hy926, which has been used extensively in the past as an endothelial cell model (434). As depicted in Fig.3, all types of HDL were able to induce the expression of human ANGPTL4 gene when compared to the PBS-treated cells.

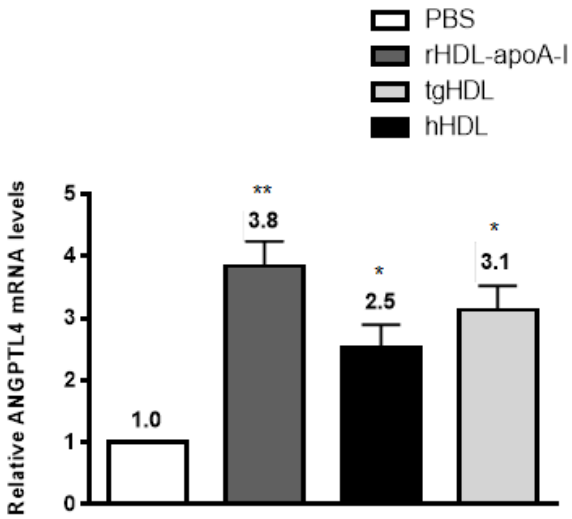

<u>Figure 3.3</u> Native HDL isolated from either transgenic mice (tgHDL) or human healthy donors (hHDL) increases the endothelial ANGPTL4 levels. The endothelial human cell line EA.hy926 was treated with tgHDL or hHDL or rHDL-AI for 12h or with vehicle (PBS, untreated sample). Total RNA was extracted and quantitative RT-PCR was performed to determine ANGPTL4 mRNA levels, which were normalized relative to the RPLPO mRNA levels. The relative ANGPTL4 mRNA levels are expressed as mean (±SD) from at least three independent experiments and shown as a histograph as fold activations in the presence of HDL versus in the absence of it. Symbols: *, $p \leq 0.05$; **, $p \leq 0.01$.

HDL induces the expression of the ANGPTL4 gene in endothelial cells in a dose and time-dependent manner

We sought to determine the mechanisms by which HDL regulates the expression of ANGPTL4 gene in endothelial cells. For this purpose, the endothelial cells were treated with tgHDL and the ANGPTL4 mRNA levels were monitored. Treatments with two different concentrations of tgHDL (100 and 250 μg/ml) for 12 h induced the expression of the ANGPTL4 gene in a dose-dependent manner (Fig. 3.4A). Moreover, treatments with 250μg/ml of tgHDL at different time points revealed a transient increase in ANGPTL4 mRNA, which reached a peak at 2 h, and started to decline at 12 h post-induction until it was restored to the original unstimulated levels at 24 h post-induction (Fig. 3.4B).

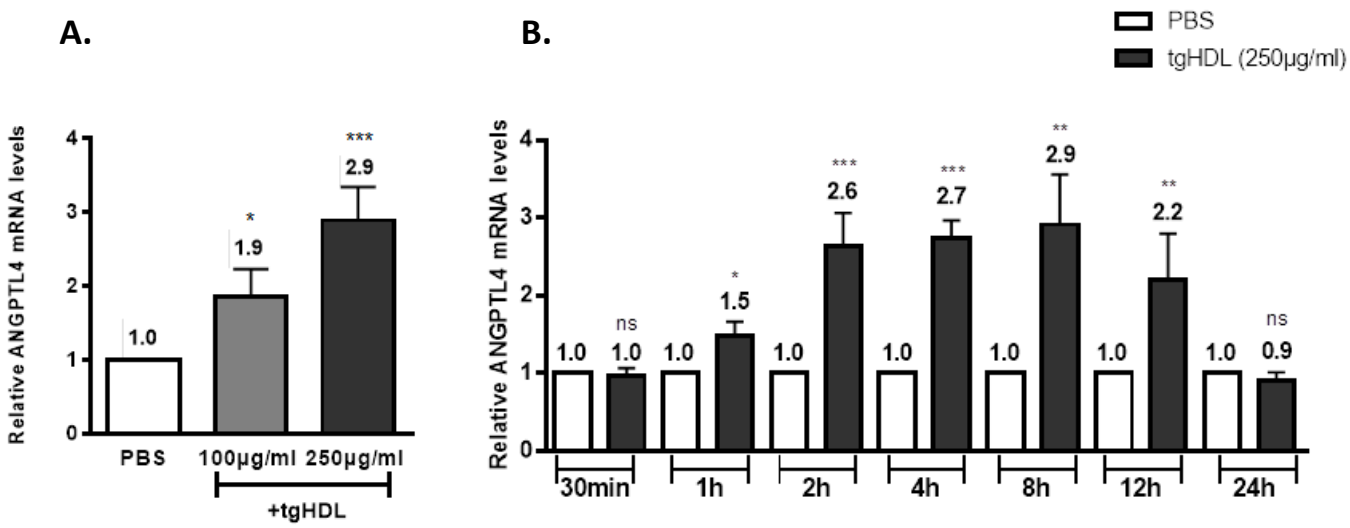

Figure. 3.4 HDL induces ANGPTL4 at the mRNA level in a dose and in a time dependent manner. (A) EA.hy926 cells were treated for 12h with 100 or 250 μg/ml of tgHDL or with PBS. Total RNA was extracted and quantitative RT-PCR was performed to determine ANGPTL4 mRNA levels. The normalized ANGPTL4 mRNA levels relative to the RPLPO mRNA levels are expressed as mean (±SD) from at least three independent experiments. B) EA.hy926 cells were treated with 250 μg/ml of tgHDL or with PBS for the indicated time periods. Total RNA was extracted and quantitative RT-PCR was performed to determine ANGPTL4 mRNA levels, which were normalized relative to the RPLPO mRNA levels. The relative ANGPTL4 mRNA levels in the absence (white bars) and in the presence (black bars) of tgHDL (mean ± SD) from at least four independent experiments are shown for each time point. Symbols: ns, not significant; *, $p \leq 0.05$; **, $p \leq 0.01$; ***, $p \leq 0.001$.

Next, we examined the effect of tgHDL on the protein levels of ANGPTL4. Treatment of endothelial cells with tgHDL induced the secreted protein levels of ANGPTL4 both in a dose (Fig. 3.5A) and in a time dependent manner (Fig. 3.5B upper panel). However, the cytoplasmic levels of ANGPTL4 were not changed after treatment with the high dose of tgHDL (Fig. 3.5B middle panel). Interestingly, the secreted ANGPTL4 was found to be associated with the mature α1 sub-class of tgHDL in native gel electrophoresis experiments (Fig. 3.5C) in agreement with previous studies which had shown that circulating ANGPTL4 was physically associated with HDL in mice (398). As expected, in the presence of cyclohexamide (CHX), an inhibitor of protein synthesis, HDL could not induce the secreted protein levels of ANGPTL4 (Fig. 3.5C, lane4).

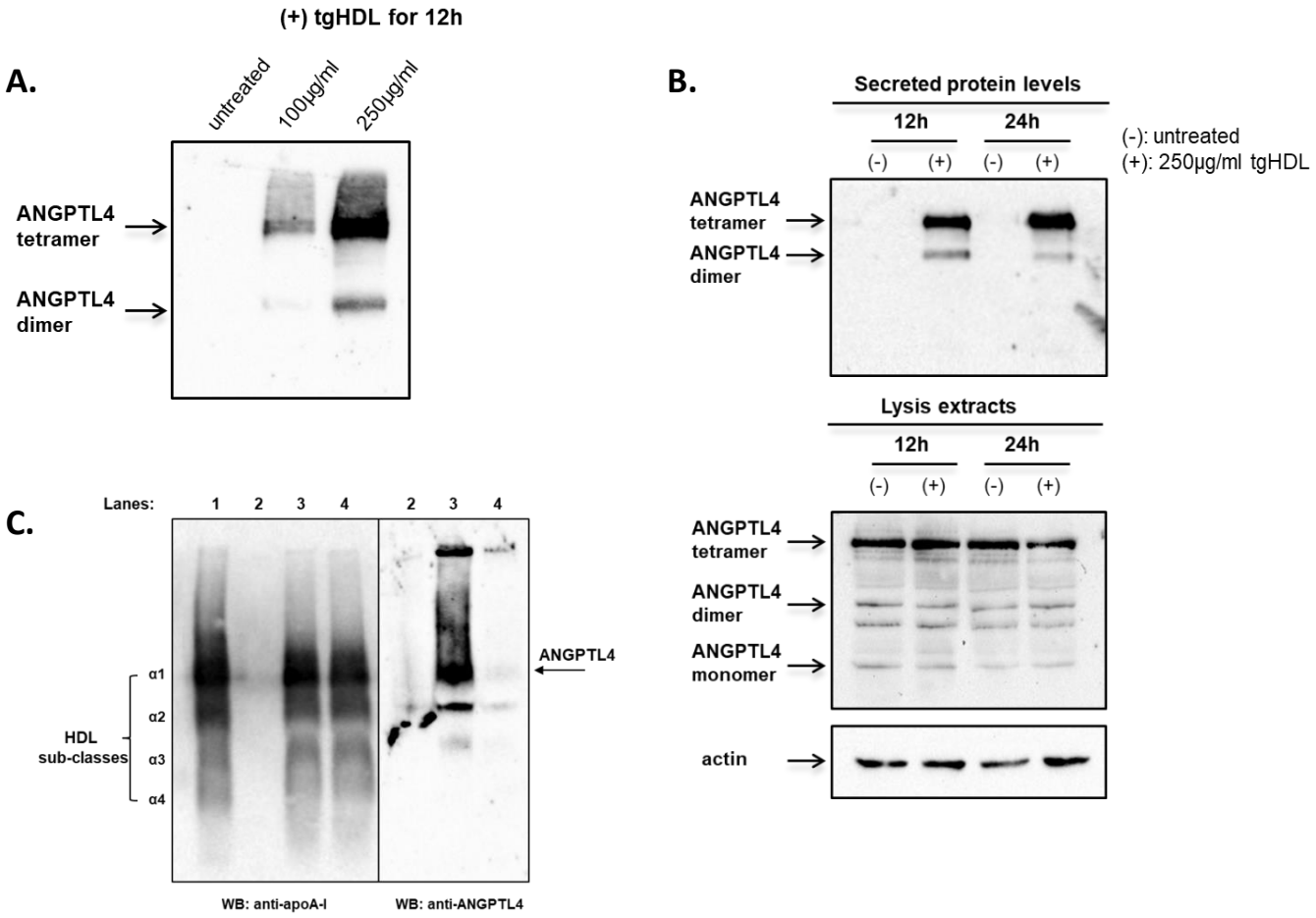

Lanes:
1: purified tgHDL
2: untreated cells
3: cells treated with tgHDL
4: cells treated with tgHDL and CHX

<u>Figure 3.5</u> HDL induces the secreted protein levels of ANGPTL4 but not the cytoplasmic one. A) EA.hy926 cells were treated with two different doses (100 and 250 μg/ml) of tgHDL or with PBS. Medium was collected and the secreted ANGPTL4 protein levels were determined by immunoblotting using ananti-ANGPTL4 antibody. B) EA.hy926 cells were treated with 250μg/ml tgHDL or with PBS for 12h or for 24h. Then, the medium (upper panel) and the whole cell extracts (middle and below panel) were collected and the protein levels of ANGPTL4 and actin were determined by immunoblotting with the corresponding antibodies. C) EA.hy926 cells were pretreated with 5μg/ml cyclohexamide (CHX) for 1h or left untreated and subsequently treated with tg-HDL (250 μg/ml) or PBS (untreated) for additional 12 h. Medium was collected and non-denaturing PAGE was performed. The HDL sub-classes were identified by immunoblotting using an antibody against human apolipoprotein A-I, whereas purified tgHDL was used as a positive control. The ANGPTL4 protein was determined by immunoblotting using the corresponding antibody. All experiments were performed at least twice, and a representative image is shown.

ANGPTL4 is a direct transcriptional target of HDL in endothelial cells

We wanted to investigate whether the observed increase in ANGPTL4 mRNA and protein levels by tgHDL in endothelial cells is direct or indirect by using the protein synthesis inhibitor cycloheximide (CHX). As shown in Fig. 3.6, treatment of EA.hy926 cells with 5 μg/ml CHX for 12 h increased significantly (19-fold) the basal mRNA levels of the human ANGPTL4 gene. Most importantly, induction of ANGPTL4 by tgHDL in the presence of CHX was much higher (33-fold). CHX did not affect the induction of ANGPTL4 by tgHDL suggesting that the mechanism by which tgHDL upregulated the ANGPTL4 gene is direct.

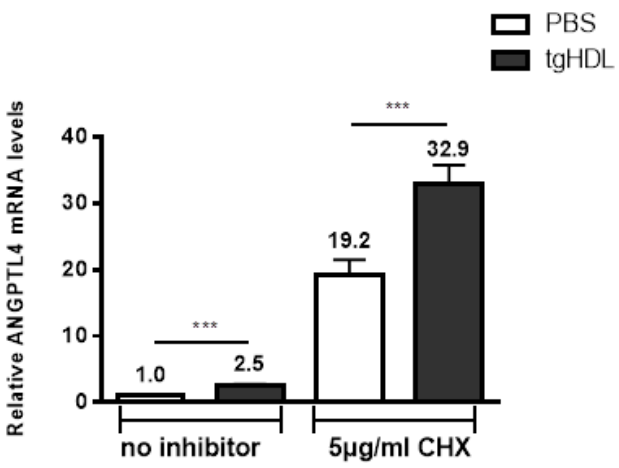

Figure 3.6 ANGTPL4 is a direct transcriptional target of HDL.
(A) EA.hy926 cells were pretreated with 5 μg/ml cycloheximide (CHX) or DMSO (no inhibitor) for 1 h and then treated with tgHDL or PBS for additional 8 h. Total RNA was extracted and quantitative RT-PCR was performed to determine ANGPTL4 mRNA levels, which were normalized relative to the RPLPO mRNA levels. The relative ANGPTL4 mRNA levels are expressed as mean (±SD) from at least four independent experiments. Symbols: *, $p \leq 0.05$; ***, $p \leq 0.001$.

The PI3K and p38 signaling pathways are implicated in the regulation of ANGPTL4 gene by tgHDL in endothelial cells

We next sought to delineate the signaling pathway(s) that are induced by tgHDL in endothelial cells and culminate in the overexpression of the ANGPTL4 gene. First we established that tgHDL was able to stimulate the phosphorylation of the signaling kinases AKT, p38, ERK and JNK with different kinetics (Fig. 3.7A). Specifically, the activation of MAP kinases JNK and p38 was very fast, reached a peak at 5 min post-induction and declined thereafter. The activation of AKT and ERK reached a peak at 30 min post-HDL treatment. However, ERK phosphorylation was more stable and started to decline after 2 h of stimulation with tgHDL.

To address the contribution of each kinase in ANGPTL4 regulation by HDL we used specific inhibitors. As shown in Figs. 3.7B-D, treatment of EA.hy926 cells with specific inhibitors of PI3 kinase (LY) or p38MAP kinase (SB) independently or in combination abolished the induction of the ANGPTL4 gene by tgHDL. In contrast, inhibitors for JNK or ERK kinases had no effect on the upregulation of ANGPTL4 mRNA levels by tgHDL in endothelial cells (Fig. 3.7E and F).

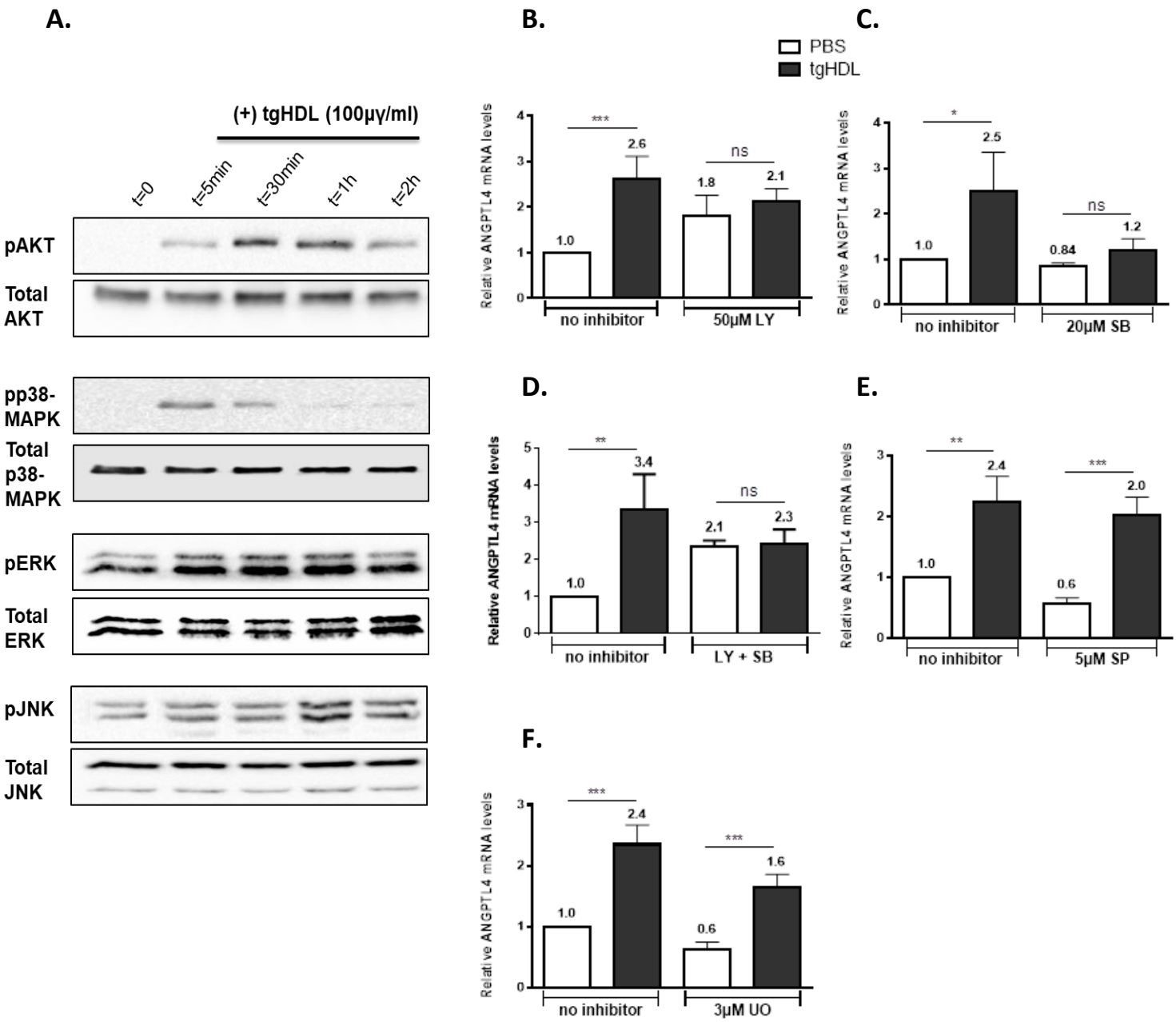

Figure 3.7 HDL induces ANGTPL4mRNA levels through the activation of PI3K/AKT and p38MAPK pathways. A) EA.hy926 cells were treated with tgHDL (100 μg/ml) for the indicated time periods. Cell extracts were collected and the total and phosphorylated levels of kinases AKT, p38, ERK and JNK were determined by immunoblotting using the corresponding antibodies. The experiment was performed three times and representative images are shown. B–F) EA.hy926 cells were pretreated for 1 h with 50 μM LY (PI3K/AKT inhibitor) (B), 20 μM SB (p38 inhibitor)(C), both 50 μM LY and 20 μM SB (D), 3 μM UO (ERK inhibitor) (E), 5 μM SP (JNK inhibitor) (F), or with DMSO (no inhibitor) and then treated with tgHDL or PBS (control) for additional 8 h. Total RNA was extracted and quantitative RT-PCR was performed to determine ANGPTL4 mRNA levels, which were normalized relative to the RPLPO mRNA levels. The relative ANGPTL4 mRNA levels are expressed as mean (±SD)

from at least three independent experiments. Symbols: ns, not significant; *, p ≤ 0.05; **, p ≤ 0.01; ***, p ≤ 0.001

It has been shown previously that HDL by activating the AKT pathway in the endothelium induces the activation of the endothelial nitric oxide synthase (eNOS) resulting in the production of NO (220, 229). Therefore, we investigated whether eNOS activation is required for the regulation of ANGPTL4 gene by tgHDL. We also observed that treatment of endothelial cells with tgHDL induced a rapid eNOS phosphorylation which peaked at 5 min and declined after 1 h of stimulation (Fig. 3.8A). Then, we treated endothelial cells with tgHDL in the presence and in the absence of an inhibitor for eNOS (L-NMMA) and we determined the ANGPTL4 mRNA levels by RT-qPCR. The data showed that the inhibitor of eNOS had no effect on ANGPTL4 gene induction by tgHDL (Fig. 3.8B) suggesting that the eNOS-mediated pathway is not implicated in the HDL-mediated induction of ANGPTL4.

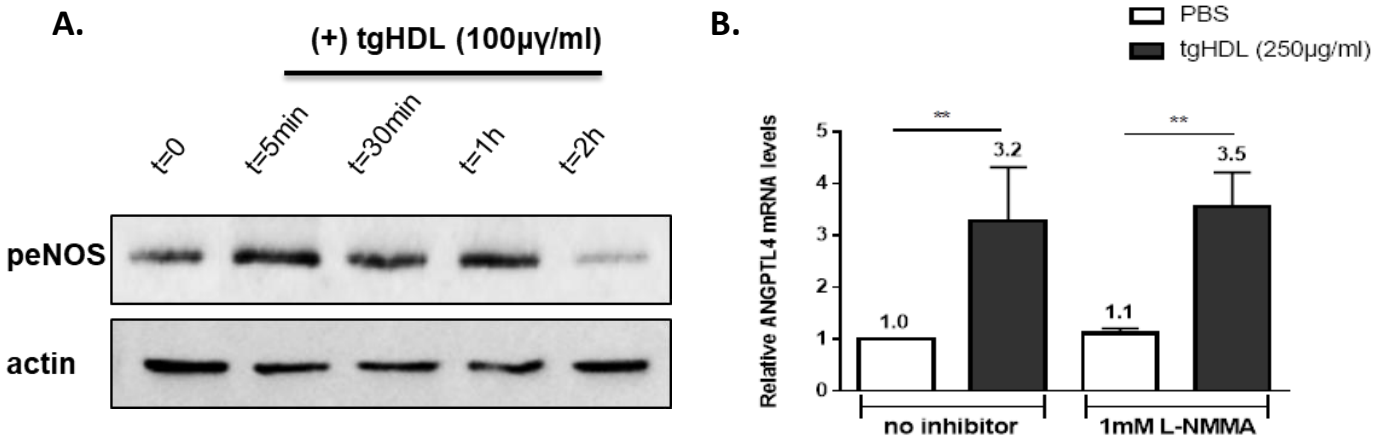

<u>Figure 3.8</u> eNOS activation by tgHDL is not implicated in the HDL-mediated induction of ANGPTL4 A) EA.hy926 cells were treated with tgHDL (100 μg/ml) for the indicated time periods. Cell extracts were collected and the phosphorylated levels of kinase eNOS as well as the protein levels of actin were determined by immunoblotting using the corresponding antibodies. The experiment was performed three times and representative images are shown. B) EA.hy926 cells were pretreated for 1 h with 1 mM L-NMMA (eNOS inhibitor) or with DMSO (no inhibitor) and then treated with tgHDL or PBS (control) for additional 8 h. Total RNA was extracted and quantitative RT-PCR was performed to determine ANGPTL4 mRNA levels, which were normalized relative to the RPLPO mRNA levels. The relative ANGPTL4 mRNA levels are expressed as mean (±SD) from at least three independent experiments. Symbols: **, p ≤ 0.01;

HDL Induces AKT-mediated phosphorylation of FOXO1 and its translocation to the cytoplasm

Stimulation of the PI3K/AKT signaling pathway leads to the phosphorylation of several downstream effectors including the transcription factor FOXO1 (435). To investigate the potential regulation of FOXO1 localization and functions by HDL, we treated EA.hy926 cells with tgHDL (250 μg/ml) or PBS for a range of time points while monitoring the levels of phosphorylated and total FOXO1 in cytoplasmic and nuclear extracts by western blotting using the corresponding antibodies. As shown in Fig. 3.9A, incubation of EA. hy926 cells with tgHDL caused a very rapid phosphorylation of FOXO1 in the nucleus which peaked at 5 min and declined to non-stimulated levels at 1 h post-stimulation. At the same time point (5 min), the levels of total FOXO1 in the nucleus started to decline and the levels of total FOXO1 in the cytoplasm strongly increased at 30 min of treatment. This increase in total cytoplasmic FOXO1 was transient since it returned to pre-stimulated levels at 2 h post-induction and at the same time, the levels of total FOXO1 in the nucleus increased. On the contrary, the mRNA levels of FOXO1 were not changed after treatment of endothelial cells with tgHDL for different time points (Fig. 3.9B), indicating that tgHDL regulates FOXO1 through post-translational modifications.

The data of the immunoblotting analysis were validated by immunofluorescence experiments. These experiments showed that prior to treatment with tgHDL, FOXO1 was localized exclusively in the nucleus of EA.hy926 cells (Fig. 3.9C first row), whereas following 30 min treatment with tgHDL (250 μg/ml) there was a significant nuclear exclusion of FOXO1 (Fig. 3.9C second row). In agreement with the data of Fig. 3.7B nuclear exclusion of FOXO1 by tgHDL was prevented using an inhibitor of PI3K (LY) whereas an inhibitor of p38 MAP kinase (SB) had a minor effect (Fig. 3.7B third and fourth rows respectively).

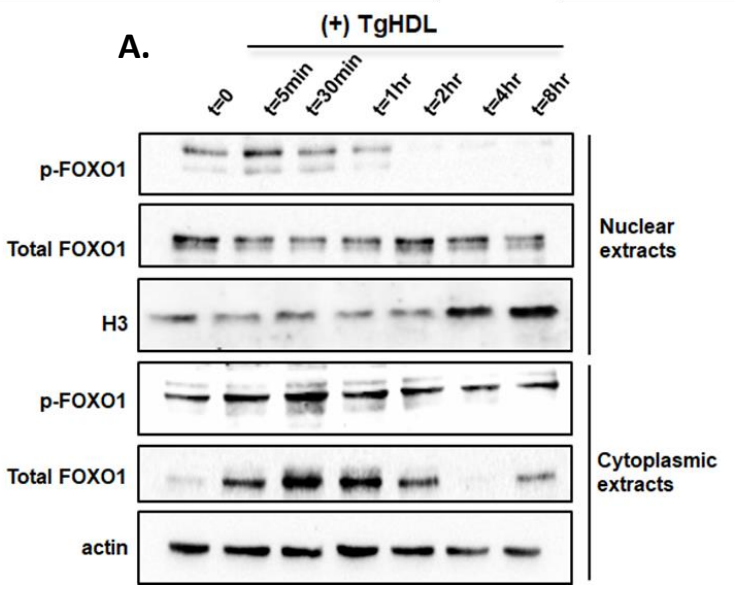
A.
(+) TgHDL
t=0
t=5min
t=30min
t=1hr
t=2hr
t=4hr
t=8hr
p-FOXO1
Total FOXO1
H3
Nuclear extracts
p-FOXO1
Total FOXO1
actin
Cytoplasmic extracts

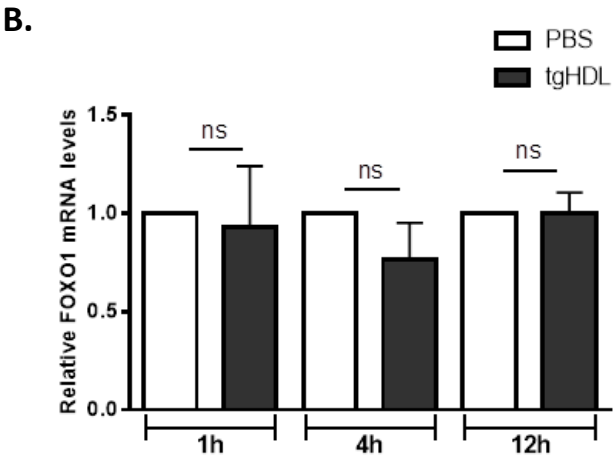
B.
PBS
tgHDL
Relative FOXO1 mRNA levels
1.5
1.0
0.5
0.0
ns
ns
ns
1h
4h
12h

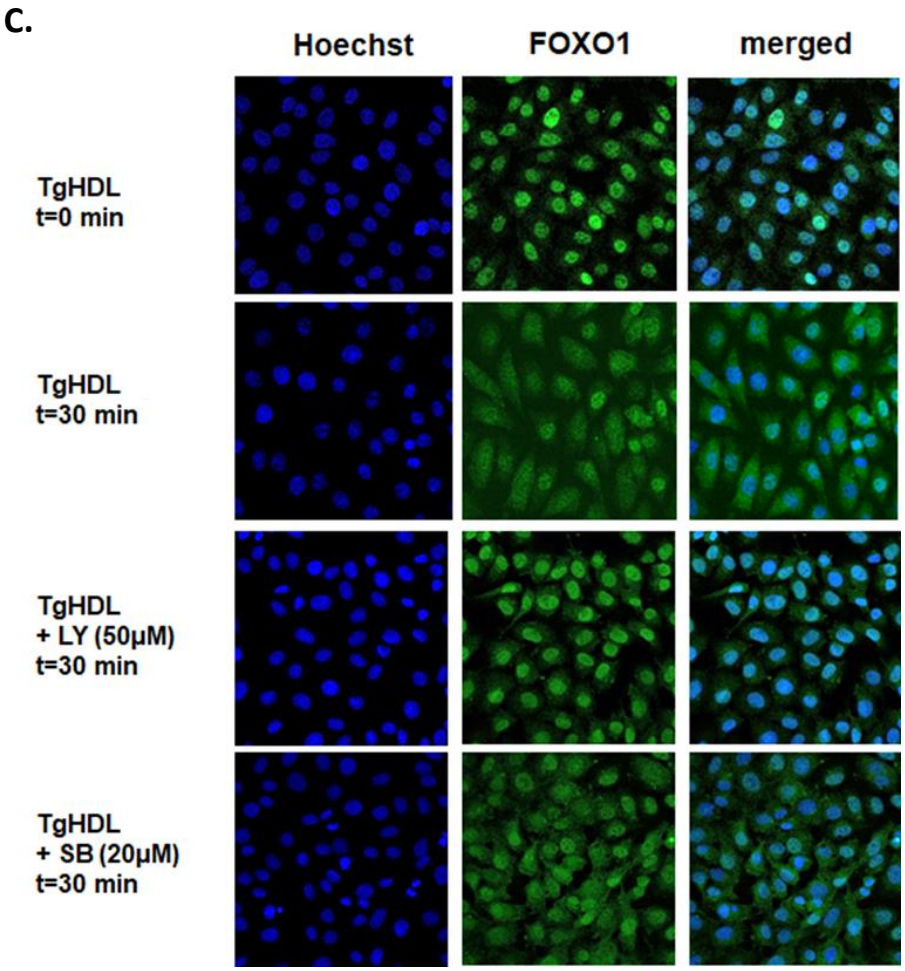
C.
Hoechst
FOXO1
merged
TgHDL
t=0 min
TgHDL
t=30 min
TgHDL
+ LY (50μM)
t=30 min
TgHDL
+ SB (20μM)
t=30 min

Figure 3.9 HDL induces the phosphorylation of FOXO1 and its translocation to the cytoplasm. A) EA.hy926 cells were treated with tgHDL (100 μg/ml) for the indicated time periods. Cell lysates were collected and the nuclear extracts were separated from the cytoplasmic extracts as described in Methods. The total and phosphorylated levels of FOXO1 in both nuclear and cytoplasmic extracts were determined by Western Blotting using the corresponding antibodies. The protein levels of histone H3 and actin were used as nuclear and cytoplasmic markers respectively. The experiment was performed three times and representative images are shown. B) EA.hy926 cells were treated with 250 μg/ml of tgHDL or PBS for the indicated time periods. Total RNA was extracted and quantitative RT-PCR was performed to determine FOXO1 mRNA levels, which were normalized relative to the RPLPO mRNA levels. The relative ANGPTL4 mRNA levels in the absence (white bars) and in the presence (black bars) of tgHDL (mean ± SD) from at least four independent experiments are shown for each time point. C) EA.hy926 cells were treated with tgHDL (100 μg/ml) in the absence and in the presence of the inhibitors LY (50 μM) or SB (20 μM) for the indicated time periods. The intracellular localization of FOXO1 was determined by immunofluorescence using an antibody for total FOXO1. Nuclei were stained with Hoechst dye. Confocal images were overlaid with Z-projection. Symbols: ns, not significant.

Induction of ANGPTL4 by tgHDL is mediated by FOXO1

Having established that tgHDL regulates FOXO1 phosphorylation and intracellular localization, we wondered whether FOXO1 is implicated on the tgHDL-mediated induction of the ANGPTL4 gene. To assess this question, we utilized the FOXO1 inhibitor AS1842856 (AS), which blocks the transcription activity of FOXO1. Firstly, we examined the effect of AS in the regulation of ANGPTL4 gene expression and we observed that treatment of EA.hy926 cells for 9h with increasing concentrations of AS (5 nM to 10 μM), increased ANGPTL4 mRNA levels in a dose dependent manner suggesting that FOXO1 is a negative regulator of the ANGPTL4 gene in endothelial cells (Fig. 3.10A). We found that low AS concentrations (50 nM–100 nM) had a moderate effect (1.5–1.8 fold induction) on ANGPTL4 mRNA levels which was not statistically significant whereas higher AS concentration (5–10 μM) were required to increase ANGPTL4 gene transcription (Fig. 3.10A). A further increase in AS concentration to 20 μM apparently had non-specific effects (Fig. 3.10A).

Then, we investigated the effect of AS in the tgHDL-mediated induction of ANGPTL4. Therefore, EA.hy926 cells were pre-treated for 1h with two different concentrations of AS or

with no inhibitor and then treated with tgHDL or PBS for additional 8h. Figure 10B shows that in the presence of 5μM concentration of AS the mRNA levels of ANGPTL4 were increased about 2 folds, whereas co-treatment with 5μM AS and tgHDL lead to a higher increase in the mRNA levels of ANGPTL4. Moreover, we identified found again that in the presence of 10μM of AS, the mRNA levels of ANGPTL4 were increased higher compared to 5μM AS (Fig. 3.10B). Interestingly, in the presence of 10μM AS, the tgHDL was not able to further induce ANGPTL4 gene expression (Fig. 3.10B).

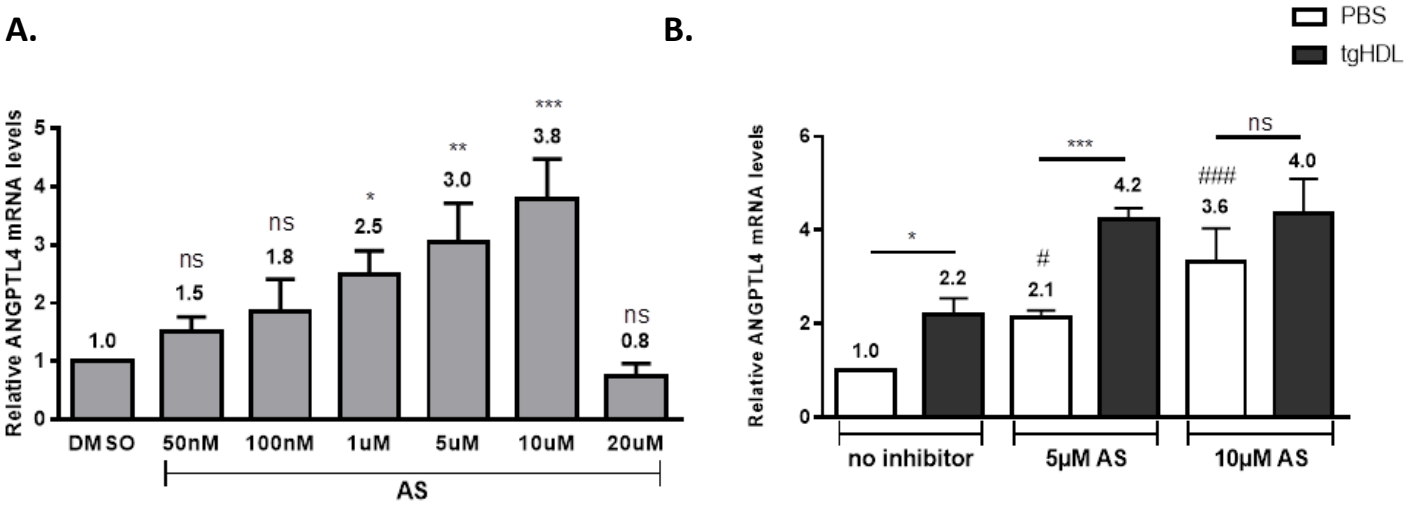

<u>Figure 3.10</u> FOXO1 inhibition increases ANGPTL4 mRNA levels and abolishes ANGPTL4 gene induction by HDL. A) EA.hy926 cells were treated with the indicated concentrations of AS1842856 (AS) for 9h. Total RNA was extracted and quantitative RT-PCR was performed to determine ANGPTL4 mRNA levels, which were normalized relative to the RPLPO mRNA levels. The relative ANGPTL4 mRNA levels are expressed as mean (±SD) from three independent experiments. B) EA.hy926 cells were pre-treated for 1 h with AS in two different concentrations (5 μM or 10μM) or with DMSO (no inhibitor). Then 250 μg/ml of tgHDL or PBS was added for additional 8 h. Total RNA was extracted and quantitative RT-PCR was performed to determine ANGPTL4mRNA levels, which were normalized relative to the RPLPO mRNA levels. The relative ANGPTL4mRNA levels are expressed as mean (±SD) from at least four independent experiments Symbols: ns, not significant; *, $p \leq 0.05$; **, $p \leq 0.01$; ***, $p \leq 0.001$; #, $p \leq 0.05$; ###, $p \leq 0.001$. In panel B * indicates the statistical difference between the absence and the presence of tgHDL for each concentration of inhibitor or no inhibitor. # indicates the statistical difference between the absence and the presence of the FOXO1 inhibitor (in untreated cells only).

The role of FOXO1 in tgHDL-mediated induction of the ANGPTL4 gene was further established by a gene silencing experiment. The efficiency of FOXO1 gene silencing by a FOXO1-specific siRNA and the non-specific (scrambled) siRNA was determined by RT-qPCR and western blotting experiment (Fig. 3.11A and B). As shown in Fig. 3.11C, the siRNA for FOXO1 increased ANGPTL4 mRNA levels 3-fold in EA.hy926 cells whereas the scrambled siRNA had no effect on ANGPTL4 expression. Treatment of EA.hy926 cells with tgHDL caused a 3.5-fold induction in ANGPTL4 mRNA levels but most importantly, this induction could not be further increased in the presence of the FOXO1 siRNA (Fig. 3.11C). The combined data of Figs. 9, 10 and 11 indicates that the induction of ANGPTL4 gene by tgHDL via the PI3K/AKT pathway requires the inhibition of FOXO1 by phosphorylation and nuclear exclusion.

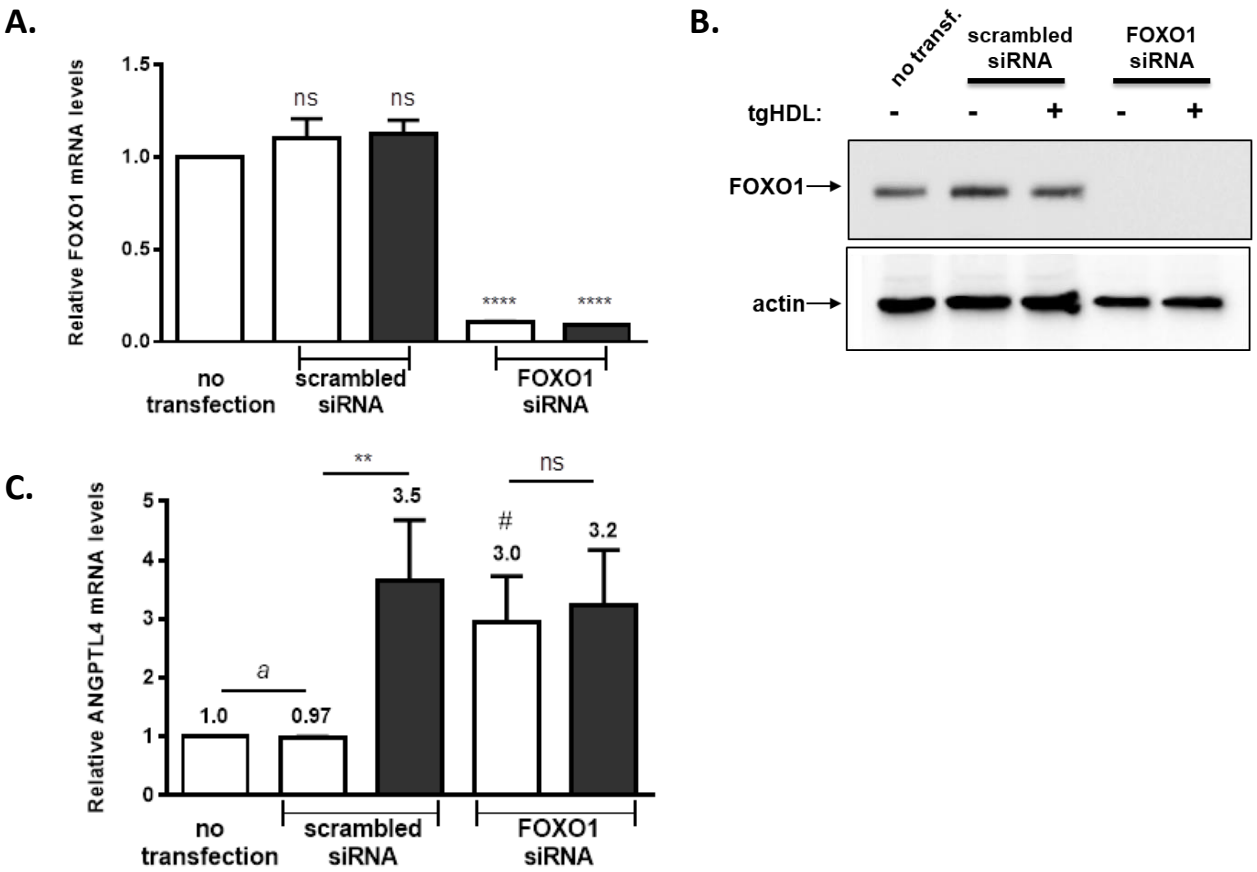

<u>Figure 3.11</u> FOXO1 silencing increases ANGPTL4 mRNA levels and abolishes ANGPTL4 gene induction by HDL. A-C) EA.hy926 cells were transfected with 100 nM of FOXO1 siRNA or with a control siRNA (scrambled) or were non-transfected. Endothelial cells were treated with 250 μg/ml of tgHDL or with PBS (untreated) for 8 h. Total RNA was extracted and quantitative RT-PCR was performed to determine FOXO1 (A) and ANGPTL4 (C) mRNA levels, which were normalized relative to the RPLPO mRNA levels. The relative ANGPTL4 and FOXO1 mRNA levels are expressed as mean (±SD) from three independent experiments. Cell lysates were collected (B) and the protein levels of FOXO1 were determined by Western Blotting using the corresponding antibody. The protein levels of actin were used for normalization. The experiment was performed three times and representative images are shown. Symbols: ns, not significant; *, $p \leq 0.05$; **, $p \leq 0.01$; ***, $p \leq 0.001$;*a*, not significant #, $p \leq 0.05$; ###, $p \leq 0.001$. In panels C * indicates the statistical difference between treated (with tgHDL) and untreated cells, while *a and* # indicate the statistical difference between the transfected and the non-transfected cells.

The human ANGPTL4 promoter is not activated by HDL

Next, we investigated whether the effect of HDL on ANGPTL4 gene expression is mediated through regulatory elements in the promoter of this gene. For this reason, we constructed a plasmid containing the -2.362/+77 region of human ANGPTL4 promoter upstream to the luciferase gene (-2.362/+77-ANGPTL4 promoter). The EA.hy926 cells were transfected with this plasmid and then were treated with 250μg/ml tgHDL or PBS for 24h. As depicted in Fig. 3.12, tgHDL could not induce the activity of the -2.362/+77 ANGPTL4 promoter suggesting that this promoter region is not required for the induction of the ANGPTL4 gene by HDL in endothelial cells and that either a different regulatory region in required or the induction is post-transcriptional.

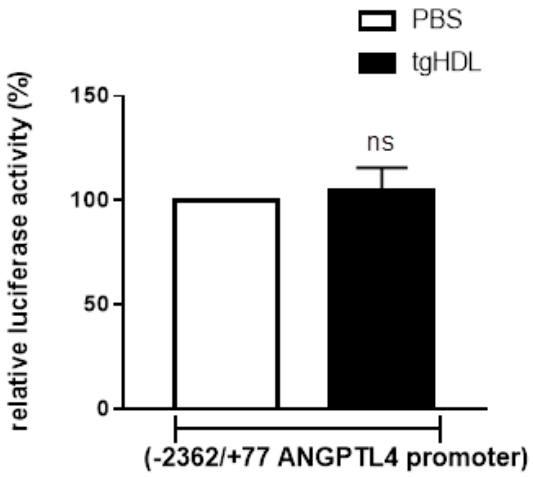

Figure 3.12 HDL does not regulate the human ANGPTL4 promoter.
EA.hy926 cells were transiently transfected with the (-2362/+77) ANGPTL4 promoter (0.5 μg) along with a β-galactosidase expression vector (0.5 μg) and 48h after transfection, cells were treated with 250μg/ml tgHDL or PBS for additional 24h. The (%) normalized relative promoter activity (±SD) was calculated from at least three independent experiments performed in duplicates. Symbols: ns, not significant.

Part I: Discussion

Low levels of plasma HDL cholesterol (HDL-C) are a strong and independent risk factor for the development of atherosclerotic CVD in humans (207). Additionally, a great number of reports have revealed that HDL exerts atheroprotection through a wide range of effects including cholesterol efflux from macrophage foam cells, protection of LDL particles against oxidation, preservation of the physiological function of the endothelium and an anti-thrombotic role (36). However, till today, drugs that were designed to increase HDL-C levels failed to counteract CVD risk in human clinical studies (354, 436). Moreover, several studies showed that HDL isolated from patients with CVDs not only was unable to exert the known anti-atherosclerotic functions, but in some cases also displayed pro-atherosclerotic properties (255, 284, 317). These findings indicated that by simply increasing the plasma HDL-C levels we cannot safely predict CVD risk and that HDL functionality is what determines atheroprotection. Therefore, a better understanding of the mechanisms underlying HDL functionality is needed. We focused on the impact of HDL on endothelium, since endothelium is an important regulator of cardiovascular homeostasis (17, 19), and also dysfunctional endothelium is associated with the initiation and the progression of atherosclerosis (17, 23). *In vitro* and *in vivo* studies have revealed that HDL protects endothelium against injury by promoting proliferation, migration and angiogenesis, while it also promotes the production of eNOS-dependent nitric oxide (NO) and also has anti-inflammatory, anti-apoptotic and anti-thrombotic effects (4, 235, 255).

Therefore, we aimed at identifying key molecular players mediating the effects of HDL on endothelium in an effort to better understand its molecular functions and pinpoint new potential therapeutic targets. As a starting point we utilized microarray data that had been generated following the treatment of human aortic endothelial cells with rHDL-apoA-I. Among the 410 significant gene expression changes, corresponding to a range of molecular pathways and cellular functions, we focused on ANGPTL4 (Fig. 3.1) due to its recently demonstrated atheroprotective properties (395, 396). ANGPTL4 is a protein known primarily

for its role as an inhibitor of lipoprotein lipase (LPL) and consequently as an important regulator of lipid metabolism (433). Additionally, ANGPTL4 is widely expressed in endothelial cells regulating endothelial cell integrity, vascular permeability and angiogenesis (437). However, its exact role in these processes is controversial, since Galaup and colleagues reported that ANPTL4 inhibits the increase in vascular permeability caused by histamine (438), while another study reported that the C-terminal fibrinogen-like domain of ANGPTL4 (cANGPTL4) disrupted the integrity of the endothelium by weakening cell-cell contacts (439). Today, ANGPTL4 is characterized as a 'gatekeeper' that regulates vascular integrity and angiogenesis in a context-dependent manner (440), and thus it emerges as an important target of HDL. Therefore, we initially validated the microarray data by performing qPCR analysis in the endothelial cell line EA.hy926 following treatment with rHDL-AI (Fig. 3.3). Importantly, we observed that both reconstituted and natural spherical HDL isolated either from transgenic mice (tgHDL) or healthy humans (hHDL) were able to induce the expression of this gene, indicating that ANGPTL4 is a true HDL-target gene (Fig. 3.3). Additionally, HDL was able to induce both the mRNA (Fig. 3.4) and the protein levels of ANGPTL4 (Fig. 3.5A). Actually, ANGTPL4 seems to be an early response gene in HDL treatment, since its induction occurred already 1h after the treatment with HDL (Fig. 3.4B). Although we observed that the secreted protein levels of ANGPTL4 were induced after treatment with HDL, its endogenous levels were not altered (Fig. 3.5A, B). Most likely, the more ANGPTL4 protein is produced the more is secreted but whether HDL also affects the secretory mechanism of ANGPTL4 could not be excluded.

Furthermore, we observed that HDL induces the expression of ANGTPL4 through the activation of both PI3K/AKT (Fig. 3.7B) and p38-MAPK (Fig. 3.7C) pathways. Since several effects of HDL on endothelium are mediated through the PI3K/AKT/eNOS axis (441), we investigated whether eNOS activation and subsequently NO production is also involved in ANGPTL4 gene induction by HDL. Although HDL induced the activation of eNOS, the effect on ANGPTL4 expression was independent of NO-production (Fig. 3.8). An additional

downstream target of PI3K/AKT axis is the transcription factor FOXO1. AKT activation phosphorylates nuclear FOXO1 promoting its translocation to the cytoplasm and consequently its inactivation (442). FOXO1 is a widely expressed transcription factor and regulates directly genes involved in the cell cycle and cellular metabolism (443). In the liver, FOXO1 promotes gluconeogenesis by positively regulating the expression of phosphoenolpyruvate carboxykinase 1 (PEPCK) and glucose-6-phosphatase (G6pc) (444), while in the adipose tissue it induces lipolysis by stimulating the expression of adipose triacylglycerol (TAG) lipase (ATGL) (445). The importance of FOXO1 in endothelium metabolism was demonstrated recently, where FOXO1 reduces the metabolic activity of endothelial cells maintaining them at quiesecence and restricting their proliferation (446). Therefore, it was of great interest to observe that tgHDL induced the rapid phosphorylation of FOXO1 and its nuclear export (Fig. 3.9). The effect of tgHDL was mediated through PI3K/AKT pathway as expected (Fig. 3.9C). Furthermore, using a specific inhibitor of the transcriptional activity of FOXO1 and a potent FOXO1-specific siRNA we were able to demonstrate that FOXO1 is an inhibitor of ANGPTL4 gene expression in endothelial cells (Fig. 3.10A, 3.10B, 3.11C). Of note, co-incubation of endothelial cells with tgHDL and FOXO1 inhibitor or siFOXO1 did not further increase the expression of ANGPTL4 (Fig. 3.10B, 3.11C) indicating that these two molecules (tgHDL and FOXO1) function in the same pathway and so, HDL induces the expression of ANGPTL4 by “removing”’ FOXO1.

How FOXO1 downregulates the expression of this gene remains unexplored. We did not observe a direct binding of FOXO1 to the promoter region of ANGPTL4 (Fig. 3.12). However, it cannot be excluded that FOXO1 may bind to an enhancer region. For instance, in rat ANGPTL4, FOXO1 binds to a FOXO1 site located 6kb upstream of the TTS upregulating the expression of this gene in the liver (447). An alternative mechanism of ANGPTL4 regulation by HDL could be indirect and more specific via the nuclear receptor PPARγ. A functional PPAR-responsive enhancer has been identified at the third intron of ANGPTL4 gene, through which PPARs activate this gene (402, 448). Additionally, it has

been reported that binding of PPARβ/δ to this enhancer, in the absence of its ligand, recruits corepressors in order to inhibit the expression of ANGPTL4 (399). Interestingly, it was shown that FOXO1 can be converted from a transcriptional activator to a transcriptional repressor in adipocytes by trans-repressing PPARγ through direct protein-protein interactions (449). FOXO1 is recruited to PPRE on target genes and interferes with promoter DNA occupancy by PPARγ. Insulin prevents FOXO1-PPARγ interactions and rescues trans-repression (449). Moreover, a novel mechanism of FOXO1-mediated transcriptional repression was revealed in liver cells involving the recruitment of corepressors, such as SIN3A and histone deacetylases to the promoters of FOXO1 target genes such as the glycolytic enzyme glucokinase (gck) via physical interactions with FOXO1 (450). Interestingly, no FOXO1 binding site could be identified on the gck gene promoter and it was hypothesized that FOXO1 associates with the gck promoter indirectly via physical interactions with Hepatocyte Nuclear Factor 4 (HNF-4), which binds to the gck promoter in liver cells and activates its transcription (451).

A schematic representation of the proposed model of ANGPTL4 gene regulation by HDL and FOXO1 via the PI3K/AKT signaling pathway is shown in Figure 3.13 These findings are very important to understand how HDL exerts atheroprotection on endothelium. Initially, the activation of endothelial FOXO1 has been associated with atherosclerosis (452). Specifically, FOXO1 downregulates the expression of the eNOS gene by directly binding to its promoter (453), while it also directly upregulates the expression of the inducible NOS (iNOS) (454). iNOS produces large quantities of NO for prolonged periods of time and thus iNOS-derived NO reacts with superoxide to yield peroxinitrite, a highly reactive oxidant (455). Interestingly, FOXO1 activated by hyperglycemia or a FOXO1 gain-of-function mutant promotes iNOS-dependent NO-peroxynitrite generation, which leads in turn to LDL oxidation and eNOS dysfunction (454). Furthermore, in a mouse model of atherosclerosis ($LDLr^{-/-}$ mice) the depletion of endothelium-specific FOXO isoforms (FOXO1, FOXO-3a and FOXO-4) resulted in reduced endothelial inflammation, oxidative stress and atherosclerosis induced

by western diet (456). As a consequence, our finding that endothelial FOXO1 inactivation is mediated by HDL, could be intergraded into the broader atheroprotective program of HDL. On the other hand, upregulation of macrophage ANGPTL4 also has been characterized as anti-atherogenic (395, 396). However, how the endothelial ANGPTL4 contribute to the atheroprotective effects of HDL is not clear and it should be studied further. We could hypothesize three potent roles of endothelial ANGPTL4. Firstly, ANGPTL4 may protect HDL from hydrolysis by LIPG and/or LPL. It has been reported that circulating ANGPTL4 is physically associated with HDL in mice (398) and we also observed that the majority of the newly synthesized ANGPTL4 is associated with tgHDL (Fig. 3.5C). Secondly, ANGPTL4 may have an autocrine effect regulating endothelial integrity and angiogenesis. Interestingly, Prosser and colleagues have demonstrated that rHDL-AI augmented hypoxia-induced angiogenesis but inhibited the inflammation-induced angiogenesis (275). Since ANGPTL4 has been characterized as a context-dependent modulator of vascular permeability and angiogenesis (440), it would be interesting to investigate whether ANGPTL4 is the mediator of these opposite effects of HDL (440). Thirdly, ANGPTL4 may also have a paracrine effect on the foam cells accumulated in the atheromatic artery. Indeed, macrophage ANGPTL4 reduces foam cell formation as well as the inflammatory content in the lesions resulting in a reduction of atherosclerosis (395, 396). However, it should be mentioned that the effect of ANGPTL4 on atherosclerosis is tissue specific, since mice with ANGPTL4 deficiency in adipocytes presented reduced atherosclerosis (397). Although endothelial ANGPTL4 seems to be beneficial for the physiology of cardiovascular system, studies with mice deficient for endothelial-specific ANGPTL4 expression could elucidate the exact role of this protein during atherosclerosis.

In conclusion, our findings reveal novel molecular mechanisms through which HDL exerts atheroprotection. Moreover, the identification of ANGPTL4 as one of the most biologically relevant target genes and the elucidation of the key role of FOXO1 in HDL-mediated atheroprotection could be exploited for the design of novel therapeutic tools for

patients with atherosclerotic cardiovascular disease. Additionally, both the induction of ANGPTL4 and the inactivation of FOXO1 could be utilized as markers of HDL functionality.

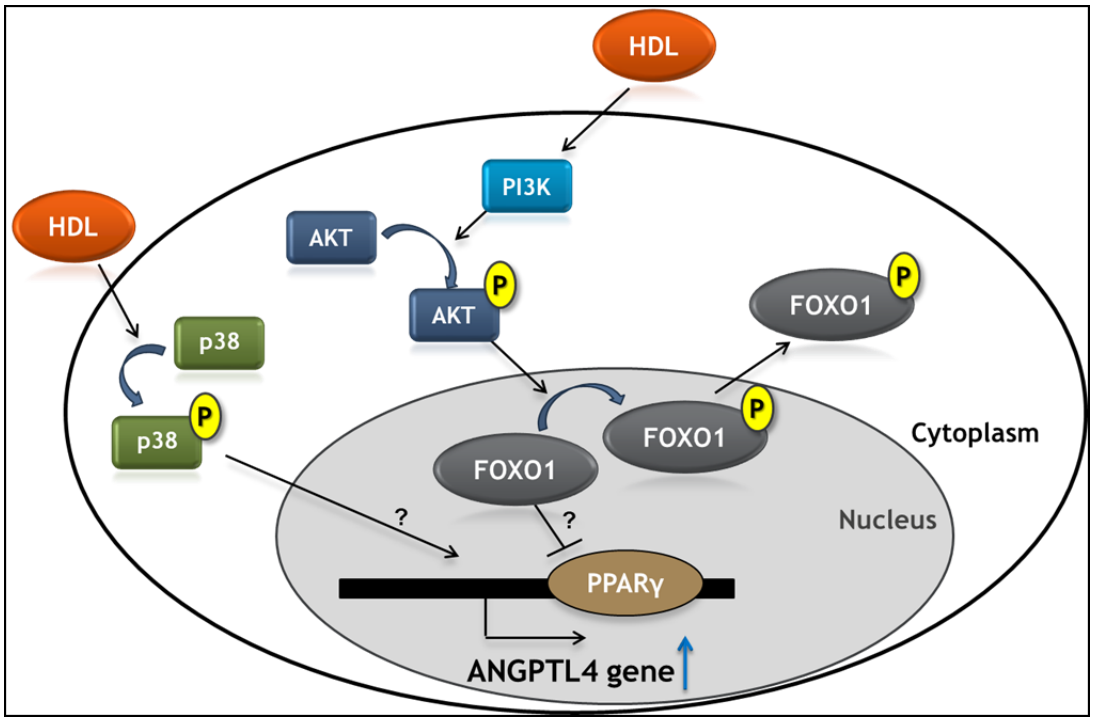

Figure 3.13 Proposed mechanism through which HDL regulates the expression of the ANGPTL4 gene

<u>Part II:</u> The role of HDL in the regulation of the endothelial lipase gene (LIPG) in endothlelial cells

As shown in Figure 3.1 of this chapter, at rHDL-AI has a great impact on the transcriptomic profile of endothelial cells as it affects the mRNA levels of 410 transcripts. We focused again on the transcripts coding for secreted proteins. Besides ANGPTL4, which was studied extensively in part I, we observed that the transcript for the endothelial lipase (LIPG) was among the most profoundly upregulated transcripts (Fig. 3.1B). LIPG is a lipase hydrolyzing mainly phospholipids and it is a characterized negative regulator of HDL levels in the serum (paper). This observation indicates a negative feedback for the control of HDL levels. Therefore we focused on the mechanisms through which HDL affects the expression of LIPG.

Native HDL and rHDL-AI have opposite effects onthe expression levels of LIPG

Initially, we examined whether LIPG is a common gene-target of all types of HDL (spherical type and discoidal type). For this reason, we utilized rHDL-AI, which resembles to the discoidal type, and native HDL, which contains the spherical type in abundance. Native HDL was isolated either from human healthy donors (hHDL) or from transgenic mice expressing the human apoA-I gene (tgHDL). The endothelial cell line EA.hy926 was treated for 12h with the above types of HDL or with PBS (control experiment). In contrast to the microarray experiments (Fig.1B), rHDL-AI did not affect the expression levels of LIPG (Fig. 3.14). More interestingly, we observed that native HDL (either tgHDL or hHDL) inhibited the expression of LIPG suggesting an opposite effect on the regulation of LIPG gene by discoidal and spherical HDL.

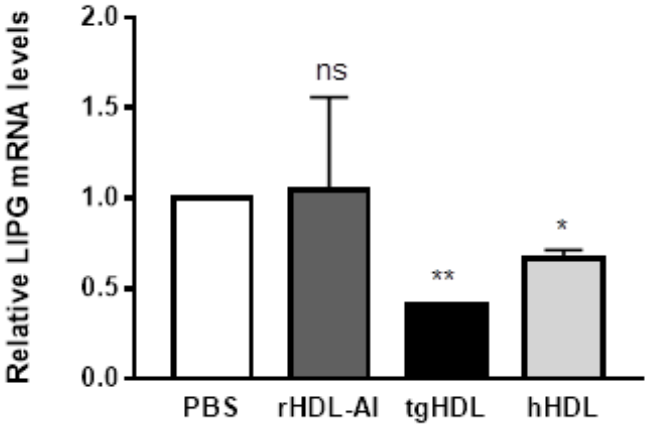

Figure 3.14 Native HDL and rHDL-AI have opposite effects on the endothelial LIPG levels EA.hy926 cells were treated with tgHDL, hHDL or rHDL-AI for 12h or with vehicle (PBS). Total RNA was extracted and quantitative RT-PCR was performed to determine LIPG mRNA levels, which were normalized relative to the RPLPO mRNA levels. The relative LIPG mRNA levels are expressed as mean (±SD) from at least two independent experiments and shown as a histograph. Symbols: ns, not significant;*, $p \leq 0.05$; **, $p \leq 0.01$

Since the main type of native HDL circulating in the blood of healthy people is the spherical one, we further investigated the role of native HDL in the regulation of *LIPG*. For this purpose, we utilized tgHDL which was shown to be functional (Fig. 3.2) and also mimics hHDL functionality in the regulation of both *ANGPTL4* (Fig. 3.3) and *LIPG* (Fig. 3.14) genes. We measured the mRNA levels of LIPG after treatment of endothelial cells with tgHDL in different concentrations (100μg/ml and 250μg/ml) for 12h. As Fig. 3.15 depicts, LIPG mRNA levels were decreased in a dose dependent manner in the presence of the different concentrations tgHDL compared to the PBS-treated cells.

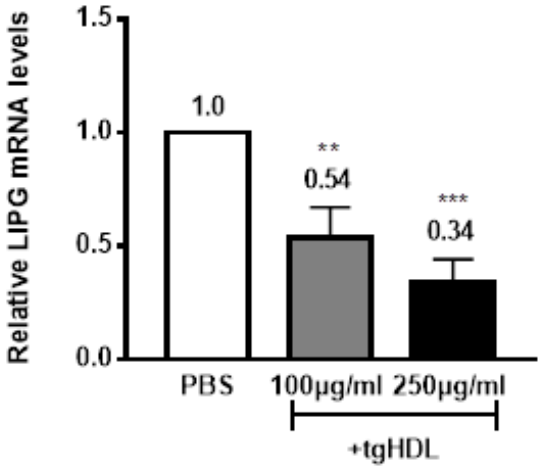

Figure 3.15 HDL decreases LIPG mRNA levels in a dose-dependent manner.
EA.hy926 cells were treated for 12h with 100 or 250 µg/ml of tgHDL. Total RNA was extracted and quantitative RT-PCR was performed to determine LIPG mRNA levels. The normalized LIPG mRNA levels relative to the RPLPO mRNA levels are expressed as mean (±SD) from at least two independent experiments.. Symbols: **, $p \leq 0.01$; ***, $p \leq 0.001$.

HDL represses the starvation-mediated induction of LIPG

The expression of LIPG gene has been shown to be induced in endothelial cells under starvation (426). To identify whether HDL modulates this starvation-mediated induction of LIPG, we cultured the EA.hy926 cells for 12h either in full medium (DMEM with 10% FBS) or in starvation medium (DMEM, without FBS) supplemented with either tgHDL(250µg/ml) or PBS (as negative control). In line with the published data, we observed that starvation provoked a 3-fold induction in the mRNA levels of LIPG (Fig. 3.16A). Interestingly, we observed that in the presence of tgHDL this induction was abolished (Fig. 3.16A).

Next, we monitored the mRNA levels of LIPG after culturing the endothelial cells in starvation medium supplemented with either PBS or tgHDL for different time points. T=0h corresponds to the starting time point at which tgHDL was added to the cells. We considered the expression levels of LIPG at t=0 as the basal levels for this gene. As shown in Fig.

3.16B, at early time points (t=1h, t=4h) starvation did not affect the mRNA levels of LIPG. However, after culturing the cells for 8h in starved conditions, the mRNA levels of LIPG were induced compared to the starting time point (Fig. 3.16B). We observed that as the starvation period was extended, the induction of LIPG was increased, reaching a peak after 24h of starvation (Fig. 3.16B). Importantly, we determined that the starvation-mediated induction of LIPG at 8h and 12h was prevented in the presence of tgHDL (Fig. 3.16B). However, this inhibitory effect of tgHDL was attenuated after 24h of treatment.

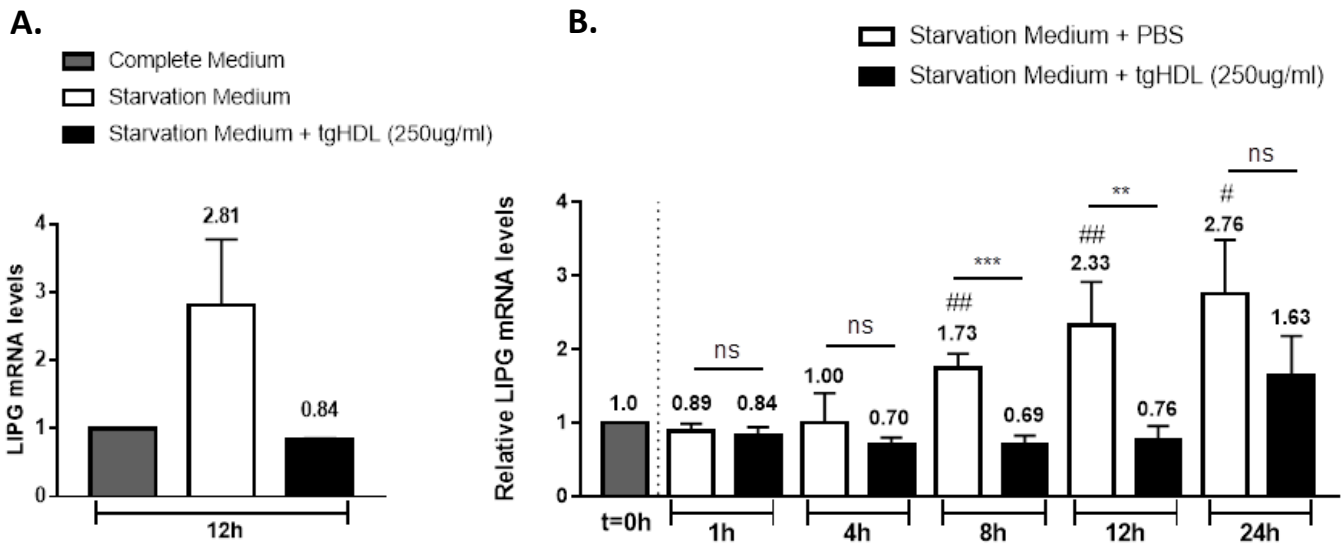

<u>Figure. 3.16</u> Starvation induces the expression of LIPG, while in the presence of tgHDL this effect was blocked. A) EA.hy926 cells were cultured for 12h either with complete medium, or with starvation medium supplemented with either tgHDL (250μg/ml) or PBS. Total RNA was extracted and quantitative RT-PCR was performed to determine LIPG mRNA levels. The normalized LIPG mRNA levels relative to the RPLPO mRNA levels are expressed as mean (±SD) from two independent experiments. B) EA.hy926 cells were cultured in starvation medium in the presence and in the absence of tgHDL (250μg/ml) for the indicated time periods. At the time point t=0h (starting time point), cells were either collected or treated with tgHDL (or PBS) respectively. Total RNA was extracted and quantitative RT-PCR was performed to determine LIPG mRNA levels, which were normalized relative to the RPLPO mRNA levels. The relative LIPG mRNA levels are expressed as (mean ± SD) from four independent experiments are shown. Symbols: ns, not significant; #, $p \leq 0.05$; ** or ##, $p \leq 0.01$; ***, $p \leq 0.001$.. In panel B ns and * indicate the statistical difference between treated (with tgHDL) and untreated (with PBS) cells within each time point, while # indicates the statistical difference between the starved cells without tgHDL and the cells at the starting time point.

Protein synthesis inhibition prevents the induction of LIPG by starvation

Next we wanted to investigate whether the observed increase in the mRNA levels of LIPG by starvation and the inhibitory effect of tgHDL are facilitated by directly affecting the expression of the LIPG gene or not. Therefore, we utilized the protein synthesis inhibitor cyclohexamide (CHX). Specifically, endothelial cells were treated with either CHX or DMSO (negative control) in starvation medium for 1h and then (at time point t=0) tgHDL was added for additional 8h. Figure 3.17 depicts that in the presence of CHX the mRNA levels of LIPG were equal to those of the time point t=0, indicating that the starvation-mediated induction of LIPG was abolished. Moreover, we observed that the co-treatment of endothelial cells with CHX and tgHDL did not promote further downregulation of LIPG mRNA levels (Fig. 3.17), indicating that CHX and tgHDL prevent the effect of starvation in the expression of LIPG via similar mechanisms. The above results suggest that LIPG is a direct transcriptional target neither of starvation nor of tgHDL. So, we can hypothesize that the regulation of the expression levels of an intermediate transcription factor is required, which in turn affects the expression of LIPG. Importantly, it seems that both tgHDL and starvation target, with differential effects, this intermediate transcription factor.

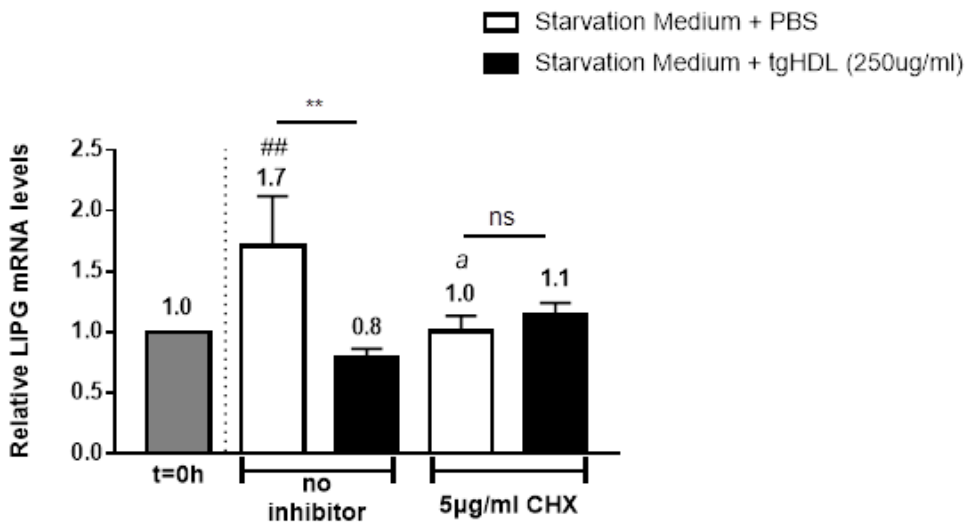

Figure 3.17 LIPG is not a direct transcriptional target of neither starvation nor tgHDL. EA.hy926 cells were pre-treated with 5 µg/ml cycloheximide (CHX) or DMSO (no inhibitor) for 1h in starvation medium and then treated with tgHDL or PBS for additional 8 h. At the time point t=0h (starting time point), cells were either collected or treated with tgHDL (or PBS) respectively. Total RNA was extracted and quantitative RT-PCR was performed to determine LIPG mRNA levels, which were normalized relative to the RPLPO mRNA levels. The relative LIPG mRNA levels are expressed as mean (±SD) from at least three independent experiments. Symbols: ns or *a*, not significant; ** or ##, $p \leq 0.01$. In the panel ns and * indicate the statistical difference between treated (with tgHDL) and untreated (with PBS) cells, while *a and* # indicates the statistical difference between the starved cells without tgHDL and the cells at the starting time point.

FOXO1 regulates the basal levels of LIPG expression

In the first part of this study, we established that tgHDL by promoting the translocation of FOXO1 to the cytoplasm inhibits its transcriptional activity and subsequently induces ANGPTL4 expression (Fig. 3.9). Therefore, we wondered whether FOXO1 is also implicated in the regulatory effects of HDL on the expression of *LIPG*. For this purpose, we performed gene silencing experiments by transfected EA.hy926 cells with siFOXO1. The efficiency of this siFOXO1 was confirmed in the first part of this study (Fig. 3.11A and B). Of note, we observed that silencing of FOXO1 eliminated the basal expression of *LIPG* (3.18).

The effect of 8h-starvation in the expression of *LIPG* was abolished in the presence of siFOXO1, while co-treatment of siFOXO1 and tgHDL could not promote a further decrease in the expression levels of *LIPG* (3.18). These results indicate that FOXO1 is an important activator of *LIPG* and is participating in the regulation of *LIPG* by starvation. Additionally, one mechanism of the inhibitory effect of tgHDL in this gene is by inactivating FOXO1.

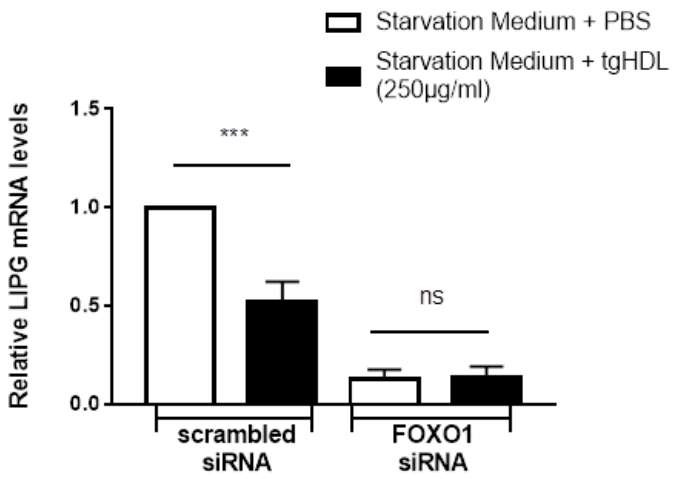

Figure 3.18 FOXO1 inhibition prevents LIPG expression. EA.hy926 cells were transfected with 100 nM of FOXO1 siRNA or with a control siRNA (scrambled). Then, endothelial cells were treated with 250 µg/ml of tgHDL or with PBS (untreated) for 8 h in starvation medium. Total RNA was extracted and quantitative RT-PCR was performed to determine LIPG mRNA levels, which were normalized relative to the RPLPO mRNA levels. The relative LIPG mRNA levels are expressed as mean (±SD) from at least three independent experiments. Symbols: ns, not significant; ***, $p \leq 0.001$;

As we discussed above, the starvation-mediated induction of LIPG requires the participation of an intermediate transcription factor which is inhibited by tgHDL. To address whether FOXO1 is this intermediate transcription factor, we measured the mRNA levels of FOXO1 at different time points after culturing the endothelial cells in starved conditions. We observed a slight but not statistically significant induction of FOXO1 mRNA levels after 1h and 12h of culture (Fig. 3.19). Moreover, we studied whether tgHDL affects the mRNA levels of FOXO1. In line with Fig. 3.9B, we, observed that FOXO1 mRNA levels are not affected in the presence of tgHDL (Fig. 3.19). The results from Fig. 3.9B and Fig. 3.19 suggest that FOXO1 is important for the starvation-mediated induction of LIPG but its transcriptional induction during starvation is not required for this function.

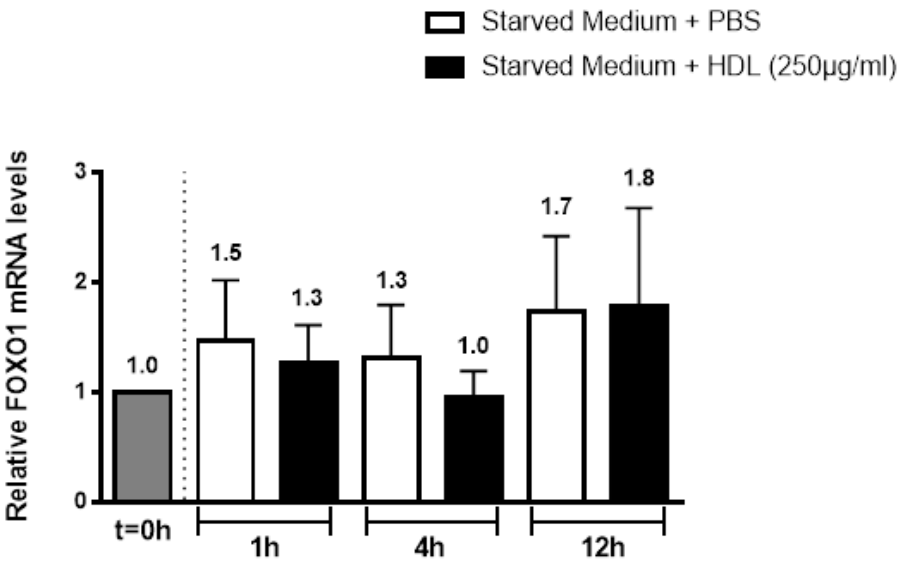

<u>Figure 3.19</u> The mRNA levels of FOXO1 were not affected either by starvation or by tgHDL. EA.hy926 cells were treated with 250 µg/ml of tgHDL or PBS for the indicated time periods. At the time point t=0h (starting time point), cells were either collected or treated with tgHDL (or PBS) respectively. Total RNA was extracted and quantitative RT-PCR was performed to determine FOXO1 mRNA levels, which were normalized relative to the RPLPO mRNA levels. The relative FOXO1 mRNA levels are expressed as mean (±SD) from two independent experiments.

ERK and JNK kinases are not implicated in the regulation of LIPG

HDL exerts its function in the endothelium through the activation of various signaling cascades and in the first part of this study we observed that tgHDL activates the signaling pathways of ERK and JNK by promoting the phosphorylation of the relative kinases (Fig. 3.7). To address the contribution of the above kinases in the inhibitory effect of tgHDL on the starvation-mediated induction of LIPG, we utilized specific kinase inhibitors. Specifically, endothelial cells were pre-treated with these inhibitors in starvation medium and were then treated with either tgHDL or PBS for additional 8h. We observed that the inhibitors for the above signaling cascades had no effect either on the upregulation of LIPG by starvation or in the subsequent inhibitory effect of tgHDL (Fig. 3.20).

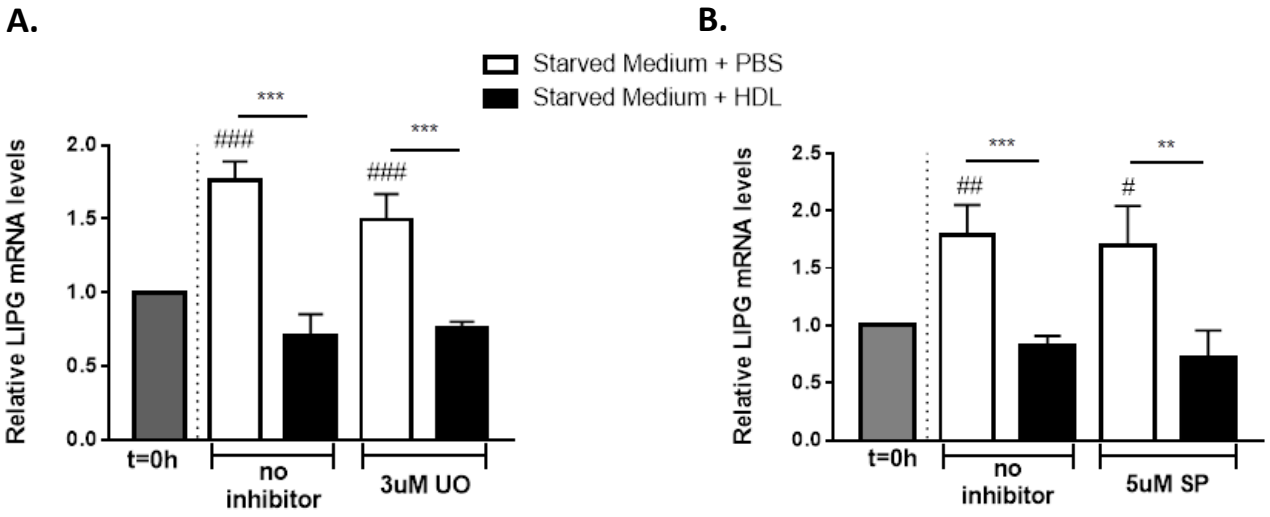

<u>Figure 3.20</u> ERK and JNK kinases are not implicated in the regulatory mechanisms underlying LIPG expression. EA.hy926 cells were pre-treated for 1 h with 3 μM UO (ERK inhibitor) (A), 5 μM SP (JNK inhibitor) (B), or with DMSO (no inhibitor) and then treated with tgHDL or PBS (control) for additional 8 h. At the time point t=0h (starting time point), cells were either collected or treated with either tgHDL or PBS respectively. Total RNA was extracted and quantitative RT-PCR was performed to determine LIPG mRNA levels, which were normalized relative to the RPLPO mRNA levels. The relative LIPG mRNA levels are expressed as mean (±SD) from at least three independent experiments. Symbols: * or # $p \leq 0.05$; ** or ##, $p \leq 0.01$; *** or ###, $p \leq 0.001$. *,** and *** indicate the statistical difference between treated (with tgHDL) and untreated (with PBS) cells, while #,## *and* ### indicates the statistical difference between the starved cells (without tgHDL) and the cells at the starting time point

Part II: Discussion

Endothelial lipase (LIPG) is a phospholipase that belongs to the triglyceride lipase family and its preferred substrates are the phospholipids of the HDL particles (457, 458). Several studies have reported that LIPG facilitates HDL catabolism and thus it is considered as a major determinant of HDL concentration in the plasma (457, 458). Specifically, hydrolysis of HDL-phospholipids by LIPG results in the generation of smaller HDL or lipid-poor apoA-I particles, which in turn are cleared from the circulation either by the SR-BI mediated selective uptake in the liver or by the kidney leading to the final catabolism of apoA-I (459, 460). Moreover, GWAS studies have shown a strong correlation between loss-of-function LIPG variants and elevated plasma HDL-C levels (417). Therefore, it was of great interest that we observed that tgHDL downregulates the expression of LIPG in endothelial cells (Fig 3.14) indicating a potential protective mechanism of HDL against its catabolism.

Of note, we observed that tgHDL had the opposite effect in the regulation of LIPG expression compared to rHDL-AI. Microarray data from endothelial cells treated with rHDL-AI showed LIPG among the most upregulated genes (Fig. 3.1). On the contrary, treatment of endothelial cells with natural HDL isolated either from human subjects (hHDL) or from transgenic mice overexpressing human apoA-I (tgHDL) resulted in the downregulation of LIPG (Fig 3.14). The molecular basis of this discrepancy could be explained by the different protein and lipid cargo among the two types of HDL. As we discussed in the introduction, several proteins, lipids and miRNAs are associated with the natural HDL affecting its functionality (38, 86), while rHDL-AI particles consist only of apoA-I, cholesterol and phospholipids. For instance, the apoM-S1P complex which is naturally bound to HDL and has been identified to exert a plethora of atheroprotective functions by activating cellular signaling cascades (164) is missing from rHDL-AI particles. Whether HDL subpopulations have differential effects on the regulation of the LIPG gene is not known and should be studied further. In our experiments, the majority of tgHDL particles are detected in the HDL3 subfraction which contains the most dense HDL particles with characterized atheroprotective

roles (60). Thus, plasma LIPG levels could be potentially utilized as a marker of HDL structure and functionality.

Since the main type of native HDL circulating in the blood of healthy people is the spherical one, we investigated further the role of native HDL in the regulation of LIPG. Previous studies have reported that endothelial LIPG expression is induced by growth deprivation (starvation) (426). In our study, we observed that tgHDL inhibited the induction of LIPG by starvation (Fig 3.16A, B). Interestingly, we found that the mechanisms underlying this regulation of LIPG by tgHDL involve both FOXO1 inactivation (Fig 3.18) and active protein synthesis (Fig 3.17). In the presence of a specific siRNA for FOXO1 (siFOXO1), the mRNA levels of LIPG were strongly reduced indicating that FOXO1 is important for the basal expression of this gene (Fig. 3.18). FOXO1 has also been identified to upregulate the expression of another member of triglyceride family, the lipoprotein lipase (LPL), in skeletal muscle (461). It has been reported that starvation promotes endothelial FOXO1 activation (454) and it appears that FOXO1 mediates the effect of starvation by upregulating the expression of LIPG. In contrast, as we observed in the first part of this study (Fig. 3.9), tgHDL promotes the inactivation of endothelial FOXO1 and consequently the downregulation of LIPG. Besides FOXO1 inactivation, tgHDL may also block the induction of an intermediate transcription factor in order to inhibit LIPG expression. This hypothesis is supported by two observations: 1) treatment with cyclohexamide (protein synthesis inhibitor) mimics the effect of tgHDL on the starvation-mediated induction of LIPG (Fig. 3.17); 2) the mRNA levels of FOXO1 were not changed after treatment with tgHDL (Fig. 3.9B and 3.19). Further studies should be done in order to identify which is this intermediate transcription factor and its exact role in the regulation of LIPG. However, since FOXO1 regulates the basal levels of LIPG expression, it is more likely that it also regulates the expression of this intermediate transcription factor.

There are controversial results on the exact role of LIPG in the development of atherosclerosis (418, 419). In addition, it is not clear whether LIPG exerts pro-inflammatory

or anti-inflammatory properties. Although LIPG is upregulated by inflammatory stimuli, some studies have reported that LIPG enhances monocyte adhesion to the vessel wall (418, 462), while another study revealed that LIPG decreases endothelial adhesion molecules (412). However, it is clear that LIPG is overexpressed in the aortas during atherosclerosis (463) thus contributing to the development of an environment that is not 'friendly' for HDL. Our findings elucidate a mechanism through which HDL tries to 'escape' from the inhibitory effect of LIPG. Taking into consideration the results from the first part of the study, HDL both downregulates the expression of LIPG and upregulates the expression of ANGPTL4, which is a physical inhibitor of LIPG (Fig. 3.21). It seems that HDL regulates its own catabolism while FOXO1 emerges as a crucial mediator of the atheroprotective effects of HDL on the vascular endothelium.

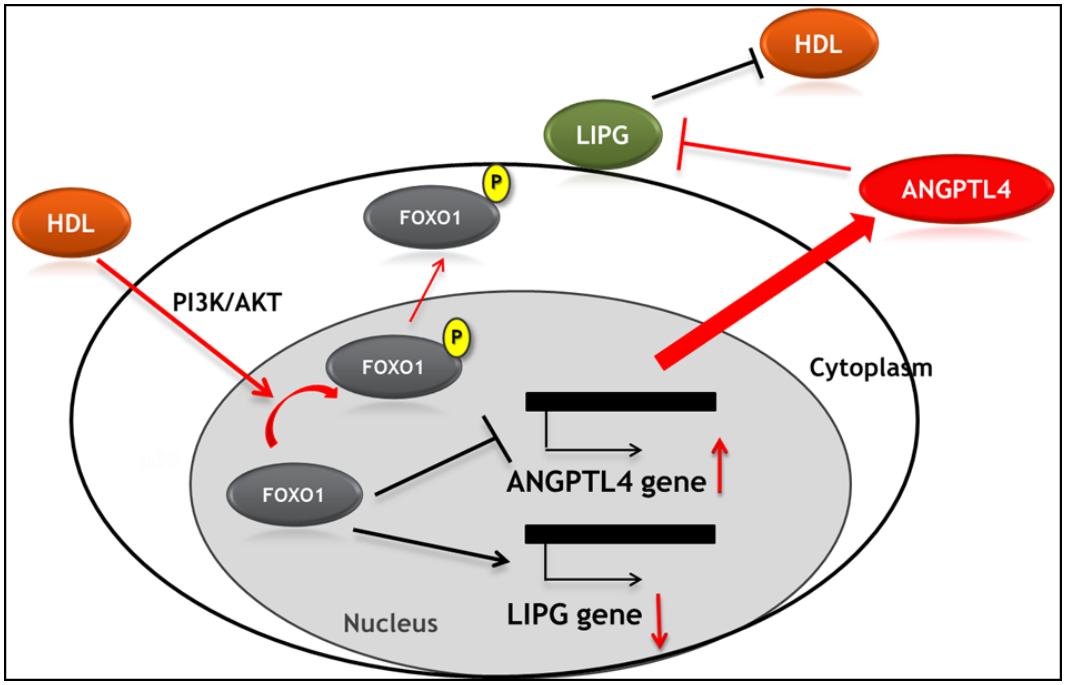

Figure 3.21 Proposed model through which HDL regulates the inhibitory effect of LIPG. Black arrows indicate the untreated state, while red arrows indicate treatment with HDL.

<u>Part III:</u> HDL functionality is disturbed in patients with Chronic Inflammatory Diseases

It is well established that HDL is a molecule with beneficial effects against the development of atherosclerosis. However, numerous studies have shown that HDL from patients with cardiovascular diseases fails to induce its atheroprotective program (255, 317, 441). In the first two parts of this chapter, we investigated the ability of native HDL to activate signaling pathways and change the expression of genes in order to mediate its atheroprotective properties. In the third part, we utilized these properties and specifically the HDL-mediated activation of AKT pathway, in order to examine the functionality of HDL isolated from patients with chronic inflammatory diseases.

The Effect of HDL isolated from patients with Ankylosing Spondylitis on the AKT-activating pathway

Ankylosing spondylitis (AS) is a chronic inflammatory disease affecting mainly the spine (464). Many clinical studies have shown that there is a strong correlation between AS and the development of cardiovascular diseases such as ischemic heart disease, congestive heart failure, peripheral vascular disease, arterial hypertension and cerebrovascular disease (465, 466).

Therefore, we examined the functionality of HDL that was isolated from these patients (HDL_{AS}). Specifically, we examined the ability of HDL_{AS} to induce the phosphorylation of AKT in endothelial cells compared to HDL isolated from healthy human donors (hHDL). For this purpose, HDL was isolated from 70 donors (35 healthy and 35 with AS) and then endothelial cells were treated with each HDL separately for 30 min. The activation of AKT from all treatments was compared to the untreated cells. We observed that HDL from AS patients caused a lower activation of AKT than HDLs from healthy donors,

indicating complications in its functionality (Fig. 3.22). In line with our results, it has been shown that additional functions of HDL from patients with AS are affected (467).

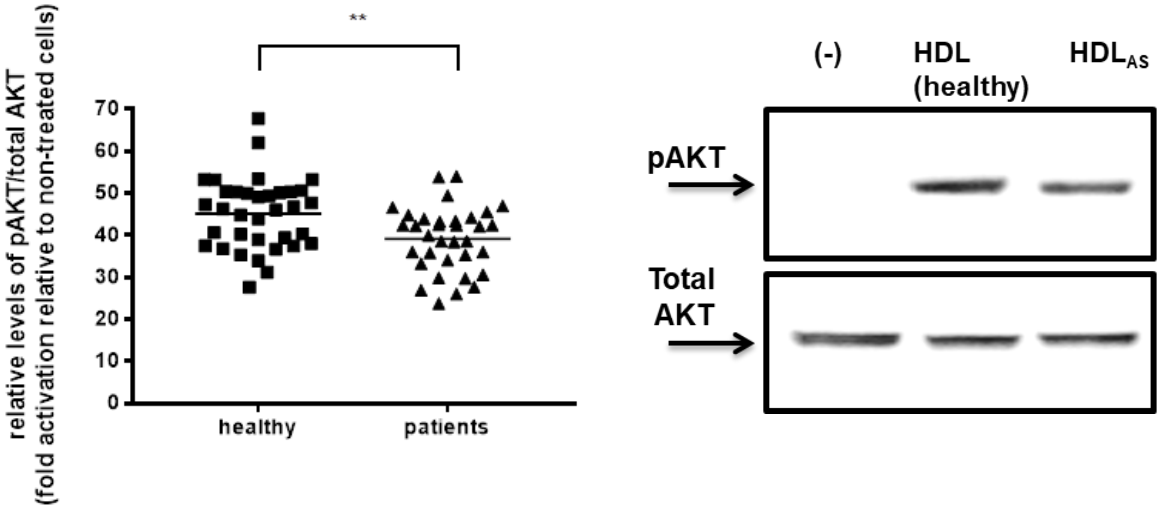

<u>Figure 3.22</u> Differential activation of AKT kinase by HDL from patients with AS and healthy donors. HDL was isolated from 70 donors (35 healthy and 35 with AS). 40μg/ml of each HDL was used for separate treatments of EA.hy926 cells for 30minutes. Cell extracts were collected and the total and phosphorylated levels of the kinase AKT were determined by immunoblotting using the corresponding antibodies. The quantification of the bands in immunoblots was performed by using the Image Lab software, whereas the levels of pAKT were normalized against the levels of total AKT. The normalized levels of pAKT in the treated cells are shown as fold activation relative to the non-treated cells (left Panel). A representative set of Western blot image is shown (Right Panel).

Part III: Discussion

Autoimmune rheumatic diseases have been associated with atherosclerosis and increased risk of cardiovascular morbidity and mortality (468). Importantly, the existence of impaired/dysfunctional HDL in some of these diseases has been reported. Specifically, patients with rheumatoid arthritis (RA) and systemic lupus erythematosus (SLE) were found to have proinflammatory HDL (469, 470). In addition, the cholesterol efflux capacity of HDL was impaired in RA patients with high disease activity, as well as in SLE patients with the disease under control (326, 471). Although the pathogenesis of Ankylosing spondilitis (AS) differs from RA and SLE (464), AS is also a chronic inflammatory disease and has been associated with increased cardiovascular risk (472). Interestingly, previous studies reported changes in the composition of HDL isolated from patients with AS. Particularly, the levels of HDL-associated serum amyloid A were found to be increased, while the levels of PON1 were reduced, suggesting impaired HDL anti-atherogenic functions (473-475). In line with these findings, we observed that HDL particles isolated from patients with AS caused a lower phosphorylation of AKT and subsequently its activation compared to the particles isolated from healthy subjects (Fig. 3.22). Further studies from Gkolifinopoulou et al. (467) revealed that HDL_{AS} particles had decreased antioxidant capacity and decreased ability to promote cholesterol efflux from macrophages compared to healthy controls.

These findings contribute to the understanding of HDL functionality in healthy humans and its dysfunction in disease. Nowadays, it is clear that under an inflammatory and oxidative environment the protein and lipid cargo of HDL is altered (329, 330). As described above, HDL particles from patients with AS are enriched in the SAA, while PON1 levels are reduced (473-475). In addition to composition changes, proteins and lipids of HDL undergo modifications which compromise their physiological role (330). For instance, dysfunctional apoA-I containing post-translational modifications mediated by MPO has been detected in atherosclerotic aortas (338, 340). Taking into account that several chronic inflammatory diseases such as atherosclerosis progress slowly and silently and are not early detectable,

the assays validating HDL functionality could be utilized as a marker of both the presence of the disease and its progress during the treatment.

Chapter II: The regulatory mechanisms controlling the expression of hepatic genes participating in HDL metabolism.

As we discussed in the introduction, many therapeutical approaches for the prevention against cardiovascular diseases focus on the increase of HDL levels in the serum. Therefore, many drugs have been developed affecting different steps of HDL metabolic pathway. However, several clinical trials in patients with Coronary Heart Disease using selective CETP inhibitors or other HDL raising drugs (fibrates, niacin) did not prove that these drugs have beneficial effects for them and even worse caused significant side effects (476) indicating that a better understanding of the mechanisms controlling HDL metabolism is needed. In this Chapter, we wanted to elucidate novel regulatory mechanisms controlling the expression of genes that participate in HDL biogenesis. In part IV, we focused on the regulatory mechanism underlying the transcription of LXRα, which by controlling the expression of ABCA1 is master regulator of HDL biogenesis (105, 106). In part V, we investigated the role of the microRNA let-7b in the expression of apolipoprotein E gene

<u>Part IV</u>: Regulatory mechanisms involved in the regulation of hLXRα expression by HNF-4α

The hLXRa promoter is regulated in hepatic cells by a combination of negative and positive regulatory elements

Our first objective was to map the region upstream from the human LXRa gene that could contribute to its transcriptional regulation in hepatic cells. For this purpose we performed a deletion analysis of the (-2625/+384)-hLXRa promoter and measured the activity of each promoter fragment by luciferase assays in human hepatoblastoma cell line HepG2. We generated by PCR the following serial deletions of the hLXRa promoter: -844/ +384, -457/+384, -300/+384, -111/+384, -42/+384 and -25/ +384 (Fig. 3.23A). As shown in Fig. 3.23B, deletion of the hLXRa promoter to position -457 caused a gradual increase in its activity from 2,1- to 4,1-fold relative to the larger promoter fragment tested (-2625/+384) suggesting the presence of negative regulatory elements inside the -2625/+457 region. The LXRa promoter activity did not decrease further by extending the deletions to positions -300 and -111. However, a significant drop in the activity of the promoter was observed when the region between nucleotides -111 and -42 was deleted suggesting the presence of strong positive regulatory elements inside the -111/+42 region. Finally, deleting the LXRa promoter to nucleotide -25 caused only a minor drop in LXRa promoter activity (Fig. 3.23B).

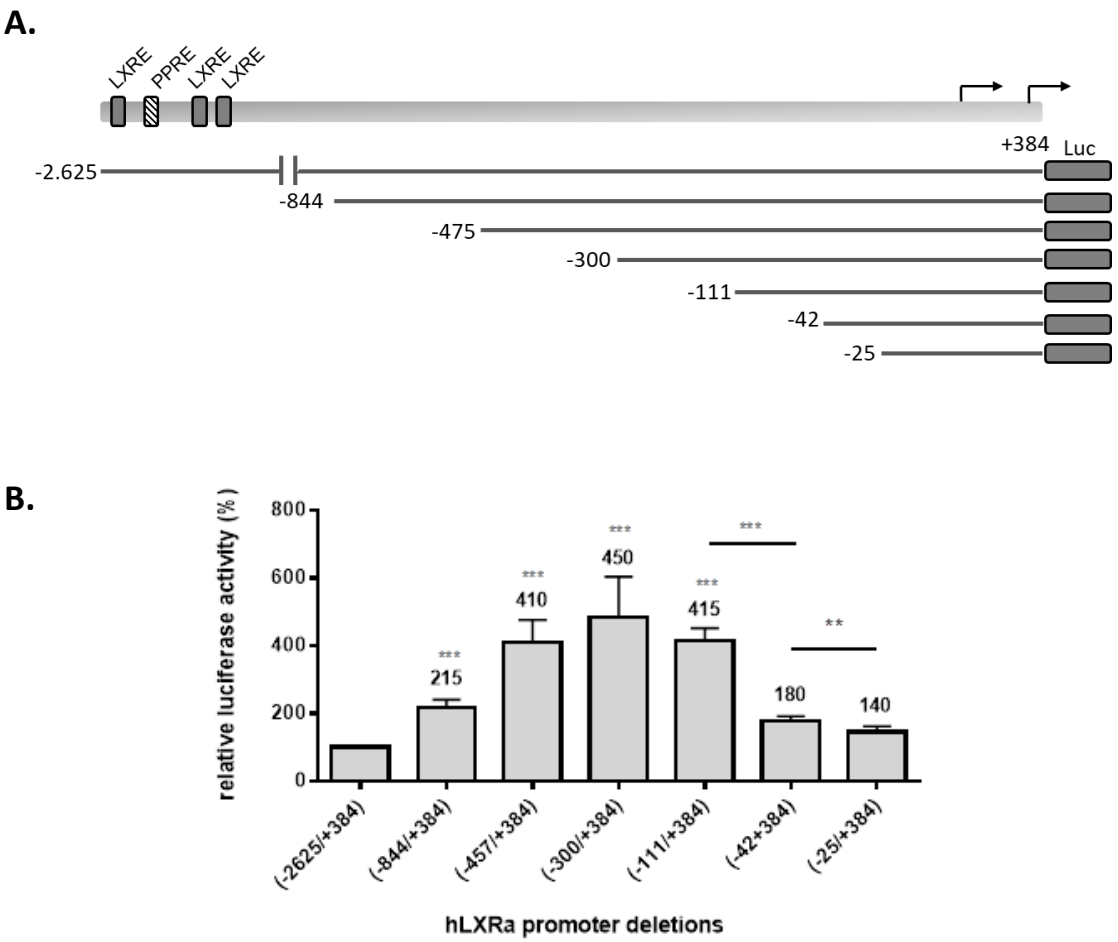

Figure 3.23 The human LXRa promoter is regulated by a combination of positive and negative regulatory elements. A) Schematic representation of the hLXRa promoter. The two transcription start sites, the distal LXREs and the PPRE are depicted. The hLXRa promoter fragments which were used in transfection experiments are shown at the bottom. B) HepG2 cells were transiently transfected with the hLXRa promoter constructs indicated along with a β-galactosidase expression vector. The (%) normalized relative promoter activity (±SD) was calculated from at least three independent experiments performed in duplicate. Symbols: **, $p \leq 0.01$; ***, $p \leq 0.001$.

HNF-4a binds to a novel HNF-4-specific binding motif present in the -50/-40 region of the human LXRa promoter

Close examination of the human proximal LXRa promoter region -111/-42 revealed the presence of a DNA motif in the -50/ -40 region (5' TGGGACCTTTG 3') with significant homology to the previously identified HNF-4a-specific binding motif or H4-SBM (149) having the sequence: 5' TGGACTTTG 3' (Fig. 3.24A and B). The binding of HNF-4 to this proximal hLXRa promoter region is also supported by previous ChIP-seq data (Fig. 3.24C red rectangle) obtained from the ENCODE project. Furthermore, by utilizing the Biobase platform for conserved transcription factor binding sites we observed that in the proximal region there is a conserved binding site for the transcription factor COUP-TF, which binds to the same regions as HNF-4α (Fig. 3.24C grey rectangle).

A.

```
-123 TTCCCAGAGGCAAGGGAGGAGGAGGGAGGC

 -93 TGGGAAAGCCGCTGGGGCTCAGTGTCGCAA

                  -50   HNF-4α   -40
 -63 TTCCGGGCCGTGCTGGGACCTTTGCTCCAC

 -33 GAGGTGCCTATGGAGGGGAGGGAACACGAT

  -3 TCTGGAGGCTGCTGGGATTGGGGTGGGGGT

 +28 TCCTGGGAGGCAGTCCTTTTGCAAGAGCTG

 +58 CTAAGAGCGC
```

B.

```
          hLXRα  5′ TGCTGGGACCTTTGCT 3′
                    *  ***  *****
Consensus H4-SBM     5′ T-GGA-CTTTG 3′
```

C.

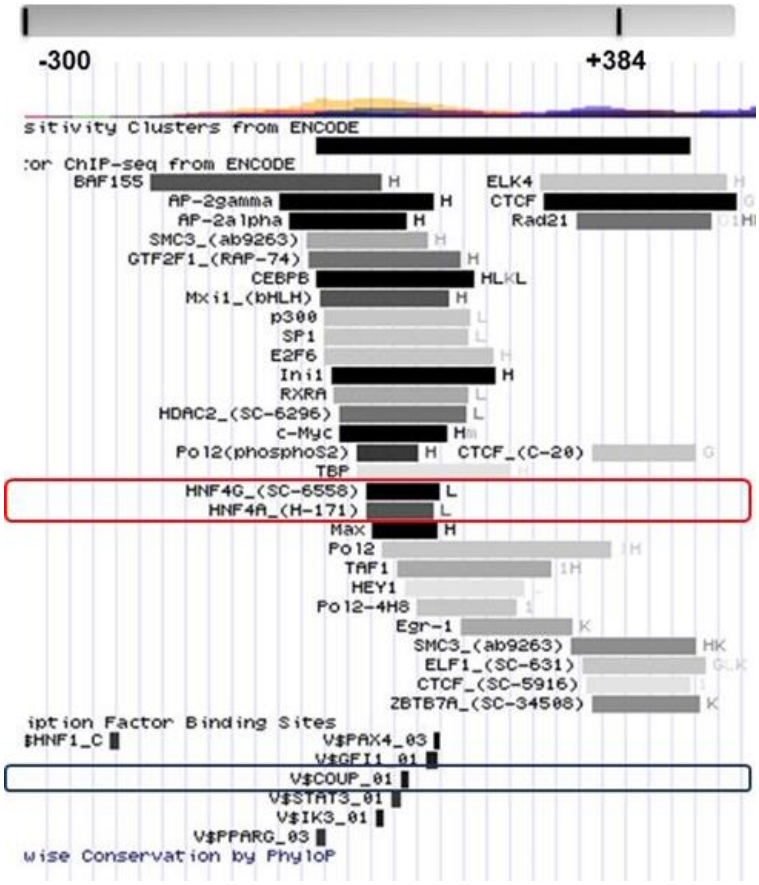

Figure 3.24 The human LXRa promoter contains a putative HNF-4a specific binding motif. A) Sequence of the proximal hLXRa promoter region spanning nucleotides -123 to +67. The putative HNF-4a binding site in the -50/-40 region of hLXRa promoter is underlined and in bold. B) Homology of the putative HNF-4 binding site in the -50/-40 region of the human LXRa promoter with the consensus H4-SBM. Identity in the nucleotide sequence is indicated with the asterisks. C) Bioinformatical analysis of the -300/+384 region of the human LXRa promoter. UCSC genome data were utilized to identify transcription factors binding to the hLXRα promoter. ChIP seq data as well as data for conservation of sites for transcription factors in the -2625/+384 promoter region were obtained from UCSC browser using the ENCODE project (v2.0) and Transfac Matrix Database (v7.0, Biobase). For the analysis, the Feb. 2009(GRCh37/hg19) genome assembly was used.

In order to confirm that HNF-4α binds to the proximal region of the human LXRa promoter in vivo, we performed chromatin immunoprecipitation (ChIP) experiment in HepG2 cells. We utilized primers for the region -147/+48 of the human LXRa promoter which contains the putative HNF-4a binding site (Fig. 3.25A). As shown in Fig. 3.25B, an antibody against HNF-4a immunoprecipitated a chromatin fragment containing the above region. In contrast, this antibody did not immunoprecipitate a distal region of the human LXRa gene (-3461/-3694) that was used as a negative control suggesting that binding of HNF-4a to the proximal LXRa promoter was specific.

Next, we performed DNA affinity precipitation (DNAP) assays so as to validate the functionality of the -50/-40 element of the hLXRa promoter. For this purpose, we generated biotinylated LXRa promoter fragments covering the regions -111/+384 and -25/+384 (Fig. 3.25A). As shown in Fig. 3.25C, HNF-4a bound to the -111/+384 but not to the -25/+384 promoter fragment. As anticipated, HNF-4a bound to a wild type but not to a mutated -40/+14 apoM oligonucleotide (96) that were used as positive and negative controls respectively (Fig. 3.25C). We then performed DNAP assays using biotinylated oligonucleotides corresponding to the wild type -53/-23 region or to the same region bearing three point mutations in the putative motif (Fig. 3.3D). We observed that HNF-4a bound to the wild type oligonucleotide but not to the mutated one. Furthermore, we examined whether

the same LXRa protein can be bound in this HNF-4a site. By performing DNAP assay using the wild type -53/ -23 bio-oligonucleotide, we did not observe binding of LXRa in this region indicating that this motif appears to be specific for HNF-4a (Fig. 3.3E). For positive control of this experiment, we utilized a biotinylated oligonucleotide corresponding to the -71/-38 region of the ABCA1 gene, which contains an established LXRa element (477) and we observed the binding of LXRa in this site.

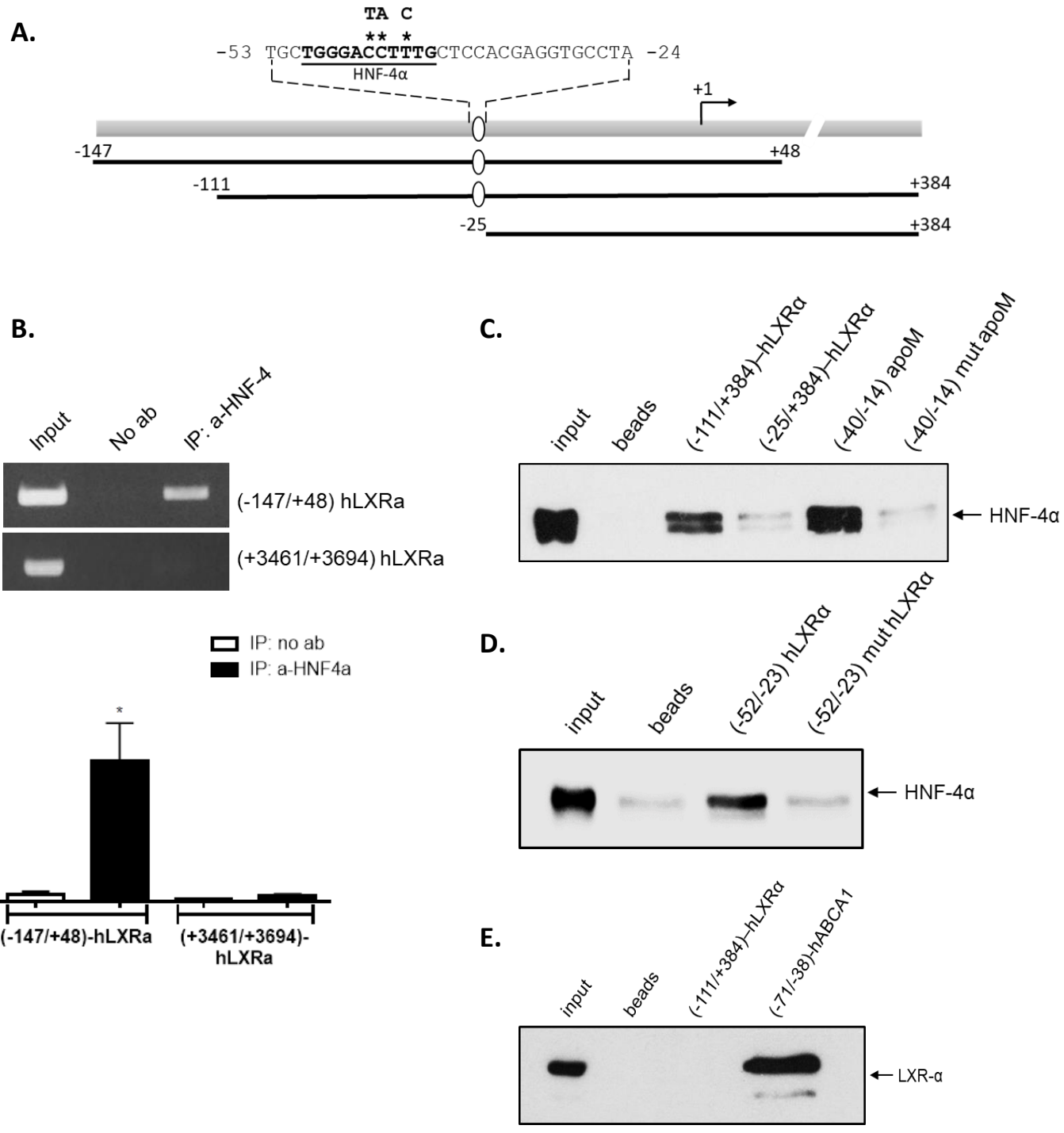

Figure 3.25 HNF-4a binds to the hLXRa promoter in vitro and in vivo.
A) Schematic representation of the human LXRa promoter showing the HNF-4a binding site (bold and underlined). The mutations that were introduced into the site are shown above the sequence. The DNA fragments used for the experiments of panels B-F are shown at the bottom. B) HepG2 cells were subjected to chromatin immunoprecipitation using the a-HNF-4α antibody or no antibody as a negative control. The immunoprecipitated chromatin was detected by both standard PCR (top) and quantitative PCR (bottom) using primers corresponding to the human LXRa promoter -147/+48 or to a distal region inside the LXRa gene. Results from qPCR are expressed as binding relative to the input (%). Each data point represents the average (±SD) of three different chromatin samples. C) DNA-affinity precipitation experiment using nuclear extracts from HepG2 cells and biotinylated PCR products corresponding to the -111/+384 or -25/+384 regions of the hLXRa promoter. Biotinylated oligonucleotides (wt and mut) corresponding to the (-40/-14) region of apolipoprotein M promoter were used as positive (wt) or negative (mut) controls respectively. D) DNA-affinity precipitation experiment using nuclear extracts from HepG2 cells and biotinylated oligonucleotides (wt and mut) corresponding to the -53/-24 region of the hLXRa promoter (their sequence is depicted in panel A). E) DNA-affinity precipitation experiment using whole extracts from HEK293T overexpressing the hLXRa protein and biotinylated PCR product corresponding to the -111/+384 region of the hLXRa promoter. Biotinylated oligonucleotide corresponding to the (-71/-38) region of ABCA1 promoter was used as positive control. In all DNAP experiments, the uncoupled beads were utilized as negative control (beads). HNF-4a or LXRa binding was detected by Western blotting using the corresponding antibodies. The arrow shows the position of HNF-4a. IP, Immunoprecipitation. Symbols: *, $p \leq 0.05$.

The novel H4-SBM present in the -50/-40 region of the human LXRa promoter is required for the transactivation of this promoter by HNF-4a

We then performed transactivation experiments in human embryonic kidney HEK293T cells that do not express endogenous HNF-4a. As shown in Fig. 3.26A, HNF-4a transactivated the full length -2625/+384 hLXRa promoter 2,8-fold confirming that this nuclear receptor plays a role in the regulation of this promoter. The data of Fig. 3.26A also shows that all LXRa promoter deletion fragments that contain the HNF-4 binding motif were transactivated by HNF- 4a. In contrast, the -42/+384 promoter deletion fragment that does not include the HNF-4a binding motif could not be transactivated by HNF-4a.

To investigate the regulatory role of the triple mutation in the HNF-4 binding site (Fig. 3.26A and D) in the HNF4-a-mediated transactivation of LXRa promoter, we introduced the triple nucleotide substitutions in the corresponding sites of -844/+384-hLXRa construct. Interestingly, HNF-4a could not transactivate this mutated construct (Fig. 3.26B).

Comparative sequence analysis of the mouse and human LXRa promoters revealed that the novel H4-SBM is conserved between the two species (Fig. 3.26C). In order to confirm that this motif is also functional in mice, we used the mouse LXRa promoter -3000/+30 in transactivation assays. As shown in Fig. 3.26D, HNF-4a transactivated the -3000/+30 mouse LXRa promoter in HEK293T cells about 24-fold. In conclusion, the combined data of Figures 3 and 4 suggest that the DNA sequence of the proximal LXRa promoter between nucleotides -50 and -40 is a true HNF-4 binding motif that mediates the transactivation of this promoter by HNF-4a.

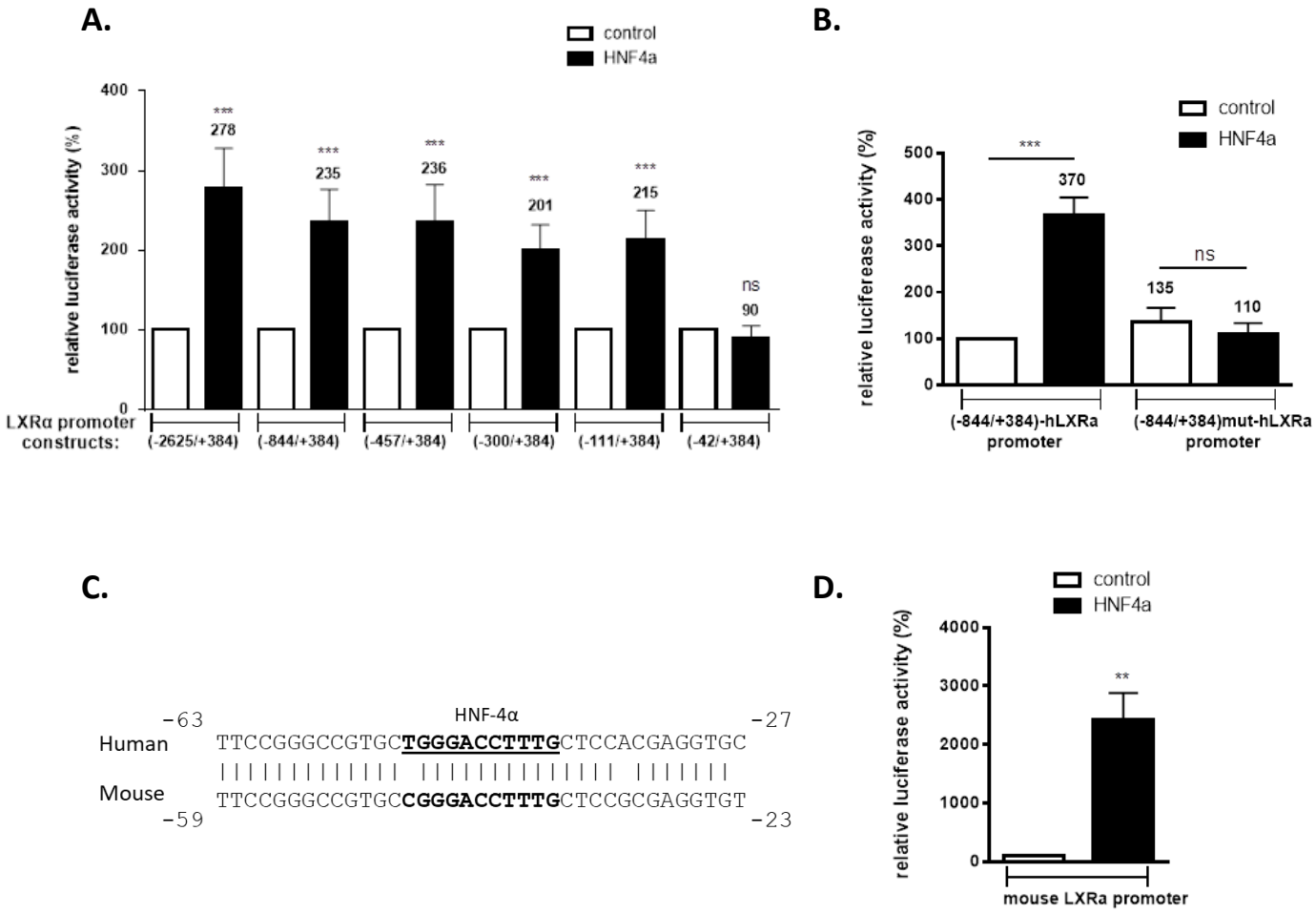

Figure 3.26 HNF-4a transactivates the hLXRa promoter through the HNF-4a binding site. A) HEK293T cells were transiently co-transfected with the indicated hLXRa reporter plasmids along with an expression vector for HNF-4a or an empty vector (control). The (%) normalized relative promoter activity (±SD) was calculated from at least three independent experiments performed in duplicate. B) HEK293T cells were transiently co-transfected with the (-844/+384)-hLXRa construct or with its mutant form (-844/+384)mut-hLXRa in the presence of an expression vector for HNF-4a or an empty vector (control). The (%) normalized relative promoter activity (±SD) was calculated from three independent experiments performed in duplicate. C) Alignment of the human and mouse LXRa promoter in the region of the HNF-4a binding site. D) HEK293T cells were co-transfected with the (-3000/+30)-mouse-LXRa luc reporter construct along with an expression vector for HNF-4a or an empty vector control). The (%) normalized relative promoter activity (±SD) was calculated from three independent experiments performed in duplicate. Symbols: ns, non-significant **, $p \leq 0.01$; ***, $p \leq 0.001$.

Silencing of the HNF-4a gene is associated with reduced LXRa protein levels and promoter activity in hepatic cells

Having established that HFN-4a is a positive regulator of the promoter of hLXRa in hepatic cells, we investigated further the effect of HNF4a on the expression levels of endogenous LXRa. For this purpose, HepG2 cells were transfected with a HNF-4a-specific siRNA or with a non-specific (scrambled) siRNA and the protein levels of LXRa were measured. Silencing of HNF-4a caused a statistically significant decrease in the protein levels of HNF-4a and LXRa (30% and 42% decrease respectively, Fig. 3.27A), indicating that LXRa is a transcriptional target of HNF-4a.

Moreover, we examined the effect of silencing HNF-4a in the basal activity of LXRa promoter constructs in HepG2 cells. The HNF-4a specific shRNA reduced the basal activity of the hLXRa promoter fragments -300/+384 and -111/ +384 bearing the HNF-4a binding motif by 35% but not of the -42/+384 promoter fragment lacking this motif (Fig. 3.27B). Finally we showed that the triple mutation in the -50/-40 HNF-4a binding motif of the human LXRa promoter reduced the basal activity of the -844/+384 promoter by 40% but most importantly, we showed that the activity of this mutated promoter could not be reduced further by the HNF-4a specific siRNA (Fig. 3.27C).

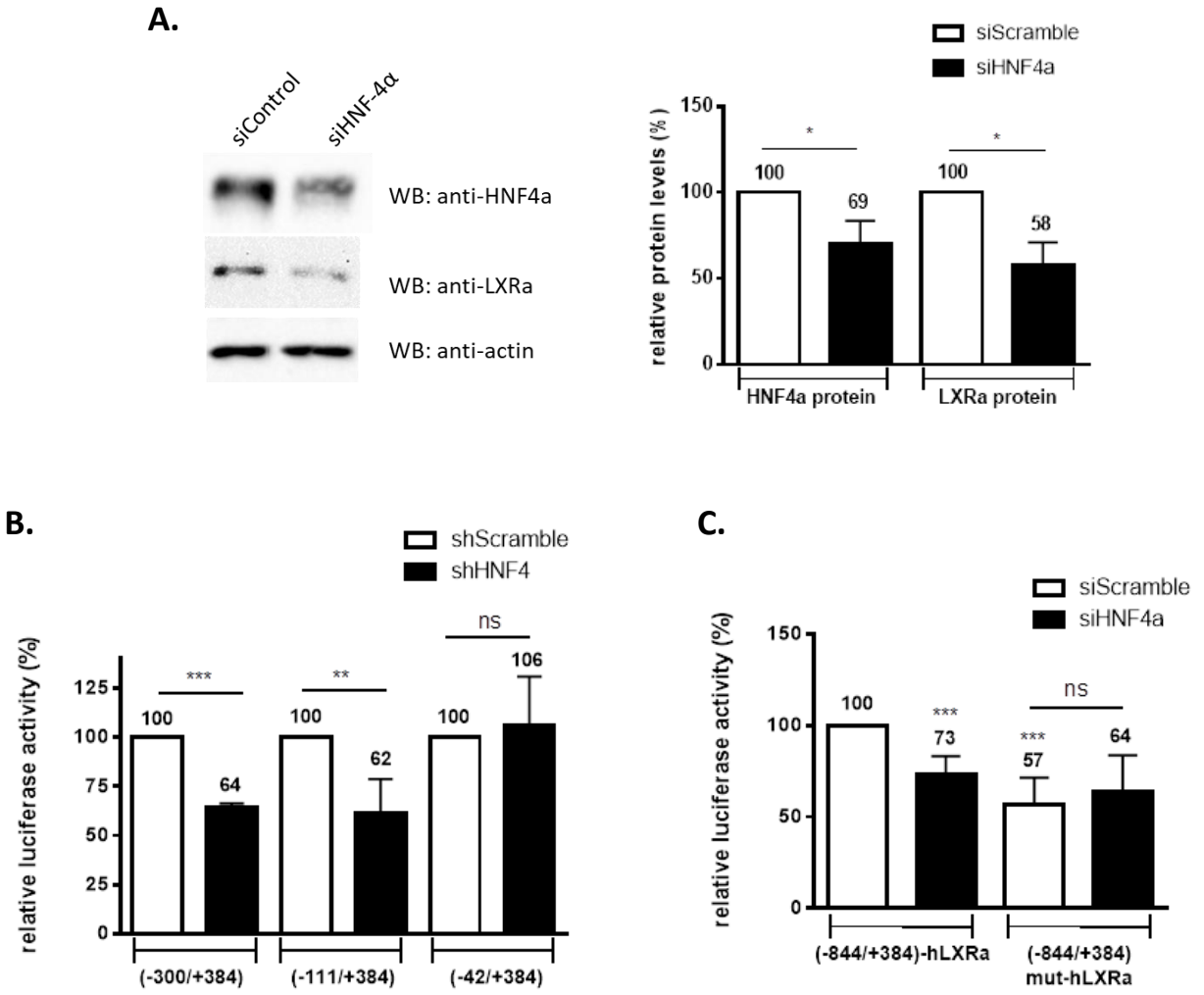

Figure 3.27 Silencing of the endogenous HNF-4a gene in HepG2 cells results in the downregulation of both hLXRa protein and hLXRa promoter activity. A) Left: HepG2 cells were transfected with 100 nM of scrambled (siControl) or HNF-4a specific si-RNA (siHNF-4a). Cell extracts were analysed for the protein levels of HNF-4a, LXRa and actin by immunoblotting using the corresponding antibodies. Right: the density of the bands was normalized to the density of actin and the normalized relative protein levels (±SD) were calculated from three independent experiments. B) HepG2 cells were co-transfected with the indicated hLXRa reporter plasmids along with a vector expressing a shRNA for HNF- 4a (shHNF-4a) or a vector expressing a shRNA with non-related sequence (shScramble). The (%) normalized relative promoter activity (±SD) was calculated from three independent experiments performed in duplicate. C) HepG2 cells were transiently co-transfected with the (-844/+384)-hLXRa construct or with its mutant form (-844/+384)mut-hLXRa in the presence of 100 nM of scrambled (siScramble) si-RNA or HNF-4a specific si-RNA (siHNF4a). The (%) normalized relative promoter activity (±SEM) was calculated from three independent experiments performed in duplicate. Symbols: ns, not significant; *, $p \leq 0.05$; **, $p \leq 0.01$; ***, $p \leq 0.001$

Part IV: Discussion

LXRs play critical roles in intracellular and plasma cholesterol homeostasis regulating the expression of a large number of genes in various cell types and tissues such as the macrophages, the liver and the intestine (119, 120, 478). In the liver, LXRs by inducing the expression of ABCA1 gene are master regulators of HDL biosynthesis, the first step of RCT (119, 120, 478). Additionally, they control the last phase of RCT by activating the expression of the hepatic bile acid transporters ABCG5 and ABCG8 facilitating the transfer of excess cholesterol to the bile (119, 120, 478). Interestingly, the same two transporters are also targets of HNF-4α, which binds to HREs present in the intergenic promoter and activates the expression of the two genes in a coordinate manner (479), suggesting a dual mechanism of regulation of these bile acid transporters by HNF-4α in the liver.

The conservation of the newly identified H4-SBM (149) in the LXRα promoter in human and mouse DNA suggested that HNF-4α may be essential for the regulation of the LXRα gene. Indeed, overexpression of HNF-4α in HEK293T cells caused a strong transactivation of both the human (hLXRα) and mouse (mLXRα) LXRα promoters containing the H4-SBM (Fig.3.26A and D). Disruption of the H4-SBM site in the hLXRα promoter with site specific mutagenesis abolished the transactivation by HNF-4α (Fig. 3.26B) Furthermore, silencing of HNF-4α in the human hepatic cell line HepG2 resulted in reduction of LXRα protein (Fig. 3.27A). However, inactivation of the mouse HNF-4α gene in adult mouse liver was not associated with a statistically significant decrease in the mRNA levels of the mouse LXRα gene (152, 162). Interestingly, a recent study revealed that inactivation of the HNF-4α gene in the liver was associated with an increase in the expression of the paralogous gene HNF-4γ (480) which is not normally expressed in the liver (481) suggesting that HNF-4γ could replace HNF-4α in its absence. This is supported by previous ChiP-seq data which showed that both HNF-4α and HNF-4γ are recruited to the proximal LXRα promoter (Fig. 3.24C). HNF-4α and HNF-4γ share high homology in their DNA binding and ligand binding domains and they also regulate common sets of genes (480, 481).

In the present study we provide new evidence for the regulation of gene expression by the sequential action of two different members of the hormone nuclear receptor superfamily: HNF-4α and LXRα. A similar mechanism of coordinated nuclear receptor action has been demonstrated in the past (141, 142, 482-486). In the majority of these cases, the promoter of one nuclear receptor gene harbors HREs that serve as binding and regulatory sites for the same (autoregulation) or other nuclear receptors thus leading to the formation of a large network of interactions controlling the expression of hundreds of genes (485). A well characterized example is the HNF-4α/PPARα cascade. The promoter of the human PPARα gene contains a regulatory element consisting of a degenerate hexamer repeat with a single nucleotide spacer (direct repeat 1), termed alphaHNF4-RE, which binds HNF-4α and PPARα and mediates the induction of this promoter by HNF-4α and PPARα itself (autoregulation) (487). These findings were confirmed recently *in vivo* using HNF-4α liver-specific knockout mice (486). The latter study showed that HNF-4α controls a transcription factor network in the liver that coordinates the reciprocal expression of fatty acid transport and metabolizing enzymes during fasting and feeding conditions (486).

Beside the beneficial effects of LXRs in the induction of HDL biosynthesis, they also induce de novo lipogenesis in the liver by directly mediating the transcription of the master regulator of fatty acid biosynthesis *SREBP-1c,* as well as other lipogenic genes (119, 120, 478). As a consequence, synthetic ligands that were produced to activate LXRs, although they increased HDL-C levels in the plasma and reduced atherosclerosis, they also resulted in an increase of liver triglycerides promoting hepatic steatosis (350, 488). Therefore, several strategies were developed to minimize the adverse effects of pan-LXR activation. Recently, a strategy focusing at post-translational modifications of LXRα was described (489). Specifically, mice deficient for the tetratricopeptide repeat (TPR) domain protein 39B (TTC39B) which promotes the ubiquitination and degradation of LXR protein, stabilize LXRα and activates a beneficial profile of gene expression that promotes cholesterol removal and inhibits lipogenesis (489). Our strategy focuses on the elucidation of the mechanisms

governing LXRα transcription. It has been reported that the expression of LXRα is driven by two promoters, with approximately 9.0 kb distance between each other, that give rise to five transcript variants (LXRα1-5) (Fig. 3.28) (138, 139). Promoter 1 is considered as the main promoter, since it transcribes the main transcript variants LXRα1 (138, 141). Although it has been observed that LXRα variants differ from each other in transactivation activity and tissue distribution (138, 139), their roles in the different aspects of LXRα biology remain unexplored. Additionally, transcription of LXRα1 gene is induced by LXRs (autoregulation) (140, 141) and PPARs (141) through their corresponding binding sites in a distal region of the promoter 1 of hLXRα gene (Fig. 3.28). In contrast to the distal localization, we detected a functional HNF-4α site in the proximal region of the main promoter of LXRα making HNF-4α a potent master regulator of this gene (Fig. 3.28). It would be very interesting to investigate further whether HNF-4α, either through its site or after conformational proximity with the other sites, promotes differential expression among LXRα transcript variants. Of note, liver-specific inactivation of HNF-4α was associated with decreased plasma HDL levels in mice (152, 162). Given the strong and reverse association between plasma HDL levels and the risk for CVDs, our findings suggest that HNF-4α could be a novel target for therapeutic interventions in patients with low HDL levels and increased risk for CVDs.

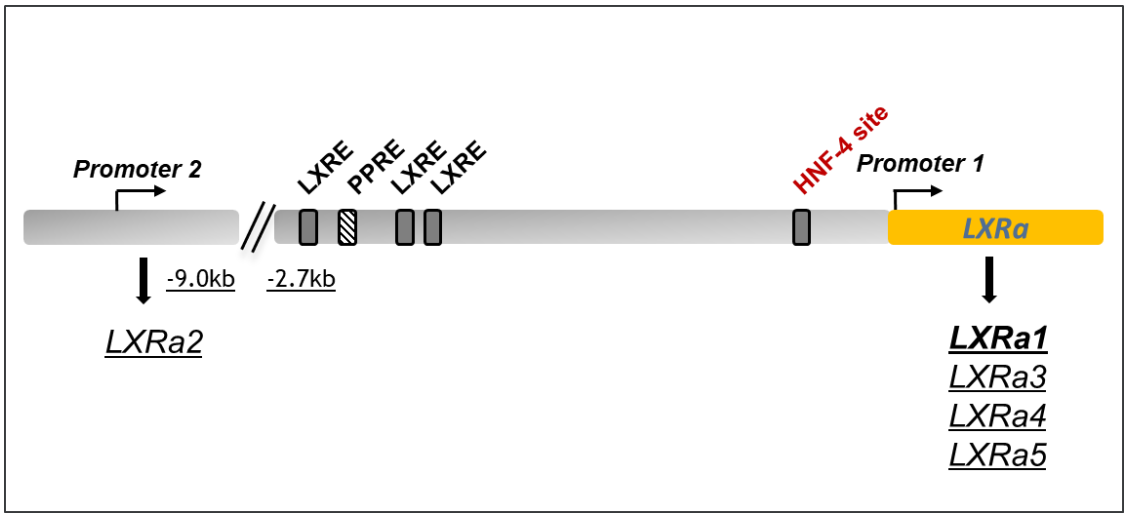

Figure 3.28 Summary of the regulatory elements that participate in the control of human LXRα gene transcription.

Part V: The role of let-7b in the regulation of apolipoprotein E gene expression

apoE mRNA and protein levels are affected by let-7b overexpression

Previous studies have shown an opposite correlation between let-7b and apoE expression levels. Specifically, a dominant negative isoform of c-Jun promotes the induction of apolipoprotein E gene expression while downregulating the mRNA levels of let-7b in hepatic cells (490, 491). Therefore, we asked whether apoE expression is under the regulation of let-7b.

To investigate the above question, we measured both the mRNA and protein levels of apoE after overexpressing let-7b or by inhibiting its expression in HepG2 cells. As shown in Fig. 3.29A, the expression levels of let-7b were increased after transfection of HepG2 cells with a double-stranded RNA that mimics the mature let-7b (let-7b mimics) compared to the cells that were transfected with a scrambled molecule (NC-miR), while the transfection of HepG2 cells with an antisense inhibitor for let-7b (as-let-7b) caused a 4-fold downregulation of the expression levels of let-7b compared to the cells transfected with the control scrambled molecule (as-miR-NC). Interestingly, we observed that both the mRNA and protein levels of apoE were reduced to half after overexpression of let-7b in HepG2 cells (Fig. 3.29B, C). However, in the presence of let-7b inhibitor neither the mRNA nor the protein levels of apoE were affected.

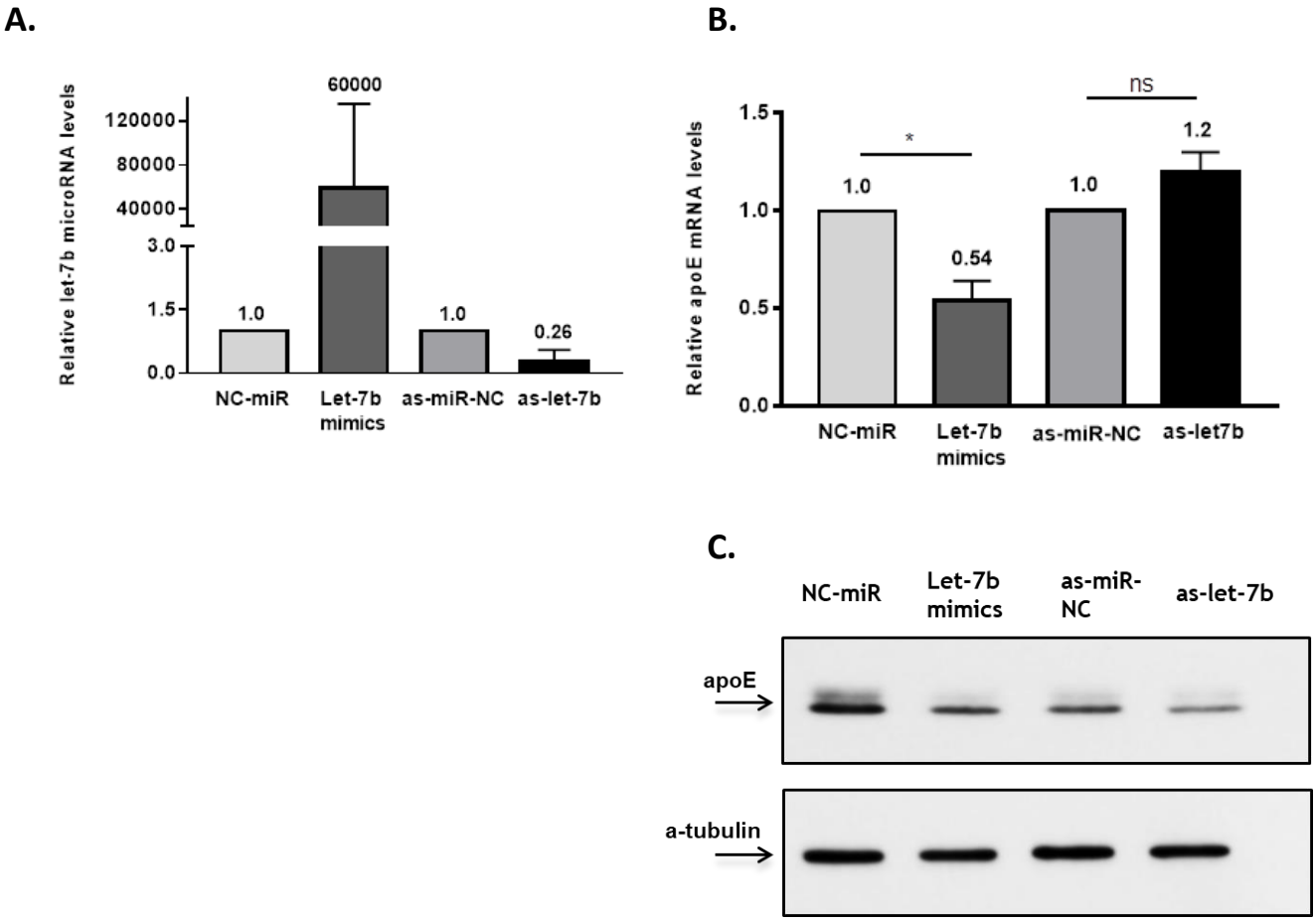

Figure 3.29 Let-7b overexpression decreases the mRNA levels of apoE.
A-C) HepG2 cells were transiently transfected with 50nM let-7b mimics, 50nM NC-miR, 50nM as-let-7b or 50nM as-miR-NC. 48h after transfection, total RNA was extracted, and quantitative RT-PCR was performed to determine let-7b (A) and ApoE (B) mRNA levels. Let-7b microRNA levels were normalized relative to 5S microRNA levels. apoE mRNA levels were normalized relative to the RPLPO mRNA levels. The relative let-7b and apoE mRNA levels are expressed as mean (±SD) from three independent experiments. Cell lysates were collected (C) and the protein levels of apoE and tubulin were determined by Western Blotting using the corresponding antibodies. The experiment was performed two times and representative images are shown. Symbols: ns, not significant; *, $p \leq 0.05$.

The mRNA of apoE is not a direct target of let-7b

miRNAs exert their function by directly binding to the 3'-untranslated region (3'-UTR) of the mRNA-target resulting in the degradation or translation inhibition of this transcript (168). The binding is achieved through complementarity between the sequence of the miRNA and a corresponding site in the 3'-UTR (168) . For this reason, we examined whether the mRNA of apoE is a direct target of let-7b. Bio-informatic analysis performed by Dr Dimitris Iliopoulos (Center for Systems Biomedicine, David Geffen School of Medicine at the University of California at Los Angeles, USA) revealed complementarity between let-7b and the site 33-53 of the 3'UTR of apoE indicating a potential binding of let-7b to this site (Fig. 3.30).

To confirm this in silico prediction, we utilized a plasmid containing the 3'UTR of apoE downstream of the luciferase gene (apoE-3'UTR) or a mutated isoform containing two serial mutations in the potential let-7b site (apoE-3'UTR mutated) and we measured their activity following let-7b overexpression in HepG2 cells. As Fig. 3.31 depicts, let-7b overexpression did not affect the luciferase activity of none of the constructs, suggesting that the mRNA of apoE is not a direct target of let-7b.

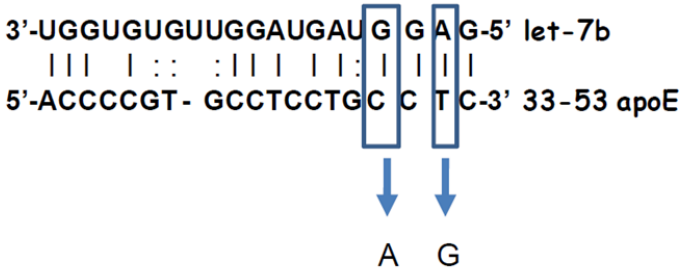

Figure 3.30 Conserved let-7b sites in the 3'-UTR of the mRNA of apoE.
Alignment of the let-7b sequence and the 3'UTR region of apoE. Nucleotide substitutions in the seed base-pairing sequence of the predicted let-7b target site generated in the apoE-3'UTR reporter are indicated by arrows

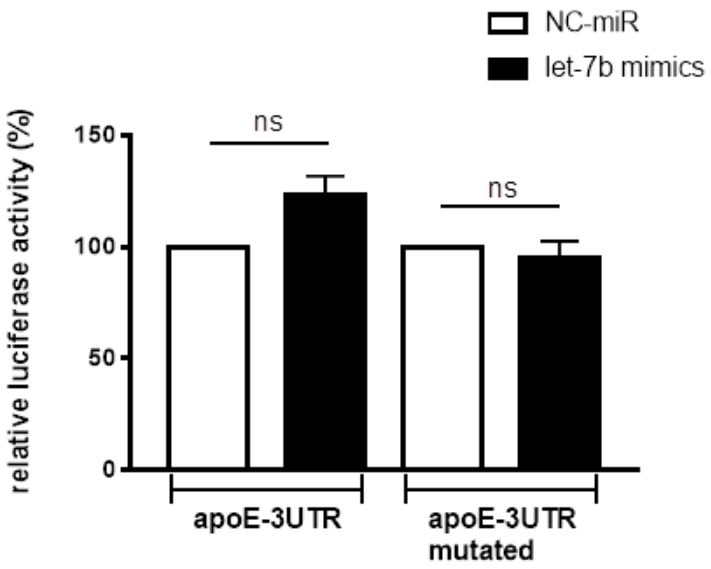

Figure 3.31 let-7b does not target the 3'UTR of apoE mRNA.
HepG2 cells were transiently co-transfected with the apoE-3UTR or apoE-3'UTR mutated luciferase plasmids along with 50nM let-7b or NC-miR. The (%) normalized relative promoter activity (±SD) was calculated from three independent experiments performed in duplicate. Symbols: ns, non-significant

let-7b is a negative regulator of the transcriptional activity of the apoE promoter

Next, we investigated whether let-7b affects the transcriptional activity of the apoE gene. For this purpose, HepG2 cells were co-transfected with a plasmid containing the (-500/+73) region of the apoE promoter in the absence or in the presence of let-7b mimics. As a positive control for the experiment, HepG2 cells were also transfected with a plasmid expressing a promoter with 3 binding sites of NF-κB (3x-kB), as NF-κB has been indicated to be targeted by let-7b (492). The luciferase activity of the apoE promoter was downregulated after overexpression of let-7b (Figure 3.32). This result confirms that let-7b affects the expression of apoE, however does not seem to be mediated by directly targeting the 3' UTR of the apoE mRNA.

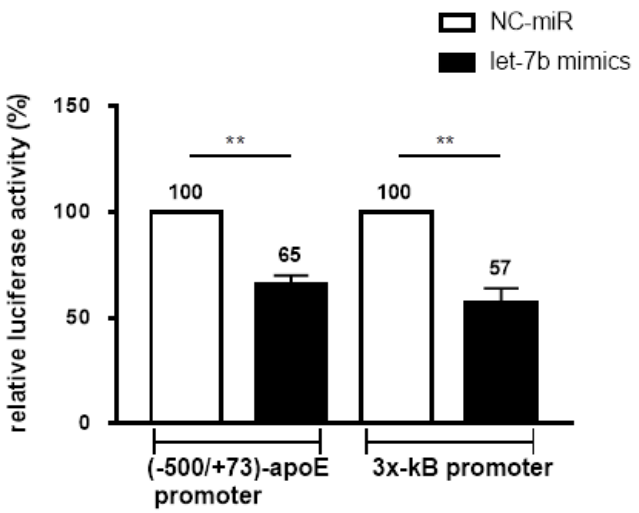

Figure 3.32 let-7b decreases the luciferase activity of the apoE promoter.
HepG2 cells were transiently co-transfected with the -500/+73 apoE reporter plasmid or with 3x-kB reporter plasmid (as a positive control) along with 50nM let-7b or NC-miR. The (%) normalized relative promoter activity (±SD) was calculated from three independent experiments performed in duplicate. Symbols: **, $p \leq 0.01$.

let-7b is a negative regulator of apolipoprotein A-I gene expression

Next, we questioned whether let-7b affects the transcriptional activity of other apolipoproteins and so we focused on apolipoprotein A-I (apoA-I) and apolipoprotein C-III (apoC-III). Firstly, we examined the promoter activity of these genes in HepG2 cells by overexpressing let-7b along with reporter plasmids containing the (-1020/-24) region of the apoA-I promoter and the (-890/+24) of the apoC-III promoter. As shown in Fig. 3.33, let-7b overexpression downregulated the activity of the (-1020/-24)-apoA-I promoter, while the activity of the (-890/+24)-apoC-III promoter was not affected.

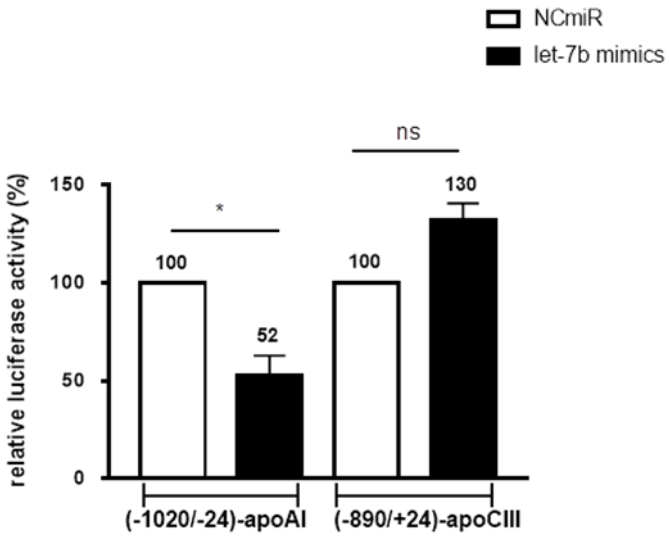

Figure 3.33 let-7b downregulates the promoter activity of apoA-I but not of apoC-III genes. HepG2 cells were transiently co-transfected with the (-1020/+24)-apoA-I promoter or the (-890/+24)-apoC-III promoter along with 50nM let-7b or NC-miR. The (%) normalized relative promoter activity (±SD) was calculated from three independent experiments performed in duplicate. Symbols: ns, not significant; *, $p \leq 0.05$.

To investigate further the let-7b-mediated regulation of apoA-I, we monitored the mRNA levels of apoA-I after overexpressing let-7b or inhibiting its expression in HepG2 cells. As shown in figure 3.34 apoA-I mRNA levels were also downregulated in the presence of let-7b. We also observed that inhibition of let-7b resulted in an increase of apoA-I mRNA levels, however this increase did not reach statistical significance. The above results indicate that the transcriptionof apo-AI is targeted by let-7b.

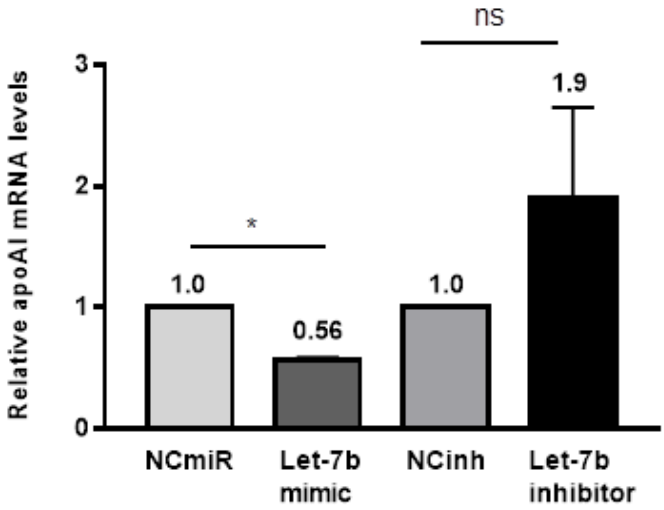

Figure 3.34 let-7b decreases the mRNA levels of apoA-I.
HepG2 cells were transiently transfected with 50nM let-7b mimics, 50nM NC-miR, 50nM as-let-7b or 50nM as-miR-NC. 48h after transfection, total RNA was extracted, and quantitative RT-PCR was performed to determine apoA-I mRNA levels, which were normalized relative to the RPLPO mRNA levels. The relative apoA-I mRNA levels are expressed as mean (±SD) from three independent experiments. Symbols: ns, not significant; *, $p \leq 0.05$.

Part V- Discussion

ApoE is an apolipoprotein with a central role in cholesterol and triglyceride homeostasis (493, 494). On the one hand, apoE is bound to triglyceride-rich lipoproteins and mediates their clearance from the circulation (76-78). On the other hand, apoE by promoting cholesterol efflux generates HDL-apoE particles contributing to RCT (43, 79). Meanwhile, the maintenance of apoE concentration into normal levels is equally important. Deficiency of apoE in mice promotes hypercholesterolemia and spontaneous atherosclerosis under normal diet (81, 495), while overexpression of apoE results in hypertriglyceridemia (496). Interestingly, epidemiological studies showed that low levels of apoE have been associated with high risk of dementia (497, 498), while high levels of apoE have been associated with high risk of ischemic heart disease in men (499) and these results were independent of *APOE* genotype. These findings highlighted that the expression of *apoE* should be under strict regulation.

Therefore, it was of great interest to observe that hepatic apoE mRNA levels were negatively associated with let-7b levels (490, 491), indicating a potential regulatory mechanism of apoE by this microRNA. We focused on hepatic apoE, since liver is the major source of plasma apoE and we validated that both mRNA and protein levels of apoE are decreased after let-7b overexpression (Fig. 3.29). However, this effect was not mediated by direct binding of let-7b to the 3-UTR of apoE mRNA (Fig. 3.31). This observation suggests that let-7b inhibits directly an upstream regulator of apoE expression. In line with this result, we observed that the promoter activity of apoE was downregulated after let-7b overexpression (Fig. 3.32). Although the main hypothesis suggests an indirect regulation of apoE by let-7b, we could not exclude a direct effect through promoter binding. Interestingly, it has been shown that another member of let-7 family, let-7f, was bound to microRNA response elements found in the promoters of two E2F target genes, CDCA8 and CDC2, and by cooperating with retinoblastoma (Rb) suppressed their transcription in an argonaute2-dependent manner in senescent fibroblasts (500).

Importantly, in addition to the regulation of apoE, we observed that let-7b controls also the transcription of the apoA-I gene, which is the major component of HDL (39). Overexpression of let-7b decreased the mRNA levels of apoA-I (Fig. 3.33) as well as the transcriptional activity of its promoter (Fig. 3.34). Bioinformatic analysis in the 3'-UTR region of apoA-I mRNA did not reveal a conserved site for let-7b (data not shown) indicating that alternative mechanisms may be involved in this regulation by let-7b. This is not the first evidence that a single microRNA can regulate the expression of more than one genes participating in the same biological process. For instance, miRNA-33a/b is known to regulate the expression of several genes involved in the pathway of cholesterol metabolism such as ABCA1, ABCG1 and CYP7A1 (181). Since the expression of both apolipoproteins is regulated by let-7b independent of their 3'-UTR, we could hypothesize that either a common upstream inducer of both *apoE* and *apoA-I* is a direct target of let-7b or a novel mechanism implicating miRNA-promoter binding could be occurred.

Our findings reveal new potent roles for all participants in this regulatory mechanism. Let-7b is mainly known as a tumor-suppressor since low levels of let-7b is a poor prognostic indicator of survival in serous ovarian cancer, acute lymphoblastic leukemia and melanoma (192, 501-503) and thus possible roles of apoA-I and apoE beyond lipid metabolism could not be excluded. Inversely, since both apoE and apoA-I are major apolipoproteins in the formation and function of lipid particles, from our results let-7b emerges as an important regulator of cholesterol homeostasis. However, the functional consequences of the let-7b-driven downregulation of *apoE* and *apoA-I* expression have not been tested. Given the important functions of these apolipoproteins in lipid metabolism and protection from atherosclerosis and the need for identification of new mechanisms to treat atherosclerosis-associated diseases, the potential roles of let-7b on reverse cholesterol transport, triglyceride clearance and atherosclerosis development need to be explored.

4. References

1. Collaborators GBDCoD. Global, regional, and national age-sex-specific mortality for 282 causes of death in 195 countries and territories, 1980-2017: a systematic analysis for the Global Burden of Disease Study 2017. Lancet. 2018;392(10159):1736-88.
2. Townsend N, Wilson L, Bhatnagar P, Wickramasinghe K, Rayner M, Nichols M. Cardiovascular disease in Europe: epidemiological update 2016. European heart journal. 2016;37(42):3232-45.
3. Mensah GA, Jaquish C, Srinivas P, Papanicolaou GJ, Wei GS, Redmond N, et al. Emerging Concepts in Precision Medicine and Cardiovascular Diseases in Racial and Ethnic Minority Populations. Circulation research. 2019;125(1):7-13.
4. Badimon L, Vilahur G. LDL-cholesterol versus HDL-cholesterol in the atherosclerotic plaque: inflammatory resolution versus thrombotic chaos. Annals of the New York Academy of Sciences. 2012;1254:18-32.
5. Falk E. Pathogenesis of atherosclerosis. Journal of the American College of Cardiology. 2006;47(8 Suppl):C7-12.
6. Rader DJ, Daugherty A. Translating molecular discoveries into new therapies for atherosclerosis. Nature. 2008;451(7181):904-13.
7. Strong JP, Malcom GT, McMahan CA, Tracy RE, Newman WP, 3rd, Herderick EE, et al. Prevalence and extent of atherosclerosis in adolescents and young adults: implications for prevention from the Pathobiological Determinants of Atherosclerosis in Youth Study. Jama. 1999;281(8):727-35.
8. Moss JW, Ramji DP. Nutraceutical therapies for atherosclerosis. Nature reviews Cardiology. 2016;13(9):513-32.
9. Huang L, Chambliss KL, Gao X, Yuhanna IS, Behling-Kelly E, Bergaya S, et al. SR-B1 drives endothelial cell LDL transcytosis via DOCK4 to promote atherosclerosis. Nature. 2019;569(7757):565-9.
10. Flood C, Gustafsson M, Pitas RE, Arnaboldi L, Walzem RL, Boren J. Molecular mechanism for changes in proteoglycan binding on compositional changes of the core and the surface of low-density lipoprotein-containing human apolipoprotein B100. Arteriosclerosis, thrombosis, and vascular biology. 2004;24(3):564-70.
11. Miller YI, Shyy JY. Context-Dependent Role of Oxidized Lipids and Lipoproteins in Inflammation. Trends in endocrinology and metabolism: TEM. 2017;28(2):143-52.
12. Gistera A, Hansson GK. The immunology of atherosclerosis. Nature reviews Nephrology. 2017;13(6):368-80.
13. Bekkering S, Quintin J, Joosten LA, van der Meer JW, Netea MG, Riksen NP. Oxidized low-density lipoprotein induces long-term proinflammatory cytokine production and foam cell formation via epigenetic reprogramming of monocytes. Arteriosclerosis, thrombosis, and vascular biology. 2014;34(8):1731-8.
14. Van Vre EA, Ait-Oufella H, Tedgui A, Mallat Z. Apoptotic cell death and efferocytosis in atherosclerosis. Arteriosclerosis, thrombosis, and vascular biology. 2012;32(4):887-93.
15. Chistiakov DA, Orekhov AN, Bobryshev YV. Vascular smooth muscle cell in atherosclerosis. Acta physiologica. 2015;214(1):33-50.
16. Steinl DC, Kaufmann BA. Ultrasound imaging for risk assessment in atherosclerosis. International journal of molecular sciences. 2015;16(5):9749-69.
17. Gimbrone MA, Jr., Garcia-Cardena G. Endothelial Cell Dysfunction and the Pathobiology of Atherosclerosis. Circulation research. 2016;118(4):620-36.
18. Vanhoutte PM, Shimokawa H, Feletou M, Tang EH. Endothelial dysfunction and vascular disease - a 30th anniversary update. Acta physiologica. 2017;219(1):22-96.
19. Cahill PA, Redmond EM. Vascular endothelium - Gatekeeper of vessel health. Atherosclerosis. 2016;248:97-109.

20. Vanhoutte PM, Zhao Y, Xu A, Leung SW. Thirty Years of Saying NO: Sources, Fate, Actions, and Misfortunes of the Endothelium-Derived Vasodilator Mediator. Circulation research. 2016;119(2):375-96.
21. Yau JW, Teoh H, Verma S. Endothelial cell control of thrombosis. BMC cardiovascular disorders. 2015;15:130.
22. Rahimi N. Defenders and Challengers of Endothelial Barrier Function. Frontiers in immunology. 2017;8:1847.
23. Wang D, Wang Z, Zhang L, Wang Y. Roles of Cells from the Arterial Vessel Wall in Atherosclerosis. Mediators of inflammation. 2017;2017:8135934.
24. Hamburg NM, Keyes MJ, Larson MG, Vasan RS, Schnabel R, Pryde MM, et al. Cross-sectional relations of digital vascular function to cardiovascular risk factors in the Framingham Heart Study. Circulation. 2008;117(19):2467-74.
25. Gradinaru D, Borsa C, Ionescu C, Prada GI. Oxidized LDL and NO synthesis--Biomarkers of endothelial dysfunction and ageing. Mechanisms of ageing and development. 2015;151:101-13.
26. Steyers CM, 3rd, Miller FJ, Jr. Endothelial dysfunction in chronic inflammatory diseases. International journal of molecular sciences. 2014;15(7):11324-49.
27. Tanaka KA, Key NS, Levy JH. Blood coagulation: hemostasis and thrombin regulation. Anesthesia and analgesia. 2009;108(5):1433-46.
28. Schafer A, Bauersachs J. Endothelial dysfunction, impaired endogenous platelet inhibition and platelet activation in diabetes and atherosclerosis. Current vascular pharmacology. 2008;6(1):52-60.
29. Zannis VI, Kardassis D, Zanni EE. Genetic mutations affecting human lipoproteins, their receptors, and their enzymes. Advances in human genetics. 1993;21:145-319.
30. Sips FL, Tiemann CA, Oosterveer MH, Groen AK, Hilbers PA, van Riel NA. A computational model for the analysis of lipoprotein distributions in the mouse: translating FPLC profiles to lipoprotein metabolism. PLoS computational biology. 2014;10(5):e1003579.
31. Murphy HC, Burns SP, White JJ, Bell JD, Iles RA. Investigation of human low-density lipoprotein by (1)H nuclear magnetic resonance spectroscopy: mobility of phosphatidylcholine and sphingomyelin headgroups characterizes the surface layer. Biochemistry. 2000;39(32):9763-70.
32. Zannis VI, Kypreos, K. E., Chroni, A., Kardassis, D., and Zanni, E. E. Lipoproteins and atherogenesis In Molecular Mechanisms of Atherosclerosis. J Loscalzo, ed Taylor & Francis, Abingdon, UK 154-244. 2004.
33. Feingold KR, Grunfeld C. Introduction to Lipids and Lipoproteins. In: Feingold KR, Anawalt B, Boyce A, Chrousos G, Dungan K, Grossman A, et al., editors. Endotext. South Dartmouth (MA)2000.
34. Julve J, Martin-Campos JM, Escola-Gil JC, Blanco-Vaca F. Chylomicrons: Advances in biology, pathology, laboratory testing, and therapeutics. Clinica chimica acta; international journal of clinical chemistry. 2016;455:134-48.
35. Babin PJ, Gibbons GF. The evolution of plasma cholesterol: direct utility or a "spandrel" of hepatic lipid metabolism? Progress in lipid research. 2009;48(2):73-91.
36. Zannis VI, Kateifides, A. K., Fotakis, P., Zanni, E. E., and Kardassis, D. Pleiotropic functions of HDL lead to protection from atherosclerosis and other diseases. In Kelishadi, R, editor Dyslipidemia - From Prevention to Treatment, Intech 173-196. 2012.
37. Davidson WS, Thompson TB. The structure of apolipoprotein A-I in high density lipoproteins. The Journal of biological chemistry. 2007;282(31):22249-53.
38. Kontush A, Lindahl M, Lhomme M, Calabresi L, Chapman MJ, Davidson WS. Structure of HDL: particle subclasses and molecular components. Handbook of experimental pharmacology. 2015;224:3-51.
39. Zannis VI, Fotakis P, Koukos G, Kardassis D, Ehnholm C, Jauhiainen M, et al. HDL biogenesis, remodeling, and catabolism. Handbook of experimental pharmacology. 2015;224:53-111.

40. Zannis VI, Cole FS, Jackson CL, Kurnit DM, Karathanasis SK. Distribution of apolipoprotein A-I, C-II, C-III, and E mRNA in fetal human tissues. Time-dependent induction of apolipoprotein E mRNA by cultures of human monocyte-macrophages. Biochemistry. 1985;24(16):4450-5.
41. Genest J, Schwertani A, Choi HY. Membrane microdomains and the regulation of HDL biogenesis. Current opinion in lipidology. 2018;29(1):36-41.
42. Zannis VI, Chroni A, Krieger M. Role of apoA-I, ABCA1, LCAT, and SR-BI in the biogenesis of HDL. Journal of molecular medicine. 2006;84(4):276-94.
43. Kypreos KE, Zannis VI. Pathway of biogenesis of apolipoprotein E-containing HDL in vivo with the participation of ABCA1 and LCAT. The Biochemical journal. 2007;403(2):359-67.
44. Duka A, Fotakis P, Georgiadou D, Kateifides A, Tzavlaki K, von Eckardstein L, et al. ApoA-IV promotes the biogenesis of apoA-IV-containing HDL particles with the participation of ABCA1 and LCAT. Journal of lipid research. 2013;54(1):107-15.
45. Wang N, Lan D, Chen W, Matsuura F, Tall AR. ATP-binding cassette transporters G1 and G4 mediate cellular cholesterol efflux to high-density lipoproteins. Proceedings of the National Academy of Sciences of the United States of America. 2004;101(26):9774-9.
46. Lusa S, Jauhiainen M, Metso J, Somerharju P, Ehnholm C. The mechanism of human plasma phospholipid transfer protein-induced enlargement of high-density lipoprotein particles: evidence for particle fusion. The Biochemical journal. 1996;313 (Pt 1):275-82.
47. Hoekstra M. SR-BI as target in atherosclerosis and cardiovascular disease - A comprehensive appraisal of the cellular functions of SR-BI in physiology and disease. Atherosclerosis. 2017;258:153-61.
48. Barter PJ, Brewer HB, Jr., Chapman MJ, Hennekens CH, Rader DJ, Tall AR. Cholesteryl ester transfer protein: a novel target for raising HDL and inhibiting atherosclerosis. Arteriosclerosis, thrombosis, and vascular biology. 2003;23(2):160-7.
49. Chroni A, Kardassis D. HDL Dysfunction Caused by Mutations in apoA-I and Other Genes that are Critical for HDL Biogenesis and Remodeling. Current medicinal chemistry. 2019;26(9):1544-75.
50. Martinez LO, Najib S, Perret B, Cabou C, Lichtenstein L. Ecto-F1-ATPase/P2Y pathways in metabolic and vascular functions of high density lipoproteins. Atherosclerosis. 2015;238(1):89-100.
51. Kardassis D, Mosialou I, Kanaki M, Tiniakou I, Thymiakou E. Metabolism of HDL and its regulation. Current medicinal chemistry. 2014;21(25):2864-80.
52. Hafiane A, Genest J. High density lipoproteins: Measurement techniques and potential biomarkers of cardiovascular risk. BBA clinical. 2015;3:175-88.
53. Kulkarni KR, Marcovina SM, Krauss RM, Garber DW, Glasscock AM, Segrest JP. Quantification of HDL2 and HDL3 cholesterol by the Vertical Auto Profile-II (VAP-II) methodology. Journal of lipid research. 1997;38(11):2353-64.
54. Blanche PJ, Gong EL, Forte TM, Nichols AV. Characterization of human high-density lipoproteins by gradient gel electrophoresis. Biochimica et biophysica acta. 1981;665(3):408-19.
55. Rosenson RS, Brewer HB, Jr., Chapman MJ, Fazio S, Hussain MM, Kontush A, et al. HDL measures, particle heterogeneity, proposed nomenclature, and relation to atherosclerotic cardiovascular events. Clinical chemistry. 2011;57(3):392-410.
56. Cheung MC, Albers JJ. Characterization of lipoprotein particles isolated by immunoaffinity chromatography. Particles containing A-I and A-II and particles containing A-I but no A-II. The Journal of biological chemistry. 1984;259(19):12201-9.
57. Castro GR, Fielding CJ. Early incorporation of cell-derived cholesterol into pre-beta-migrating high-density lipoprotein. Biochemistry. 1988;27(1):25-9.
58. Huang Y, von Eckardstein A, Wu S, Maeda N, Assmann G. A plasma lipoprotein containing only apolipoprotein E and with gamma mobility on electrophoresis releases cholesterol from cells. Proceedings of the National Academy of Sciences of the United States of America. 1994;91(5):1834-8.
59. Freeman LA. Native-native 2D gel electrophoresis for HDL subpopulation analysis. Methods in molecular biology. 2013;1027:353-67.

60. Camont L, Chapman MJ, Kontush A. Biological activities of HDL subpopulations and their relevance to cardiovascular disease. Trends in molecular medicine. 2011;17(10):594-603.
61. Zannis VI, Kurnit DM, Breslow JL. Hepatic apo-A-I and apo-E and intestinal apo-A-I are synthesized in precursor isoprotein forms by organ cultures of human fetal tissues. The Journal of biological chemistry. 1982;257(1):536-44.
62. Zannis VI, Karathanasis SK, Keutmann HT, Goldberger G, Breslow JL. Intracellular and extracellular processing of human apolipoprotein A-I: secreted apolipoprotein A-I isoprotein 2 is a propeptide. Proceedings of the National Academy of Sciences of the United States of America. 1983;80(9):2574-8.
63. Mei X, Atkinson D. Lipid-free Apolipoprotein A-I Structure: Insights into HDL Formation and Atherosclerosis Development. Archives of medical research. 2015;46(5):351-60.
64. Chroni A, Koukos G, Duka A, Zannis VI. The carboxy-terminal region of apoA-I is required for the ABCA1-dependent formation of alpha-HDL but not prebeta-HDL particles in vivo. Biochemistry. 2007;46(19):5697-708.
65. Chroni A, Liu T, Gorshkova I, Kan HY, Uehara Y, Von Eckardstein A, et al. The central helices of ApoA-I can promote ATP-binding cassette transporter A1 (ABCA1)-mediated lipid efflux. Amino acid residues 220-231 of the wild-type ApoA-I are required for lipid efflux in vitro and high density lipoprotein formation in vivo. The Journal of biological chemistry. 2003;278(9):6719-30.
66. Fotakis P, Kateifides AK, Gkolfinopoulou C, Georgiadou D, Beck M, Grundler K, et al. Role of the hydrophobic and charged residues in the 218-226 region of apoA-I in the biogenesis of HDL. Journal of lipid research. 2013;54(12):3281-92.
67. Fotakis P, Tiniakou I, Kateifides AK, Gkolfinopoulou C, Chroni A, Stratikos E, et al. Significance of the hydrophobic residues 225-230 of apoA-I for the biogenesis of HDL. Journal of lipid research. 2013;54(12):3293-302.
68. Tiniakou I, Kanaki Z, Georgopoulos S, Chroni A, Van Eck M, Fotakis P, et al. Natural human apoA-I mutations L141RPisa and L159RFIN alter HDL structure and functionality and promote atherosclerosis development in mice. Atherosclerosis. 2015;243(1):77-85.
69. Ignatius MJ, Gebicke-Harter PJ, Skene JH, Schilling JW, Weisgraber KH, Mahley RW, et al. Expression of apolipoprotein E during nerve degeneration and regeneration. Proceedings of the National Academy of Sciences of the United States of America. 1986;83(4):1125-9.
70. Kraft HG, Menzel HJ, Hoppichler F, Vogel W, Utermann G. Changes of genetic apolipoprotein phenotypes caused by liver transplantation. Implications for apolipoprotein synthesis. The Journal of clinical investigation. 1989;83(1):137-42.
71. Zannis VI, Breslow JL, Utermann G, Mahley RW, Weisgraber KH, Havel RJ, et al. Proposed nomenclature of apoE isoproteins, apoE genotypes, and phenotypes. Journal of lipid research. 1982;23(6):911-4.
72. Ordovas JM, Litwack-Klein L, Wilson PW, Schaefer MM, Schaefer EJ. Apolipoprotein E isoform phenotyping methodology and population frequency with identification of apoE1 and apoE5 isoforms. Journal of lipid research. 1987;28(4):371-80.
73. Mahley RW, Huang Y, Rall SC, Jr. Pathogenesis of type III hyperlipoproteinemia (dysbetalipoproteinemia). Questions, quandaries, and paradoxes. Journal of lipid research. 1999;40(11):1933-49.
74. Roses AD. Apolipoprotein E alleles as risk factors in Alzheimer's disease. Annual review of medicine. 1996;47:387-400.
75. Lund-Katz S, Phillips MC. High density lipoprotein structure-function and role in reverse cholesterol transport. Sub-cellular biochemistry. 2010;51:183-227.
76. Li X, Kypreos K, Zanni EE, Zannis V. Domains of apoE required for binding to apoE receptor 2 and to phospholipids: implications for the functions of apoE in the brain. Biochemistry. 2003;42(35):10406-17.
77. Kypreos KE, Zannis VI. LDL receptor deficiency or apoE mutations prevent remnant clearance and induce hypertriglyceridemia in mice. Journal of lipid research. 2006;47(3):521-9.

78. Herz J, Willnow TE. Lipoprotein and receptor interactions in vivo. Current opinion in lipidology. 1995;6(2):97-103.
79. Filou S, Lhomme M, Karavia EA, Kalogeropoulou C, Theodoropoulos V, Zvintzou E, et al. Distinct Roles of Apolipoproteins A1 and E in the Modulation of High-Density Lipoprotein Composition and Function. Biochemistry. 2016;55(27):3752-62.
80. Zannis VI, Koukos G, Drosatos K, Vezeridis A, Zanni EE, Kypreos KE, et al. Discrete roles of apoA-I and apoE in the biogenesis of HDL species: lessons learned from gene transfer studies in different mouse models. Annals of medicine. 2008;40 Suppl 1:14-28.
81. Plump AS, Smith JD, Hayek T, Aalto-Setala K, Walsh A, Verstuyft JG, et al. Severe hypercholesterolemia and atherosclerosis in apolipoprotein E-deficient mice created by homologous recombination in ES cells. Cell. 1992;71(2):343-53.
82. Breslow JL. Mouse models of atherosclerosis. Science. 1996;272(5262):685-8.
83. Daugherty A. Mouse models of atherosclerosis. The American journal of the medical sciences. 2002;323(1):3-10.
84. Shao B, Heinecke JW. Quantifying HDL proteins by mass spectrometry: how many proteins are there and what are their functions? Expert review of proteomics. 2018;15(1):31-40.
85. Kontush A, Lhomme M, Chapman MJ. Unraveling the complexities of the HDL lipidome. Journal of lipid research. 2013;54(11):2950-63.
86. Michell DL, Vickers KC. Lipoprotein carriers of microRNAs. Biochimica et biophysica acta. 2016;1861(12 Pt B):2069-74.
87. Kardassis D, Gafencu A, Zannis VI, Davalos A. Regulation of HDL genes: transcriptional, posttranscriptional, and posttranslational. Handbook of experimental pharmacology. 2015;224:113-79.
88. Canfran-Duque A, Lin CS, Goedeke L, Suarez Y, Fernandez-Hernando C. Micro-RNAs and High-Density Lipoprotein Metabolism. Arteriosclerosis, thrombosis, and vascular biology. 2016;36(6):1076-84.
89. van Solingen C, Scacalossi KR, Moore KJ. Long noncoding RNAs in lipid metabolism. Current opinion in lipidology. 2018;29(3):224-32.
90. Rudraiah S, Zhang X, Wang L. Nuclear Receptors as Therapeutic Targets in Liver Disease: Are We There Yet? Annual review of pharmacology and toxicology. 2016;56:605-26.
91. Gronemeyer H, Gustafsson JA, Laudet V. Principles for modulation of the nuclear receptor superfamily. Nature reviews Drug discovery. 2004;3(11):950-64.
92. Tran M, Liu Y, Huang W, Wang L. Nuclear receptors and liver disease: Summary of the 2017 basic research symposium. Hepatology communications. 2018;2(7):765-77.
93. Rochel N, Ciesielski F, Godet J, Moman E, Roessle M, Peluso-Iltis C, et al. Common architecture of nuclear receptor heterodimers on DNA direct repeat elements with different spacings. Nature structural & molecular biology. 2011;18(5):564-70.
94. Kardassis D, Drosatos, C., Zannis, V. Regulation of Genes Involved in the Biogenesis and the Remodeling of HDL in *High-Density Lipoproteins From Basic*

Biology to Clinical Aspects. Wiley-VCH, Weinheim. 2007.
95. Veras Ribeiro Filho H, Tambones IL, Mariano Goncalves Dias M, Bernardi Videira N, Bruder M, Amorim Amato A, et al. Modulation of nuclear receptor function: Targeting the protein-DNA interface. Molecular and cellular endocrinology. 2019;484:1-14.
96. Mosialou I, Zannis VI, Kardassis D. Regulation of human apolipoprotein m gene expression by orphan and ligand-dependent nuclear receptors. The Journal of biological chemistry. 2010;285(40):30719-30.
97. Apfel R, Benbrook D, Lernhardt E, Ortiz MA, Salbert G, Pfahl M. A novel orphan receptor specific for a subset of thyroid hormone-responsive elements and its interaction with the retinoid/thyroid hormone receptor subfamily. Molecular and cellular biology. 1994;14(10):7025-35.

98. Willy PJ, Umesono K, Ong ES, Evans RM, Heyman RA, Mangelsdorf DJ. LXR, a nuclear receptor that defines a distinct retinoid response pathway. Genes & development. 1995;9(9):1033-45.
99. Repa JJ, Mangelsdorf DJ. The role of orphan nuclear receptors in the regulation of cholesterol homeostasis. Annual review of cell and developmental biology. 2000;16:459-81.
100. Annicotte JS, Schoonjans K, Auwerx J. Expression of the liver X receptor alpha and beta in embryonic and adult mice. The anatomical record Part A, Discoveries in molecular, cellular, and evolutionary biology. 2004;277(2):312-6.
101. Ma L, Nelson ER. Oxysterols and nuclear receptors. Molecular and cellular endocrinology. 2019;484:42-51.
102. Spann NJ, Garmire LX, McDonald JG, Myers DS, Milne SB, Shibata N, et al. Regulated accumulation of desmosterol integrates macrophage lipid metabolism and inflammatory responses. Cell. 2012;151(1):138-52.
103. Lehmann JM, Kliewer SA, Moore LB, Smith-Oliver TA, Oliver BB, Su JL, et al. Activation of the nuclear receptor LXR by oxysterols defines a new hormone response pathway. The Journal of biological chemistry. 1997;272(6):3137-40.
104. Peet DJ, Turley SD, Ma W, Janowski BA, Lobaccaro JM, Hammer RE, et al. Cholesterol and bile acid metabolism are impaired in mice lacking the nuclear oxysterol receptor LXR alpha. Cell. 1998;93(5):693-704.
105. Costet P, Luo Y, Wang N, Tall AR. Sterol-dependent transactivation of the ABC1 promoter by the liver X receptor/retinoid X receptor. The Journal of biological chemistry. 2000;275(36):28240-5.
106. Repa JJ, Turley SD, Lobaccaro JA, Medina J, Li L, Lustig K, et al. Regulation of absorption and ABC1-mediated efflux of cholesterol by RXR heterodimers. Science. 2000;289(5484):1524-9.
107. Venkateswaran A, Repa JJ, Lobaccaro JM, Bronson A, Mangelsdorf DJ, Edwards PA. Human white/murine ABC8 mRNA levels are highly induced in lipid-loaded macrophages. A transcriptional role for specific oxysterols. The Journal of biological chemistry. 2000;275(19):14700-7.
108. Laffitte BA, Joseph SB, Chen M, Castrillo A, Repa J, Wilpitz D, et al. The phospholipid transfer protein gene is a liver X receptor target expressed by macrophages in atherosclerotic lesions. Molecular and cellular biology. 2003;23(6):2182-91.
109. Luo Y, Tall AR. Sterol upregulation of human CETP expression in vitro and in transgenic mice by an LXR element. The Journal of clinical investigation. 2000;105(4):513-20.
110. Zhang Y, Repa JJ, Gauthier K, Mangelsdorf DJ. Regulation of lipoprotein lipase by the oxysterol receptors, LXRalpha and LXRbeta. The Journal of biological chemistry. 2001;276(46):43018-24.
111. Mak PA, Laffitte BA, Desrumaux C, Joseph SB, Curtiss LK, Mangelsdorf DJ, et al. Regulated expression of the apolipoprotein E/C-I/C-IV/C-II gene cluster in murine and human macrophages. A critical role for nuclear liver X receptors alpha and beta. The Journal of biological chemistry. 2002;277(35):31900-8.
112. Laffitte BA, Repa JJ, Joseph SB, Wilpitz DC, Kast HR, Mangelsdorf DJ, et al. LXRs control lipid-inducible expression of the apolipoprotein E gene in macrophages and adipocytes. Proceedings of the National Academy of Sciences of the United States of America. 2001;98(2):507-12.
113. Yu L, Hammer RE, Li-Hawkins J, Von Bergmann K, Lutjohann D, Cohen JC, et al. Disruption of Abcg5 and Abcg8 in mice reveals their crucial role in biliary cholesterol secretion. Proceedings of the National Academy of Sciences of the United States of America. 2002;99(25):16237-42.
114. Berge KE, Tian H, Graf GA, Yu L, Grishin NV, Schultz J, et al. Accumulation of dietary cholesterol in sitosterolemia caused by mutations in adjacent ABC transporters. Science. 2000;290(5497):1771-5.
115. Repa JJ, Berge KE, Pomajzl C, Richardson JA, Hobbs H, Mangelsdorf DJ. Regulation of ATP-binding cassette sterol transporters ABCG5 and ABCG8 by the liver X receptors alpha and beta. The Journal of biological chemistry. 2002;277(21):18793-800.

116. Duval C, Touche V, Tailleux A, Fruchart JC, Fievet C, Clavey V, et al. Niemann-Pick C1 like 1 gene expression is down-regulated by LXR activators in the intestine. Biochemical and biophysical research communications. 2006;340(4):1259-63.
117. Sallam T, Jones MC, Gilliland T, Zhang L, Wu X, Eskin A, et al. Feedback modulation of cholesterol metabolism by the lipid-responsive non-coding RNA LeXis. Nature. 2016;534(7605):124-8.
118. Zelcer N, Hong C, Boyadjian R, Tontonoz P. LXR regulates cholesterol uptake through Idol-dependent ubiquitination of the LDL receptor. Science. 2009;325(5936):100-4.
119. Jakobsson T, Treuter E, Gustafsson JA, Steffensen KR. Liver X receptor biology and pharmacology: new pathways, challenges and opportunities. Trends in pharmacological sciences. 2012;33(7):394-404.
120. Rasheed A, Cummins CL. Beyond the Foam Cell: The Role of LXRs in Preventing Atherogenesis. International journal of molecular sciences. 2018;19(8).
121. Schuster GU, Parini P, Wang L, Alberti S, Steffensen KR, Hansson GK, et al. Accumulation of foam cells in liver X receptor-deficient mice. Circulation. 2002;106(9):1147-53.
122. Zhang Y, Breevoort SR, Angdisen J, Fu M, Schmidt DR, Holmstrom SR, et al. Liver LXRalpha expression is crucial for whole body cholesterol homeostasis and reverse cholesterol transport in mice. The Journal of clinical investigation. 2012;122(5):1688-99.
123. Lo Sasso G, Murzilli S, Salvatore L, D'Errico I, Petruzzelli M, Conca P, et al. Intestinal specific LXR activation stimulates reverse cholesterol transport and protects from atherosclerosis. Cell metabolism. 2010;12(2):187-93.
124. Tangirala RK, Bischoff ED, Joseph SB, Wagner BL, Walczak R, Laffitte BA, et al. Identification of macrophage liver X receptors as inhibitors of atherosclerosis. Proceedings of the National Academy of Sciences of the United States of America. 2002;99(18):11896-901.
125. Joseph SB, McKilligin E, Pei L, Watson MA, Collins AR, Laffitte BA, et al. Synthetic LXR ligand inhibits the development of atherosclerosis in mice. Proceedings of the National Academy of Sciences of the United States of America. 2002;99(11):7604-9.
126. Teupser D, Kretzschmar D, Tennert C, Burkhardt R, Wilfert W, Fengler D, et al. Effect of macrophage overexpression of murine liver X receptor-alpha (LXR-alpha) on atherosclerosis in LDL-receptor deficient mice. Arteriosclerosis, thrombosis, and vascular biology. 2008;28(11):2009-15.
127. Joseph SB, Castrillo A, Laffitte BA, Mangelsdorf DJ, Tontonoz P. Reciprocal regulation of inflammation and lipid metabolism by liver X receptors. Nature medicine. 2003;9(2):213-9.
128. Ghisletti S, Huang W, Ogawa S, Pascual G, Lin ME, Willson TM, et al. Parallel SUMOylation-dependent pathways mediate gene- and signal-specific transrepression by LXRs and PPARgamma. Molecular cell. 2007;25(1):57-70.
129. Ito A, Hong C, Rong X, Zhu X, Tarling EJ, Hedde PN, et al. LXRs link metabolism to inflammation through Abca1-dependent regulation of membrane composition and TLR signaling. eLife. 2015;4:e08009.
130. Schultz JR, Tu H, Luk A, Repa JJ, Medina JC, Li L, et al. Role of LXRs in control of lipogenesis. Genes & development. 2000;14(22):2831-8.
131. Joseph SB, Laffitte BA, Patel PH, Watson MA, Matsukuma KE, Walczak R, et al. Direct and indirect mechanisms for regulation of fatty acid synthase gene expression by liver X receptors. The Journal of biological chemistry. 2002;277(13):11019-25.
132. Chu K, Miyazaki M, Man WC, Ntambi JM. Stearoyl-coenzyme A desaturase 1 deficiency protects against hypertriglyceridemia and increases plasma high-density lipoprotein cholesterol induced by liver X receptor activation. Molecular and cellular biology. 2006;26(18):6786-98.
133. Laffitte BA, Chao LC, Li J, Walczak R, Hummasti S, Joseph SB, et al. Activation of liver X receptor improves glucose tolerance through coordinate regulation of glucose metabolism in liver and adipose tissue. Proceedings of the National Academy of Sciences of the United States of America. 2003;100(9):5419-24.

134. Cao G, Liang Y, Broderick CL, Oldham BA, Beyer TP, Schmidt RJ, et al. Antidiabetic action of a liver x receptor agonist mediated by inhibition of hepatic gluconeogenesis. The Journal of biological chemistry. 2003;278(2):1131-6.
135. Alberti S, Schuster G, Parini P, Feltkamp D, Diczfalusy U, Rudling M, et al. Hepatic cholesterol metabolism and resistance to dietary cholesterol in LXRbeta-deficient mice. The Journal of clinical investigation. 2001;107(5):565-73.
136. Bischoff ED, Daige CL, Petrowski M, Dedman H, Pattison J, Juliano J, et al. Non-redundant roles for LXRalpha and LXRbeta in atherosclerosis susceptibility in low density lipoprotein receptor knockout mice. Journal of lipid research. 2010;51(5):900-6.
137. Bradley MN, Hong C, Chen M, Joseph SB, Wilpitz DC, Wang X, et al. Ligand activation of LXR beta reverses atherosclerosis and cellular cholesterol overload in mice lacking LXR alpha and apoE. The Journal of clinical investigation. 2007;117(8):2337-46.
138. Chen M, Beaven S, Tontonoz P. Identification and characterization of two alternatively spliced transcript variants of human liver X receptor alpha. Journal of lipid research. 2005;46(12):2570-9.
139. Endo-Umeda K, Uno S, Fujimori K, Naito Y, Saito K, Yamagishi K, et al. Differential expression and function of alternative splicing variants of human liver X receptor alpha. Molecular pharmacology. 2012;81(6):800-10.
140. Whitney KD, Watson MA, Goodwin B, Galardi CM, Maglich JM, Wilson JG, et al. Liver X receptor (LXR) regulation of the LXRalpha gene in human macrophages. The Journal of biological chemistry. 2001;276(47):43509-15.
141. Laffitte BA, Joseph SB, Walczak R, Pei L, Wilpitz DC, Collins JL, et al. Autoregulation of the human liver X receptor alpha promoter. Molecular and cellular biology. 2001;21(22):7558-68.
142. Hashimoto K, Matsumoto S, Yamada M, Satoh T, Mori M. Liver X receptor-alpha gene expression is positively regulated by thyroid hormone. Endocrinology. 2007;148(10):4667-75.
143. Kim MS, Sweeney TR, Shigenaga JK, Chui LG, Moser A, Grunfeld C, et al. Tumor necrosis factor and interleukin 1 decrease RXRalpha, PPARalpha, PPARgamma, LXRalpha, and the coactivators SRC-1, PGC-1alpha, and PGC-1beta in liver cells. Metabolism: clinical and experimental. 2007;56(2):267-79.
144. Tobin KA, Ulven SM, Schuster GU, Steineger HH, Andresen SM, Gustafsson JA, et al. Liver X receptors as insulin-mediating factors in fatty acid and cholesterol biosynthesis. The Journal of biological chemistry. 2002;277(12):10691-7.
145. Chen G, Liang G, Ou J, Goldstein JL, Brown MS. Central role for liver X receptor in insulin-mediated activation of Srebp-1c transcription and stimulation of fatty acid synthesis in liver. Proceedings of the National Academy of Sciences of the United States of America. 2004;101(31):11245-50.
146. Tian J, Goldstein JL, Brown MS. Insulin induction of SREBP-1c in rodent liver requires LXRalpha-C/EBPbeta complex. Proceedings of the National Academy of Sciences of the United States of America. 2016;113(29):8182-7.
147. Sladek FM. What are nuclear receptor ligands? Molecular and cellular endocrinology. 2011;334(1-2):3-13.
148. Yuan X, Ta TC, Lin M, Evans JR, Dong Y, Bolotin E, et al. Identification of an endogenous ligand bound to a native orphan nuclear receptor. PloS one. 2009;4(5):e5609.
149. Fang B, Mane-Padros D, Bolotin E, Jiang T, Sladek FM. Identification of a binding motif specific to HNF4 by comparative analysis of multiple nuclear receptors. Nucleic acids research. 2012;40(12):5343-56.
150. Chen WS, Manova K, Weinstein DC, Duncan SA, Plump AS, Prezioso VR, et al. Disruption of the HNF-4 gene, expressed in visceral endoderm, leads to cell death in embryonic ectoderm and impaired gastrulation of mouse embryos. Genes & development. 1994;8(20):2466-77.

151. Sladek FM, Zhong WM, Lai E, Darnell JE, Jr. Liver-enriched transcription factor HNF-4 is a novel member of the steroid hormone receptor superfamily. Genes & development. 1990;4(12B):2353-65.
152. Hayhurst GP, Lee YH, Lambert G, Ward JM, Gonzalez FJ. Hepatocyte nuclear factor 4alpha (nuclear receptor 2A1) is essential for maintenance of hepatic gene expression and lipid homeostasis. Molecular and cellular biology. 2001;21(4):1393-403.
153. Inoue Y, Hayhurst GP, Inoue J, Mori M, Gonzalez FJ. Defective ureagenesis in mice carrying a liver-specific disruption of hepatocyte nuclear factor 4alpha (HNF4alpha). HNF4alpha regulates ornithine transcarbamylase in vivo. The Journal of biological chemistry. 2002;277(28):25257-65.
154. Inoue Y, Yu AM, Yim SH, Ma X, Krausz KW, Inoue J, et al. Regulation of bile acid biosynthesis by hepatocyte nuclear factor 4alpha. Journal of lipid research. 2006;47(1):215-27.
155. Rhee J, Inoue Y, Yoon JC, Puigserver P, Fan M, Gonzalez FJ, et al. Regulation of hepatic fasting response by PPARgamma coactivator-1alpha (PGC-1): requirement for hepatocyte nuclear factor 4alpha in gluconeogenesis. Proceedings of the National Academy of Sciences of the United States of America. 2003;100(7):4012-7.
156. Kyrmizi I, Hatzis P, Katrakili N, Tronche F, Gonzalez FJ, Talianidis I. Plasticity and expanding complexity of the hepatic transcription factor network during liver development. Genes & development. 2006;20(16):2293-305.
157. Odom DT, Zizlsperger N, Gordon DB, Bell GW, Rinaldi NJ, Murray HL, et al. Control of pancreas and liver gene expression by HNF transcription factors. Science. 2004;303(5662):1378-81.
158. Yeh MM, Bosch DE, Daoud SS. Role of hepatocyte nuclear factor 4-alpha in gastrointestinal and liver diseases. World journal of gastroenterology. 2019;25(30):4074-91.
159. Yamagata K, Furuta H, Oda N, Kaisaki PJ, Menzel S, Cox NJ, et al. Mutations in the hepatocyte nuclear factor-4alpha gene in maturity-onset diabetes of the young (MODY1). Nature. 1996;384(6608):458-60.
160. Pearson ER, Pruhova S, Tack CJ, Johansen A, Castleden HA, Lumb PJ, et al. Molecular genetics and phenotypic characteristics of MODY caused by hepatocyte nuclear factor 4alpha mutations in a large European collection. Diabetologia. 2005;48(5):878-85.
161. Lau HH, Ng NHJ, Loo LSW, Jasmen JB, Teo AKK. The molecular functions of hepatocyte nuclear factors - In and beyond the liver. Journal of hepatology. 2018;68(5):1033-48.
162. Yin L, Ma H, Ge X, Edwards PA, Zhang Y. Hepatic hepatocyte nuclear factor 4alpha is essential for maintaining triglyceride and cholesterol homeostasis. Arteriosclerosis, thrombosis, and vascular biology. 2011;31(2):328-36.
163. Kathiresan S, Willer CJ, Peloso GM, Demissie S, Musunuru K, Schadt EE, et al. Common variants at 30 loci contribute to polygenic dyslipidemia. Nature genetics. 2009;41(1):56-65.
164. Christoffersen C, Obinata H, Kumaraswamy SB, Galvani S, Ahnstrom J, Sevvana M, et al. Endothelium-protective sphingosine-1-phosphate provided by HDL-associated apolipoprotein M. Proceedings of the National Academy of Sciences of the United States of America. 2011;108(23):9613-8.
165. Babeu JP, Boudreau F. Hepatocyte nuclear factor 4-alpha involvement in liver and intestinal inflammatory networks. World journal of gastroenterology. 2014;20(1):22-30.
166. Xie X, Liao H, Dang H, Pang W, Guan Y, Wang X, et al. Down-regulation of hepatic HNF4alpha gene expression during hyperinsulinemia via SREBPs. Molecular endocrinology. 2009;23(4):434-43.
167. Lu H. Crosstalk of HNF4alpha with extracellular and intracellular signaling pathways in the regulation of hepatic metabolism of drugs and lipids. Acta pharmaceutica Sinica B. 2016;6(5):393-408.
168. Bartel DP. MicroRNAs: target recognition and regulatory functions. Cell. 2009;136(2):215-33.
169. Carthew RW, Sontheimer EJ. Origins and Mechanisms of miRNAs and siRNAs. Cell. 2009;136(4):642-55.
170. Zhang J, Zhou W, Liu Y, Liu T, Li C, Wang L. Oncogenic role of microRNA-532-5p in human colorectal cancer via targeting of the 5'UTR of RUNX3. Oncology letters. 2018;15(5):7215-20.

171. Tay Y, Zhang J, Thomson AM, Lim B, Rigoutsos I. MicroRNAs to Nanog, Oct4 and Sox2 coding regions modulate embryonic stem cell differentiation. Nature. 2008;455(7216):1124-8.
172. Vasudevan S, Tong Y, Steitz JA. Switching from repression to activation: microRNAs can up-regulate translation. Science. 2007;318(5858):1931-4.
173. Dharap A, Pokrzywa C, Murali S, Pandi G, Vemuganti R. MicroRNA miR-324-3p induces promoter-mediated expression of RelA gene. PloS one. 2013;8(11):e79467.
174. Xiao M, Li J, Li W, Wang Y, Wu F, Xi Y, et al. MicroRNAs activate gene transcription epigenetically as an enhancer trigger. RNA biology. 2017;14(10):1326-34.
175. Friedman RC, Farh KK, Burge CB, Bartel DP. Most mammalian mRNAs are conserved targets of microRNAs. Genome research. 2009;19(1):92-105.
176. Vishnoi A, Rani S. MiRNA Biogenesis and Regulation of Diseases: An Overview. Methods in molecular biology. 2017;1509:1-10.
177. Vickers KC, Palmisano BT, Shoucri BM, Shamburek RD, Remaley AT. MicroRNAs are transported in plasma and delivered to recipient cells by high-density lipoproteins. Nature cell biology. 2011;13(4):423-33.
178. Roderburg C, Luedde T. Circulating microRNAs as markers of liver inflammation, fibrosis and cancer. Journal of hepatology. 2014;61(6):1434-7.
179. Zhang X, Price NL, Fernandez-Hernando C. Non-coding RNAs in lipid metabolism. Vascular pharmacology. 2019;114:93-102.
180. Zaiou M, Rihn BH, Bakillah A. Epigenetic regulation of genes involved in the reverse cholesterol transport through interaction with miRNAs. Frontiers in bioscience. 2018;23:2090-105.
181. Aryal B, Singh AK, Rotllan N, Price N, Fernandez-Hernando C. MicroRNAs and lipid metabolism. Current opinion in lipidology. 2017;28(3):273-80.
182. Rotllan N, Ramirez CM, Aryal B, Esau CC, Fernandez-Hernando C. Therapeutic silencing of microRNA-33 inhibits the progression of atherosclerosis in Ldlr-/- mice--brief report. Arteriosclerosis, thrombosis, and vascular biology. 2013;33(8):1973-7.
183. Rayner KJ, Sheedy FJ, Esau CC, Hussain FN, Temel RE, Parathath S, et al. Antagonism of miR-33 in mice promotes reverse cholesterol transport and regression of atherosclerosis. The Journal of clinical investigation. 2011;121(7):2921-31.
184. Horie T, Baba O, Kuwabara Y, Chujo Y, Watanabe S, Kinoshita M, et al. MicroRNA-33 deficiency reduces the progression of atherosclerotic plaque in ApoE-/- mice. Journal of the American Heart Association. 2012;1(6):e003376.
185. Liang B, Wang X, Song X, Bai R, Yang H, Yang Z, et al. MicroRNA-20a/b regulates cholesterol efflux through post-transcriptional repression of ATP-binding cassette transporter A1. Biochimica et biophysica acta Molecular and cell biology of lipids. 2017;1862(9):929-38.
186. Ren K, Zhu X, Zheng Z, Mo ZC, Peng XS, Zeng YZ, et al. MicroRNA-24 aggravates atherosclerosis by inhibiting selective lipid uptake from HDL cholesterol via the post-transcriptional repression of scavenger receptor class B type I. Atherosclerosis. 2018;270:57-67.
187. Reinhart BJ, Slack FJ, Basson M, Pasquinelli AE, Bettinger JC, Rougvie AE, et al. The 21-nucleotide let-7 RNA regulates developmental timing in Caenorhabditis elegans. Nature. 2000;403(6772):901-6.
188. Pasquinelli AE, Reinhart BJ, Slack F, Martindale MQ, Kuroda MI, Maller B, et al. Conservation of the sequence and temporal expression of let-7 heterochronic regulatory RNA. Nature. 2000;408(6808):86-9.
189. Hertel J, Bartschat S, Wintsche A, Otto C, Students of the Bioinformatics Computer L, Stadler PF. Evolution of the let-7 microRNA family. RNA biology. 2012;9(3):231-41.
190. Su JL, Chen PS, Johansson G, Kuo ML. Function and regulation of let-7 family microRNAs. MicroRNA. 2012;1(1):34-9.
191. Lee H, Han S, Kwon CS, Lee D. Biogenesis and regulation of the let-7 miRNAs and their functional implications. Protein & cell. 2016;7(2):100-13.

192. Chirshev E, Oberg KC, Ioffe YJ, Unternaehrer JJ. Let-7 as biomarker, prognostic indicator, and therapy for precision medicine in cancer. Clinical and translational medicine. 2019;8(1):24.
193. Kumar MS, Erkeland SJ, Pester RE, Chen CY, Ebert MS, Sharp PA, et al. Suppression of non-small cell lung tumor development by the let-7 microRNA family. Proceedings of the National Academy of Sciences of the United States of America. 2008;105(10):3903-8.
194. Yu F, Yao H, Zhu P, Zhang X, Pan Q, Gong C, et al. let-7 regulates self renewal and tumorigenicity of breast cancer cells. Cell. 2007;131(6):1109-23.
195. Li XX, Di X, Cong S, Wang Y, Wang K. The role of let-7 and HMGA2 in the occurrence and development of lung cancer: a systematic review and meta-analysis. European review for medical and pharmacological sciences. 2018;22(23):8353-66.
196. Sampson VB, Rong NH, Han J, Yang Q, Aris V, Soteropoulos P, et al. MicroRNA let-7a down-regulates MYC and reverts MYC-induced growth in Burkitt lymphoma cells. Cancer research. 2007;67(20):9762-70.
197. Bao MH, Feng X, Zhang YW, Lou XY, Cheng Y, Zhou HH. Let-7 in cardiovascular diseases, heart development and cardiovascular differentiation from stem cells. International journal of molecular sciences. 2013;14(11):23086-102.
198. Cuaz-Perolin C, Jguirim I, Larigauderie G, Jlassi A, Furman C, Moreau M, et al. Apolipoprotein E knockout mice over-expressing human tissue inhibitor of metalloproteinase 1 are protected against aneurysm formation but not against atherosclerotic plaque development. Journal of vascular research. 2006;43(6):493-501.
199. Fichtlscherer S, De Rosa S, Fox H, Schwietz T, Fischer A, Liebetrau C, et al. Circulating microRNAs in patients with coronary artery disease. Circulation research. 2010;107(5):677-84.
200. Satoh M, Tabuchi T, Minami Y, Takahashi Y, Itoh T, Nakamura M. Expression of let-7i is associated with Toll-like receptor 4 signal in coronary artery disease: effect of statins on let-7i and Toll-like receptor 4 signal. Immunobiology. 2012;217(5):533-9.
201. Kin K, Miyagawa S, Fukushima S, Shirakawa Y, Torikai K, Shimamura K, et al. Tissue- and plasma-specific MicroRNA signatures for atherosclerotic abdominal aortic aneurysm. Journal of the American Heart Association. 2012;1(5):e000745.
202. Wang YS, Hsi E, Cheng HY, Hsu SH, Liao YC, Juo SH. Let-7g suppresses both canonical and non-canonical NF-kappaB pathways in macrophages leading to anti-atherosclerosis. Oncotarget. 2017;8(60):101026-41.
203. Zhu H, Shyh-Chang N, Segre AV, Shinoda G, Shah SP, Einhorn WS, et al. The Lin28/let-7 axis regulates glucose metabolism. Cell. 2011;147(1):81-94.
204. Frost RJ, Olson EN. Control of glucose homeostasis and insulin sensitivity by the Let-7 family of microRNAs. Proceedings of the National Academy of Sciences of the United States of America. 2011;108(52):21075-80.
205. Barr DP, Russ EM, Eder HA. Protein-lipid relationships in human plasma. II. In atherosclerosis and related conditions. The American journal of medicine. 1951;11(4):480-93.
206. Gordon T, Castelli WP, Hjortland MC, Kannel WB, Dawber TR. High density lipoprotein as a protective factor against coronary heart disease. The Framingham Study. The American journal of medicine. 1977;62(5):707-14.
207. Assmann G, Schulte H, von Eckardstein A, Huang Y. High-density lipoprotein cholesterol as a predictor of coronary heart disease risk. The PROCAM experience and pathophysiological implications for reverse cholesterol transport. Atherosclerosis. 1996;124 Suppl:S11-20.
208. Toth PP, Barter PJ, Rosenson RS, Boden WE, Chapman MJ, Cuchel M, et al. High-density lipoproteins: a consensus statement from the National Lipid Association. Journal of clinical lipidology. 2013;7(5):484-525.
209. Barter P, Gotto AM, LaRosa JC, Maroni J, Szarek M, Grundy SM, et al. HDL cholesterol, very low levels of LDL cholesterol, and cardiovascular events. The New England journal of medicine. 2007;357(13):1301-10.

210. Bortnick AE, Rothblat GH, Stoudt G, Hoppe KL, Royer LJ, McNeish J, et al. The correlation of ATP-binding cassette 1 mRNA levels with cholesterol efflux from various cell lines. The Journal of biological chemistry. 2000;275(37):28634-40.
211. Yvan-Charvet L, Ranalletta M, Wang N, Han S, Terasaka N, Li R, et al. Combined deficiency of ABCA1 and ABCG1 promotes foam cell accumulation and accelerates atherosclerosis in mice. The Journal of clinical investigation. 2007;117(12):3900-8.
212. Phillips MC. Molecular mechanisms of cellular cholesterol efflux. The Journal of biological chemistry. 2014;289(35):24020-9.
213. Acton S, Rigotti A, Landschulz KT, Xu S, Hobbs HH, Krieger M. Identification of scavenger receptor SR-BI as a high density lipoprotein receptor. Science. 1996;271(5248):518-20.
214. Wang X, Collins HL, Ranalletta M, Fuki IV, Billheimer JT, Rothblat GH, et al. Macrophage ABCA1 and ABCG1, but not SR-BI, promote macrophage reverse cholesterol transport in vivo. The Journal of clinical investigation. 2007;117(8):2216-24.
215. Zhao Y, Pennings M, Hildebrand RB, Ye D, Calpe-Berdiel L, Out R, et al. Enhanced foam cell formation, atherosclerotic lesion development, and inflammation by combined deletion of ABCA1 and SR-BI in Bone marrow-derived cells in LDL receptor knockout mice on western-type diet. Circulation research. 2010;107(12):e20-31.
216. Rosenson RS, Brewer HB, Jr., Davidson WS, Fayad ZA, Fuster V, Goldstein J, et al. Cholesterol efflux and atheroprotection: advancing the concept of reverse cholesterol transport. Circulation. 2012;125(15):1905-19.
217. von Eckardstein A, Rohrer L. Transendothelial lipoprotein transport and regulation of endothelial permeability and integrity by lipoproteins. Current opinion in lipidology. 2009;20(3):197-205.
218. Rodman JS, Mercer RW, Stahl PD. Endocytosis and transcytosis. Current opinion in cell biology. 1990;2(4):664-72.
219. Zanoni P, Velagapudi S, Yalcinkaya M, Rohrer L, von Eckardstein A. Endocytosis of lipoproteins. Atherosclerosis. 2018;275:273-95.
220. Yuhanna IS, Zhu Y, Cox BE, Hahner LD, Osborne-Lawrence S, Lu P, et al. High-density lipoprotein binding to scavenger receptor-BI activates endothelial nitric oxide synthase. Nature medicine. 2001;7(7):853-7.
221. Uittenbogaard A, Shaul PW, Yuhanna IS, Blair A, Smart EJ. High density lipoprotein prevents oxidized low density lipoprotein-induced inhibition of endothelial nitric-oxide synthase localization and activation in caveolae. The Journal of biological chemistry. 2000;275(15):11278-83.
222. Ramet ME, Ramet M, Lu Q, Nickerson M, Savolainen MJ, Malzone A, et al. High-density lipoprotein increases the abundance of eNOS protein in human vascular endothelial cells by increasing its half-life. Journal of the American College of Cardiology. 2003;41(12):2288-97.
223. Levkau B, Hermann S, Theilmeier G, van der Giet M, Chun J, Schober O, et al. High-density lipoprotein stimulates myocardial perfusion in vivo. Circulation. 2004;110(21):3355-9.
224. Spieker LE, Sudano I, Hurlimann D, Lerch PG, Lang MG, Binggeli C, et al. High-density lipoprotein restores endothelial function in hypercholesterolemic men. Circulation. 2002;105(12):1399-402.
225. Mineo C, Shaul PW. Modulation of endothelial NO production by high-density lipoprotein. Cold Spring Harbor symposia on quantitative biology. 2002;67:459-69.
226. Kimura T, Tomura H, Sato K, Ito M, Matsuoka I, Im DS, et al. Mechanism and role of high density lipoprotein-induced activation of AMP-activated protein kinase in endothelial cells. The Journal of biological chemistry. 2010;285(7):4387-97.
227. Assanasen C, Mineo C, Seetharam D, Yuhanna IS, Marcel YL, Connelly MA, et al. Cholesterol binding, efflux, and a PDZ-interacting domain of scavenger receptor-BI mediate HDL-initiated signaling. The Journal of clinical investigation. 2005;115(4):969-77.
228. Saddar S, Carriere V, Lee WR, Tanigaki K, Yuhanna IS, Parathath S, et al. Scavenger receptor class B type I is a plasma membrane cholesterol sensor. Circulation research. 2013;112(1):140-51.

229. Nofer JR, van der Giet M, Tolle M, Wolinska I, von Wnuck Lipinski K, Baba HA, et al. HDL induces NO-dependent vasorelaxation via the lysophospholipid receptor S1P3. The Journal of clinical investigation. 2004;113(4):569-81.
230. Igarashi J, Miyoshi M, Hashimoto T, Kubota Y, Kosaka H. Statins induce S1P1 receptors and enhance endothelial nitric oxide production in response to high-density lipoproteins. British journal of pharmacology. 2007;150(4):470-9.
231. Gonzalez E, Kou R, Michel T. Rac1 modulates sphingosine 1-phosphate-mediated activation of phosphoinositide 3-kinase/Akt signaling pathways in vascular endothelial cells. The Journal of biological chemistry. 2006;281(6):3210-6.
232. Igarashi J, Michel T. Agonist-modulated targeting of the EDG-1 receptor to plasmalemmal caveolae. eNOS activation by sphingosine 1-phosphate and the role of caveolin-1 in sphingolipid signal transduction. The Journal of biological chemistry. 2000;275(41):32363-70.
233. Terasaka N, Yu S, Yvan-Charvet L, Wang N, Mzhavia N, Langlois R, et al. ABCG1 and HDL protect against endothelial dysfunction in mice fed a high-cholesterol diet. The Journal of clinical investigation. 2008;118(11):3701-13.
234. Terasaka N, Westerterp M, Koetsveld J, Fernandez-Hernando C, Yvan-Charvet L, Wang N, et al. ATP-binding cassette transporter G1 and high-density lipoprotein promote endothelial NO synthesis through a decrease in the interaction of caveolin-1 and endothelial NO synthase. Arteriosclerosis, thrombosis, and vascular biology. 2010;30(11):2219-25.
235. Kratzer A, Giral H, Landmesser U. High-density lipoproteins as modulators of endothelial cell functions: alterations in patients with coronary artery disease. Cardiovascular research. 2014;103(3):350-61.
236. Cockerill GW, Rye KA, Gamble JR, Vadas MA, Barter PJ. High-density lipoproteins inhibit cytokine-induced expression of endothelial cell adhesion molecules. Arteriosclerosis, thrombosis, and vascular biology. 1995;15(11):1987-94.
237. Calabresi L, Franceschini G, Sirtori CR, De Palma A, Saresella M, Ferrante P, et al. Inhibition of VCAM-1 expression in endothelial cells by reconstituted high density lipoproteins. Biochemical and biophysical research communications. 1997;238(1):61-5.
238. Mackness B, Hine D, Liu Y, Mastorikou M, Mackness M. Paraoxonase-1 inhibits oxidised LDL-induced MCP-1 production by endothelial cells. Biochemical and biophysical research communications. 2004;318(3):680-3.
239. Maier JA, Barenghi L, Pagani F, Bradamante S, Comi P, Ragnotti G. The protective role of high-density lipoprotein on oxidized-low-density-lipoprotein-induced U937/endothelial cell interactions. European journal of biochemistry. 1994;221(1):35-41.
240. Dimayuga P, Zhu J, Oguchi S, Chyu KY, Xu XO, Yano J, et al. Reconstituted HDL containing human apolipoprotein A-1 reduces VCAM-1 expression and neointima formation following periadventitial cuff-induced carotid injury in apoE null mice. Biochemical and biophysical research communications. 1999;264(2):465-8.
241. Nicholls SJ, Dusting GJ, Cutri B, Bao S, Drummond GR, Rye KA, et al. Reconstituted high-density lipoproteins inhibit the acute pro-oxidant and proinflammatory vascular changes induced by a periarterial collar in normocholesterolemic rabbits. Circulation. 2005;111(12):1543-50.
242. Puranik R, Bao S, Nobecourt E, Nicholls SJ, Dusting GJ, Barter PJ, et al. Low dose apolipoprotein A-I rescues carotid arteries from inflammation in vivo. Atherosclerosis. 2008;196(1):240-7.
243. Li J, Wang W, Han L, Feng M, Lu H, Yang L, et al. Human apolipoprotein A-I exerts a prophylactic effect on high-fat diet-induced atherosclerosis via inflammation inhibition in a rabbit model. Acta biochimica et biophysica Sinica. 2017;49(2):149-58.
244. Patel S, Drew BG, Nakhla S, Duffy SJ, Murphy AJ, Barter PJ, et al. Reconstituted high-density lipoprotein increases plasma high-density lipoprotein anti-inflammatory properties and cholesterol efflux capacity in patients with type 2 diabetes. Journal of the American College of Cardiology. 2009;53(11):962-71.

245. Kimura T, Tomura H, Mogi C, Kuwabara A, Damirin A, Ishizuka T, et al. Role of scavenger receptor class B type I and sphingosine 1-phosphate receptors in high density lipoprotein-induced inhibition of adhesion molecule expression in endothelial cells. The Journal of biological chemistry. 2006;281(49):37457-67.
246. Wu BJ, Chen K, Shrestha S, Ong KL, Barter PJ, Rye KA. High-density lipoproteins inhibit vascular endothelial inflammation by increasing 3beta-hydroxysteroid-Delta24 reductase expression and inducing heme oxygenase-1. Circulation research. 2013;112(2):278-88.
247. Galvani S, Sanson M, Blaho VA, Swendeman SL, Obinata H, Conger H, et al. HDL-bound sphingosine 1-phosphate acts as a biased agonist for the endothelial cell receptor S1P1 to limit vascular inflammation. Science signaling. 2015;8(389):ra79.
248. Whetzel AM, Sturek JM, Nagelin MH, Bolick DT, Gebre AK, Parks JS, et al. ABCG1 deficiency in mice promotes endothelial activation and monocyte-endothelial interactions. Arteriosclerosis, thrombosis, and vascular biology. 2010;30(4):809-17.
249. Cheng AM, Handa P, Tateya S, Schwartz J, Tang C, Mitra P, et al. Apolipoprotein A-I attenuates palmitate-mediated NF-kappaB activation by reducing Toll-like receptor-4 recruitment into lipid rafts. PloS one. 2012;7(3):e33917.
250. Baker PW, Rye KA, Gamble JR, Vadas MA, Barter PJ. Phospholipid composition of reconstituted high density lipoproteins influences their ability to inhibit endothelial cell adhesion molecule expression. Journal of lipid research. 2000;41(8):1261-7.
251. Nofer JR, Geigenmuller S, Gopfert C, Assmann G, Buddecke E, Schmidt A. High density lipoprotein-associated lysosphingolipids reduce E-selectin expression in human endothelial cells. Biochemical and biophysical research communications. 2003;310(1):98-103.
252. Sugano M, Tsuchida K, Makino N. High-density lipoproteins protect endothelial cells from tumor necrosis factor-alpha-induced apoptosis. Biochemical and biophysical research communications. 2000;272(3):872-6.
253. Suc I, Escargueil-Blanc I, Troly M, Salvayre R, Negre-Salvayre A. HDL and ApoA prevent cell death of endothelial cells induced by oxidized LDL. Arteriosclerosis, thrombosis, and vascular biology. 1997;17(10):2158-66.
254. Nofer JR, Levkau B, Wolinska I, Junker R, Fobker M, von Eckardstein A, et al. Suppression of endothelial cell apoptosis by high density lipoproteins (HDL) and HDL-associated lysosphingolipids. The Journal of biological chemistry. 2001;276(37):34480-5.
255. Riwanto M, Rohrer L, Roschitzki B, Besler C, Mocharla P, Mueller M, et al. Altered activation of endothelial anti- and proapoptotic pathways by high-density lipoprotein from patients with coronary artery disease: role of high-density lipoprotein-proteome remodeling. Circulation. 2013;127(8):891-904.
256. de Souza JA, Vindis C, Hansel B, Negre-Salvayre A, Therond P, Serrano CV, Jr., et al. Metabolic syndrome features small, apolipoprotein A-I-poor, triglyceride-rich HDL3 particles with defective anti-apoptotic activity. Atherosclerosis. 2008;197(1):84-94.
257. Radojkovic C, Genoux A, Pons V, Combes G, de Jonge H, Champagne E, et al. Stimulation of cell surface F1-ATPase activity by apolipoprotein A-I inhibits endothelial cell apoptosis and promotes proliferation. Arteriosclerosis, thrombosis, and vascular biology. 2009;29(7):1125-30.
258. Ruiz M, Okada H, Dahlback B. HDL-associated ApoM is anti-apoptotic by delivering sphingosine 1-phosphate to S1P1 & S1P3 receptors on vascular endothelium. Lipids in health and disease. 2017;16(1):36.
259. Sutter I, Velagapudi S, Othman A, Riwanto M, Manz J, Rohrer L, et al. Plasmalogens of high-density lipoproteins (HDL) are associated with coronary artery disease and anti-apoptotic activity of HDL. Atherosclerosis. 2015;241(2):539-46.
260. Jin F, Hagemann N, Sun L, Wu J, Doeppner TR, Dai Y, et al. High-density lipoprotein (HDL) promotes angiogenesis via S1P3-dependent VEGFR2 activation. Angiogenesis. 2018;21(2):381-94.

261. Tso C, Martinic G, Fan WH, Rogers C, Rye KA, Barter PJ. High-density lipoproteins enhance progenitor-mediated endothelium repair in mice. Arteriosclerosis, thrombosis, and vascular biology. 2006;26(5):1144-9.
262. Tan JT, Prosser HC, Vanags LZ, Monger SA, Ng MK, Bursill CA. High-density lipoproteins augment hypoxia-induced angiogenesis via regulation of post-translational modulation of hypoxia-inducible factor 1alpha. FASEB journal : official publication of the Federation of American Societies for Experimental Biology. 2014;28(1):206-17.
263. Castaing-Berthou A, Malet N, Radojkovic C, Cabou C, Gayral S, Martinez LO, et al. PI3Kbeta Plays a Key Role in Apolipoprotein A-I-Induced Endothelial Cell Proliferation Through Activation of the Ecto-F1-ATPase/P2Y1 Receptors. Cellular physiology and biochemistry : international journal of experimental cellular physiology, biochemistry, and pharmacology. 2017;42(2):579-93.
264. Seetharam D, Mineo C, Gormley AK, Gibson LL, Vongpatanasin W, Chambliss KL, et al. High-density lipoprotein promotes endothelial cell migration and reendothelialization via scavenger receptor-B type I. Circulation research. 2006;98(1):63-72.
265. Kimura T, Sato K, Malchinkhuu E, Tomura H, Tamama K, Kuwabara A, et al. High-density lipoprotein stimulates endothelial cell migration and survival through sphingosine 1-phosphate and its receptors. Arteriosclerosis, thrombosis, and vascular biology. 2003;23(7):1283-8.
266. Zhu W, Saddar S, Seetharam D, Chambliss KL, Longoria C, Silver DL, et al. The scavenger receptor class B type I adaptor protein PDZK1 maintains endothelial monolayer integrity. Circulation research. 2008;102(4):480-7.
267. Edwards N, Langford-Smith AWW, Wilkinson FL, Alexander MY. Endothelial Progenitor Cells: New Targets for Therapeutics for Inflammatory Conditions With High Cardiovascular Risk. Frontiers in medicine. 2018;5:200.
268. Feng Y, Jacobs F, Van Craeyveld E, Brunaud C, Snoeys J, Tjwa M, et al. Human ApoA-I transfer attenuates transplant arteriosclerosis via enhanced incorporation of bone marrow-derived endothelial progenitor cells. Arteriosclerosis, thrombosis, and vascular biology. 2008;28(2):278-83.
269. Feng Y, van Eck M, Van Craeyveld E, Jacobs F, Carlier V, Van Linthout S, et al. Critical role of scavenger receptor-BI-expressing bone marrow-derived endothelial progenitor cells in the attenuation of allograft vasculopathy after human apo A-I transfer. Blood. 2009;113(3):755-64.
270. Sumi M, Sata M, Miura S, Rye KA, Toya N, Kanaoka Y, et al. Reconstituted high-density lipoprotein stimulates differentiation of endothelial progenitor cells and enhances ischemia-induced angiogenesis. Arteriosclerosis, thrombosis, and vascular biology. 2007;27(4):813-8.
271. Noor R, Shuaib U, Wang CX, Todd K, Ghani U, Schwindt B, et al. High-density lipoprotein cholesterol regulates endothelial progenitor cells by increasing eNOS and preventing apoptosis. Atherosclerosis. 2007;192(1):92-9.
272. Shi Y, Lv X, Liu Y, Li B, Liu M, Yan M, et al. Elevating ATP-binding cassette transporter G1 improves re-endothelialization function of endothelial progenitor cells via Lyn/Akt/eNOS in diabetic mice. FASEB journal : official publication of the Federation of American Societies for Experimental Biology. 2018;32(12):6525-36.
273. Miura S, Fujino M, Matsuo Y, Kawamura A, Tanigawa H, Nishikawa H, et al. High density lipoprotein-induced angiogenesis requires the activation of Ras/MAP kinase in human coronary artery endothelial cells. Arteriosclerosis, thrombosis, and vascular biology. 2003;23(5):802-8.
274. Ware JA, Simons M. Angiogenesis in ischemic heart disease. Nature medicine. 1997;3(2):158-64.
275. Prosser HC, Tan JT, Dunn LL, Patel S, Vanags LZ, Bao S, et al. Multifunctional regulation of angiogenesis by high-density lipoproteins. Cardiovascular research. 2014;101(1):145-54.
276. Tsatralis T, Ridiandries A, Robertson S, Vanags LZ, Lam YT, Tan JT, et al. Reconstituted high-density lipoproteins promote wound repair and blood flow recovery in response to ischemia in aged mice. Lipids in health and disease. 2016;15(1):150.

277. Tan JT, Prosser HC, Dunn LL, Vanags LZ, Ridiandries A, Tsatralis T, et al. High-Density Lipoproteins Rescue Diabetes-Impaired Angiogenesis via Scavenger Receptor Class B Type I. Diabetes. 2016;65(10):3091-103.
278. Pajkrt D, Lerch PG, van der Poll T, Levi M, Illi M, Doran JE, et al. Differential effects of reconstituted high-density lipoprotein on coagulation, fibrinolysis and platelet activation during human endotoxemia. Thrombosis and haemostasis. 1997;77(2):303-7.
279. Norata GD, Callegari E, Inoue H, Catapano AL. HDL3 induces cyclooxygenase-2 expression and prostacyclin release in human endothelial cells via a p38 MAPK/CRE-dependent pathway: effects on COX-2/PGI-synthase coupling. Arteriosclerosis, thrombosis, and vascular biology. 2004;24(5):871-7.
280. Vane JR, Botting RM. Pharmacodynamic profile of prostacyclin. The American journal of cardiology. 1995;75(3):3A-10A.
281. Pomerantz KB, Fleisher LN, Tall AR, Cannon PJ. Enrichment of endothelial cell arachidonate by lipid transfer from high density lipoproteins: relationship to prostaglandin I2 synthesis. Journal of lipid research. 1985;26(10):1269-76.
282. Liu D, Ji L, Tong X, Pan B, Han JY, Huang Y, et al. Human apolipoprotein A-I induces cyclooxygenase-2 expression and prostaglandin I-2 release in endothelial cells through ATP-binding cassette transporter A1. American journal of physiology Cell physiology. 2011;301(3):C739-48.
283. Zhang QH, Zu XY, Cao RX, Liu JH, Mo ZC, Zeng Y, et al. An involvement of SR-B1 mediated PI3K-Akt-eNOS signaling in HDL-induced cyclooxygenase 2 expression and prostacyclin production in endothelial cells. Biochemical and biophysical research communications. 2012;420(1):17-23.
284. Holy EW, Besler C, Reiner MF, Camici GG, Manz J, Beer JH, et al. High-density lipoprotein from patients with coronary heart disease loses anti-thrombotic effects on endothelial cells: impact on arterial thrombus formation. Thrombosis and haemostasis. 2014;112(5):1024-35.
285. Viswambharan H, Ming XF, Zhu S, Hubsch A, Lerch P, Vergeres G, et al. Reconstituted high-density lipoprotein inhibits thrombin-induced endothelial tissue factor expression through inhibition of RhoA and stimulation of phosphatidylinositol 3-kinase but not Akt/endothelial nitric oxide synthase. Circulation research. 2004;94(7):918-25.
286. Ossoli A, Remaley AT, Vaisman B, Calabresi L, Gomaraschi M. Plasma-derived and synthetic high-density lipoprotein inhibit tissue factor in endothelial cells and monocytes. The Biochemical journal. 2016;473(2):211-9.
287. Chung DW, Chen J, Ling M, Fu X, Blevins T, Parsons S, et al. High-density lipoprotein modulates thrombosis by preventing von Willebrand factor self-association and subsequent platelet adhesion. Blood. 2016;127(5):637-45.
288. Karlsson H, Kontush A, James RW. Functionality of HDL: antioxidation and detoxifying effects. Handbook of experimental pharmacology. 2015;224:207-28.
289. Kontush A, Chapman MJ. Antiatherogenic function of HDL particle subpopulations: focus on antioxidative activities. Current opinion in lipidology. 2010;21(4):312-8.
290. Christison JK, Rye KA, Stocker R. Exchange of oxidized cholesteryl linoleate between LDL and HDL mediated by cholesteryl ester transfer protein. Journal of lipid research. 1995;36(9):2017-26.
291. Navab M, Hama SY, Cooke CJ, Anantharamaiah GM, Chaddha M, Jin L, et al. Normal high density lipoprotein inhibits three steps in the formation of mildly oxidized low density lipoprotein: step 1. Journal of lipid research. 2000;41(9):1481-94.
292. Garner B, Waldeck AR, Witting PK, Rye KA, Stocker R. Oxidation of high density lipoproteins. II. Evidence for direct reduction of lipid hydroperoxides by methionine residues of apolipoproteins AI and AII. The Journal of biological chemistry. 1998;273(11):6088-95.
293. Zerrad-Saadi A, Therond P, Chantepie S, Couturier M, Rye KA, Chapman MJ, et al. HDL3-mediated inactivation of LDL-associated phospholipid hydroperoxides is determined by the redox status of apolipoprotein A-I and HDL particle surface lipid rigidity: relevance to inflammation and atherogenesis. Arteriosclerosis, thrombosis, and vascular biology. 2009;29(12):2169-75.

294. Riwanto M, Rohrer L, von Eckardstein A, Landmesser U. Dysfunctional HDL: from structure-function-relationships to biomarkers. Handbook of experimental pharmacology. 2015;224:337-66.
295. Davidson WS, Silva RA, Chantepie S, Lagor WR, Chapman MJ, Kontush A. Proteomic analysis of defined HDL subpopulations reveals particle-specific protein clusters: relevance to antioxidative function. Arteriosclerosis, thrombosis, and vascular biology. 2009;29(6):870-6.
296. Shih DM, Gu L, Xia YR, Navab M, Li WF, Hama S, et al. Mice lacking serum paraoxonase are susceptible to organophosphate toxicity and atherosclerosis. Nature. 1998;394(6690):284-7.
297. Garcia-Heredia A, Marsillach J, Rull A, Triguero I, Fort I, Mackness B, et al. Paraoxonase-1 inhibits oxidized low-density lipoprotein-induced metabolic alterations and apoptosis in endothelial cells: a nondirected metabolomic study. Mediators of inflammation. 2013;2013:156053.
298. Catapano AL, Pirillo A, Bonacina F, Norata GD. HDL in innate and adaptive immunity. Cardiovascular research. 2014;103(3):372-83.
299. Murphy AJ, Woollard KJ, Hoang A, Mukhamedova N, Stirzaker RA, McCormick SP, et al. High-density lipoprotein reduces the human monocyte inflammatory response. Arteriosclerosis, thrombosis, and vascular biology. 2008;28(11):2071-7.
300. Murphy AJ, Woollard KJ, Suhartoyo A, Stirzaker RA, Shaw J, Sviridov D, et al. Neutrophil activation is attenuated by high-density lipoprotein and apolipoprotein A-I in in vitro and in vivo models of inflammation. Arteriosclerosis, thrombosis, and vascular biology. 2011;31(6):1333-41.
301. Liu G, Yang H. Modulation of macrophage activation and programming in immunity. Journal of cellular physiology. 2013;228(3):502-12.
302. Feig JE, Rong JX, Shamir R, Sanson M, Vengrenyuk Y, Liu J, et al. HDL promotes rapid atherosclerosis regression in mice and alters inflammatory properties of plaque monocyte-derived cells. Proceedings of the National Academy of Sciences of the United States of America. 2011;108(17):7166-71.
303. Suzuki M, Pritchard DK, Becker L, Hoofnagle AN, Tanimura N, Bammler TK, et al. High-density lipoprotein suppresses the type I interferon response, a family of potent antiviral immunoregulators, in macrophages challenged with lipopolysaccharide. Circulation. 2010;122(19):1919-27.
304. Medzhitov R, Horng T. Transcriptional control of the inflammatory response. Nature reviews Immunology. 2009;9(10):692-703.
305. De Nardo D, Labzin LI, Kono H, Seki R, Schmidt SV, Beyer M, et al. High-density lipoprotein mediates anti-inflammatory reprogramming of macrophages via the transcriptional regulator ATF3. Nature immunology. 2014;15(2):152-60.
306. van der Vorst EPC, Theodorou K, Wu Y, Hoeksema MA, Goossens P, Bursill CA, et al. High-Density Lipoproteins Exert Pro-inflammatory Effects on Macrophages via Passive Cholesterol Depletion and PKC-NF-kappaB/STAT1-IRF1 Signaling. Cell metabolism. 2017;25(1):197-207.
307. Duewell P, Kono H, Rayner KJ, Sirois CM, Vladimer G, Bauernfeind FG, et al. NLRP3 inflammasomes are required for atherogenesis and activated by cholesterol crystals. Nature. 2010;464(7293):1357-61.
308. Li WL, Hua LG, Qu P, Yan WH, Ming C, Jun YD, et al. NLRP3 inflammasome: a novel link between lipoproteins and atherosclerosis. Archives of medical science : AMS. 2016;12(5):950-8.
309. Thacker SG, Zarzour A, Chen Y, Alcicek MS, Freeman LA, Sviridov DO, et al. High-density lipoprotein reduces inflammation from cholesterol crystals by inhibiting inflammasome activation. Immunology. 2016;149(3):306-19.
310. Spillmann F, De Geest B, Muthuramu I, Amin R, Miteva K, Pieske B, et al. Apolipoprotein A-I gene transfer exerts immunomodulatory effects and reduces vascular inflammation and fibrosis in ob/ob mice. Journal of inflammation. 2016;13:25.
311. Westerterp M, Fotakis P, Ouimet M, Bochem AE, Zhang H, Molusky MM, et al. Cholesterol Efflux Pathways Suppress Inflammasome Activation, NETosis, and Atherogenesis. Circulation. 2018;138(9):898-912.
312. Haghikia A, Landmesser U. High-Density Lipoproteins: Effects on Vascular Function and Role in the Immune Response. Cardiology clinics. 2018;36(2):317-27.

313. Sorci-Thomas MG, Thomas MJ. Microdomains, Inflammation, and Atherosclerosis. Circulation research. 2016;118(4):679-91.
314. Wang SH, Yuan SG, Peng DQ, Zhao SP. HDL and ApoA-I inhibit antigen presentation-mediated T cell activation by disrupting lipid rafts in antigen presenting cells. Atherosclerosis. 2012;225(1):105-14.
315. Tiniakou I, Drakos E, Sinatkas V, Van Eck M, Zannis VI, Boumpas D, et al. High-density lipoprotein attenuates Th1 and th17 autoimmune responses by modulating dendritic cell maturation and function. Journal of immunology. 2015;194(10):4676-87.
316. Bonacina F, Coe D, Wang G, Longhi MP, Baragetti A, Moregola A, et al. Myeloid apolipoprotein E controls dendritic cell antigen presentation and T cell activation. Nature communications. 2018;9(1):3083.
317. Besler C, Heinrich K, Rohrer L, Doerries C, Riwanto M, Shih DM, et al. Mechanisms underlying adverse effects of HDL on eNOS-activating pathways in patients with coronary artery disease. The Journal of clinical investigation. 2011;121(7):2693-708.
318. Hafiane A, Jabor B, Ruel I, Ling J, Genest J. High-density lipoprotein mediated cellular cholesterol efflux in acute coronary syndromes. The American journal of cardiology. 2014;113(2):249-55.
319. Navab M, Hama SY, Anantharamaiah GM, Hassan K, Hough GP, Watson AD, et al. Normal high density lipoprotein inhibits three steps in the formation of mildly oxidized low density lipoprotein: steps 2 and 3. Journal of lipid research. 2000;41(9):1495-508.
320. Kim JB, Hama S, Hough G, Navab M, Fogelman AM, Maclellan WR, et al. Heart failure is associated with impaired anti-inflammatory and antioxidant properties of high-density lipoproteins. The American journal of cardiology. 2013;112(11):1770-7.
321. Patel PJ, Khera AV, Wilensky RL, Rader DJ. Anti-oxidative and cholesterol efflux capacities of high-density lipoprotein are reduced in ischaemic cardiomyopathy. European journal of heart failure. 2013;15(11):1215-9.
322. Ortiz-Munoz G, Couret D, Lapergue B, Bruckert E, Meseguer E, Amarenco P, et al. Dysfunctional HDL in acute stroke. Atherosclerosis. 2016;253:75-80.
323. Srivastava RAK. Dysfunctional HDL in diabetes mellitus and its role in the pathogenesis of cardiovascular disease. Molecular and cellular biochemistry. 2018;440(1-2):167-87.
324. Kaseda R, Jabs K, Hunley TE, Jones D, Bian A, Allen RM, et al. Dysfunctional high-density lipoproteins in children with chronic kidney disease. Metabolism: clinical and experimental. 2015;64(2):263-73.
325. Vaziri ND. HDL abnormalities in nephrotic syndrome and chronic kidney disease. Nature reviews Nephrology. 2016;12(1):37-47.
326. Ronda N, Favari E, Borghi MO, Ingegnoli F, Gerosa M, Chighizola C, et al. Impaired serum cholesterol efflux capacity in rheumatoid arthritis and systemic lupus erythematosus. Annals of the rheumatic diseases. 2014;73(3):609-15.
327. Ganjali S, Momtazi AA, Banach M, Kovanen PT, Stein EA, Sahebkar A. HDL abnormalities in familial hypercholesterolemia: Focus on biological functions. Progress in lipid research. 2017;67:16-26.
328. Bellanger N, Orsoni A, Julia Z, Fournier N, Frisdal E, Duchene E, et al. Atheroprotective reverse cholesterol transport pathway is defective in familial hypercholesterolemia. Arteriosclerosis, thrombosis, and vascular biology. 2011;31(7):1675-81.
329. Connelly MA, Shalaurova I, Otvos JD. High-density lipoprotein and inflammation in cardiovascular disease. Translational research : the journal of laboratory and clinical medicine. 2016;173:7-18.
330. Annema W, von Eckardstein A. Dysfunctional high-density lipoproteins in coronary heart disease: implications for diagnostics and therapy. Translational research : the journal of laboratory and clinical medicine. 2016;173:30-57.

331. Van Lenten BJ, Hama SY, de Beer FC, Stafforini DM, McIntyre TM, Prescott SM, et al. Anti-inflammatory HDL becomes pro-inflammatory during the acute phase response. Loss of protective effect of HDL against LDL oxidation in aortic wall cell cocultures. The Journal of clinical investigation. 1995;96(6):2758-67.
332. Rached F, Lhomme M, Camont L, Gomes F, Dauteuille C, Robillard P, et al. Defective functionality of small, dense HDL3 subpopulations in ST segment elevation myocardial infarction: Relevance of enrichment in lysophosphatidylcholine, phosphatidic acid and serum amyloid A. Biochimica et biophysica acta. 2015;1851(9):1254-61.
333. Alwaili K, Bailey D, Awan Z, Bailey SD, Ruel I, Hafiane A, et al. The HDL proteome in acute coronary syndromes shifts to an inflammatory profile. Biochimica et biophysica acta. 2012;1821(3):405-15.
334. Rosenson RS, Brewer HB, Jr., Ansell BJ, Barter P, Chapman MJ, Heinecke JW, et al. Dysfunctional HDL and atherosclerotic cardiovascular disease. Nature reviews Cardiology. 2016;13(1):48-60.
335. Keul P, Polzin A, Kaiser K, Graler M, Dannenberg L, Daum G, et al. Potent anti-inflammatory properties of HDL in vascular smooth muscle cells mediated by HDL-S1P and their impairment in coronary artery disease due to lower HDL-S1P: a new aspect of HDL dysfunction and its therapy. FASEB journal : official publication of the Federation of American Societies for Experimental Biology. 2019;33(1):1482-95.
336. Shao B, Oda MN, Oram JF, Heinecke JW. Myeloperoxidase: an oxidative pathway for generating dysfunctional high-density lipoprotein. Chemical research in toxicology. 2010;23(3):447-54.
337. Baldus S, Eiserich JP, Mani A, Castro L, Figueroa M, Chumley P, et al. Endothelial transcytosis of myeloperoxidase confers specificity to vascular ECM proteins as targets of tyrosine nitration. The Journal of clinical investigation. 2001;108(12):1759-70.
338. Shao B, Pennathur S, Heinecke JW. Myeloperoxidase targets apolipoprotein A-I, the major high density lipoprotein protein, for site-specific oxidation in human atherosclerotic lesions. The Journal of biological chemistry. 2012;287(9):6375-86.
339. DiDonato JA, Aulak K, Huang Y, Wagner M, Gerstenecker G, Topbas C, et al. Site-specific nitration of apolipoprotein A-I at tyrosine 166 is both abundant within human atherosclerotic plaque and dysfunctional. The Journal of biological chemistry. 2014;289(15):10276-92.
340. Huang Y, DiDonato JA, Levison BS, Schmitt D, Li L, Wu Y, et al. An abundant dysfunctional apolipoprotein A1 in human atheroma. Nature medicine. 2014;20(2):193-203.
341. Zheng L, Settle M, Brubaker G, Schmitt D, Hazen SL, Smith JD, et al. Localization of nitration and chlorination sites on apolipoprotein A-I catalyzed by myeloperoxidase in human atheroma and associated oxidative impairment in ABCA1-dependent cholesterol efflux from macrophages. The Journal of biological chemistry. 2005;280(1):38-47.
342. Hewing B, Parathath S, Barrett T, Chung WK, Astudillo YM, Hamada T, et al. Effects of native and myeloperoxidase-modified apolipoprotein a-I on reverse cholesterol transport and atherosclerosis in mice. Arteriosclerosis, thrombosis, and vascular biology. 2014;34(4):779-89.
343. Baigent C, Keech A, Kearney PM, Blackwell L, Buck G, Pollicino C, et al. Efficacy and safety of cholesterol-lowering treatment: prospective meta-analysis of data from 90,056 participants in 14 randomised trials of statins. Lancet. 2005;366(9493):1267-78.
344. Cholesterol Treatment Trialists C, Mihaylova B, Emberson J, Blackwell L, Keech A, Simes J, et al. The effects of lowering LDL cholesterol with statin therapy in people at low risk of vascular disease: meta-analysis of individual data from 27 randomised trials. Lancet. 2012;380(9841):581-90.
345. Sampson UK, Fazio S, Linton MF. Residual cardiovascular risk despite optimal LDL cholesterol reduction with statins: the evidence, etiology, and therapeutic challenges. Current atherosclerosis reports. 2012;14(1):1-10.

346. Gomaraschi M, Adorni MP, Banach M, Bernini F, Franceschini G, Calabresi L. Effects of established hypolipidemic drugs on HDL concentration, subclass distribution, and function. Handbook of experimental pharmacology. 2015;224:593-615.
347. Talbot D, Delaney JAC, Sandfort V, Herrington DM, McClelland RL. Importance of the lipid-related pathways in the association between statins, mortality, and cardiovascular disease risk: The Multi-Ethnic Study of Atherosclerosis. Pharmacoepidemiology and drug safety. 2018;27(4):365-72.
348. Group AS, Ginsberg HN, Elam MB, Lovato LC, Crouse JR, 3rd, Leiter LA, et al. Effects of combination lipid therapy in type 2 diabetes mellitus. The New England journal of medicine. 2010;362(17):1563-74.
349. Investigators A-H, Boden WE, Probstfield JL, Anderson T, Chaitman BR, Desvignes-Nickens P, et al. Niacin in patients with low HDL cholesterol levels receiving intensive statin therapy. The New England journal of medicine. 2011;365(24):2255-67.
350. Balder JW, Staels B, Kuivenhoven JA. Pharmacological interventions in human HDL metabolism. Current opinion in lipidology. 2013;24(6):500-9.
351. Remaley AT, Norata GD, Catapano AL. Novel concepts in HDL pharmacology. Cardiovascular research. 2014;103(3):423-8.
352. Colin S, Chinetti-Gbaguidi G, Kuivenhoven JA, Staels B. Emerging small molecule drugs. Handbook of experimental pharmacology. 2015;224:617-30.
353. Luscher TF, Landmesser U, von Eckardstein A, Fogelman AM. High-density lipoprotein: vascular protective effects, dysfunction, and potential as therapeutic target. Circulation research. 2014;114(1):171-82.
354. Sposito AC, Carmo HR, Barreto J, Sun L, Carvalho LSF, Feinstein SB, et al. HDL-Targeted Therapies During Myocardial Infarction. Cardiovascular drugs and therapy. 2019;33(3):371-81.
355. Barter PJ, Caulfield M, Eriksson M, Grundy SM, Kastelein JJ, Komajda M, et al. Effects of torcetrapib in patients at high risk for coronary events. The New England journal of medicine. 2007;357(21):2109-22.
356. Frikke-Schmidt R, Nordestgaard BG, Stene MC, Sethi AA, Remaley AT, Schnohr P, et al. Association of loss-of-function mutations in the ABCA1 gene with high-density lipoprotein cholesterol levels and risk of ischemic heart disease. Jama. 2008;299(21):2524-32.
357. Haase CL, Tybjaerg-Hansen A, Qayyum AA, Schou J, Nordestgaard BG, Frikke-Schmidt R. LCAT, HDL cholesterol and ischemic cardiovascular disease: a Mendelian randomization study of HDL cholesterol in 54,500 individuals. The Journal of clinical endocrinology and metabolism. 2012;97(2):E248-56.
358. Voight BF, Peloso GM, Orho-Melander M, Frikke-Schmidt R, Barbalic M, Jensen MK, et al. Plasma HDL cholesterol and risk of myocardial infarction: a mendelian randomisation study. Lancet. 2012;380(9841):572-80.
359. Zanoni P, Khetarpal SA, Larach DB, Hancock-Cerutti WF, Millar JS, Cuchel M, et al. Rare variant in scavenger receptor BI raises HDL cholesterol and increases risk of coronary heart disease. Science. 2016;351(6278):1166-71.
360. Madsen CM, Varbo A, Nordestgaard BG. Extreme high high-density lipoprotein cholesterol is paradoxically associated with high mortality in men and women: two prospective cohort studies. European heart journal. 2017;38(32):2478-86.
361. Nissen SE, Tsunoda T, Tuzcu EM, Schoenhagen P, Cooper CJ, Yasin M, et al. Effect of recombinant ApoA-I Milano on coronary atherosclerosis in patients with acute coronary syndromes: a randomized controlled trial. Jama. 2003;290(17):2292-300.
362. Nicholls SJ, Puri R, Ballantyne CM, Jukema JW, Kastelein JJP, Koenig W, et al. Effect of Infusion of High-Density Lipoprotein Mimetic Containing Recombinant Apolipoprotein A-I Milano on Coronary Disease in Patients With an Acute Coronary Syndrome in the MILANO-PILOT Trial: A Randomized Clinical Trial. JAMA cardiology. 2018;3(9):806-14.
363. Stoekenbroek RM, Stroes ES, Hovingh GK. ApoA-I mimetics. Handbook of experimental pharmacology. 2015;224:631-48.

364. Kootte RS, Smits LP, van der Valk FM, Dasseux JL, Keyserling CH, Barbaras R, et al. Effect of open-label infusion of an apoA-I-containing particle (CER-001) on RCT and artery wall thickness in patients with FHA. Journal of lipid research. 2015;56(3):703-12.
365. Hovingh GK, Smits LP, Stefanutti C, Soran H, Kwok S, de Graaf J, et al. The effect of an apolipoprotein A-I-containing high-density lipoprotein-mimetic particle (CER-001) on carotid artery wall thickness in patients with homozygous familial hypercholesterolemia: The Modifying Orphan Disease Evaluation (MODE) study. American heart journal. 2015;169(5):736-42 e1.
366. Gibson CM, Kerneis M, Yee MK, Daaboul Y, Korjian S, Mehr AP, et al. The CSL112-2001 trial: Safety and tolerability of multiple doses of CSL112 (apolipoprotein A-I [human]), an intravenous formulation of plasma-derived apolipoprotein A-I, among subjects with moderate renal impairment after acute myocardial infarction. American heart journal. 2019;208:81-90.
367. Wirka RC, Pjanic M, Quertermous T. Advances in Transcriptomics: Investigating Cardiovascular Disease at Unprecedented Resolution. Circulation research. 2018;122(9):1200-20.
368. Pedrotty DM, Morley MP, Cappola TP. Transcriptomic biomarkers of cardiovascular disease. Progress in cardiovascular diseases. 2012;55(1):64-9.
369. Fotakis P. Exploring the pathway of biogenesis of HDL by gene mutation. PhD Thesis, School of Medicine, University of Crete. 2014.
370. Oike Y, Yasunaga K, Suda T. Angiopoietin-related/angiopoietin-like proteins regulate angiogenesis. International journal of hematology. 2004;80(1):21-8.
371. Dijk W, Kersten S. Regulation of lipid metabolism by angiopoietin-like proteins. Current opinion in lipidology. 2016;27(3):249-56.
372. Zhu H, Li J, Qin W, Yang Y, He X, Wan D, et al. [Cloning of a novel gene, ANGPTL4 and the functional study in angiogenesis]. Zhonghua yi xue za zhi. 2002;82(2):94-9.
373. Grootaert C, Van de Wiele T, Verstraete W, Bracke M, Vanhoecke B. Angiopoietin-like protein 4: health effects, modulating agents and structure-function relationships. Expert review of proteomics. 2012;9(2):181-99.
374. Yin W, Romeo S, Chang S, Grishin NV, Hobbs HH, Cohen JC. Genetic variation in ANGPTL4 provides insights into protein processing and function. The Journal of biological chemistry. 2009;284(19):13213-22.
375. Yau MH, Wang Y, Lam KS, Zhang J, Wu D, Xu A. A highly conserved motif within the NH2-terminal coiled-coil domain of angiopoietin-like protein 4 confers its inhibitory effects on lipoprotein lipase by disrupting the enzyme dimerization. The Journal of biological chemistry. 2009;284(18):11942-52.
376. Lei X, Shi F, Basu D, Huq A, Routhier S, Day R, et al. Proteolytic processing of angiopoietin-like protein 4 by proprotein convertases modulates its inhibitory effects on lipoprotein lipase activity. The Journal of biological chemistry. 2011;286(18):15747-56.
377. Xu A, Lam MC, Chan KW, Wang Y, Zhang J, Hoo RL, et al. Angiopoietin-like protein 4 decreases blood glucose and improves glucose tolerance but induces hyperlipidemia and hepatic steatosis in mice. Proceedings of the National Academy of Sciences of the United States of America. 2005;102(17):6086-91.
378. La Paglia L, Listi A, Caruso S, Amodeo V, Passiglia F, Bazan V, et al. Potential Role of ANGPTL4 in the Cross Talk between Metabolism and Cancer through PPAR Signaling Pathway. PPAR research. 2017;2017:8187235.
379. Goldberg IJ. Lipoprotein lipase and lipolysis: central roles in lipoprotein metabolism and atherogenesis. Journal of lipid research. 1996;37(4):693-707.
380. Koster A, Chao YB, Mosior M, Ford A, Gonzalez-DeWhitt PA, Hale JE, et al. Transgenic angiopoietin-like (angptl)4 overexpression and targeted disruption of angptl4 and angptl3: regulation of triglyceride metabolism. Endocrinology. 2005;146(11):4943-50.
381. Aryal B, Price NL, Suarez Y, Fernandez-Hernando C. ANGPTL4 in Metabolic and Cardiovascular Disease. Trends in molecular medicine. 2019;25(8):723-34.

382. Zhu P, Goh YY, Chin HF, Kersten S, Tan NS. Angiopoietin-like 4: a decade of research. Bioscience reports. 2012;32(3):211-9.
383. Kersten S. New insights into angiopoietin-like proteins in lipid metabolism and cardiovascular disease risk. Current opinion in lipidology. 2019;30(3):205-11.
384. Mysling S, Kristensen KK, Larsson M, Kovrov O, Bensadouen A, Jorgensen TJ, et al. The angiopoietin-like protein ANGPTL4 catalyzes unfolding of the hydrolase domain in lipoprotein lipase and the endothelial membrane protein GPIHBP1 counteracts this unfolding. eLife. 2016;5.
385. Romeo S, Pennacchio LA, Fu Y, Boerwinkle E, Tybjaerg-Hansen A, Hobbs HH, et al. Population-based resequencing of ANGPTL4 uncovers variations that reduce triglycerides and increase HDL. Nature genetics. 2007;39(4):513-6.
386. Helgadottir A, Gretarsdottir S, Thorleifsson G, Hjartarson E, Sigurdsson A, Magnusdottir A, et al. Variants with large effects on blood lipids and the role of cholesterol and triglycerides in coronary disease. Nature genetics. 2016;48(6):634-9.
387. Dewey FE, Gusarova V, O'Dushlaine C, Gottesman O, Trejos J, Hunt C, et al. Inactivating Variants in ANGPTL4 and Risk of Coronary Artery Disease. The New England journal of medicine. 2016;374(12):1123-33.
388. Liu DJ, Peloso GM, Yu H, Butterworth AS, Wang X, Mahajan A, et al. Exome-wide association study of plasma lipids in >300,000 individuals. Nature genetics. 2017;49(12):1758-66.
389. Myocardial Infarction G, Investigators CAEC, Stitziel NO, Stirrups KE, Masca NG, Erdmann J, et al. Coding Variation in ANGPTL4, LPL, and SVEP1 and the Risk of Coronary Disease. The New England journal of medicine. 2016;374(12):1134-44.
390. Lotta LA, Stewart ID, Sharp SJ, Day FR, Burgess S, Luan J, et al. Association of Genetically Enhanced Lipoprotein Lipase-Mediated Lipolysis and Low-Density Lipoprotein Cholesterol-Lowering Alleles With Risk of Coronary Disease and Type 2 Diabetes. JAMA cardiology. 2018;3(10):957-66.
391. Talmud PJ, Smart M, Presswood E, Cooper JA, Nicaud V, Drenos F, et al. ANGPTL4 E40K and T266M: effects on plasma triglyceride and HDL levels, postprandial responses, and CHD risk. Arteriosclerosis, thrombosis, and vascular biology. 2008;28(12):2319-25.
392. Muendlein A, Saely CH, Leiherer A, Fraunberger P, Kinz E, Rein P, et al. Angiopoietin-like protein 4 significantly predicts future cardiovascular events in coronary patients. Atherosclerosis. 2014;237(2):632-8.
393. Lichtenstein L, Mattijssen F, de Wit NJ, Georgiadi A, Hooiveld GJ, van der Meer R, et al. Angptl4 protects against severe proinflammatory effects of saturated fat by inhibiting fatty acid uptake into mesenteric lymph node macrophages. Cell metabolism. 2010;12(6):580-92.
394. Oteng AB, Bhattacharya A, Brodesser S, Qi L, Tan NS, Kersten S. Feeding Angptl4(-/-) mice trans fat promotes foam cell formation in mesenteric lymph nodes without leading to ascites. Journal of lipid research. 2017;58(6):1100-13.
395. Georgiadi A, Wang Y, Stienstra R, Tjeerdema N, Janssen A, Stalenhoef A, et al. Overexpression of angiopoietin-like protein 4 protects against atherosclerosis development. Arteriosclerosis, thrombosis, and vascular biology. 2013;33(7):1529-37.
396. Aryal B, Rotllan N, Araldi E, Ramirez CM, He S, Chousterman BG, et al. ANGPTL4 deficiency in haematopoietic cells promotes monocyte expansion and atherosclerosis progression. Nature communications. 2016;7:12313.
397. Aryal B, Singh AK, Zhang X, Varela L, Rotllan N, Goedeke L, et al. Absence of ANGPTL4 in adipose tissue improves glucose tolerance and attenuates atherogenesis. JCI insight. 2018;3(6).
398. Mandard S, Zandbergen F, van Straten E, Wahli W, Kuipers F, Muller M, et al. The fasting-induced adipose factor/angiopoietin-like protein 4 is physically associated with lipoproteins and governs plasma lipid levels and adiposity. The Journal of biological chemistry. 2006;281(2):934-44.
399. Jin Q, Yu LR, Wang L, Zhang Z, Kasper LH, Lee JE, et al. Distinct roles of GCN5/PCAF-mediated H3K9ac and CBP/p300-mediated H3K18/27ac in nuclear receptor transactivation. The EMBO journal. 2011;30(2):249-62.

400. Mimura I, Nangaku M, Kanki Y, Tsutsumi S, Inoue T, Kohro T, et al. Dynamic change of chromatin conformation in response to hypoxia enhances the expression of GLUT3 (SLC2A3) by cooperative interaction of hypoxia-inducible factor 1 and KDM3A. Molecular and cellular biology. 2012;32(15):3018-32.
401. Inoue T, Kohro T, Tanaka T, Kanki Y, Li G, Poh HM, et al. Cross-enhancement of ANGPTL4 transcription by HIF1 alpha and PPAR beta/delta is the result of the conformational proximity of two response elements. Genome biology. 2014;15(4):R63.
402. Kaddatz K, Adhikary T, Finkernagel F, Meissner W, Muller-Brusselbach S, Muller R. Transcriptional profiling identifies functional interactions of TGF beta and PPAR beta/delta signaling: synergistic induction of ANGPTL4 transcription. The Journal of biological chemistry. 2010;285(38):29469-79.
403. Jaye M, Lynch KJ, Krawiec J, Marchadier D, Maugeais C, Doan K, et al. A novel endothelial-derived lipase that modulates HDL metabolism. Nature genetics. 1999;21(4):424-8.
404. Miller GC, Long CJ, Bojilova ED, Marchadier D, Badellino KO, Blanchard N, et al. Role of N-linked glycosylation in the secretion and activity of endothelial lipase. Journal of lipid research. 2004;45(11):2080-7.
405. Hirata K, Dichek HL, Cioffi JA, Choi SY, Leeper NJ, Quintana L, et al. Cloning of a unique lipase from endothelial cells extends the lipase gene family. The Journal of biological chemistry. 1999;274(20):14170-5.
406. McCoy MG, Sun GS, Marchadier D, Maugeais C, Glick JM, Rader DJ. Characterization of the lipolytic activity of endothelial lipase. Journal of lipid research. 2002;43(6):921-9.
407. Ishida T, Choi S, Kundu RK, Hirata K, Rubin EM, Cooper AD, et al. Endothelial lipase is a major determinant of HDL level. The Journal of clinical investigation. 2003;111(3):347-55.
408. Ma K, Cilingiroglu M, Otvos JD, Ballantyne CM, Marian AJ, Chan L. Endothelial lipase is a major genetic determinant for high-density lipoprotein concentration, structure, and metabolism. Proceedings of the National Academy of Sciences of the United States of America. 2003;100(5):2748-53.
409. Jin W, Millar JS, Broedl U, Glick JM, Rader DJ. Inhibition of endothelial lipase causes increased HDL cholesterol levels in vivo. The Journal of clinical investigation. 2003;111(3):357-62.
410. Broedl UC, Maugeais C, Millar JS, Jin W, Moore RE, Fuki IV, et al. Endothelial lipase promotes the catabolism of ApoB-containing lipoproteins. Circulation research. 2004;94(12):1554-61.
411. Riederer M, Kofeler H, Lechleitner M, Tritscher M, Frank S. Impact of endothelial lipase on cellular lipid composition. Biochimica et biophysica acta. 2012;1821(7):1003-11.
412. Ahmed W, Orasanu G, Nehra V, Asatryan L, Rader DJ, Ziouzenkova O, et al. High-density lipoprotein hydrolysis by endothelial lipase activates PPARalpha: a candidate mechanism for high-density lipoprotein-mediated repression of leukocyte adhesion. Circulation research. 2006;98(4):490-8.
413. Tatematsu S, Francis SA, Natarajan P, Rader DJ, Saghatelian A, Brown JD, et al. Endothelial lipase is a critical determinant of high-density lipoprotein-stimulated sphingosine 1-phosphate-dependent signaling in vascular endothelium. Arteriosclerosis, thrombosis, and vascular biology. 2013;33(8):1788-94.
414. Robert J, Lehner M, Frank S, Perisa D, von Eckardstein A, Rohrer L. Interleukin 6 stimulates endothelial binding and transport of high-density lipoprotein through induction of endothelial lipase. Arteriosclerosis, thrombosis, and vascular biology. 2013;33(12):2699-706.
415. Strauss JG, Zimmermann R, Hrzenjak A, Zhou Y, Kratky D, Levak-Frank S, et al. Endothelial cell-derived lipase mediates uptake and binding of high-density lipoprotein (HDL) particles and the selective uptake of HDL-associated cholesterol esters independent of its enzymic activity. The Biochemical journal. 2002;368(Pt 1):69-79.
416. Fuki IV, Blanchard N, Jin W, Marchadier DH, Millar JS, Glick JM, et al. Endogenously produced endothelial lipase enhances binding and cellular processing of plasma lipoproteins via heparan sulfate proteoglycan-mediated pathway. The Journal of biological chemistry. 2003;278(36):34331-8.

417. Vitali C, Khetarpal SA, Rader DJ. HDL Cholesterol Metabolism and the Risk of CHD: New Insights from Human Genetics. Current cardiology reports. 2017;19(12):132.
418. Ishida T, Choi SY, Kundu RK, Spin J, Yamashita T, Hirata K, et al. Endothelial lipase modulates susceptibility to atherosclerosis in apolipoprotein-E-deficient mice. The Journal of biological chemistry. 2004;279(43):45085-92.
419. Ko KW, Paul A, Ma K, Li L, Chan L. Endothelial lipase modulates HDL but has no effect on atherosclerosis development in apoE-/- and LDLR-/- mice. Journal of lipid research. 2005;46(12):2586-94.
420. Hara T, Ishida T, Kojima Y, Tanaka H, Yasuda T, Shinohara M, et al. Targeted deletion of endothelial lipase increases HDL particles with anti-inflammatory properties both in vitro and in vivo. Journal of lipid research. 2011;52(1):57-67.
421. Wang C, Nishijima K, Kitajima S, Niimi M, Yan H, Chen Y, et al. Increased Hepatic Expression of Endothelial Lipase Inhibits Cholesterol Diet-Induced Hypercholesterolemia and Atherosclerosis in Transgenic Rabbits. Arteriosclerosis, thrombosis, and vascular biology. 2017;37(7):1282-9.
422. Jin W, Sun GS, Marchadier D, Octtaviani E, Glick JM, Rader DJ. Endothelial cells secrete triglyceride lipase and phospholipase activities in response to cytokines as a result of endothelial lipase. Circulation research. 2003;92(6):644-50.
423. Shimokawa Y, Hirata K, Ishida T, Kojima Y, Inoue N, Quertermous T, et al. Increased expression of endothelial lipase in rat models of hypertension. Cardiovascular research. 2005;66(3):594-600.
424. Kempe S, Kestler H, Lasar A, Wirth T. NF-kappaB controls the global pro-inflammatory response in endothelial cells: evidence for the regulation of a pro-atherogenic program. Nucleic acids research. 2005;33(16):5308-19.
425. Jung UJ, Torrejon C, Chang CL, Hamai H, Worgall TS, Deckelbaum RJ. Fatty acids regulate endothelial lipase and inflammatory markers in macrophages and in mouse aorta: a role for PPARgamma. Arteriosclerosis, thrombosis, and vascular biology. 2012;32(12):2929-37.
426. Kivela AM, Dijkstra MH, Heinonen SE, Gurzeler E, Jauhiainen S, Levonen AL, et al. Regulation of endothelial lipase and systemic HDL cholesterol levels by SREBPs and VEGF-A. Atherosclerosis. 2012;225(2):335-40.
427. Georgopoulos S, Kan HY, Reardon-Alulis C, Zannis V. The SP1 sites of the human apoCIII enhancer are essential for the expression of the apoCIII gene and contribute to the hepatic and intestinal expression of the apoA-I gene in transgenic mice. Nucleic acids research. 2000;28(24):4919-29.
428. Chroni A, Duka A, Kan HY, Liu T, Zannis VI. Point mutations in apolipoprotein A-I mimic the phenotype observed in patients with classical lecithin:cholesterol acyltransferase deficiency. Biochemistry. 2005;44(43):14353-66.
429. Anestis A. Diploma Thesis. School of Medicine, University of Crete. 2011.
430. Mosialou I. Regulatory mechanisms underlying transcription of human apolipoprotein genes *in vivo*. PhD Thesis, School of Medicine, University of Crete. 2010.
431. Durocher Y, Perret S, Kamen A. High-level and high-throughput recombinant protein production by transient transfection of suspension-growing human 293-EBNA1 cells. Nucleic acids research. 2002;30(2):E9.
432. Jiang L, He L, Fountoulakis M. Comparison of protein precipitation methods for sample preparation prior to proteomic analysis. Journal of chromatography A. 2004;1023(2):317-20.
433. Dijk W, Kersten S. Regulation of lipoprotein lipase by Angptl4. Trends in endocrinology and metabolism: TEM. 2014;25(3):146-55.
434. Edgell CJ, McDonald CC, Graham JB. Permanent cell line expressing human factor VIII-related antigen established by hybridization. Proceedings of the National Academy of Sciences of the United States of America. 1983;80(12):3734-7.
435. Tzivion G, Dobson M, Ramakrishnan G. FoxO transcription factors; Regulation by AKT and 14-3-3 proteins. Biochimica et biophysica acta. 2011;1813(11):1938-45.

436. Nicholls SJ, Nelson AJ. HDL and cardiovascular disease. Pathology. 2019;51(2):142-7.
437. Xu L, Guo ZN, Yang Y, Xu J, Burchell SR, Tang J, et al. Angiopoietin-like 4: A double-edged sword in atherosclerosis and ischemic stroke? Experimental neurology. 2015;272:61-6.
438. Galaup A, Cazes A, Le Jan S, Philippe J, Connault E, Le Coz E, et al. Angiopoietin-like 4 prevents metastasis through inhibition of vascular permeability and tumor cell motility and invasiveness. Proceedings of the National Academy of Sciences of the United States of America. 2006;103(49):18721-6.
439. Huang RL, Teo Z, Chong HC, Zhu P, Tan MJ, Tan CK, et al. ANGPTL4 modulates vascular junction integrity by integrin signaling and disruption of intercellular VE-cadherin and claudin-5 clusters. Blood. 2011;118(14):3990-4002.
440. Yang X, Cheng Y, Su G. A review of the multifunctionality of angiopoietin-like 4 in eye disease. Bioscience reports. 2018;38(5).
441. Riwanto M, Landmesser U. High density lipoproteins and endothelial functions: mechanistic insights and alterations in cardiovascular disease. Journal of lipid research. 2013;54(12):3227-43.
442. Oellerich MF, Potente M. FOXOs and sirtuins in vascular growth, maintenance, and aging. Circulation research. 2012;110(9):1238-51.
443. Xing YQ, Li A, Yang Y, Li XX, Zhang LN, Guo HC. The regulation of FOXO1 and its role in disease progression. Life sciences. 2018;193:124-31.
444. Puigserver P, Rhee J, Donovan J, Walkey CJ, Yoon JC, Oriente F, et al. Insulin-regulated hepatic gluconeogenesis through FOXO1-PGC-1alpha interaction. Nature. 2003;423(6939):550-5.
445. Chakrabarti P, Kandror KV. FoxO1 controls insulin-dependent adipose triglyceride lipase (ATGL) expression and lipolysis in adipocytes. The Journal of biological chemistry. 2009;284(20):13296-300.
446. Wilhelm K, Happel K, Eelen G, Schoors S, Oellerich MF, Lim R, et al. FOXO1 couples metabolic activity and growth state in the vascular endothelium. Nature. 2016;529(7585):216-20.
447. Kuo T, Chen TC, Yan S, Foo F, Ching C, McQueen A, et al. Repression of glucocorticoid-stimulated angiopoietin-like 4 gene transcription by insulin. Journal of lipid research. 2014;55(5):919-28.
448. Mandard S, Zandbergen F, Tan NS, Escher P, Patsouris D, Koenig W, et al. The direct peroxisome proliferator-activated receptor target fasting-induced adipose factor (FIAF/PGAR/ANGPTL4) is present in blood plasma as a truncated protein that is increased by fenofibrate treatment. The Journal of biological chemistry. 2004;279(33):34411-20.
449. Fan W, Imamura T, Sonoda N, Sears DD, Patsouris D, Kim JJ, et al. FOXO1 transrepresses peroxisome proliferator-activated receptor gamma transactivation, coordinating an insulin-induced feed-forward response in adipocytes. The Journal of biological chemistry. 2009;284(18):12188-97.
450. Langlet F, Haeusler RA, Linden D, Ericson E, Norris T, Johansson A, et al. Selective Inhibition of FOXO1 Activator/Repressor Balance Modulates Hepatic Glucose Handling. Cell. 2017;171(4):824-35 e18.
451. Hirota K, Sakamaki J, Ishida J, Shimamoto Y, Nishihara S, Kodama N, et al. A combination of HNF-4 and Foxo1 is required for reciprocal transcriptional regulation of glucokinase and glucose-6-phosphatase genes in response to fasting and feeding. The Journal of biological chemistry. 2008;283(47):32432-41.
452. Tsuchiya K, Ogawa Y. Forkhead box class O family member proteins: The biology and pathophysiological roles in diabetes. Journal of diabetes investigation. 2017;8(6):726-34.
453. Potente M, Urbich C, Sasaki K, Hofmann WK, Heeschen C, Aicher A, et al. Involvement of Foxo transcription factors in angiogenesis and postnatal neovascularization. The Journal of clinical investigation. 2005;115(9):2382-92.
454. Tanaka J, Qiang L, Banks AS, Welch CL, Matsumoto M, Kitamura T, et al. Foxo1 links hyperglycemia to LDL oxidation and endothelial nitric oxide synthase dysfunction in vascular endothelial cells. Diabetes. 2009;58(10):2344-54.

455. Heeringa P, van Goor H, Moshage H, Klok PA, Huitema MG, de Jager A, et al. Expression of iNOS, eNOS, and peroxynitrite-modified proteins in experimental anti-myeloperoxidase associated crescentic glomerulonephritis. Kidney international. 1998;53(2):382-93.
456. Tsuchiya K, Tanaka J, Shuiqing Y, Welch CL, DePinho RA, Tabas I, et al. FoxOs integrate pleiotropic actions of insulin in vascular endothelium to protect mice from atherosclerosis. Cell metabolism. 2012;15(3):372-81.
457. Yu JE, Han SY, Wolfson B, Zhou Q. The role of endothelial lipase in lipid metabolism, inflammation, and cancer. Histology and histopathology. 2018;33(1):1-10.
458. Yasuda T, Ishida T, Rader DJ. Update on the role of endothelial lipase in high-density lipoprotein metabolism, reverse cholesterol transport, and atherosclerosis. Circulation journal : official journal of the Japanese Circulation Society. 2010;74(11):2263-70.
459. Nijstad N, Wiersma H, Gautier T, van der Giet M, Maugeais C, Tietge UJ. Scavenger receptor BI-mediated selective uptake is required for the remodeling of high density lipoprotein by endothelial lipase. The Journal of biological chemistry. 2009;284(10):6093-100.
460. Maugeais C, Tietge UJ, Broedl UC, Marchadier D, Cain W, McCoy MG, et al. Dose-dependent acceleration of high-density lipoprotein catabolism by endothelial lipase. Circulation. 2003;108(17):2121-6.
461. Kamei Y, Mizukami J, Miura S, Suzuki M, Takahashi N, Kawada T, et al. A forkhead transcription factor FKHR up-regulates lipoprotein lipase expression in skeletal muscle. FEBS letters. 2003;536(1-3):232-6.
462. Kojma Y, Hirata K, Ishida T, Shimokawa Y, Inoue N, Kawashima S, et al. Endothelial lipase modulates monocyte adhesion to the vessel wall. A potential role in inflammation. The Journal of biological chemistry. 2004;279(52):54032-8.
463. Azumi H, Hirata K, Ishida T, Kojima Y, Rikitake Y, Takeuchi S, et al. Immunohistochemical localization of endothelial cell-derived lipase in atherosclerotic human coronary arteries. Cardiovascular research. 2003;58(3):647-54.
464. Smith JA. Update on ankylosing spondylitis: current concepts in pathogenesis. Current allergy and asthma reports. 2015;15(1):489.
465. Han C, Robinson DW, Jr., Hackett MV, Paramore LC, Fraeman KH, Bala MV. Cardiovascular disease and risk factors in patients with rheumatoid arthritis, psoriatic arthritis, and ankylosing spondylitis. The Journal of rheumatology. 2006;33(11):2167-72.
466. Szabo SM, Levy AR, Rao SR, Kirbach SE, Lacaille D, Cifaldi M, et al. Increased risk of cardiovascular and cerebrovascular diseases in individuals with ankylosing spondylitis: a population-based study. Arthritis and rheumatism. 2011;63(11):3294-304.
467. Gkolfinopoulou C, Stratikos E, Theofilatos D, Kardassis D, Voulgari PV, Drosos AA, et al. Impaired Antiatherogenic Functions of High-density Lipoprotein in Patients with Ankylosing Spondylitis. The Journal of rheumatology. 2015;42(9):1652-60.
468. Shoenfeld Y, Gerli R, Doria A, Matsuura E, Cerinic MM, Ronda N, et al. Accelerated atherosclerosis in autoimmune rheumatic diseases. Circulation. 2005;112(21):3337-47.
469. McMahon M, Grossman J, FitzGerald J, Dahlin-Lee E, Wallace DJ, Thong BY, et al. Proinflammatory high-density lipoprotein as a biomarker for atherosclerosis in patients with systemic lupus erythematosus and rheumatoid arthritis. Arthritis and rheumatism. 2006;54(8):2541-9.
470. Charles-Schoeman C, Watanabe J, Lee YY, Furst DE, Amjadi S, Elashoff D, et al. Abnormal function of high-density lipoprotein is associated with poor disease control and an altered protein cargo in rheumatoid arthritis. Arthritis and rheumatism. 2009;60(10):2870-9.
471. Charles-Schoeman C, Lee YY, Grijalva V, Amjadi S, FitzGerald J, Ranganath VK, et al. Cholesterol efflux by high density lipoproteins is impaired in patients with active rheumatoid arthritis. Annals of the rheumatic diseases. 2012;71(7):1157-62.
472. Haque S, Mirjafari H, Bruce IN. Atherosclerosis in rheumatoid arthritis and systemic lupus erythematosus. Current opinion in lipidology. 2008;19(4):338-43.

473. van Eijk IC, de Vries MK, Levels JH, Peters MJ, Huizer EE, Dijkmans BA, et al. Improvement of lipid profile is accompanied by atheroprotective alterations in high-density lipoprotein composition upon tumor necrosis factor blockade: a prospective cohort study in ankylosing spondylitis. Arthritis and rheumatism. 2009;60(5):1324-30.
474. Cece H, Yazgan P, Karakas E, Karakas O, Demirkol A, Toru I, et al. Carotid intima-media thickness and paraoxonase activity in patients with ankylosing spondylitis. Clinical and investigative medicine Medecine clinique et experimentale. 2011;34(4):E225.
475. Olama SM, Elarman MM. Evaluation of paraoxonase and arylesterase activities in Egyptian patients with ankylosing spondylitis. Rheumatology international. 2013;33(6):1487-94.
476. Kingwell BA, Chapman MJ, Kontush A, Miller NE. HDL-targeted therapies: progress, failures and future. Nature reviews Drug discovery. 2014;13(6):445-64.
477. Thymiakou E, Zannis VI, Kardassis D. Physical and functional interactions between liver X receptor/retinoid X receptor and Sp1 modulate the transcriptional induction of the human ATP binding cassette transporter A1 gene by oxysterols and retinoids. Biochemistry. 2007;46(41):11473-83.
478. Wang B, Tontonoz P. Liver X receptors in lipid signalling and membrane homeostasis. Nature reviews Endocrinology. 2018;14(8):452-63.
479. Sumi K, Tanaka T, Uchida A, Magoori K, Urashima Y, Ohashi R, et al. Cooperative interaction between hepatocyte nuclear factor 4 alpha and GATA transcription factors regulates ATP-binding cassette sterol transporters ABCG5 and ABCG8. Molecular and cellular biology. 2007;27(12):4248-60.
480. Sasaki S, Urabe M, Maeda T, Suzuki J, Irie R, Suzuki M, et al. Induction of Hepatic Metabolic Functions by a Novel Variant of Hepatocyte Nuclear Factor 4gamma. Molecular and cellular biology. 2018;38(24).
481. Taraviras S, Mantamadiotis T, Dong-Si T, Mincheva A, Lichter P, Drewes T, et al. Primary structure, chromosomal mapping, expression and transcriptional activity of murine hepatocyte nuclear factor 4gamma. Biochimica et biophysica acta. 2000;1490(1-2):21-32.
482. Chawla A, Boisvert WA, Lee CH, Laffitte BA, Barak Y, Joseph SB, et al. A PPAR gamma-LXR-ABCA1 pathway in macrophages is involved in cholesterol efflux and atherogenesis. Molecular cell. 2001;7(1):161-71.
483. Chinetti G, Lestavel S, Bocher V, Remaley AT, Neve B, Torra IP, et al. PPAR-alpha and PPAR-gamma activators induce cholesterol removal from human macrophage foam cells through stimulation of the ABCA1 pathway. Nature medicine. 2001;7(1):53-8.
484. Hatzis P, Talianidis I. Regulatory mechanisms controlling human hepatocyte nuclear factor 4alpha gene expression. Molecular and cellular biology. 2001;21(21):7320-30.
485. Karagianni P, Talianidis I. Transcription factor networks regulating hepatic fatty acid metabolism. Biochimica et biophysica acta. 2015;1851(1):2-8.
486. Martinez-Jimenez CP, Kyrmizi I, Cardot P, Gonzalez FJ, Talianidis I. Hepatocyte nuclear factor 4alpha coordinates a transcription factor network regulating hepatic fatty acid metabolism. Molecular and cellular biology. 2010;30(3):565-77.
487. Pineda Torra I, Jamshidi Y, Flavell DM, Fruchart JC, Staels B. Characterization of the human PPARalpha promoter: identification of a functional nuclear receptor response element. Molecular endocrinology. 2002;16(5):1013-28.
488. Subedi BH, Joshi PH, Jones SR, Martin SS, Blaha MJ, Michos ED. Current guidelines for high-density lipoprotein cholesterol in therapy and future directions. Vascular health and risk management. 2014;10:205-16.
489. Hsieh J, Koseki M, Molusky MM, Yakushiji E, Ichi I, Westerterp M, et al. TTC39B deficiency stabilizes LXR reducing both atherosclerosis and steatohepatitis. Nature. 2016;535(7611):303-7.
490. Drosatos K, Sanoudou D, Kypreos KE, Kardassis D, Zannis VI. A dominant negative form of the transcription factor c-Jun affects genes that have opposing effects on lipid homeostasis in mice. The Journal of biological chemistry. 2007;282(27):19556-64.

491. Iliopoulos D, Drosatos K, Hiyama Y, Goldberg IJ, Zannis VI. MicroRNA-370 controls the expression of microRNA-122 and Cpt1alpha and affects lipid metabolism. Journal of lipid research. 2010;51(6):1513-23.
492. Teng GG, Wang WH, Dai Y, Wang SJ, Chu YX, Li J. Let-7b is involved in the inflammation and immune responses associated with Helicobacter pylori infection by targeting Toll-like receptor 4. PloS one. 2013;8(2):e56709.
493. Marais AD. Apolipoprotein E in lipoprotein metabolism, health and cardiovascular disease. Pathology. 2019;51(2):165-76.
494. Liehn EA, Ponomariov V, Diaconu R, Streata I, Ioana M, Crespo-Avilan GE, et al. Apolipoprotein E in Cardiovascular Diseases: Novel Aspects of an Old-fashioned Enigma. Archives of medical research. 2018;49(8):522-9.
495. Rosenfeld ME, Polinsky P, Virmani R, Kauser K, Rubanyi G, Schwartz SM. Advanced atherosclerotic lesions in the innominate artery of the ApoE knockout mouse. Arteriosclerosis, thrombosis, and vascular biology. 2000;20(12):2587-92.
496. Huang Y, Liu XQ, Rall SC, Jr., Taylor JM, von Eckardstein A, Assmann G, et al. Overexpression and accumulation of apolipoprotein E as a cause of hypertriglyceridemia. The Journal of biological chemistry. 1998;273(41):26388-93.
497. Rasmussen KL, Tybjaerg-Hansen A, Nordestgaard BG, Frikke-Schmidt R. Plasma levels of apolipoprotein E and risk of dementia in the general population. Annals of neurology. 2015;77(2):301-11.
498. Wolters FJ, Koudstaal PJ, Hofman A, van Duijn CM, Ikram MA. Serum apolipoprotein E is associated with long-term risk of Alzheimer's disease: The Rotterdam Study. Neuroscience letters. 2016;617:139-42.
499. Rasmussen KL, Tybjaerg-Hansen A, Nordestgaard BG, Frikke-Schmidt R. Plasma levels of apolipoprotein E and risk of ischemic heart disease in the general population. Atherosclerosis. 2016;246:63-70.
500. Benhamed M, Herbig U, Ye T, Dejean A, Bischof O. Senescence is an endogenous trigger for microRNA-directed transcriptional gene silencing in human cells. Nature cell biology. 2012;14(3):266-75.
501. Nam EJ, Yoon H, Kim SW, Kim H, Kim YT, Kim JH, et al. MicroRNA expression profiles in serous ovarian carcinoma. Clinical cancer research : an official journal of the American Association for Cancer Research. 2008;14(9):2690-5.
502. Mi S, Lu J, Sun M, Li Z, Zhang H, Neilly MB, et al. MicroRNA expression signatures accurately discriminate acute lymphoblastic leukemia from acute myeloid leukemia. Proceedings of the National Academy of Sciences of the United States of America. 2007;104(50):19971-6.
503. Schultz J, Lorenz P, Gross G, Ibrahim S, Kunz M. MicroRNA let-7b targets important cell cycle molecules in malignant melanoma cells and interferes with anchorage-independent growth. Cell research. 2008;18(5):549-57.

Metabolism Clinical and Experimental 87 (2018) 36–47

Contents lists available at ScienceDirect

Metabolism Clinical and Experimental

journal homepage: www.metabolismjournal.com

HDL-apoA-I induces the expression of angiopoietin like 4 (ANGPTL4) in endothelial cells via a PI3K/AKT/FOXO1 signaling pathway

Dimitris Theofilatos [a,b], Panagiotis Fotakis [c,1], Efi Valanti [d], Despina Sanoudou [d], Vassilis Zannis [c], Dimitris Kardassis [a,b,*]

[a] Laboratory of Biochemistry, University of Crete School of Medicine, Heraklion, Greece
[b] Institute of Molecular Biology and Biotechnology, Foundation for Research and Technology of Hellas, Heraklion, Greece
[c] Section of Molecular Genetics, Boston University Medical School, Boston, USA
[d] 4th Department of Internal Medicine, "Attikon" Hospital, Medical School, National and Kapodistrian University of Athens, Athens, Greece

ARTICLE INFO

Article history:
Received 19 December 2017
Accepted 17 June 2018
Available online xxxx

Keywords:
High Density Lipoprotein
Apolipoprotein A-I
Endothelial cells
Microarrays
Angiopoietin like 4
Forkhead box 1

ABSTRACT

Background: High Density Lipoprotein (HDL) and its main protein component, apolipoprotein A-I (apoA-I), have numerous atheroprotective functions on various tissues including the endothelium. Therapies based on reconstituted HDL containing apoA-I (rHDL-apoA-I) have been used successfully in patients with acute coronary syndrome, peripheral vascular disease or diabetes but very little is known about the genomic effects of rHDL-apoA-I and how they could contribute to atheroprotection.
Objective: The present study aimed to understand the endothelial signaling pathways and the genes that may contribute to rHDL-apoA-I-mediated atheroprotection.
Methods: Human aortic endothelial cells (HAECs) were treated with rHDL-apoA-I and their total RNA was analyzed with whole genome microarrays. Validation of microarray data was performed using multiplex RT-qPCR. The expression of ANGPTL4 in EA.hy926 endothelial cells was determined by RT-qPCR and Western blotting. The contribution of signaling kinases and transcription factors in ANGPTL4 gene regulation by HDL-apoA-I was assessed by RT-qPCR, Western blotting and immunofluorescence using chemical inhibitors or siRNA-mediated gene silencing.
Results: It was found that 410 transcripts were significantly changed in the presence of rHDL-apoA-I and that angiopoietin like 4 (ANGPTL4) was one of the most upregulated and biologically relevant molecules. In validation experiments rHDL-apoA-I, as well as natural HDL from human healthy donors or from transgenic mice overexpressing human apoA-I (TgHDL-apoA-I), increased ANGPTL4 mRNA and protein levels. ANGPTL4 gene induction by HDL was direct and was blocked in the presence of inhibitors for the AKT or the p38 MAP kinases. TgHDL-apoA-I caused phosphorylation of the transcription factor forkhead box O1 (FOXO1) and its translocation from the nucleus to the cytoplasm. Importantly, a FOXO1 inhibitor or a FOXO1-specific siRNA enhanced ANGPTL4 expression, whereas administration of TgHDL-apoA-I in the presence of the FOXO1 inhibitor or the FOXO1-specific siRNA did not induce further ANGPTL4 expression. These data suggest that FOXO1 functions as an inhibitor of ANGPTL4, while HDL-apoA-I blocks FOXO1 activity and induces ANGPTL4 through the activation of AKT.
Conclusion: Our data provide novel insights into the global molecular effects of HDL-apoA-I on endothelial cells and identify ANGPTL4 as a putative mediator of the atheroprotective functions of HDL-apoA-I on the artery wall, with notable therapeutic potential.

Abbreviations: apoA-I, apolipoprotein A-I; ANGPTL4, angiopoietin like 4; CETP, cholesterol ester transfer protein; CHX, cycloheximide; CVD, cardiovascular disease; EBM, endothelial cell basal medium; eNOS, endothelial NO synthase; ERK, extracellular signal-regulated kinase; FPLC, fast protein liquid chromatography; FOXO1, forkhead box O1; gck, glucokinase; HAECs, human aortic endothelial cells; HDL, High Density Lipoprotein; ICAM-1, Intercellular Adhesion Molecule 1; IPA, Ingenuity Pathway Analysis; JKN, Jun N-terminal kinase; LPDS, lipoprotein deficient serum; LPL, lipoprotein lipase; MCP-1, monocyte chemoattractant protein 1; NO, nitric oxide; PCR, polymerase chain reaction; PI3K, phosphatidylinositol 3-kinase; qRT-PCR, quantitative reverse transcription PCR; RCT, reverse cholesterol transport; rHDL-A-I, reconstituted HDL containing apoA-I; siRNA, small interfering RNA; TgHDL-apoA-I, HDL isolated from transgenic mice expressing human apoA-I.

* Corresponding author at: University of Crete School of Medicine and Institute of Molecular Biology and Biotechnology, Foundation for Research and Technology of Hellas, Heraklion 71003, Greece.
E-mail address: kardasis@imbb.forth.gr (D. Kardassis).
[1] Current address: Columbia University School of Medicine, New York, USA.

https://doi.org/10.1016/j.metabol.2018.06.002
0026-0495/

1. Introduction

Multiple epidemiological studies have established an inverse association between plasma levels of High Density Lipoprotein cholesterol (HDL-C) and the risk for developing cardiovascular disease (CVD), which is the leading cause of death in Western societies [1]. However, the original "HDL hypothesis", based on which the risk for developing CVD would be decreased by an increase in the plasma HDL-C levels, has not been validated by clinical studies using HDL-raising drugs such as the cholesterol ester transfer protein (CETP) inhibitors or by genetic studies in humans and animals [2]. On the other hand, a wealth of information coming from experiments in vitro and ex vivo indicated that the functionality of HDL particles is more important than the concentration of HDL-C for atheroprotection, thus shifting the attention of the research community to more functional studies of HDL [3]. The most well studied HDL function is the efflux of cholesterol from peripheral cells, such as the macrophages, and its transport back to the liver for excretion, a process that has been termed the reverse cholesterol transport (RCT) [4]. The clinical significance of this function is the unloading of cholesterol from macrophage foam cells of the arterial intima and the protection from atherosclerosis [3]. Furthermore, chronic diseases with an inflammatory component, such as obesity, diabetes, rheumatoid arthritis or inflammatory bowel diseases, are characterized by dysfunctional, pro-inflammatory HDL [5]. Research is now underway, mainly via proteomics and lipidomics approaches, to identify critical changes in HDL protein and lipid composition that could account for the transformation of an anti-inflammatory to a pro-inflammatory particle [6,7].

The integrity of the vascular endothelium is essential for the protection against atherosclerosis [8]. In response to inflammation, oxidative stress or other causes, endothelial cells are activated to produce adhesion proteins and chemoattractants, such as the monocyte chemoattractant protein 1 (MCP-1), resulting in the recruitment of circulating monocytes into the intima which will become the precursors of the cholesterol-rich macrophage foam cells of the atherosclerotic plaques [9]. HDL plays a protective role on the endothelium by securing endothelial integrity, reducing endothelial cell apoptosis [10–12], stimulating endothelial cell proliferation [13] and inducing the production of nitric oxide (NO) from endothelial NO synthase (eNOS) [14]. The upstream events in these endothelial cell responses to HDL have been studied in detail. The interaction of HDL particles with SR-BI on endothelial cells has been shown to alter the cholesterol content of caveolae which are rich in eNOS thus inducing the production of nitric oxide [15,16]. Sphingosine 1 phosphate (S1P) which is a minor component of HDL carried by apoM (5% of total HDL particles) also triggers cellular signaling pathways leading to nitric oxide production, proliferation and migration in endothelial cells and survival in cardiomyocytes by interacting with specific G protein coupled receptors (S1P3) [17]. However, the downstream signaling pathways that mediate the HDL-induced cell responses and the signaling molecules (proteins, lipids) involved are poorly understood.

Therapies based on reconstituted HDL containing human apoA-I (rHDL-apoA-I), wild type or apoA-I $(R173C)_{Milano}$, have shown encouraging results both in mice with atherogenic backgrounds and in human patients with acute coronary syndrome, peripheral vascular disease or type II diabetes [18–24]. Previous studies had shown that rHDL-apoA-I infusion was well tolerated by healthy humans and caused an increase in plasma HDL and apoA-I levels [25]. The combined data from these intervention studies strongly suggested a promising future for the use of rHDL-apoA-I in the clinic. However, the mechanisms by which rHDL-apoA-I exerts its various atheroprotective and anti-inflammatory functions are still not understood. The present study aimed to identify genes that could mediate the protective functions of rHDL-apoA-I in endothelial cells and to understand the mechanisms and the signaling pathways that are involved in endothelial gene regulation by HDL. Our data show that treatment with rHDL-apoA-I was associated with significant changes in the transcriptome of cultured endothelial cells and the bioinformatics analysis of the microarray data identified angiopoietin like 4 (ANGPTL4) as one of the most highly upregulated and biologically relevant molecules. Using specific chemical inhibitors we delineated the signaling pathway that leads to the transcriptional activation of the ANGPTL4 gene which includes the kinases PI3K and AKT, and the transcription factor FOXO1. The global gene expression changes induced by rHDL-apoA-I that were identified in this study and the identification of ANGPTL4 as one of the most biologically relevant target genes could be exploited for the design of novel therapeutic tools for patients with atherosclerotic cardiovascular disease.

2. Materials and Methods

Materials and additional methods can be found in the Supplementary material.

2.1. Cell Cultures

Human aortic endothelial cells (HAEC) (Lonza Inc. MD), were cultured in endothelial cell basal medium (EBM-2) as recommended by the supplier. The endothelial cell line EA.hy926 was cultured in DMEM containing 1 g/l glucose, pyruvate and GlutaMax supplemented with 10% fetal bovine serum and 2% penicillin/streptomycin solution. All cells were maintained in 37 °C in a 5% CO_2 atmosphere.

2.2. Preparation of HDL

Natural HDL was purified from the pooled plasma of transgenic mice expressing human apoA-I (TgHDL-apoA-I) or from human healthy volunteers (hHDL) using density gradient ultracentrifugation as described previously [26]. The apolipoprotein composition of each fraction was determined by SDS–PAGE and Coomassie Brilliant Blue staining. Fractions containing apoA-I were pooled and the HDL was concentrated using Amicon Ultra-0.5 Centrifugal Filter Devices (Millipore). HDL was sterilized through a 0.22-μm filter, and stored at 4°C. Since apoA-I is the main protein that is present in the HDL preparation, HDL concentration was determined by the Lowry method.

2.3. Preparation of Reconstituted HDL

Reconstituted HDL (rHDL) particles were prepared by mixing 1-palmitoyl-2-oleoyl-sn-glycero-3-phosphocholine (POPC), cholesterol, purified human apolipoprotein A-I and sodium cholate at a molar ratio of 100:10:1:100 as described previously [27].

2.4. Animal Models

Transgenic mice carrying the human apoA-I/apoC-III gene cluster have been described previously [28]. These mice were lacking the expression of the endogenous mouse apoA-I gene. Mice were maintained at the animal facility of the Institute of Molecular Biology and Biotechnology of Crete on a 12 h light/dark cycle and fed standard rodent chow. For the isolation of HDL, blood was collected by cardiac puncture following a 4 h fasting period.

2.5. Microarray Experiments

For the microarray experiments HAEC were cultured for 4 h in EBM-2 basal medium supplemented with 0.5% Fetal Bovine Serum and 5% Lipoprotein Deficient Serum (LPDS). The medium was then replaced with EBM-2 basal medium containing 5% LPDS and the cells were incubated for 12 h in the presence of rHDL-apoA-I at a final concentration of 250 μg/ml. PBS was used in the control experiments. All experiments were repeated five times. RNA purification was performed using the Trizol reagent according to the manufacturer's protocol. Following

integrity and purity assessment, each sample was processed using Affymetrix recommended protocols for target preparation and hybridization to GeneChip Human Gene 1.0 ST Arrays (Affymetrix, Santa Clara, CA, USA). Washing and staining of the arrays was performed on the Affymetrix 450 Fluidics station, and scanning with the GeneChip Scanner 3000.

2.6. Analysis of Microarray Data

The raw data (5 treated and 4 control specimens) were normalized using the Robust Multi-chip Analysis (RMA). The statistically significant gene expression changes between the two groups were identified using pairwise Welch *t*-tests (*t*-statistic, *p*-value and FDR q-value). To control for multiple testing, a false discovery rate (FDR) threshold of ≤0.05 was applied. Transcripts with a fold change of ≥ | 2.00 | were selected for further studies. The list containing the significantly changed genes was subjected to in depth data mining using the Ingenuity Pathway Analysis (IPA) software and extensive PubMed-based mining.

2.7. High Throughput Quantitative Reverse Transcription PCR (qRT-PCR)

cDNA was synthesized using Superscript II RNase H reverse transcriptase and oligo-dT primers and it was applied to dynamic array chips (BioMark 96.96 Dynamic Array, Fluidigm Biomark) according to manufacturer's instructions. The qRT-PCR data were normalized to GAPDH (reference gene) using the comparative CT method, and the ΔΔCT values were calculated relative to the PBS control group.

2.8. Cell Treatments with HDL and Inhibitors

For treatment with HDL, EA.hy926 cells were starved for 3 h and incubated with TgHDL-apoA-I for various time points. For the experiments with the inhibitors, cells were pre-incubated with inhibitors in medium containing 0.5% FBS for 1 h before the addition of TgHDL-apoA-I and remained in the culture medium for the entire duration of the experiment. The following inhibitors were used: phosphatidylinositol 3-kinase (PI3K)/Akt inhibitor LY294004, p38 mitogen-activated protein kinase inhibitor SB203580, extracellular signal-regulated kinase (ERK) inhibitor UO126, c-Jun N-terminal kinase (JNK) inhibitor SP600125, endothelial nitric oxide synthase inhibitor (L-NMMA), the protein synthesis inhibitor cycloheximide (CHX) and the forkhead box O1 (FOXO1) inhibitor AS1842856.

2.9. siRNA Silencing

EA.hy926 cells were transfected with siRNA targeting FOXO1 or with a control (scrambled) siRNA using Lipofectamine RNAiMAX according to the manufacturer's instructions. FOXO1 silencing was achieved following two rounds of 100 nM siRNA transfection. Ninety two hours after the first round of transfection, cells were treated with TgHDL-apoA-I as described above. The silencing efficiency of FOXO1 was confirmed by western blotting and RT-qPCR.

2.10. Quantitative Reverse Transcription PCR

Total RNA was isolated from EA.hy926 cells using RNAiso reagent according to the manufacturer's protocol (Takara, Japan). cDNA synthesis was performed using the M-MLV reverse transcriptase and random primers. Quantitative PCR (qPCR) was performed on a StepOnePlus Real-Time PCR system (Applied Biosystems, Foster City, CA) using KAPA SYBR FAST qPCR Master Mix (Kapa Biosystems, Wilmington, MA). The relative gene expression levels were determined by the comparative Ct method (ΔΔCt method), as described in Applied Biosystems Guide, using RPLPO levels as internal control. The primers used for RT-qPCR are shown in Table S1.

2.11. Statistical Analysis

Data are expressed as mean ± SD. Statistical significance was determined using two-tailed Student's *t*-test or one-way analysis of variance and Tukey's post-hoc test to evaluate differences between three or more groups. For all results, $p < 0.05$ was considered statistically significant. Analysis was performed using GraphPad Prism (GraphPad Software, Inc., La Jolla, USA).

3. Results

3.1. Effects of rHDL-apoA-I on Global Endothelial Gene Expression

Previous studies had shown that rHDL-apoA-I infusion into animals or humans displayed positive effects towards improved HDL functionality and protection from atherosclerosis but the mechanisms and the molecules that could mediated these atheroprotective effects of rHDL-apoA-I are not known. We addressed this issue by performing whole genome microarray experiments in primary HAECs treated with rHDL-apoA-I for 12 h. In control experiments, HAECs were treated with PBS for the same time period. The mRNAs from the rHDL-treated and PBS-treated cells were purified, labeled and hybridized with GeneChip Human Gene 1.0 ST Arrays (Affymetrix) followed by bioinformatics analysis. By applying fold change and FDR thresholds of ≥ | 2 | and <0.05, respectively, we identified 410 transcripts the expression of which was significantly changed in the presence of rHDL-apoA-I compared to PBS (Table S2). Interestingly, more than half of the differentially expressed transcripts were downregulated by rHDL-apoA-I (263 transcripts or 64% of the total) (Fig. 1). Gene ontology classification of the differentially expressed transcripts based on the cellular localization of the encoded proteins revealed that the majority of the transcripts encoded for nuclear (186), followed by cytoplasmic (103), plasma membrane (43), secreted (31), as well as other proteins with unknown localization (47) (Fig. 1, Table S2). The list with the highly up-regulated transcripts included angiopoietin like 4 (ANGPTL4, 6.1 fold), the very low density lipoprotein receptor (VLDLR, 5.8-fold), the endothelin receptor type B (EDNRB, 5.4 fold), the endothelial lipase (LIPG, 3.4 fold), and the vascular endothelial growth factor A (VEGFA, 3.3 fold). The list with the most significantly down-regulated genes included the hormone nuclear receptor retinoic acid receptor B (RARB, −10.7 fold), the sphingosine 1 phosphate receptor 3 (S1P3, −5.9 fold), and the transforming growth factor beta 2 (TGFB2, −5.5 fold) (Table S2).

Using the IPA software from Qiagen, (Germantown, USA) we grouped the 410 transcripts into 17 Molecular and Cellular Functions (Fig. 2, Table S3). The five functional categories with the strongest statistically significant changes were: 1) cell cycle; 2) cell death and survival; 3) DNA replication, recombination and repair; 4) cellular assembly and organization; and 5) post-translational modifications. Other physiologically relevant categories, pertinent to the effect of HDL on endothelial cells, were: cellular growth and proliferation; cell morphology; lipid metabolism; and gene expression.

The microarray findings were validated with high throughput RT-qPCR screening using dynamic array chips from Fluidigm (San Francisco, USA) for a set of representative genes selected among the most physiologically relevant functional categories. All RT-qPCR results were in accordance with the microarray measurements (Table S4), confirming that the interaction of rHDL-apoA-I with endothelial cells triggers events that lead to the activation or repression of target genes with diverse intracellular and extracellular functions. The RT-qPCR data also confirmed that ANGPTL4 is one of the genes with the most prominent upregulation in endothelial cells in response to rHDL-apoA-I stimulation. A closer examination of the IPA data revealed that ANGPTL4 was included in five of the functional categories, namely “Cell Death and Survival”, “Protein Synthesis”, “Cellular Development”, “Cellular Growth and Proliferation”, and “Cell Morphology” (Table S3)

which are all relevant to the biological effects of rHDL-apoA-I on endothelial cells ex vivo and in vivo (see Discussion section).

3.2. Upstream Regulator Analysis

In order to identify the molecules contributing to the ANGPTL4 upregulation by rHDL-apoA-I, we performed Upstream Regulator Analysis using the IPA software. This analysis takes into consideration transcription factors, intracellular phosphorylation cascades, receptors and molecules with an established direct or indirect regulatory effect on gene expression. Forty nine molecules were predicted to be potential regulators of ANGPTL4 (Table S5). One of the transcription factors that was identified in this group was the forkhead box O1 (FOXO1) ($p < 0.0001$) which had been previously shown to mediate the metabolic effects of insulin in several cell types, including the liver, by controlling the expression of genes involved in gluconeogenesis or lipoprotein metabolism [29]. Importantly, it was shown recently that FOXO1 plays a crucial role in the regulation of endothelial cell metabolism in the context of angiogenesis [30].

3.3. HDL Induces the Expression of the ANGPTL4 Gene in Endothelial Cells in a Dose and Time-Dependent Manner

We sought to determine the mechanisms by which HDL containing human apoA-I regulates the expression of ANGPTL4 gene in endothelial cells. For this purpose we used native HDL isolated from healthy volunteers or from transgenic mice overexpressing human apoA-I (TgHDL-apoA-I) [28]. TgHDL-apoA-I was equally effective as native human HDL (Fig. 3A and B) or rHDL-apoA-I (data not shown) to induce the expression of human ANGPTL4 gene in the endothelial cell line EA.hy926 which has been used extensively in the past as an endothelial cell model [31]. The TgHDL-apoA-I that was isolated from the human apoA-I transgenic mice had structural and functional properties similar to human HDL, such as the distribution of apoA-I in the HDL2/HDL3 region and the inhibition of TNFα-induced expression of the pro-inflammatory cytokine Intercellular Adhesion Molecule 1 (ICAM-1) in endothelial cells (Fig. S1A-C). These mice had high levels of plasma total and HDL cholesterol, a normal ratio of CE/TC and normal phospholipids and triglycerides (Fig. S1D). Treatment of human endothelial cells with two different concentrations of TgHDL-apoA-I (100 and 250 μg/ml) for 12 h induced the expression of the human ANGPTL4 gene in a dose-dependent manner (Fig. 3A). As shown in Fig. 3C, the increase in ANGPTL4 mRNA levels by TgHDL-apoA-I was transient, reached a peak at 2 h, and started to decline at 12 h post-induction until it was restored to the original unstimulated levels at 24 h post-induction. Treatment of endothelial cells with two different concentrations of TgHDL-apoA-I (100 and 250 μg/ml) for 12 h significantly increased the levels of secreted ANGPTL4 in a dose-dependent manner (Fig. 3D). The secreted ANGPTL4 was found to associate with the mature α1 sub-class of TgHDL-apoA-I in native gel electrophoresis experiments (Fig. S2) in agreement with previous studies which had shown that circulating ANGPTL4 was physically associated with HDL in mice [32].

3.4. ANGPTL4 Is a Direct Transcriptional Target of HDL in Endothelial Cells

We used the protein synthesis inhibitor cycloheximide (CHX) in order to investigate whether the observed increase in ANGPTL4 mRNA and protein levels by TgHDL-apoA-I in endothelial cells is direct or not. As shown in Fig. 4, treatment of EA.hy926 cells with 5 μg/ml CHX for 12 h increased significantly (18-fold) the basal mRNA levels of the human ANGPTL4 gene. Most importantly, induction of ANGPTL4 by TgHDL-apoA-I was not affected by CHX suggesting that the mechanism by which TgHDL-apoA-I upregulated the ANGPTL4 gene is direct.

3.5. The PI3K and p38 Signaling Pathways Are Implicated in the Regulation of ANGPTL4 Gene by TgHDL-apoA-I in Endothelial Cells

We next sought to delineate the signaling pathway(s) that are induced by TgHDL-apoA-I in endothelial cells and culminate in the overexpression of the ANGPTL4 gene. First we established that TgHDL-apoA-I was able to stimulate the phosphorylation of the signaling kinases AKT, p38, ERK and JNK with different kinetics (Fig. 5A). Specifically, the activation of MAP kinases JNK and p38 was very fast, reached a peak at 5 min post-induction and declined thereafter. The activation of AKT and ERK reached a peak at 30 min post-HDL treatment. However, ERK phosphorylation was more stable and started to decline after 2 h of stimulation with TgHDL-apoA-I. To address the contribution of each kinase in ANGPTL4 regulation by HDL we used specific inhibitors. As shown in Figs. 5B and C and S3, treatment of EA.hy926 cells with specific inhibitors of PI3 kinase (LY) or p38 MAP kinase (SB) independently or in combination abolished the induction of the ANGPTL4 gene by TgHDL-apoA-I. In contrast, inhibitors for JNK or ERK kinases had no effect on the upregulation of ANGPTL4 mRNA levels by TgHDL-apoA-I in endothelial cells (Fig. 5D and E).

We also studied the involvement of endothelial nitric oxide synthase in the regulation of ANGPTL4 gene by TgHDL-apoA-I. Specifically, we treated endothelial cells with TgHDL-apoA-I in the presence and in the absence of an inhibitor for eNOS (L-NMMA) and we determined the ANGPTL4 mRNA levels by RT-qPCR. We also measured eNOS phosphorylation by TgHDL-apoA-I. The data showed that treatment of endothelial cells with TgHDL-apoA-I induced a rapid eNOS phosphorylation which peaked at 5 min and declined after 1 h of stimulation (Fig. 5A). The data also showed that the inhibitor of eNOS had no effect on ANGPTL4 gene induction by TgHDL-apoA-I (Fig. 5F).

3.6. HDL Induces AKT-mediated Phosphorylation of FOXO1 and Its Translocation to the Cytoplasm

Stimulation of the PI3K/AKT signaling pathway leads to the phosphorylation of several downstream effectors including the transcription factor FOXO1 [29]. To investigate the potential regulation of FOXO1 localization and functions by HDL, we treated EA.hy926 cells with TgHDL-apoA-I (250 μg/ml) or PBS for a range of time points while monitoring the levels of phosphorylated and total FOXO1 in cytoplasmic and nuclear extracts by western blotting using the corresponding antibodies. As shown in Fig. 6A top, incubation of EA.hy926 cells with TgHDL-apoA-I caused a very rapid phosphorylation of FOXO1 in the nucleus which peaked at 5 min and declined to non-stimulated levels at 1 h post-stimulation. At the same time point (5 min), the levels of total FOXO1 in the nucleus started to decline and the levels of total FOXO1 in the cytoplasm strongly increased at 30 min of treatment. This increase in total cytoplasmic FOXO1 was transient since it returned to pre-stimulated levels at 2 h post-induction and at the same time, the levels of total FOXO1 in the nucleus increased.

The data of the immunoblotting analysis were validated by immunofluorescence experiments. These experiments showed that prior to treatment with TgHDL-apoA-I, FOXO1 was localized exclusively in the nucleus of EA.hy926 cells (Fig. 6B top row), whereas following 30 min treatment with TgHDL-apoA-I (250 μg/ml) there was a significant nuclear exclusion of FOXO1 (Fig. 6B second row). In agreement with the data of Fig. 5, nuclear exclusion of FOXO1 by TgHDL-apoA-I was prevented using an inhibitor of PI3K (LY) whereas an inhibitor of p38 MAP kinase (SB) had a minor effect (Fig. 6B third and fourth rows respectively).

3.7. Induction of ANGPTL4 by TgHDL-apoA-I Is Mediated by FOXO1

Having established that TgHDL-apoA-I regulates FOXO1 phosphorylation and intracellular localization, we investigated the effect of the FOXO1 inhibitor AS1842856 (AS) on the TgHDL-apoA-I-mediated

Symbol	Entrez Gene Name	Fold change
ANGPTL4	angiopoietin like 4	6,174
APOL6	apolipoprotein L6	4,744
STC2	stanniocalcin 2	4,57
LIPG	lipase G, endothelial type	3,432
VEGFA	vascular endothelial growth factor A	3,349
SLC46A3	solute carrier family 46 member 3	2,802
A2M	alpha-2-macroglobulin	2,394
ADAMTS4	ADAM metallopeptidase with thrombospondin type 1 motif 4	2,306
IL6	interleukin 6	2,223
TSLP	thymic stromal lymphopoietin	2,202
TGFB3	transforming growth factor beta 3	2,162
PAPPA2	pappalysin 2	2,039
VIP	vasoactive intestinal peptide	2,022
BMP2	bone morphogenetic protein 2	-1,999
VASH1	vasohibin 1	-2,013
LRRC17	leucine rich repeat containing 17	-2,015
CCBE1	collagen and calcium binding EGF domains 1	-2,092
FGF5	fibroblast growth factor 5	-2,129
ESM1	endothelial cell specific molecule 1	-2,183
ANGPT2	angiopoietin 2	-2,21
CXCL1	C-X-C motif chemokine ligand 1	-2,229
PRSS23	protease, serine 23	-2,408
CYTL1	cytokine like 1	-2,435
ATAD5	ATPase family, AAA domain containing 5	-2,523
CXCL8	C-X-C motif chemokine ligand 8	-2,564
MAMDC2	MAM domain containing 2	-2,936
GDF6	growth differentiation factor 6	-2,947
PLAT	plasminogen activator, tissue type	-3,239
FST	follistatin	-4,262
TGFB2	transforming growth factor beta 2	-5,529
DKK1	dickkopf WNT signaling pathway inhibitor 1	-5,934

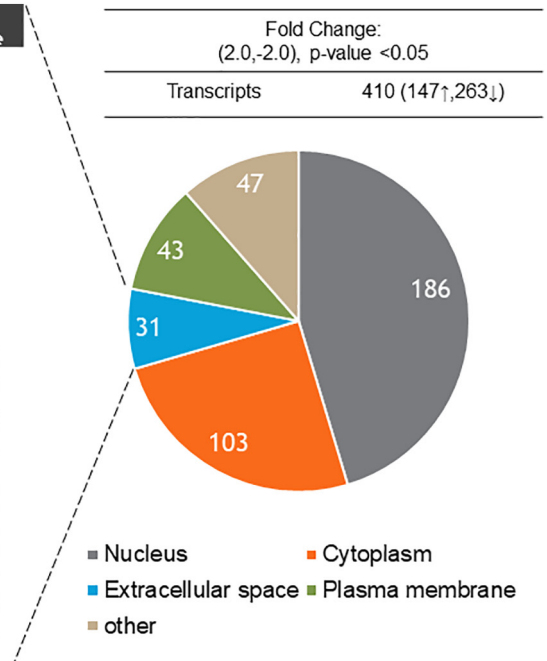

Fig. 1. Microarray analysis identified 410 differentially expressed transcripts in response to rHDL-apoAI in endothelial cells. Primary human aortic endothelial cells were treated with 250 μg/ml of rHDL-apoA-I for 12 h. Total RNA was extracted and microarray analysis was performed as described in Materials and Methods section. Transcripts with a fold change of ≥ | 2.00 | were selected and a false discovery rate (FDR) threshold of <0.05 was applied. The pie chart shows the classification of the differentially expressed transcripts based on the cellular localization of the encoded proteins. The Table shows genes encoding for extracellular proteins that were differentially expressed in response to rHDL-apoA-I. ANGPTL4 was the gene with the strongest upregulation.

induction of the ANGPTL4 gene. As shown in Fig. S4, treatment of EA.hy926 cells with increasing concentrations of the FOXO1 inhibitor (5 nM to 10 μM), increased ANGPTL4 mRNA levels in a dose-dependent manner suggesting that FOXO1 is a negative regulator of the ANGPTL4 gene in endothelial cells. It has been reported previously that low concentrations of AS (below 100 nM) are sufficient to inhibit the transcriptional activity of FOXO1 on an artificial promoter consisting of four copies of a 22-base pair insulin-responsive element identical with that of rat PEPCK promoter upstream of the firefly luciferase gene [33]. We found that low AS concentrations (50 nM–100 nM) had a moderate effect (1.4–1.8 fold induction) on ANGPTL4 mRNA levels which was not statistically significant whereas higher AS concentration (5–10 μM) were required to increase ANGPTL4 gene transcription (Fig. S4). A further increase in AS concentration to 20 μM apparently had non-specific effects (Fig. S4). As shown in Fig. 7A, in the presence of a high concentration of AS (10 μM) TgHDL-apoA-I was not able to further induce ANGPTL4 gene expression in endothelial cells. The role of FOXO1 in TgHDL-apoA-I-mediated induction of the ANGPTL4 gene was further established by a gene silencing experiment. As shown in Fig. 7B, a FOXO1-specific siRNA increased ANGPTL4 mRNA levels 3-fold in EA.hy926 cells whereas a non-specific (scrambled) siRNA had no effect on ANGPTL4 expression. Treatment of EA.hy926 cells with TgHDL-apoA-I caused a 3.7-fold induction in ANGPTL4 mRNA levels but most importantly, this induction could not be further

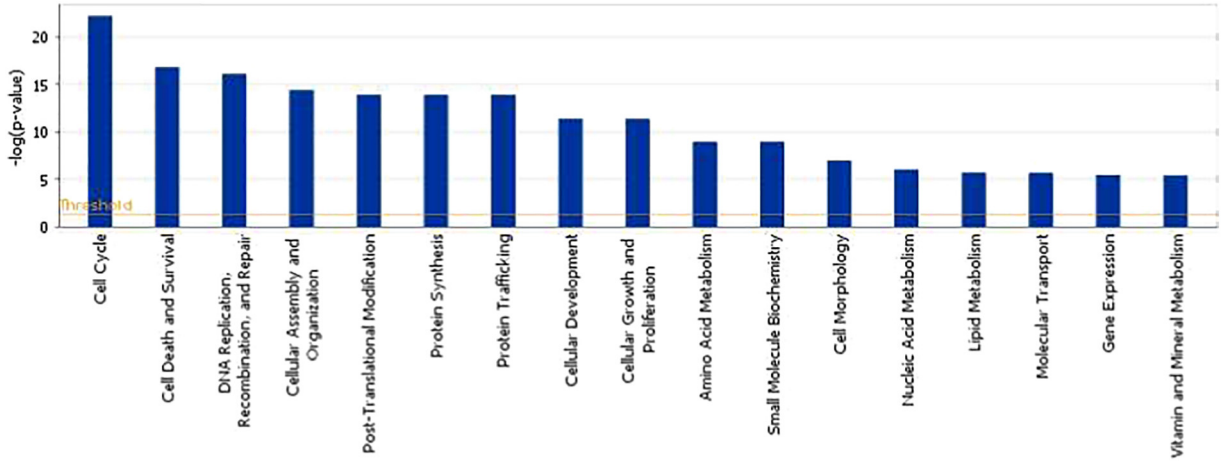

Fig. 2. Molecular and cellular functions significantly over-represented among the differentially expressed transcripts (IPA analysis). Bars indicate the likelihood [−log (*p*-value)] that the specific molecular and cellular function category was affected by the rHDL-apoA-I treatment. The results were filtered for significance using a *p*-value <0.05 (orange line) threshold. (For interpretation of the references to color in this figure legend, the reader is referred to the web version of this article.)

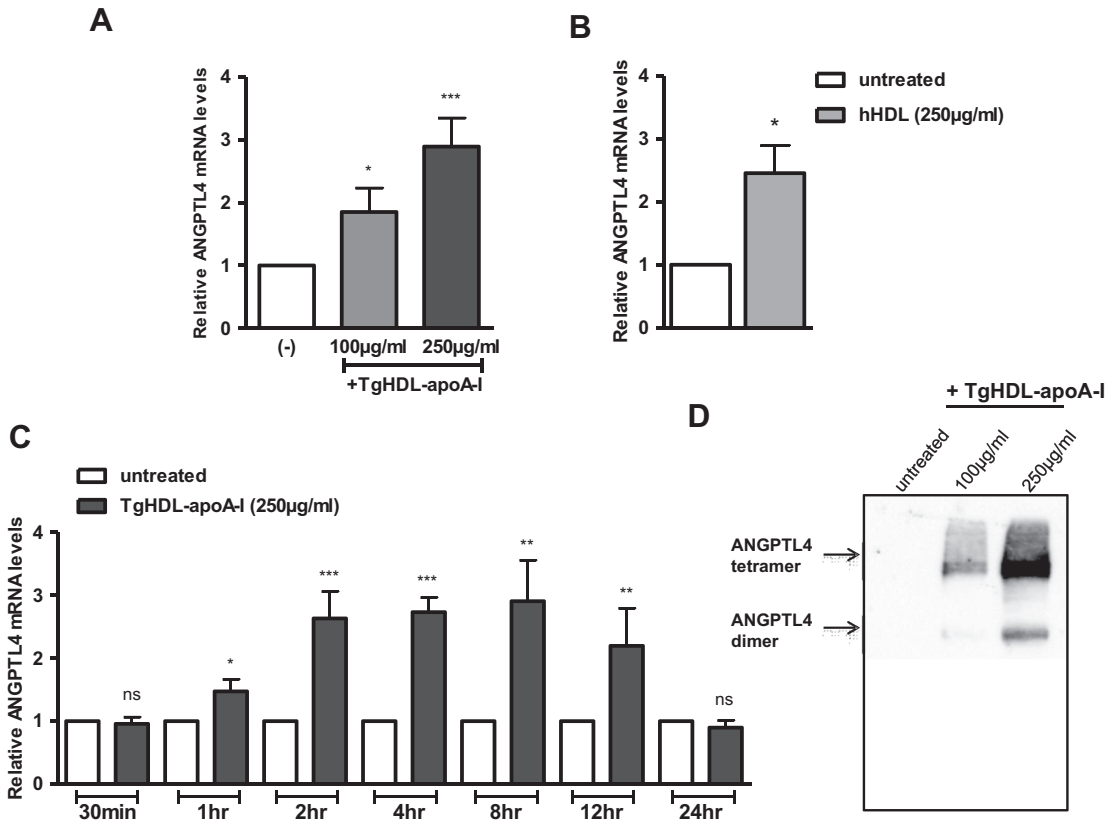

Fig. 3. Natural HDL isolated from healthy human volunteers or from transgenic mice expressing human apoA-I induces ANGPTL4 at the mRNA and protein levels. (A) The endothelial human cell line EA.hy926 was treated with two different concentrations (100 and 250 μg/ml) of natural HDL isolated from transgenic mice expressing human apoA-I (TgHDL-apoA-I) for 12 h or with PBS (−). Total RNA was extracted and quantitative RT-PCR was performed to determine ANGPTL4 mRNA levels. The ANGPTL4 mRNA levels relative to the RPLPO mRNA levels that were used as an internal control are expressed as mean (±SD) from at least three independent experiments. (B) EA.hy926 cells were treated with 250 μg/ml of HDL isolated from healthy human volunteers (hHDL) or with PBS (untreated) for 12 h. Total RNA was extracted and quantitative RT-PCR was performed to determine ANGPTL4 mRNA levels. The normalized ANGPTL4 mRNA levels relative to the RPLPO mRNA levels are expressed as mean (±SD) from at least three independent experiments. (C) EA.hy926 cells were treated with 250 μg/ml of Tg-HDL-apoA-I for the indicated time periods. Total RNA was extracted and quantitative RT-PCR was performed to determine ANGPTL4 mRNA levels, which were normalized relative to the RPLPO mRNA levels. The relative ANGPTL4 mRNA levels in the absence (white bars) and in the presence (black bars) of TgHDL-apoA-I (mean ± SD) from at least four independent experiments are shown for each time point. (D) EA.hy926 cells were treated with two different doses (100 and 250 μg/ml) of TgHDL-apoA-I or with PBS (untreated). Medium was collected and the secreted ANGPTL4 protein levels were determined by immunoblotting. The experiment was performed three times, and a representative image is shown. Symbols: ns, not significant; *, $p \le 0.05$; **, $p \le 0.01$; ***, $p \le 0.001$.

increased in the presence of the FOXO1 siRNA (Fig. 7B). The efficiency of FOXO1 gene silencing by the FOXO1 siRNA and the scrambled siRNA was determined by RT-qPCR and western blotting experiment (Fig. 7C and D).

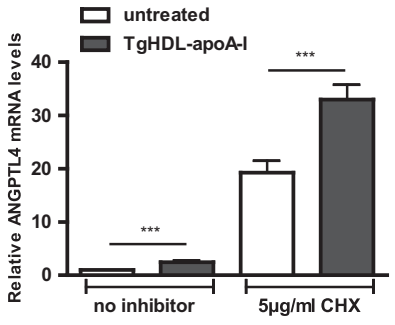

Fig. 4. ANGTPL4 is a direct transcriptional target of HDL. (A) EA.hy926 cells were pretreated with 5 μg/ml cycloheximide (CHX) or DMSO (no inhibitor) for 1 h and then treated with TgHDL-apoA-I or PBS (untreated) for additional 8 h. Total RNA was extracted and quantitative RT-PCR was performed to determine ANGPTL4 mRNA levels, which were normalized relative to the RPLPO mRNA levels. The relative ANGPTL4 mRNA levels are expressed as mean (±SD) from at least four independent experiments. Symbols: *, $p \le 0.05$; **, $p \le 0.01$.

The combined data of Figs. 6 and 7 indicated that induction of ANGPTL4 gene by TgHDL-apoA-I via the PI3K/AKT pathway requires inhibition of FOXO1 by phosphorylation and nuclear exclusion.

4. Discussion

Low levels of plasma HDL cholesterol are a strong and independent risk factor for the development of atherosclerotic CVD in humans [1]. However, numerous clinical studies in humans and studies in experimental animals have shown that by simply measuring plasma HDL-C levels we cannot safely predict CVD risk and that HDL functionality is what determines atheroprotection [3]. In addition to its anti-oxidant effects in the plasma and the cholesterol efflux capacity in macrophages, HDL exerts a plethora of effects on various cell types, including endothelial cells, which remain unexplored.

Reconstituted HDL containing apoA-I is being considered as a promising new therapeutic approach for patients with atherosclerotic CVD and this optimism is derived from the demonstration that infusion of rHDL particles containing apoA-I into healthy humans is well tolerated and increases the levels of HDL and apoA-I [25]. Two studies demonstrated the ability of rHDL to reduce atheroma volume and cause plaque remodeling in humans. In one study, Nissen and colleagues [19] administered rHDL containing apoA-I_{Milano} (ETC-216) in patients with acute coronary syndrome at a dose of five weekly

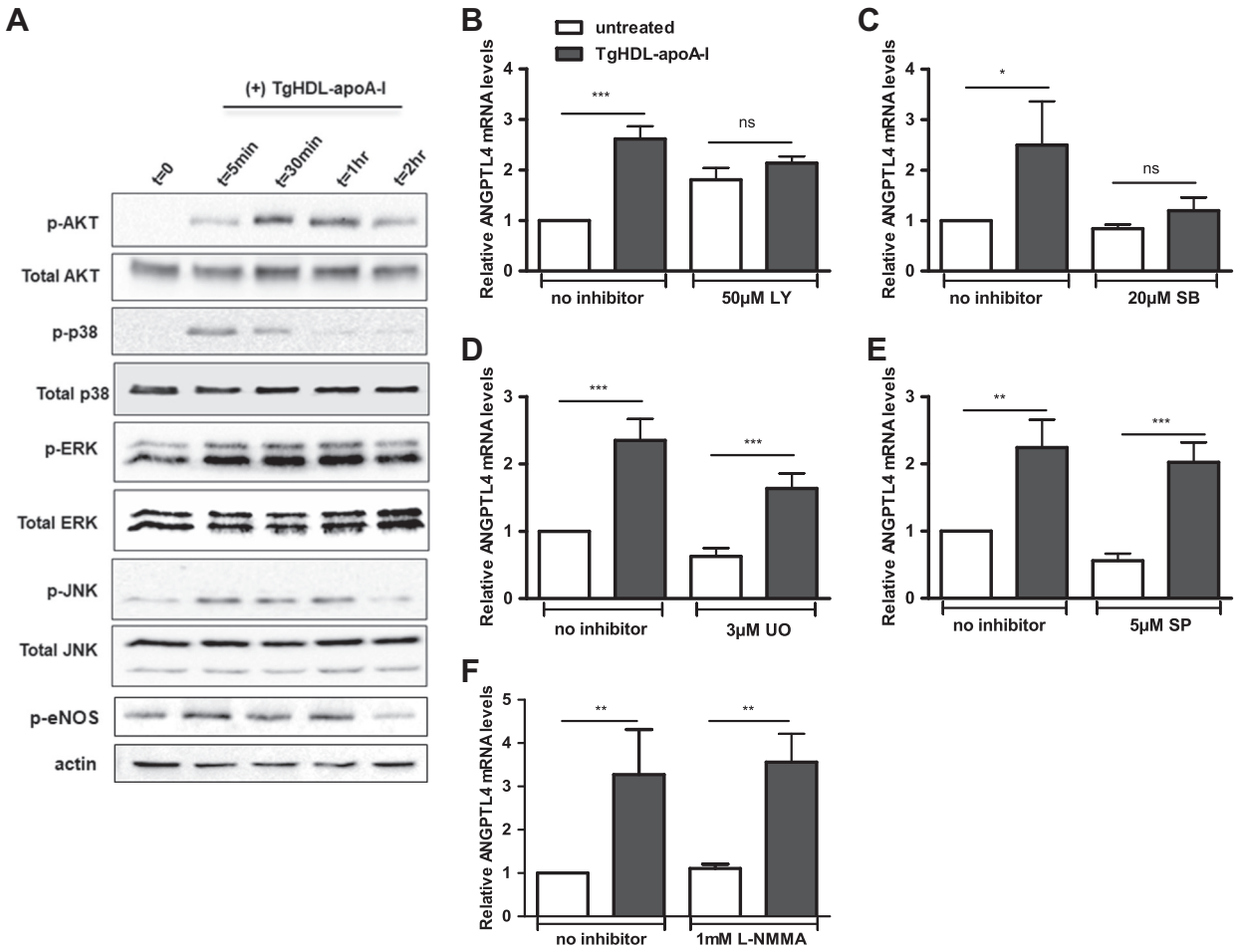

Fig. 5. HDL induces ANGTPL4 mRNA levels through the activation of PI3K/AKT and p38 MAPK pathways. (A) EA.hy926 cells were treated with TgHDL-apoA-I (100 μg/ml) for the indicated time periods. Cell extracts were collected and the total and phosphorylated levels of kinases AKT, p38, ERK and JNK as well as the phosphorylated levels of eNOS and the protein levels of actin were determined by immunoblotting using the corresponding antibodies. The experiment was performed three times and representative images are shown. (B–F) EA.hy926 cells were pretreated for 1 h with 50 μM LY (PI3K/AKT inhibitor) (B), 20 μM SB (p38 inhibitor) (C), 3 μM UO (ERK inhibitor) (D), 5 μM SP (JNK inhibitor) (E), 1 mM of L-NMMA (eNOS inhibitor) (F) or with DMSO (no inhibitor) and then treated with TgHDL-apoA-I or PBS (untreated) for additional 8 h. Total RNA was extracted and quantitative RT-PCR was performed to determine ANGPTL4 mRNA levels, which were normalized relative to the RPLPO mRNA levels. The relative ANGPTL4 mRNA levels are expressed as mean (±SD) from at least three independent experiments. Symbols: ns, not significant; *, $p \le 0.05$; **, $p \le 0.01$; ***, $p \le 0.001$.

infusions of 15 mg/kg or 45 mg/kg against placebo and they showed that ETC-216 reduced atheroma volume by 4.2% compared with baseline over a 5-week period. In the second study, Nicholls and colleagues [18] performed a similar intervention study but they also measured the external elastic membrane (EEM) and lumen volumes and they found that ETC-216 caused remodeling of the EEM without any change in the lumen size. These data are in agreement with the findings of Shaw et al. [22], who demonstrated that a single rHDL-apoA-I infusion into patients with claudication could dramatically remodel atherosclerotic plaque with a reduction in lipid content, macrophage size and markers of inflammation and of Tardif et al. [34] who showed that short-term infusions of rHDL-apoA-I (CSL-111) had no effect on atheroma volume but improved the plaque characterization index and coronary score. Infusion of rHDL-apoA-I to hypercholesterolemic men rapidly restored endothelium-dependent vasodilation by increasing NO bioavailability [35]. A number of clinical trials have demonstrated the safety and tolerability of CSL112, an infusible plasma-derived apoA-I, in patients with stable atherosclerotic disease [36] or acute myocardial infarction [37]. Reconstituted HDL was also shown to exert protective effects against diabetes. Drew et al. [24] showed that a single infusion of rHDL containing apoA-I in patients with type 2 diabetes mellitus reduced plasma glucose by increasing plasma insulin and activating AMP-activated protein kinase in skeletal muscle. These findings suggested a therapeutic role for HDL beyond atherosclerosis. Reconstituted HDL containing apoA-I was shown to have various anti-inflammatory and anti-oxidant functions and to play a role in the innate immune system in animal models of atherosclerosis or chronic inflammation [38]. We have shown recently that apoA-I$^{-/-}$ mice had exaggerated antigen-induced rheumatoid arthritis (RA) compared with wild-type mice and elevated Th1 and Th17 cell activity in the draining lymph nodes [39]. Importantly, we showed that treatment of stimulated lymphocytes with rHDL-apoA-I attenuated this rheumatic phenotype. The suppressive effects of rHDL-apoA-I on the immune cells were mediated by dendritic cells (DC) and required the SR-BI and the ABCA1 membrane transporters. Overall, our data supported a critical role of HDL in the regulation of adaptive inflammatory responses through inhibition of dendritic cell functions [39].

In light of the encouraging findings described above, we aimed at identifying key molecular players mediating the effects of rHDL-apoA-I in an effort to better understand its molecular functions and pinpoint potentially new therapeutic targets. As a starting point we selected an unbiased global screening approach involving whole transcriptome measurements following treatment of human aortic endothelial cells with rHDL-apoA-I. Among the 410 significant gene expression changes, corresponding to a range of molecular pathways and cellular functions, we focused on ANGPTL4 due to its multitier involvement in endothelial cell functions.

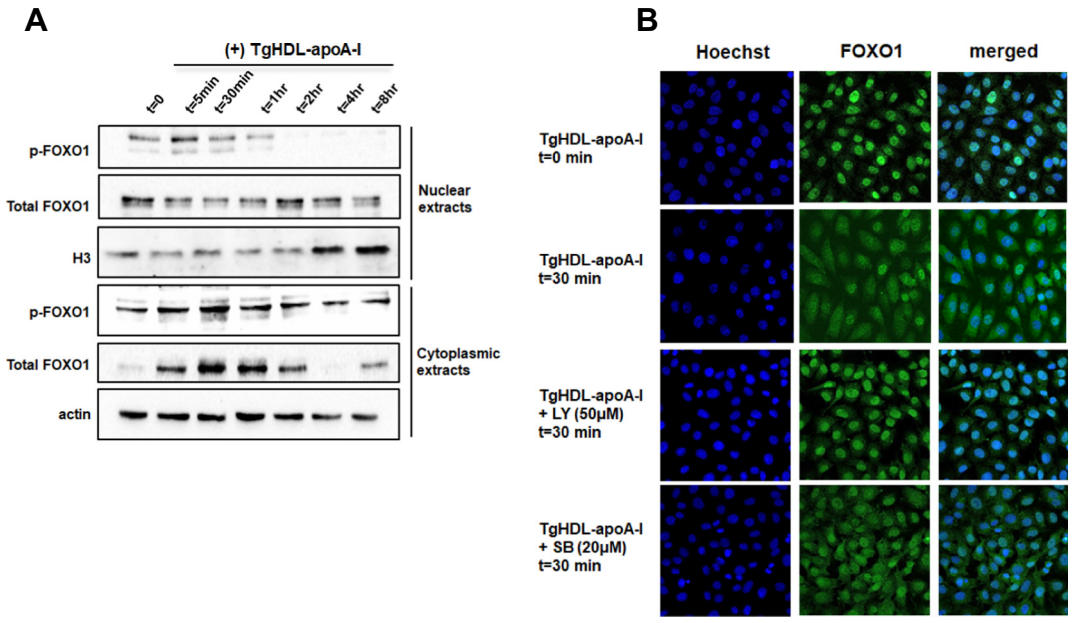

Fig. 6. HDL induces the phosphorylation of FOXO1 and its translocation to the cytoplasm. (A) EA.hy926 cells were treated with TgHDL-apoA-I (100 μg/ml) for the indicated time periods. Cell lysates were collected and the nuclear extracts were separated from the cytoplasmic extracts as described in Methods. The total and phosphorylated levels of FOXO1 in both nuclear and cytoplasmic extracts were determined by Western Blotting using the corresponding antibodies. The protein levels of histone H3 and actin were used as nuclear and cytoplasmic markers respectively. The experiment was performed three times and representative images are shown. (B) EA.hy926 cells were treated with TgHDL-apoA-I (100 μg/ml) in the absence and in the presence of the inhibitors LY (50 μM) or SB (20 μM) for the indicated time periods. The intracellular localization of FOXO1 was determined by immunofluorescence using an antibody for total FOXO1. Nuclei were stained with Hoechst dye. Confocal images were overlaid with Z-projection.

ANGPTL4 is a protein known primarily for its role as an inhibitor of lipoprotein lipase (LPL) [40]. As a result of its capacity to inhibit LPL, overexpression of ANGPTL4 in mice leads to hypertriglyceridemia, whereas its deficiency leads to reduced circulating lipids [41]. Studies in humans revealed that ANGPTL4 levels in plasma are directly associated with levels of insulin, fatty acids and leptin [42]. A genetic variant leading to loss of function of ANGPTL4 (E40K) was associated with increased coronary heart disease risk despite the atheroprotective lipid profile, suggesting that ANGPTL4 plays important atheroprotective roles that extend beyond its ability to control LPL [43]. However, the data of the DiscovEHR human genetics study [44] demonstrated that carriers of E40K and other inactivating mutations in ANGPTL4 had lower levels of triglycerides and a lower risk of coronary artery disease than did noncarriers.

Loss of endothelial integrity and functionality is one of the critical initiating events in atherosclerosis [45]. Although ANGPTL4 is widely expressed in endothelial cells, its role in endothelial cell integrity, vascular permeability and angiogenesis is controversial [46]. Some studies showed that ANGPTL4 protects endothelial cells from apoptosis [47] and inhibits the increase in vascular permeability caused by histamine [48]. However, another study reported that the C-terminal fibrinogen-like domain of ANGPTL4 (cANGPTL4) disrupted the integrity of the endothelium via its fibrinogen-like domain by weakening cell-cell contacts [49] suggesting that ANGPTL4 structure and proteolytic processing determines to a large extent its functions on the endothelium. The mechanism by which ANGPTL4 regulates endothelial permeability is under investigation. Data from previous studies suggest that ANGPTL4 inhibits VEGF signaling by prohibiting the recruitment of src to the VEGF receptor 2 via PI3 kinase/AKT signaling leading to decreased VE-cadherin phosphorylation and preserving vascular integrity [46]. Inhibition of src causes a reduction in myosin light chain kinase (MLCK) activity leading to reduced MLCK-dependent endothelial permeability [50,51]. In line with this model, we show that treatment of endothelial cells with TgHDL-apoA-I activates the PI3K/AKT pathway which leads to the induction of the ANGPTL4 gene. The subsequently secreted ANGPTL4 could act in an autocrine fashion to further enhance PI3K signaling and protect from endothelial permeability which is the primary cause of atherosclerosis and ischaemic stroke [46].

Furthermore, using a specific inhibitor of the transcriptional activity of FOXO1 and a potent FOXO1-specific siRNA we were able to demonstrate for the first time that FOXO1 is an inhibitor of ANGPTL4 gene expression in endothelial cells. TgHDL-apoA-I was found to induce the rapid phosphorylation of FOXO1 and its nuclear export, thus inhibiting FOXO1 nuclear activity and inducing ANGPTL4. A schematic representation of the proposed model of ANGPTL4 gene regulation by HDL and FOXO1 via the PI3K/AKT signaling pathway is shown in Fig. 8. Bioinformatics analysis of our microarray data revealed that FOXO1 is an upstream regulator for 29 of the significantly changed genes following rHDL-apoA-I treatment, including ANGPTL4 and other transcription factors (e.g. Jun and KLF4) (Table S5). Interestingly, half of the genes downstream of FOXO1 (15 genes) are upregulated by rHDL-apoA-I suggesting that inhibition of FOXO1 by rHDL-apoA-I may have a broader role in the regulation of endothelial gene expression.

The mechanism by which FOXO1 inhibits ANGPTL4 and possibly other genes is not known. Our IPA analysis predicted two pathways via which FOXO1 targets ANGPTL4: a direct and an indirect pathway via the PPAR gamma (PPARγ) nuclear receptor (Fig. S5). In a previous study it was shown that FOXO1 cooperates with the glucocorticoid receptor to induce the expression of ANGPTL4 in hepatic cells via binding to the corresponding response elements that are present in a region 6 kb downstream of the transcription start site of the ANGPTL4 gene [52]. Insulin inactivated FOXO1 via AKT and abolished glucocorticoid-induced ANGPTL4 gene upregulation [52]. An alternative mechanism of ANGPTL4 regulation by HDL could be via the nuclear receptor PPARγ. It was shown that PPARγ binds to a PPAR response element (PPRE) present inside the third intron of the human ANGPTL4 gene in 3T3L1 adipocytes [53]. In line with these findings, it was shown that a novel TGFβ-responsive upstream enhancer (TGF-E) in the human ANGPTL4 gene cooperates with an unusual PPARγ-responsive enhancer (PPAR-E) in the third intron of the gene to mediate synergistic ANGPTL4 upregulation by TGFβ and PPARγ ligands [54]. Interestingly, it was shown that FOXO1 can be converted from a transcriptional activator

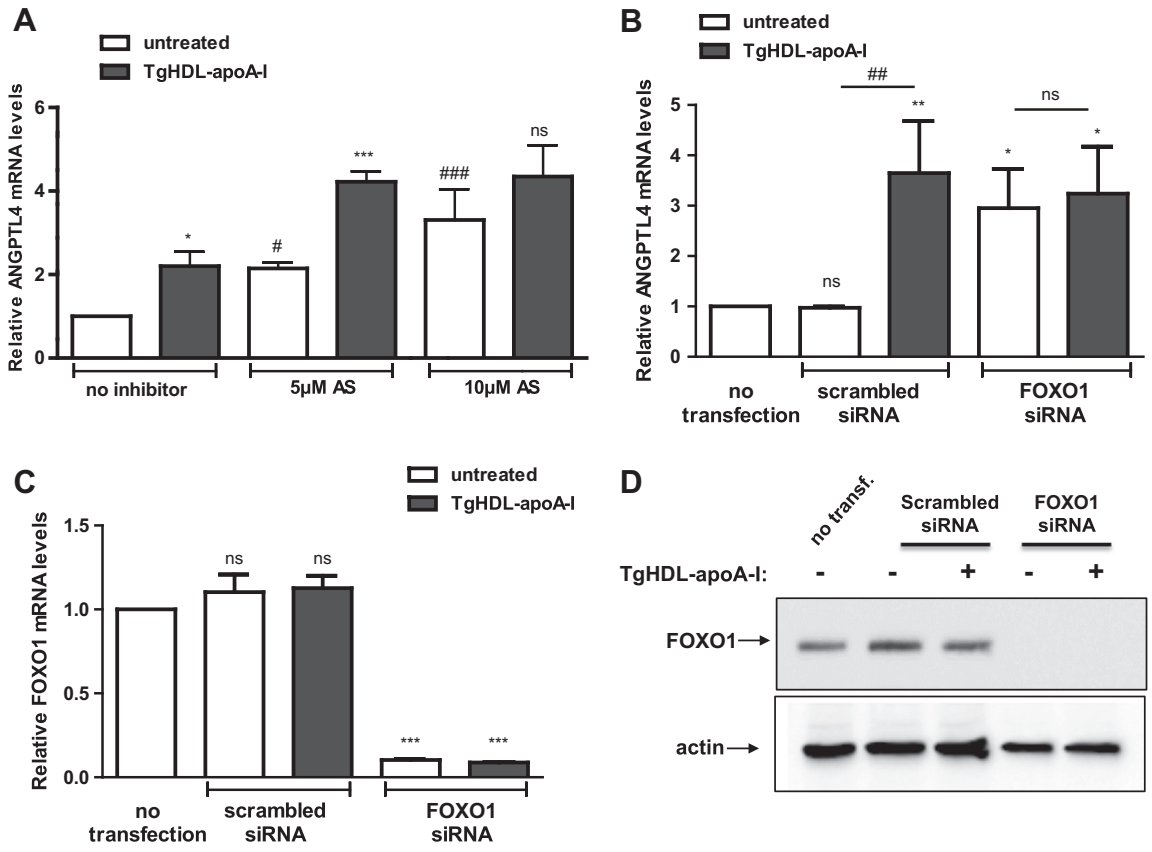

Fig. 7. FOXO1 inhibition or silencing increases ANGPTL4 mRNA levels and abolishes ANGPTL4 gene induction by HDL. (A) EA.hy926 cells were pre-treated for 1 h with an inhibitor of the transcription factor FOXO1 (AS1842856 indicated as AS) in two different concentrations (5 μM or 10 μM) or with DMSO (no inhibitor). Then 250 μg/ml of TgHDL-apoA-I or PBS (untreated) was added for additional 8 h. Total RNA was extracted and quantitative RT-PCR was performed to determine ANGPTL4 mRNA levels, which were normalized relative to the RPLPO mRNA levels. The relative ANGPTL4 mRNA levels are expressed as mean (±SD) from at least four independent experiments. (B–D) EA.hy926 cells were transfected with 100 nM of FOXO1 siRNA or with a control siRNA (scrambled) or non-transfected. Then, the endothelial cells were treated with 250 μg/ml of TgHDL-apoA-I or with PBS (untreated) for 8 h. Total RNA was extracted, and quantitative RT-PCR was performed to determine ANGPTL4 (B) and FOXO1 (C) mRNA levels, which were normalized relative to the RPLPO mRNA levels. The relative ANGPTL4 and FOXO1 mRNA levels are expressed as mean (±SD) from three independent experiments. Cell lysates were collected (D) and the protein levels of FOXO1 were determined by Western Blotting using the corresponding antibody. The protein levels of actin were used for normalization. The experiment was performed three times and representative images are shown. Symbols: ns, not significant; *, $p \le 0.05$; **, $p \le 0.01$; ***, $p \le 0.001$; #, $p \le 0.05$; ###, $p \le 0.001$. In panel A * indicates the statistical difference between the absence and the presence of TgHDL-apoA-I for each concentration of inhibitor or no inhibitor. # indicates the statistical difference between the absence and the presence of the FOXO1 inhibitor (in untreated cells only). In panels B and C * indicates the statistical difference between the transfected and the non-transfected cells and # indicates the statistical difference between treated (with TgHDL-apoA-I) and untreated cells.

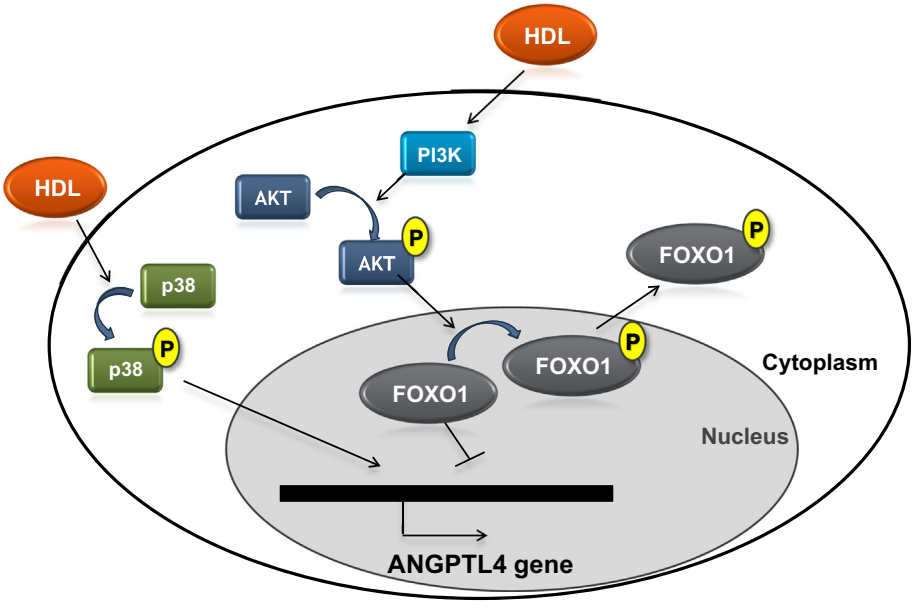

Fig. 8. Proposed mechanism through which HDL regulates the expression of the ANGPTL4 gene. See Discussion section for details.

to a transcriptional repressor in adipocytes by trans-repressing PPARγ through direct protein-protein interactions [55]. FOXO1 is recruited to PPRE on target genes and interferes with promoter DNA occupancy by PPARγ. Insulin prevents FOXO1-PPARγ interactions and rescues trans-repression [55]. Finally, a novel mechanism of FOXO1-mediated transcriptional repression was revealed in liver cells which is based on the recruitment of corepressors such as SIN3A and histone deacetylases to the promoters of FOXO1 target genes such as the glycolytic enzyme glucokinase (gck) via physical interactions with FOXO1 [56]. Interestingly, no FOXO1 binding site could be identified on the gck gene promoter and it was hypothesized that FOXO1 associates with the gck promoter indirectly via physical interactions with Hepatocyte Nuclear Factor 4 (HNF-4) which binds to the gck promoter in liver cells and activates its transcription [57].

The mechanism of ANGPTL4 gene upregulation by HDL that was described in the present study (via a PI3K/AKT/FOXO1 signaling pathway) may be cell context-specific. For instance, FOXO1 could repress ANGPTL4 gene expression by recruiting a corepressor such as a histone deacetylase that is present in endothelial cells but is absent in other cell types such as the liver or the adipose tissue. In the liver, FOXO1 activates the ANGPTL4 gene by synergizing with the glucocorticoid receptor as described above whereas insulin, by phosphorylating and inhibiting FOXO1, decreases ANGPTL4 gene expression [52]. Inhibition of ANGPTL4 by insulin in the liver or the adipose tissue, the major sites of ANGPTL4 production, could lead to increased LPL activity in the plasma and decreased levels of TGs. In contrast, insulin resistance could result in loss of AKT activation and nuclear accumulation of FOXO1 thus increasing ANGPTL4 gene expression and plasma TGs. In line with these observations, it was shown that levels of circulating ANGPTL4 are increased in patients with the metabolic syndrome which is characterized by obesity, high levels of TGs and insulin resistance [58]. Interestingly, the association between plasma ANGPTL4 levels and glucose levels or type II diabetes is not consistent [58–60] for reasons that are still unknown.

The main strength of our study is that by using an unbiased global screening approach, we identified several genes that respond to HDL in endothelial cells, which could mediate the atheroprotective functions of this lipoprotein and could be exploited for therapeutic purposes. The main limitation of our study is that the treatments and the transcriptomics were done in endothelial cells in culture which do not accurately replicate the environment of arterial endothelial cells in vivo such as exposure to pressure, strain and shear stress waveforms associated with both normal flow seen in normal sections of arteries and disturbed flow seen atherosclerosis lesions. Another limitation is that by focusing on reconstituted HDL due to its important therapeutic potential we may have missed changes in endothelial gene expression in response to other bioactive components which are present in natural HDL such as sphingolipids.

Our work has important clinical implications. The first implication comes from the novel finding that FOXO1 is a key mediator of the genomic responses of endothelial cells to rHDL-apoA-I that is currently considered as a promising therapeutic tool for patients with CAD. It was recently shown that FOXO1 is an essential regulator of vascular growth that couples glucose metabolism and mitochondrial oxidation with cell proliferation in endothelial cells [30]. It was shown that FOXO1 activation suppresses endothelial cell growth by inhibiting the c-MYC oncogene, whereas FOXO1 silencing enhances proliferation [30]. These novel findings suggest that suppression of FOXO1 by HDL-apoA-I could be required for the growth-promoting activity of HDL in endothelial cells that was described in previous studies [3]. In support to this notion, in our microarray analysis cell cycle and cell growth/proliferation were among the most significantly modulated functions (Fig. 2).

A second clinical implication is related to the potential utilization of ANGPTL4 as a biomarker of CAD or as a marker for endothelial or macrophage activation. Indeed, plasma levels of ANGPTL4, which is produced mainly in the liver or the adipose tissue, have been shown to be a risk factor for coronary heart disease independently of other traditional risk factors [58]. However, ANGPTL4 is also expressed in endothelial cells and macrophages and ANGPTL4 protein was detectable in macrophages of human atherosclerotic lesions [61]. Furthermore, overexpression of ANGPTL4 in apoE3.Leiden mice reduced atherosclerosis by 34% by decreasing the macrophage content of the plaques and the number of monocytes adhering to the endothelium [61]. Thus, overexpression of ANGPTL4 leads to a less inflammatory lesion phenotype. In a recent study it was shown that ANGPTL4 deficiency in haematopoietic cells promotes monocyte expansion and atherosclerosis progression [62]. Specifically, it was shown that ANGPTL4 was the most highly upregulated gene in macrophage foam cells and its deletion in haematopoietic cells resulted in larger plaque area with bigger necrotic core and increased macrophage apoptosis. Furthermore, ANGPTL4 deficiency in macrophages promoted foam cell formation by enhancing CD36 expression and reducing ABCA1 localization in the cell surface [62]. Based on the above studies, it could be suggested that low levels of ANGPTL4 in macrophages could be used as a marker for predisposition to atherosclerotic cardiovascular disease. More work needs to be done towards the potential utilization of ANGPTL4 (full length or the proteolytically processed form) as markers of endothelial cell activation in patients with CAD due to the controversial effects of ANGPTL4 on endothelial integrity, vascular permeability and angiogenesis as described above.

In conclusion, the global gene expression changes induced by rHDL-apoA-I that were identified in this study, the identification of ANGPTL4 as one of the most biologically relevant target genes and the elucidation of the key role of FOXO1 in HDL-mediated atheroprotection could be exploited for the design of novel therapeutic tools for patients with atherosclerotic cardiovascular disease.

Supplementary data to this article can be found online at https://doi.org/10.1016/j.metabol.2018.06.002.

Author Contributions

VZ, DS and DK conceived and designed the study. PF performed the microarray experiments and the initial validations. DT performed all the experiments on the regulation of ANGPTL4 by HDL. EV and DS performed the bioinformatics analysis of the microarray data. DK and DS interpreted the data and wrote the manuscript. All authors read and approved the manuscript.

Funding

This work was supported by a grant from the Hellenic Ministry for Education, Research and Religious Affairs (THALIS MIS 377286) to DK and DS.

Conflict of Interest

All authors declare no conflict of interest.

Acknowledgments

We would like to thank the members of Kardassis lab Katerina Karagouni-Dalakoura and Veta Papakosta for assistance with mice, Dr. Kanelina Karali for assistance with the confocal microscope and members of Kardassis and Sanoudou labs for assistance with protocols and useful suggestions.

References

[1] Gordon DJ, Probstfield JL, Garrison RJ, Neaton JD, Castelli WP, Knoke JD, et al. High-density lipoprotein cholesterol and cardiovascular disease. Four prospective American studies. Circulation 1989;79:8–15.

[2] Vergeer M, Holleboom AG, Kastelein JJ, Kuivenhoven JA. The HDL hypothesis: does high-density lipoprotein protect from atherosclerosis? J Lipid Res 2010;51:2058–73.
[3] Luscher TF, Landmesser U, von Eckardstein A, Fogelman AM. High-density lipoprotein: vascular protective effects, dysfunction, and potential as therapeutic target. Circ Res 2014;114:171–82.
[4] Hutchins PM, Heinecke JW. Cholesterol efflux capacity, macrophage reverse cholesterol transport and cardioprotective HDL. Curr Opin Lipidol 2015;26:388–93.
[5] Riwanto M, Rohrer L, von Eckardstein A, Landmesser U. Dysfunctional HDL: from structure-function-relationships to biomarkers. Handb Exp Pharmacol 2015;224:337–66.
[6] Shah AS, Tan L, Long JL, Davidson WS. Proteomic diversity of high density lipoproteins: our emerging understanding of its importance in lipid transport and beyond. J Lipid Res 2013;54:2575–85.
[7] Kontush A, Lhomme M, Chapman MJ. Unraveling the complexities of the HDL lipidome. J Lipid Res 2013;54:2950–63.
[8] Khaddaj Mallat R, Mathew John C, Kendrick DJ, Braun AP. The vascular endothelium: a regulator of arterial tone and interface for the immune system. Crit Rev Clin Lab Sci 2017;54:458–70.
[9] Rosenson RS, Brewer Jr HB, Ansell BJ, Barter P, Chapman MJ, Heinecke JW, et al. Dysfunctional HDL and atherosclerotic cardiovascular disease. Nat Rev Cardiol 2016;13:48–60.
[10] Suc I, Escargueil-Blanc I, Troly M, Salvayre R, Negre-Salvayre A. HDL and ApoA prevent cell death of endothelial cells induced by oxidized LDL. Arterioscler Thromb Vasc Biol 1997;17:2158–66.
[11] Sugano M, Tsuchida K, Makino N. High-density lipoproteins protect endothelial cells from tumor necrosis factor-alpha-induced apoptosis. Biochem Biophys Res Commun 2000;272:872–6.
[12] Nofer JR, Levkau B, Wolinska I, Junker R, Fobker M, von Eckardstein A, et al. Suppression of endothelial cell apoptosis by high density lipoproteins (HDL) and HDL-associated lysosphingolipids. J Biol Chem 2001;276:34480–5.
[13] Werner N, Junk S, Laufs U, Link A, Walenta K, Bohm M, et al. Intravenous transfusion of endothelial progenitor cells reduces neointima formation after vascular injury. Circ Res 2003;93:e17–24.
[14] Ramet ME, Ramet M, Lu Q, Nickerson M, Savolainen MJ, Malzone A, et al. High-density lipoprotein increases the abundance of eNOS protein in human vascular endothelial cells by increasing its half-life. J Am Coll Cardiol 2003;41:2288–97.
[15] Nofer JR. Signal transduction by HDL: agonists, receptors, and signaling cascades. Handb Exp Pharmacol 2015;224:229–56.
[16] Mineo C, Shaul PW. Regulation of signal transduction by HDL. J Lipid Res 2013;54:2315–24.
[17] Borup A, Christensen PM, Nielsen LB, Christoffersen C. Apolipoprotein M in lipid metabolism and cardiometabolic diseases. Curr Opin Lipidol 2015;26:48–55.
[18] Nicholls SJ, Tuzcu EM, Sipahi I, Schoenhagen P, Crowe T, Kapadia S, et al. Relationship between atheroma regression and change in lumen size after infusion of apolipoprotein A-I Milano. J Am Coll Cardiol 2006;47:992–7.
[19] Nissen SE, Tsunoda T, Tuzcu EM, Schoenhagen P, Cooper CJ, Yasin M, et al. Effect of recombinant ApoA-I Milano on coronary atherosclerosis in patients with acute coronary syndromes: a randomized controlled trial. JAMA 2003;290:2292–300.
[20] Nicholls SJ, Dusting GJ, Cutri B, Bao S, Drummond GR, Rye KA, et al. Reconstituted high-density lipoproteins inhibit the acute pro-oxidant and proinflammatory vascular changes induced by a periarterial collar in normocholesterolemic rabbits. Circulation 2005;111:1543–50.
[21] Shah PK, Nilsson J, Kaul S, Fishbein MC, Ageland H, Hamsten A, et al. Effects of recombinant apolipoprotein A-I(Milano) on aortic atherosclerosis in apolipoprotein E-deficient mice. Circulation 1998;97:780–5.
[22] Shaw JA, Bobik A, Murphy A, Kanellakis P, Blombery P, Mukhamedova N, et al. Infusion of reconstituted high-density lipoprotein leads to acute changes in human atherosclerotic plaque. Circ Res 2008;103:1084–91.
[23] Murphy AJ, Woollard KJ, Hoang A, Mukhamedova N, Stirzaker RA, McCormick SP, et al. High-density lipoprotein reduces the human monocyte inflammatory response. Arterioscler Thromb Vasc Biol 2008;28:2071–7.
[24] Drew BG, Duffy SJ, Formosa MF, Natoli AK, Henstridge DC, Penfold SA, et al. High-density lipoprotein modulates glucose metabolism in patients with type 2 diabetes mellitus. Circulation 2009;119:2103–11.
[25] Nanjee MN, Doran JE, Lerch PG, Miller NE. Acute effects of intravenous infusion of ApoA1/phosphatidylcholine discs on plasma lipoproteins in humans. Arterioscler Thromb Vasc Biol 1999;19:979–89.
[26] Tiniakou I, Kanaki Z, Georgopoulos S, Chroni A, Van Eck M, Fotakis P, et al. Natural human apoA-I mutations L141RPisa and L159RFIN alter HDL structure and functionality and promote atherosclerosis development in mice. Atherosclerosis 2015;243:77–85.
[27] Laccotripe M, Makrides SC, Jonas A, Zannis VI. The carboxyl-terminal hydrophobic residues of apolipoprotein A-I affect its rate of phospholipid binding and its association with high density lipoprotein. J Biol Chem 1997;272:17511–22.
[28] Georgopoulos S, Kan HY, Reardon-Alulis C, Zannis V. The SP1 sites of the human apoCIII enhancer are essential for the expression of the apoCIII gene and contribute to the hepatic and intestinal expression of the apoA-I gene in transgenic mice. Nucleic Acids Res 2000;28:4919–29.
[29] Tzivion G, Dobson M, Ramakrishnan G. FoxO transcription factors; regulation by AKT and 14-3-3 proteins. Biochim Biophys Acta 2011;1813:1938–45.
[30] Wilhelm K, Happel K, Eelen G, Schoors S, Oellerich MF, Lim R, et al. FOXO1 couples metabolic activity and growth state in the vascular endothelium. Nature 2016;529:216–20.
[31] Edgell CJ, McDonald CC, Graham JB. Permanent cell line expressing human factor VIII-related antigen established by hybridization. Proc Natl Acad Sci U S A 1983;80:3734–7.
[32] Mandard S, Zandbergen F, van Straten E, Wahli W, Kuipers F, Muller M, et al. The fasting-induced adipose factor/angiopoietin-like protein 4 is physically associated with lipoproteins and governs plasma lipid levels and adiposity. J Biol Chem 2006;281:934–44.
[33] Nagashima T, Shigematsu N, Maruki R, Urano Y, Tanaka H, Shimaya A, et al. Discovery of novel forkhead box O1 inhibitors for treating type 2 diabetes: improvement of fasting glycemia in diabetic db/db mice. Mol Pharmacol 2010;78:961–70.
[34] Tardif JC, Gregoire J, L'Allier PL, Ibrahim R, Lesperance J, Heinonen TM, et al. Effects of reconstituted high-density lipoprotein infusions on coronary atherosclerosis: a randomized controlled trial. JAMA 2007;297:1675–82.
[35] Spieker LE, Sudano I, Hurlimann D, Lerch PG, Lang MG, Binggeli C, et al. High-density lipoprotein restores endothelial function in hypercholesterolemic men. Circulation 2002;105:1399–402.
[36] Tricoci P, D'Andrea DM, Gurbel PA, Yao Z, Cuchel M, Winston B, et al. Infusion of reconstituted high-density lipoprotein, CSL112, in patients with atherosclerosis: safety and pharmacokinetic results from a phase 2a randomized clinical trial. J Am Heart Assoc 2015;4:e002171.
[37] Michael Gibson C, Korjian S, Tricoci P, Daaboul Y, Yee M, Jain P, et al. Safety and tolerability of CSL112, a reconstituted, infusible, plasma-derived apolipoprotein A-I, after acute myocardial infarction: the AEGIS-I trial (ApoA-I Event Reducing in Ischemic Syndromes I). Circulation 2016;134:1918–30.
[38] Murphy AJ, Chin-Dusting J, Sviridov D. Reconstituted HDL: a therapy for atherosclerosis and beyond. Clin Lipidol 2009;4:731–9.
[39] Tiniakou I, Drakos E, Sinatkas V, Van Eck M, Zannis VI, Boumpas D, et al. High-density lipoprotein attenuates Th1 and th17 autoimmune responses by modulating dendritic cell maturation and function. J Immunol 2015;194:4676–87.
[40] Dijk W, Kersten S. Regulation of lipid metabolism by angiopoietin-like proteins. Curr Opin Lipidol 2016;27:249–56.
[41] Koster A, Chao YB, Mosior M, Ford A, Gonzalez-DeWhitt PA, Hale JE, et al. Transgenic angiopoietin-like (angptl)4 overexpression and targeted disruption of angptl4 and angptl3: regulation of triglyceride metabolism. Endocrinology 2005;146:4943–50.
[42] Romeo S, Pennacchio LA, Fu Y, Boerwinkle E, Tybjaerg-Hansen A, Hobbs HH, et al. Population-based resequencing of ANGPTL4 uncovers variations that reduce triglycerides and increase HDL. Nat Genet 2007;39:513–6.
[43] Talmud PJ, Smart M, Presswood E, Cooper JA, Nicaud V, Drenos F, et al. ANGPTL4 E40K and T266M: effects on plasma triglyceride and HDL levels, postprandial responses, and CHD risk. Arterioscler Thromb Vasc Biol 2008;28:2319–25.
[44] Dewey FE, Gusarova V, O'Dushlaine C, Gottesman O, Trejos J, Hunt C, et al. Inactivating variants in ANGPTL4 and risk of coronary artery disease. N Engl J Med 2016;374:1123–33.
[45] Sitia S, Tomasoni L, Atzeni F, Ambrosio G, Cordiano C, Catapano A, et al. From endothelial dysfunction to atherosclerosis. Autoimmun Rev 2010;9:830–4.
[46] Xu L, Guo ZN, Yang Y, Xu J, Burchell SR, Tang J, et al. Angiopoietin-like 4: a double-edged sword in atherosclerosis and ischemic stroke? Exp Neurol 2015;272:61–6.
[47] Kim I, Kim HG, Kim H, Kim HH, Park SK, Uhm CS, et al. Hepatic expression, synthesis and secretion of a novel fibrinogen/angiopoietin-related protein that prevents endothelial-cell apoptosis. Biochem J 2000;346(Pt 3):603–10.
[48] Galaup A, Cazes A, Le Jan S, Philippe J, Connault E, Le Coz E, et al. Angiopoietin-like 4 prevents metastasis through inhibition of vascular permeability and tumor cell motility and invasiveness. Proc Natl Acad Sci U S A 2006;103:18721–6.
[49] Huang RL, Teo Z, Chong HC, Zhu P, Tan MJ, Tan CK, et al. ANGPTL4 modulates vascular junction integrity by integrin signaling and disruption of intercellular VE-cadherin and claudin-5 clusters. Blood 2011;118:3990–4002.
[50] Dudek SM, Birukov KG, Zhan X, Garcia JG. Novel interaction of cortactin with endothelial cell myosin light chain kinase. Biochem Biophys Res Commun 2002;298:511–9.
[51] Rigor RR, Shen Q, Pivetti CD, Wu MH, Yuan SY. Myosin light chain kinase signaling in endothelial barrier dysfunction. Med Res Rev 2013;33:911–33.
[52] Kuo T, Chen TC, Yan S, Foo F, Ching C, McQueen A, et al. Repression of glucocorticoid-stimulated angiopoietin-like 4 gene transcription by insulin. J Lipid Res 2014;55:919–28.
[53] Mandard S, Zandbergen F, Tan NS, Escher P, Patsouris D, Koenig W, et al. The direct peroxisome proliferator-activated receptor target fasting-induced adipose factor (FIAF/PGAR/ANGPTL4) is present in blood plasma as a truncated protein that is increased by fenofibrate treatment. J Biol Chem 2004;279:34411–20.
[54] Kaddatz K, Adhikary T, Finkernagel F, Meissner W, Muller-Brusselbach S, Muller R. Transcriptional profiling identifies functional interactions of TGF beta and PPAR beta/delta signaling: synergistic induction of ANGPTL4 transcription. J Biol Chem 2010;285:29469–79.
[55] Fan W, Imamura T, Sonoda N, Sears DD, Patsouris D, Kim JJ, et al. FOXO1 transrepresses peroxisome proliferator-activated receptor gamma transactivation, coordinating an insulin-induced feed-forward response in adipocytes. J Biol Chem 2009;284:12188–97.
[56] Langlet F, Haeusler RA, Linden D, Ericson E, Norris T, Johansson A, et al. Selective inhibition of FOXO1 activator/repressor balance modulates hepatic glucose handling. Cell 2017;171:824–835.e18.
[57] Hirota K, Sakamaki J, Ishida J, Shimamoto Y, Nishihara S, Kodama N, et al. A combination of HNF-4 and Foxo1 is required for reciprocal transcriptional regulation of glucokinase and glucose-6-phosphatase genes in response to fasting and feeding. J Biol Chem 2008;283:32432–41.
[58] Muendlein A, Saely CH, Leiherer A, Fraunberger P, Kinz E, Rein P, et al. Angiopoietin-like protein 4 significantly predicts future cardiovascular events in coronary patients. Atherosclerosis 2014;237:632–8.

[59] Mehta N, Qamar A, Qu L, Qasim AN, Mehta NN, Reilly MP, et al. Differential association of plasma angiopoietin-like proteins 3 and 4 with lipid and metabolic traits. Arterioscler Thromb Vasc Biol 2014;34:1057–63.
[60] Xu A, Lam MC, Chan KW, Wang Y, Zhang J, Hoo RL, et al. Angiopoietin-like protein 4 decreases blood glucose and improves glucose tolerance but induces hyperlipidemia and hepatic steatosis in mice. Proc Natl Acad Sci U S A 2005;102:6086–91.
[61] Georgiadi A, Wang Y, Stienstra R, Tjeerdema N, Janssen A, Stalenhoef A, et al. Overexpression of angiopoietin-like protein 4 protects against atherosclerosis development. Arterioscler Thromb Vasc Biol 2013;33:1529–37.
[62] Aryal B, Rotllan N, Araldi E, Ramirez CM, He S, Chousterman BG, et al. ANGPTL4 deficiency in haematopoietic cells promotes monocyte expansion and atherosclerosis progression. Nat Commun 2016;7:12313.

Biochemical and Biophysical Research Communications 469 (2016) 573–579

Contents lists available at ScienceDirect

Biochemical and Biophysical Research Communications

journal homepage: www.elsevier.com/locate/ybbrc

Transcriptional regulation of the human Liver X Receptor α gene by Hepatocyte Nuclear Factor 4α

Dimitris Theofilatos [a], Aristomenis Anestis [a], Koshi Hashimoto [b], Dimitris Kardassis [a, *]

[a] University of Crete Medical School and Institute of Molecular Biology and Biotechnology, Foundation for Research and Technology of Hellas, Heraklion, 71003, Crete, Greece

[b] Department of Preemptive Medicine and Metabolism, Tokyo Medical and Dental University, 1-5-45 Yushima, Bunkyo-city, Tokyo, 113-8510, Japan

ARTICLE INFO

Article history:
Received 27 November 2015
Accepted 8 December 2015
Available online 12 December 2015

Keywords:
LXR
HNF-4α
Gene regulation
HDL
Oxysterols

ABSTRACT

Liver X Receptors (LXRs) are sterol-activated transcription factors that play major roles in cellular cholesterol homeostasis, HDL biogenesis and reverse cholesterol transport. The aim of the present study was to investigate the mechanisms that control the expression of the human LXRα gene in hepatic cells. A series of reporter plasmids containing consecutive 5′ deletions of the hLXRα promoter upstream of the luciferase gene were constructed and the activity of each construct was measured in HepG2 cells. This analysis showed that the activity of the human LXRα promoter was significantly reduced by deleting the −111 to −42 region suggesting the presence of positive regulatory elements in this short proximal fragment. Bioinformatics data including motif search and ChIP-Seq revealed the presence of a potential binding motif for Hepatocyte Nuclear Factor 4 α (HNF-4α) in this area. Overexpression of HNF-4α in HEK 293T cells increased the expression of all LXRα promoter constructs except −42/+384. In line, silencing the expression of endogenous HNF-4α in HepG2 cells was associated with reduced LXRα protein levels and reduced activity of the −111/+384 LXRα promoter but not of the −42/+384 promoter. Using ChiP assays in HepG2 cells combined with DNAP assays we mapped the novel HNF-4α specific binding motif (H4-SBM) in the −50 to −40 region of the human LXRα promoter. A triple mutation in this H4-SBM abolished HNF-4α binding and reduced the activity of the promoter to 65% relative to the wild type. Furthermore, the mutant promoter could not be transactivated by HNF-4α. In conclusion, our data indicate that HNF-4α may have a wider role in cell and plasma cholesterol homeostasis by controlling the expression of LXRα in hepatic cells.

1. Introduction

Liver X receptors (LXRs) are members of the hormone nuclear receptor superfamily of transcription factors with key roles in intracellular and plasma cholesterol homeostasis [1]. LXRs can be activated either by natural products of cholesterol metabolism (oxysterols) or by synthetic compounds such as T0901317 [2]. There are two LXR isoforms, LXRα and LXRβ, sharing almost 80% amino acid identity in their DNA-binding and ligand-binding domains [3]. Experiments in cell cultures and in mice have shown that synthetic LXR ligands promote the efflux of cholesterol from macrophage to extracellular acceptors by up-regulating the genes encoding the membrane lipid transporters ATP Binding Cassette Transporters A1 (ABCA1) and ABCG1 [4]. In the liver, LXRs are strong inducers of hepatic lipogenesis due to the transcriptional up-regulation of Sterol Regulatory Element Binding Protein 1c (SREBP-1c) gene [5]. LXRα is expressed primarily in the liver, intestine, adipose tissue, and macrophages, whereas LXRβ is widely expressed [6]. It has been shown previously that the expression of LXRα in the liver is subject to regulation by dietary fatty acids [7] and by thyroid

Abbreviations: ABCA1, ATP Binsing Cassette Transporter A1; ChIP, Chromatin Immunoprecipitation; ChIP-seq, Chromatin Immunoprecipitation followed by sequencing; DNAP, DNA Affinity Precipitation; HNF-4, Hepatocyte Nuclear Factor 4; H4-SBM, HNF-4 specific binding motif; HRE, Hormone Response Element; LXRs, Liver X Receptors; NR, Nuclear Receptor; PPAR, Peroxisome Proliferator-Activated Receptor; RCT, Reverse Cholesterol Transport; shRNA, Short hairpin RNA; siRNA, Short interfering RNA; SREBP-1c, Sterol Regulatory Element Binding Protein 1c.

* Corresponding author. Laboratory of Biochemistry, Department of Basic Sciences, University of Crete Medical School and Institute of Molecular Biology and Biotechnology, Foundation for Research and Technology of Hellas, 71003, Heraklion, Greece.

E-mail address: kardasis@imbb.forth.gr (D. Kardassis).

http://dx.doi.org/10.1016/j.bbrc.2015.12.031
0006-291X/

hormone [8]. In macrophages, the expression of LXRα, but not LXRβ, is induced by synthetic PPARγ ligands via a PPAR response element located in the distal region of the mouse LXR promoter [9]. This distal region also contains LXR responsive elements (LXREs) that have been shown to play a role in the autoregulation of the LXRα gene in macrophages (Fig. 1A) [10].

Hepatocyte Nuclear factor 4α (HNF-4α) is an orphan member of the nuclear receptor superfamily that is expressed mainly in the liver but also in kidney, intestine and pancreas [11]. In humans, heterozygous mutations in the HNF-4α gene are associated with an early-onset form of type II diabetes called maturity onset diabetes of the young 1 [12]. Work from our group and others showed that HNF-4α binds to the promoters of various genes involved in lipid and lipoprotein metabolism [13]. HNF-4α can bind to Hormone Response Elements of the direct depeat with one nucleotide in the spacer region (DR-1) type almost exclusively as a homodimer [14]. However, a systematic examination of the DNA binding specificity of HNF-4 using protein-binding microarrays (PBMs) revealed a novel HNF-4-specific binding motif (H4-SBM) having the consensus sequence 5′ xxxxCAAAGTCCA 3′ [14] and by Chromatin Immunoprecipitation followed by sequencing (ChIP-seq) analysis it was shown that this H4-SBM is uniquely bound by HNF-4α in vivo [14].

In the present study we show that the human and the mouse LXRα genes are targets of HNF-4α in hepatic cells. We identified a novel and conserved H4-SBM in the proximal promoter of the human LXRα gene and we validated this site as a true HNF-4α responsive element using *in vitro* and *ex vivo* techniques. Furthermore, we show that silencing of the endogenous HNF-4α gene in hepatocytes was associated with a reduction in protein levels of LXRα and the activity of the LXRα promoter. These data support a novel role of HNF-4α in cell and plasma cholesterol homeostasis through LXRα.

2. Materials and methods

2.1. Plasmid constructions

The luciferase reporter constructs (−2625/+384)-hLXRα and (−3000/+30)-mLXRα, the sh-HNF-4α and sh-control expression vectors and the pMT2-HNF-4α plasmid have been described previoulsy [8,15,16]. All other reporter vectors were generated by standard cloning procedures as described in the Supplement. Oligonucleotides used as primers in PCR cloning or in mutagenesis are shown in Table 1.

2.2. Cell cultures, transient transfections, treatments, and luciferase and β-galactosidase assays

Human embryonic kidney cells (HEK293T) and human hepatoma HepG2 cells were obtained from ATCC and cultured in Dulbecco's modified Eagle's medium supplemented with 10% fetal bovine serum, L-glutamine, and penicillin/streptomycin at 37 °C in a 5% CO_2 atmosphere. Transient transfections were performed using the $Ca_3(PO_4)_2$ coprecipitation method. For co-transfection experiments with siRNAs, the Attractene transfection reagent (Qiagen) was used according to the manufacturer's instruction. Luciferase assays were performed using the luciferase assay kit from Promega Corp. according to the manufacturer's instructions. Normalization for transfection efficiency was performed by β-galactosidase assays.

2.3. Chromatin immunoprecipitation

Chromatin immunoprecipitation (ChIP) assays were performed as described previously [17] using the SYBR-Green quantitative PCR (KAPA SYBR® FAST qPCR) kit and the StepOnePlus™ Real-Time PCR System (Applied Biosystems) according ot the manufacturer's

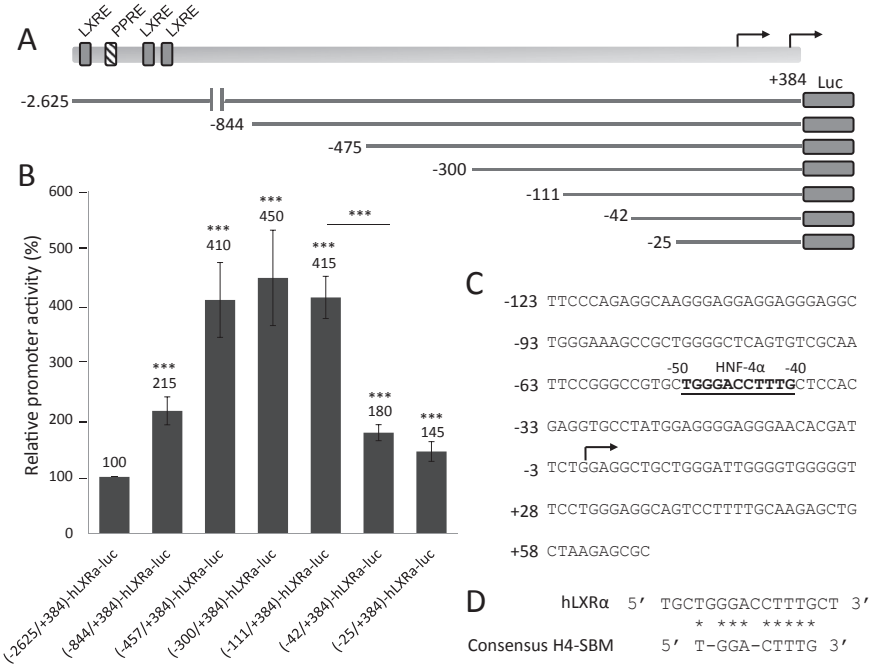

Fig. 1. The human LXRα promoter contains a putative HNF-4α specific binding motif. (A) Schematic representation of the hLXRα promoter. The two transcription start sites, the distal LXREs and the PPRE are depicted. The hLXRα promoter fragments which were used in transfection experiments are shown at the bottom. (B) HepG2 cells were transiently transfected with the hLXRα promoter constructs indicated along with a β-galactosidase expression vector. The normalized relative promoter activity (±SD) was calculated from at least three independent experiments performed in duplicate. (C) Sequence of the proximal hLXRα promoter region spanning nucleotides −123 to +67. The putative HNF-4α binding site in the −50/−40 region of hLXRα promoter is underlined and in bold. (D) Homology of the putative HNF-4 binding site in the −50/−40 region of the human LXRα promoter with the consensus H4-SBM. Identity in the nucleotide sequence is indicated with the asterisks. Key: ***, $p < 0.0001$ by t-testing.

Table 1
Primers used in cloning, mutagenesis, ChIP and DNAP assays.

Name	Sequence	Purpose
−457-hLXRa - FW	5′ - CGGGGTACCCTATAGTCTCAGTAGCTG - 3′	Cloning of the hLXRα promoter, position −457, forward primer
−300-hLXRa - FW	5′ - CGGGGTACCACTGCTCATAGCAGATTT - 3′	Cloning of the hLXRα promoter, position −300, forward primer
−111-hLXRa - FW	5′ - GGGTACCAAGGGAGGAGGAGGGAGG - 3′	Cloning of the hLXRα promoter, position −111, forward primer
−42-hLXRa - FW	5′ - GGGTACCTTTGCTCCACGAGGTGCCTA - 3′	Cloning of the hLXRα promoter, position −42, forward primer
−25-hLXRa - FW	5′ - 5′- GGGGTACCCTATGGAGGGGAGGGAA -3′ - 3′	Cloning of the hLXRα promoter, position −25, forward primer
+384-hLXRa - FW	5′ - CCAAGCTTTGTCCAGAAGTCTCGGT -3′	Cloning of the hLXRα promoter, position +384, reverse primer
+384-hLXRa-bio	5′ - bio TGTCCAGAAGTCTCGGTGGC -3′	DNAP, hLXRα promoter, position +384 reverse primer, 5′ biotinylated
−147-hLXRa-ChIP-FW	5′ - CTAGTGGGGAGAGCTTCTTGG -3′	ChIP, hLXRα promoter, position −147, forward primer
+78-hLXRa-ChIP-Rev	5′ - CTCCTTACCCAGCGCTCTTAG -3′	ChIP, hLXRα promoter, position +78, reverse primer
+3461-hLXRa-ChIP-FW	5′ - ATTTGGCCCTGTCCTTAGGTG T -3′	ChIP, hLXRα promoter, position +3461, forward primer
+3694-hLXRa-ChIP-Rev	5′ - CAAGTACCGTGACTCGAAGCC - 3′	ChIP, hLXRα promoter, position +3694, reverse primer
−52/-23-hLXRa-bio FW	5′ - bio TGCTGGGACCTTTGCTCCACGAGGTGCCTA -3′	DNAP, hLXRα promoter, position −52/-23, sense strand, 5′ biotinylated
−52/-23-hLXRa REV	5′ - TAGGCACCTCGTGGAGCAAAGGTCCCAGCA - 3′	DNAP and mutagenesis, hLXRα promoter, position −52/-23, anti-sense strand
−52/-23-hLXRa-bio mut FW	5′ - bio TGCTGGGATATCTGCTCCACGAGGTGCCTA - 3′	DNAP, hLXRα promoter, position −52/-23, mutated, sense strand, 5′ biotinylated
−52/-23-hLXRa mut FW	5′ - TAGGCACCTCGTGGAGCAGATATCCCAGCA - 3′	DNAP, hLXRα promoter, position −52/-23, mutated, anti-sense strand
−52/-23-hLXRa-FW	5′ - bio TGCTGGGACCTTTGCTCCACGAGGTGCCTA -3′	mutagenesis, hLXRα promoter, position −52/−23, sense strand

KpnI (GGTACC) and *HINDIII* (AAGCTT) restriction sites are underlined.

instructions. The CT values of the ChIP signals detected by real-time PCR were converted to the percentage of the input DNA using the "percent input method" as recommended by the manufacturer. All oligonucleotides used as primers in these assays are shown in Table 1.

2.4. DNA affinity precipitation

For the *in vitro* identificaton of DNA-protein interactions, we performed DNA affinity precipitation (DNAP) utilizing nuclear extracts from HepG2 cells and biotinylated PCR products or biotynylated oligonucleotides as described previously [17]. The complete protocol is decribed in the Supplement. All oligonucleotides used for DNA affinity prepcipitation assays are depicted in Table 1.

2.5. RNA interference

HepG2 cells were transfected with scrambled siRNA (5′-UGCGCUAGGCCUCGGUUGC -3′) or siRNA against HNF-4α (5′-AAAGCGGCCACGCGAGUCAUACUGG -3′) using the Hiperfect transfection reagent (Qiagen) according to the manufacturer's instructions. The silencing efficiency of HNF-4α was confirmed by western blotting.

2.6. Statistical analyses

Data are expressed as mean ± SD. Statistical significance was determined using paired or unpaired two-tailed Student's t test. For all results, $p < 0.05$ was considered statistically significant. Analysis was performed using GraphPad Prism software (GraphPad Software Inc., La Jolla, CA).

3. Results

3.1. The hLXRa promoter is regulated in hepatic cells by a combination of negative and positive regulatory elements

Our first objective was to map the region upstream from the human LXRα gene that could contribute to its transcriptional regulation in hepatic cells. For this purpose we performed a deletion analysis of the (−2625/+384)-hLXRα promoter [8] and measured the activity of each promoter fragment by luciferase assays in human hepatoblastoma cell line HepG2. We generated by PCR the following serial deletions of the hLXRα promoter: −844/+384, −457/+384, −300/+384, −111/+384, −42/+384 and −25/+384 (Fig. 1A). As shown in Fig. 1B, deletion of the hLXRα promoter to position −457 caused a gradual increase in its activity from 2,1- to 4,1-fold relative to the larger promoter fragment tested (−2625/+384) suggesting the presence of negative regulatory elements inside the −2625/-457 region. The LXRα promoter activity did not decrease further by extending the deletions to positions −300 and −111. However, a significant drop in the activity of the promoter was observed when the region between nucleotides −111 and −42 was deleted suggesting the presence of strong positive regulatory elements inside the −111/−42 region. Finally, deleting the LXRα promoter to nucleotide −25 caused only a minor drop in LXRα promoter activity (Fig. 1B).

3.2. HNF-4α binds to a novel HNF-4-specific binding motif present in the −50/−40 region of the human LXRα promoter

Close examination of the human proximal LXRα promoter region −111/−42 revealed the presence of a DNA motif in the −50/−40 region (5′ TGGGACCTTTG 3′) with significant homology to the previously identified HNF-4-specific binding motif or H4-SBM [14] having the sequence: 5′ TGGACTTTG 3′ (Fig. 1C and D). Binding of HNF-4 to this proximal hLXRα promoter region is also supported by previous ChIP-seq data (Suppl. Fig. 1) obtained from the USCS genome bioinformatics platform (http://genome.ucsc.edu/).

First, we confirmed that HNF-4α binds to the proximal region of the human LXRα promoter *in vivo* by performing a chromatin immunoprecipitation (ChIP) experiment in HepG2 cells. As shown in Fig. 2B, an antibody against HNF-4α immunoprecipitated a chromatin fragment containing the human LXRα promoter region −147/+48. In contrast, this antibody did not immunoprecipitate a distal region of the human LXRα gene (+3461/+3694) that was used as a negative control suggesting that binding of HNF-4α to the proximal LXRα promoter was specific.

We performed DNA affinity precipitation (DNAP) assays in order to validate the functionality of the −50/−40 element of the hLXRα promoter. For this purpose, we generated biotinylated LXRα promoter fragments covering the regions −111/+384 and −25/+384 (Fig. 2A). As shown in Fig. 2C, HNF-4α bound to the −111/+384 but not to the −25/+384 promoter fragment. As anticipated, HNF-4α bound to a wild type but not to a mutated −40/−14 apoM oligonucleotide [15] that were used as a control (Fig. 2C).

We then performed DNAP assays using biotinylated oligonucleotides corresponding to the wild type −53/−23 region or to the same region bearing three point mutations in the putative motif

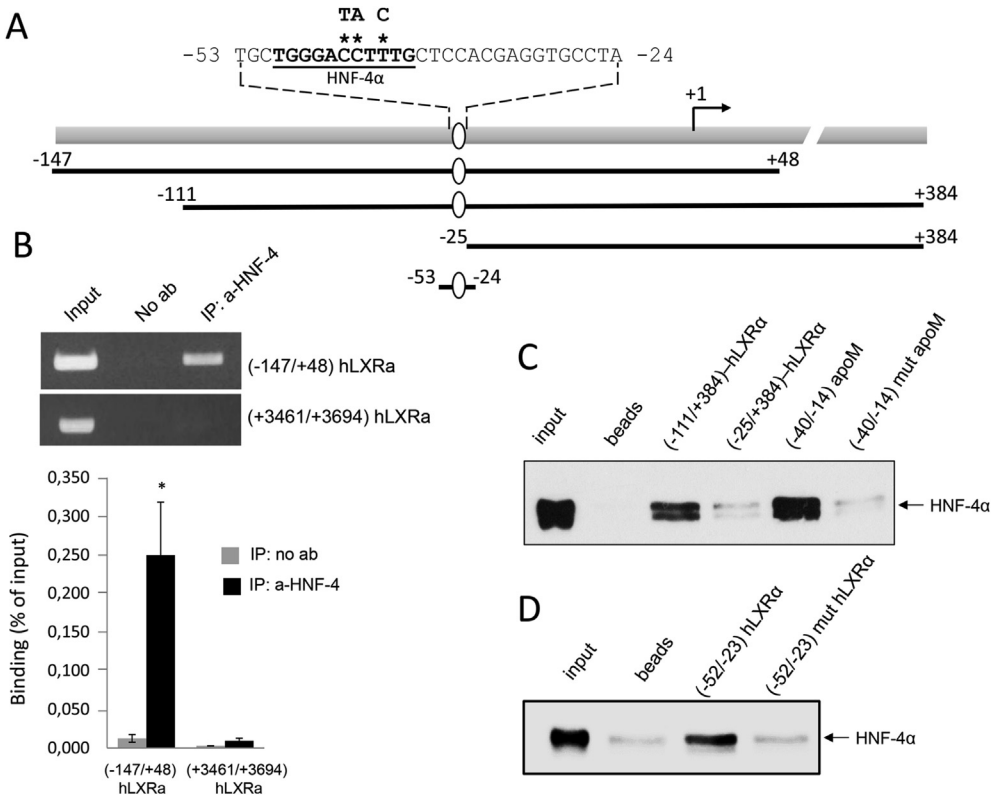

Fig. 2. HNF-4α binds to the hLXRα promoter *in vitro* and *in vivo*. (A) Schematic representation of the human LXRα promoter showing the HNF-4α binding site (bold and underlined). The mutations that were introduced into the site are shown above the sequence. The DNA fragments used for the experiments of panels B–D are shown at the bottom. (B) HepG2 cells were subjected to chromatin immunoprecipitation using the a-HNF-4α antibody or no antibody as a negative control. The immunoprecipitated chromatin was detected by both standard PCR (top) and quantitative PCR (bottom) using primers corresponding to the human LXRα promoter −147/+48 or to a distal region inside the LXRα gene. Results from qPCR are expressed as binding relative to the input (%). Each data point represents the average (±SD) of three different chromatin samples. (C) DNA-affinity precipitation experiment using nuclear extracts from HepG2 cells and biotinylated PCR products corresponding to the −111/+384 or −25/+384 regions of the hLXRα promoter. Biotinylated oligonucleotides (wt and mut) corresponding to the (−40/−14) region of apolipoprotein M promoter were used as positive (wt) or negative (mut) controls. (D) DNA-affinity precipitation experiment using nuclear extracts from HepG2 cells and biotinylated oligonucleotides (wt and mut) corresponding to the −53/+24 region of the hLXRα promoter (their sequence is depicted in panel A). Uncoupled beads were utilized as negative control (beads). HNF-4α binding was detected by Western blotting using the a-HNF-4α antibody. The arrow shows the position of HNF-4α. IP, Immunoprecipitation. Key: *, $p < 0.05$ by t-testing.

(Fig. 2A). As shown in Fig. 2D, HNF-4α bound to the wild type oligonucleotide but not to the mutated one. Binding of HNF-4α to the −50/−40 motif appears to be specific since no binding of LXRα was observed using the −53/−23 oligonucleotide in DNAP assays (data not shown).

3.3. The novel H4-SBM present in the −50/−40 region of the human LXRα promoter is required for the transactivation of this promoter by HNF-4α

We then performed transactivation experiments in human embryonic kidney HEK293T cells that do not express endogenous HNF-4α. As shown in Fig. 3A, HNF-4α transactivated the full length −2625/+384 hLXRα promoter 2,8-fold confirming that this nuclear receptor plays a role in the regulation of this promoter. The data of Fig. 3A also show that all LXRα promoter deletion fragments that contain the HNF-4 binding motif were transactivated by HNF-4α. In contrast, the −42/+384 promoter deletion fragment that does not include the HNF-4α binding motif could not be transactivated by HNF-4α. Most importantly, HNF-4α could not transactivate the −844/+384 LXRα promoter containing the triple nucleotide substitution (−844/+384 mut LXRα-luc) that abolished binding of HNF-4α (Fig. 2D and 3B).

Comparative sequence analysis of the mouse and human LXRα promoters revealed that the novel H4-SBM is conserved between the two species. In order to confirm that this motif is also functional in mice, we used the mouse LXRα promoter −3000/+30 [8] in transactivation assays. As shown in Fig. 3C, HNF-4α transactivated the −3000/+30 mouse LXRα promoter in HEK293T cells 24-fold.

In conclusion, the combined data of Figs. 2 and 3 suggest that the DNA sequence of the proximal LXRα promoter between nucleotides −50 and −40 is a true HNF-4 binding motif that mediates the transactivation of this promoter by HNF-4α.

3.4. Silencing of the HNF-4α gene is associated with reduced LXRα protein levels and promoter activity in hepatic cells

Transfection of HepG2 cells with a HNF-4α-specific siRNA [15] caused a statistically significant decrease in the protein levels of HNF-4α and LXRα (30% and 42% decrease respectively, Fig. 4A). Furthermore, the HNF-4α specific shRNA reduced the basal activity of the human LXRα promoter fragments −300/+384 and −111/+384 bearing the HNF-4α binding motif by 35% but not of the −42/+384 promoter fragment lacking this motif (Fig. 4B). Finally we showed that the triple mutation in the −50/−40 HNF-4α binding motif of the human LXRα promoter reduced the basal activity of the −844/+384 promoter by 40% but most importantly, we showed that the activity of this mutated promoter could not be reduced further by the HNF-4α specific siRNA (Fig. 4C).

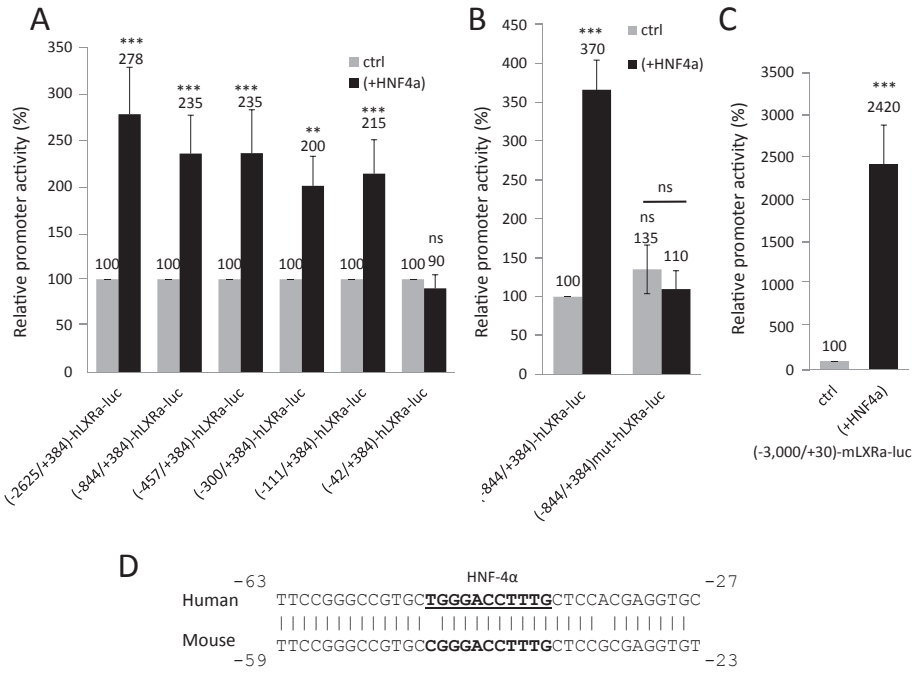

Fig. 3. HNF-4α transactivates the hLXRα promoter through the HNF-4α binding site. (A) HEK293T cells were transiently co-transfected with the indicated hLXRα reporter plasmids along with an expression vector for HNF-4α or an empty vector (ctrl). The (%) normalized relative promoter activity (±SD) was calculated from at least three independent experiments performed in duplicate. (B) HEK293T cells were transiently co-transfected with the (−844/+384)-hLXRα construct or with its mutant form (−844/+384)mut-hLXRα in the presence of an expression vector for HNF-4α or an empty vector (ctrl). The (%) normalized relative promoter activity (±SD) was calculated from three independent experiments performed in duplicate. (C) HEK293T cells were co-transfected with the (−3000/+30)-mouse LXRα luc reporter construct along with an expression vector for HNF-4α or an empty vector (ctrl). The (%) normalized relative promoter activity (±SD) was calculated from three independent experiments performed in duplicate. (D) Alignment of the human and mouse LXRα promoter in the region of the HNF-4α binding site. Key: **, $p < 0.001$, ***, $p < 0.0001$ by t-testing; ns, non-significant.

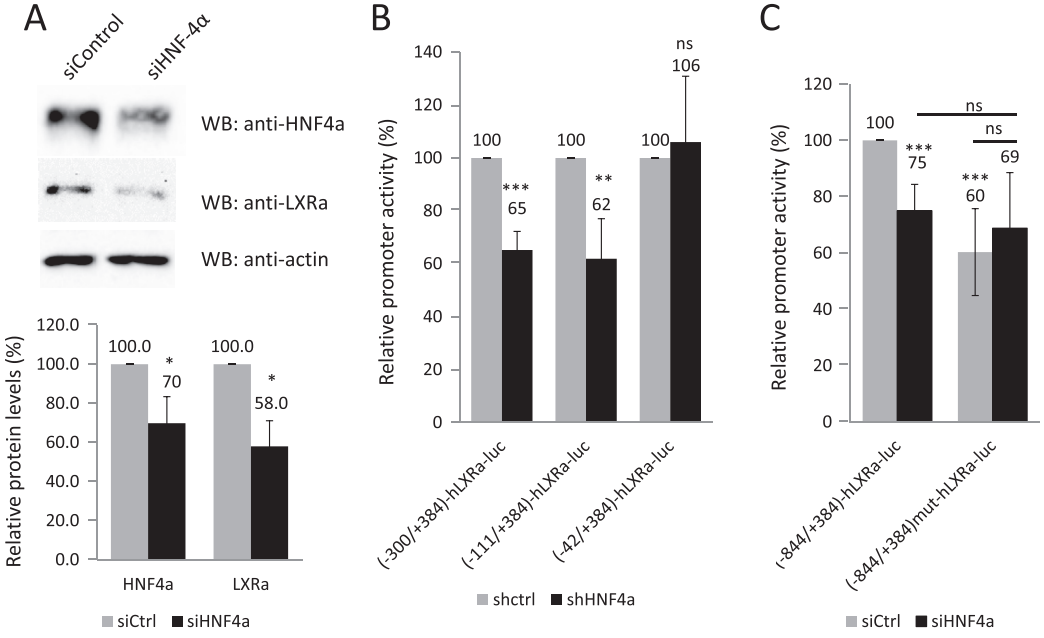

Fig. 4. Silencing of the endogenous HNF-4α gene in HepG2 cells results in the downregulation of both hLXRα protein and hLXRα promoter activity. (A) Top: HepG2 cells were transfected with 100 nM of scrambled (siControl) or HNF-4α specific si-RNA (siHNF-4α). Cell extracts were analysed for the protein levels of HNF-4α, LXRα and actin by immunoblotting using the corresponding antibodies. Bottom: the density of the bands was normalized to the density of actin and the normalized relative protein levels (±SD) were calculated from three independent experiments. (B) HepG2 cells were co-transfected with the indicated hLXRα reporter plasmids along with a vector expressing a shRNA for HNF-4α (shHNF-4α) or a vector expressing a shRNA with non-related sequence (shctrl). The (%) normalized relative promoter activity (±SD) was calculated from three independent experiments performed in duplicate. (C) HepG2 cells were transiently co-transfected with the (−844/+384)-hLXRα construct or with its mutant form (−844/+384)mut-hLXRα in the presence of 100 nM of scrambled (sictrl) si-RNA or HNF-4α specific si-RNA (siHNF4α). The (%) normalized relative promoter activity (±SEM) was calculated from three independent experiments performed in duplicate. Key: *,p < 0.05, **, $p < 0.001$, ***, $p < 0.0001$ by t-testing; ns, non-significant.

4. Discussion

LXRs play critical roles in lipid and lipoprotein metabolism by regulating the expression of a large number of genes in response to increased levels of intracellular cholesterol in various tissues such as the macrophages, the liver and the intestine [1]. In the liver, oxysterol-activated LXRs induce the transcription of the SREBP-1c gene thus causing hepatic lipogenesis [5] but they also activate the expression of the hepatic bile acid transporters ABCG5 and ABCG8 in order to facilitate the transfer of excess cholesterol to the bile [18]. Interestingly, the same two transporters are also targets of HNF-4α which binds to HREs present in the intergenic promoter and activates the expression the two genes in a coordinate manner [19] suggesting a dual mechanism of regulation of these bile acid transporters by HNF-4α in the liver.

The conservation of the newly identified H4-SBM in the LXRα promoter in mouse and human DNA suggested that HNF-4α may be essential for the regulation of the LXRα gene in the mouse. Indeed, overexpression of HNF-4α in HEK293T cells caused a strong transactivation of the mouse LXRα promoter containing the H4-SBM (Fig. 3C). Interestingly, inactivation of the mouse HNF-4α gene in adult mouse liver was not associated with a statistically significant decrease in the mRNA levels of the mouse LXRα gene (ref [20] and data not shown). However, it was observed that inactivation of the HNF-4α gene in the liver was associated with an increase in the expression of the paralogous gene HNF-4γ (Thymiakou et al., manuscript in preparation) which is not normally expressed in the liver [21] that could replace HNF-4α in its absence. This is supported by previous ChiP-seq data which showed that both HNF-4α and HNF-4γ are recruited to the proximal LXRα promoter (Suppl. Fig. 1). HNF-4α and HNF-4γ share high homology in their DNA binding and ligand binding domains [21] suggesting that they bind and regulate common sets of genes.

In the present study we provide new evidence for the regulation of gene expression by the sequential action of two different members of the hormone nuclear receptor superfamily: HNF-4α and LXRα. A similar mechanism of coordinated nuclear receptor action has been demonstrated in the past [8–10,22–25]. In the majority of these cases, the promoter of one nuclear receptor gene harbours HREs that serve as binding and regulatory sites for the same (autoregulation) or other nuclear receptors thus leading to the formation of a large network of interactions controlling the expression of hundreds of genes [24]. A well characterized example is the HNF-4/PPAR cascade. The promoter of the human PPARα gene contains a regulatory element consisting of a degenerate hexamer repeat with a single nucleotide spacer (direct repeat 1), termed alphaHNF4-RE, which binds HNF-4α and PPARα and mediates the induction of this promoter by HNF-4α and PPARα itself (autoregulation) [26]. These findings were confirmed recently *in vivo* using HNF-4α liver-specific knockout mice [23]. The latter study showed that HNF-4α controls a transcription factor network in the liver that coordinates the reciprocal expression of fatty acid transport and metabolizing enzymes during fasting and feeding conditions [23].

Finally, the regulation of the expression of the nuclear receptor LXRα by HNF-4α in the liver may be of importance for the biogenesis of High Density Lipoproteins (HDL) [13,27]. Of note, liver-specific inactivation of HNF-4α was associated with decreased plasma HDL levels in mice [20]. Given the strong and reverse association between plasma HDL levels and the risk for coronary heart disease (CHD), our findings suggest that HNF-4α could be a novel target for therapeutic interventions in patients with low HDL levels and increased risk for CHD.

Acknowledgments

This work was supported by a grant from the Hellenic Ministry for Education, Research and Relegious Affairs (THALIS MIS 377286) to DK. We would like to thank all members of the Kardassis lab for assistance with protocols and useful suggestions.

Appendix A. Supplementary data

Supplementary data related to this article can be found at http://dx.doi.org/10.1016/j.bbrc.2015.12.031.

Transparency document

Transparency document related to this article can be found online at http://dx.doi.org/10.1016/j.bbrc.2015.12.031.

References

[1] C. Zhao, K. Dahlman-Wright, Liver X receptor in cholesterol metabolism, J. Endocrinol. 204 (2010) 233–240.
[2] J.L. Collins, A.M. Fivush, M.A. Watson, C.M. Galardi, M.C. Lewis, L.B. Moore, D.J. Parks, J.G. Wilson, T.K. Tippin, J.G. Binz, K.D. Plunket, D.G. Morgan, E.J. Beaudet, K.D. Whitney, S.A. Kliewer, T.M. Willson, Identification of a nonsteroidal liver X receptor agonist through parallel array synthesis of tertiary amines, J. Med. Chem. 45 (2002) 1963–1966.
[3] J.J. Repa, D.J. Mangelsdorf, The liver X receptor gene team: potential new players in atherosclerosis, Nat. Med. 8 (2002) 1243–1248.
[4] J.J. Repa, S.D. Turley, J.A. Lobaccaro, J. Medina, L. Li, K. Lustig, B. Shan, R.A. Heyman, J.M. Dietschy, D.J. Mangelsdorf, Regulation of absorption and ABC1-mediated efflux of cholesterol by RXR heterodimers, Science 289 (2000) 1524–1529.
[5] J.J. Repa, G. Liang, J. Ou, Y. Bashmakov, J.M. Lobaccaro, I. Shimomura, B. Shan, M.S. Brown, J.L. Goldstein, D.J. Mangelsdorf, Regulation of mouse sterol regulatory element-binding protein-1c gene (SREBP-1c) by oxysterol receptors, LXRalpha and LXRbeta, Genes Dev. 14 (2000) 2819–2830.
[6] S.S. Im, T.F. Osborne, Liver x receptors in atherosclerosis and inflammation, Circ. Res. 108 (2011) 996–1001.
[7] K.A. Tobin, H.H. Steineger, S. Alberti, O. Spydevold, J. Auwerx, J.A. Gustafsson, H.I. Nebb, Cross-talk between fatty acid and cholesterol metabolism mediated by liver X receptor-alpha, Mol. Endocrinol. 14 (2000) 741–752.
[8] K. Hashimoto, S. Matsumoto, M. Yamada, T. Satoh, M. Mori, Liver X receptor-alpha gene expression is positively regulated by thyroid hormone, Endocrinology 148 (2007) 4667–4675.
[9] A. Chawla, W.A. Boisvert, C.H. Lee, B.A. Laffitte, Y. Barak, S.B. Joseph, D. Liao, L. Nagy, P.A. Edwards, L.K. Curtiss, R.M. Evans, P. Tontonoz, A PPAR gamma-LXR-ABCA1 pathway in macrophages is involved in cholesterol efflux and atherogenesis, Mol. Cell 7 (2001) 161–171.
[10] B.A. Laffitte, S.B. Joseph, R. Walczak, L. Pei, D.C. Wilpitz, J.L. Collins, P. Tontonoz, Autoregulation of the human liver X receptor alpha promoter, Mol. Cell Biol. 21 (2001) 7558–7568.
[11] F.M. Sladek, W.M. Zhong, E. Lai, J.E. Darnell Jr., Liver-enriched transcription factor HNF-4 is a novel member of the steroid hormone receptor superfamily, Genes Dev. 4 (1990) 2353–2365.
[12] K. Yamagata, H. Furuta, N. Oda, P.J. Kaisaki, S. Menzel, N.J. Cox, S.S. Fajans, S. Signorini, M. Stoffel, G.I. Bell, Mutations in the hepatocyte nuclear factor-4alpha gene in maturity-onset diabetes of the young (MODY1), Nature 384 (1996) 458–460.
[13] D. Kardassis, I. Mosialou, M. Kanaki, I. Tiniakou, E. Thymiakou, Metabolism of HDL and its regulation, Curr. Med. Chem. 21 (2014) 2864–2880.
[14] B. Fang, D. Mane-Padros, E. Bolotin, T. Jiang, F.M. Sladek, Identification of a binding motif specific to HNF4 by comparative analysis of multiple nuclear receptors, Nucleic Acids Res. 40 (2012) 5343–5356.
[15] I. Mosialou, V.I. Zannis, D. Kardassis, Regulation of human apolipoprotein m gene expression by orphan and ligand-dependent nuclear receptors, J. Biol. Chem. 285 (2010) 30719–30730.
[16] J.A. Ladias, M. Hadzopoulou-Cladaras, D. Kardassis, P. Cardot, J. Cheng, V. Zannis, C. Cladaras, Transcriptional regulation of human apolipoprotein genes ApoB, ApoCIII, and ApoAII by members of the steroid hormone receptor superfamily HNF-4, ARP-1, EAR-2, and EAR-3, J. Biol. Chem. 267 (1992) 15849–15860.
[17] E. Thymiakou, D. Kardassis, Novel mechanism of transcriptional repression of the human ATP binding cassette transporter A1 gene in hepatic cells by the winged helix/forkhead box transcription factor A2, Biochim. Biophys. Acta 1839 (2014) 526–536.
[18] J.J. Repa, K.E. Berge, C. Pomajzl, J.A. Richardson, H. Hobbs, D.J. Mangelsdorf, Regulation of ATP-binding cassette sterol transporters ABCG5 and ABCG8 by the liver X receptors alpha and beta, J. Biol. Chem. 277 (2002) 18793–18800.
[19] K. Sumi, T. Tanaka, A. Uchida, K. Magoori, Y. Urashima, R. Ohashi, H. Ohguchi,

M. Okamura, H. Kudo, K. Daigo, T. Maejima, N. Kojima, I. Sakakibara, S. Jiang, G. Hasegawa, I. Kim, T.F. Osborne, M. Naito, F.J. Gonzalez, T. Hamakubo, T. Kodama, J. Sakai, Cooperative interaction between hepatocyte nuclear factor 4 alpha and GATA transcription factors regulates ATP-binding cassette sterol transporters ABCG5 and ABCG8, Mol. Cell Biol. 27 (2007) 4248–4260.

[20] G.P. Hayhurst, Y.H. Lee, G. Lambert, J.M. Ward, F.J. Gonzalez, Hepatocyte nuclear factor 4alpha (nuclear receptor 2A1) is essential for maintenance of hepatic gene expression and lipid homeostasis, Mol. Cell Biol. 21 (2001) 1393–1403.

[21] S. Taraviras, T. Mantamadiotis, T. Dong-Si, A. Mincheva, P. Lichter, T. Drewes, G.U. Ryffel, A.P. Monaghan, G. Schutz, Primary structure, chromosomal mapping, expression and transcriptional activity of murine hepatocyte nuclear factor 4gamma, Biochim. Biophys. Acta 1490 (2000) 21–32.

[22] G. Chinetti, S. Lestavel, V. Bocher, A.T. Remaley, B. Neve, I.P. Torra, E. Teissier, A. Minnich, M. Jaye, N. Duverger, H.B. Brewer, J.C. Fruchart, V. Clavey, B. Staels, PPAR-alpha and PPAR-gamma activators induce cholesterol removal from human macrophage foam cells through stimulation of the ABCA1 pathway, Nat. Med. 7 (2001) 53–58.

[23] C.P. Martinez-Jimenez, I. Kyrmizi, P. Cardot, F.J. Gonzalez, I. Talianidis, Hepatocyte nuclear factor 4alpha coordinates a transcription factor network regulating hepatic fatty acid metabolism, Mol. Cell Biol. 30 (2010) 565–577.

[24] P. Karagianni, I. Talianidis, Transcription factor networks regulating hepatic fatty acid metabolism, Biochim. Biophys. Acta 1851 (2015) 2–8.

[25] P. Hatzis, I. Talianidis, Regulatory mechanisms controlling human hepatocyte nuclear factor 4alpha gene expression, Mol. Cell Biol. 21 (2001) 7320–7330.

[26] I. Pineda Torra, Y. Jamshidi, D.M. Flavell, J.C. Fruchart, B. Staels, Characterization of the human PPARalpha promoter: identification of a functional nuclear receptor response element, Mol. Endocrinol. 16 (2002) 1013–1028.

[27] D. Kardassis, A. Gafencu, V.I. Zannis, A. Davalos, Regulation of HDL genes: transcriptional, posttranscriptional, and posttranslational, Handb. Exp. Pharmacol. 224 (2015) 113–179.